

ЖУРНАЛ
ПРИКЛАДНОЙ ХИМИИ

Volume 32, No. 7

July, 1959

JOURNAL OF
APPLIED CHEMISTRY
OF THE USSR

(ZHURNAL PRIKLADNOI KHIMII)

IN ENGLISH TRANSLATION



CONSULTANTS BUREAU, INC.

UNDER THE DIRECTION OF THE AMERICAN CERAMIC SOCIETY...
a major source of scientific communication —

GLASS AND CERAMICS

TRANSLATED FROM RUSSIAN

This Soviet monthly, published for glass and ceramics researchers, technologists and production workers, provides Western scientists with reports on the latest technical advances from the laboratories and plants of the USSR.

Translation of GLASS AND CERAMICS, prompted by the recognition given to Soviet work in the field, permits you to take advantage of their intensified research program. Using these accurate translations by a staff of bilingual scientists can eliminate costly duplication of research. Scientists in this country can learn the *specifics* about how their Soviet counterparts upgrade products and improve processes; design unique, improved equipment; break production records and reduce costs.

GLASS AND CERAMICS will be published in the most effective manner possible to bridge the 3-year gap since this journal was last available in complete translation.

1957 issues will be published in 3 separate volumes, each of which will contain 4 issues. Nos. 1-4 March; Nos. 5-8 April; Nos. 9-12 June. The remaining 1958 and 1959 issues will be brought out in four-issue volumes on a bimonthly basis until the backlog has been diminished.

Subscription price: \$80.00 per year.

Detailed tables of contents will be sent upon request.

You will also be interested in . . .

THE STRUCTURE OF GLASS

Proceedings of a Conference Held in Leningrad on the Structure of Glass

"...The Glass Division of the American Ceramic Society and the National Science Foundation are to be congratulated for making this inspiring collection available..."

—JOURNAL OF CHEMICAL EDUCATION

"The book should be of great interest to scientific and technical personnel interested in glass technology, ceramics, the states of matter, and any work involving the vitreous state. They should all have the experience of reading this book...there exists in the scientific literature of the USSR, a whole new reference field that should be as easily available to

Western scientists and vice-versa."

—CHEMISTRY IN CANADA

"... a stimulating experience..."

—TRANS., BRITISH CERAMIC SOCIETY

"...lively discussions which show the diversity of opinions on every experimental report."

—THE GLASS INDUSTRY

"... the volume is excellent... The translation was well worth while..."

—R. W. Douglas, NATURE

"... an excellent volume..."

—SOUTH AFRICAN JOURNAL OF SCIENCE

Cloth

296 pages

profusely illustrated

\$20.00

Order on approval from

CONSULTANTS BUREAU ENTERPRISES, INC.

227 West 17th Street • New York 11, N. Y.

Volume 32, No. 7

July, 1959

JOURNAL OF
APPLIED CHEMISTRY
OF THE USSR

(ZHURNAL PRIKLADNOI KHIMII)

A publication of the Academy of Sciences of the USSR

IN ENGLISH TRANSLATION

Year and issue of first translation:

Vol. 23, No. 1

January 1950

	<i>U. S. and Canada</i>	<i>Foreign</i>
<i>Annual subscription</i>	\$60.00	\$65.00
<i>Annual subscription for libraries of nonprofit academic institutions</i>	20.00	25.00
<i>Single issue</i>	7.50	7.50

Copyright 1960

CONSULTANTS BUREAU ENTERPRISES, INC.
227 West 17th Street, New York, N. Y.

Editorial Board
(ZHURNAL PRIKLADNOI KHIMII)

P. P. Budnikov, S. I. Vol'fkovich, A. F. Dobryanskii,
O. E. Zvyagintsev, N. I. Nikitin (Editor in Chief),
G. V. Pigulevskii, M. E. Pozin, L. K. Simonova
(Secretary), V. V. Skorchellett, N. P. Fedot'ev

*Note: The sale of photostatic copies of any
portion of this copyright translation is expressly
prohibited by the copyright owners.*

Printed in the United States of America

CONTENTS

	PAGE	RUSS. PAGE
The Reaction of Spodumene with Potassium Sulfate at High Temperatures. <u>V. E. Plyushchev</u>	1451	1413
The Role of Filtration of Selenious Sulfite (Selenosulfate) Solutions in the Production of Pure Selenium. <u>O. V. Al'tshuler, E. A. Subbotina and F. F. Kharakhorin</u>	1457	1420
Thermal Production of Alkali Metals from Their Chlorides and Heat-Transfer Characteristics of Briquetted Charges. <u>N. M. Zuev</u>	1464	1426
Effect of the Composition of Glass on Diffusion of Copper Ions into It. <u>E. A. Ivanova and V. V. Vargin</u>	1469	1432
A Study of Processes of Microstructure Formation in Insulator Porcelain During Firing. <u>N. A. Toropov and A. N. Alekseeva</u>	1477	1441
The Relationship Between the Stressed State of Porcelain and Damping of Vibrations Induced in it. <u>V. Z. Petrova and A. L. Avgustinik</u>	1481	1445
A Study of the Stabilization Conditions and Stability of ZrO_2 . <u>L. P. Kachalova and A. L. Avgustinik</u>	1487	1451
Effects of Added Organosilicon Compounds on the Acid Resistance and Other Technical Characteristics of Ceramic Materials. <u>V. A. Bork and L. L. Kornblit</u>	1493	1457
Density of Solutions of N_2O_4 in Strong Nitric Acid. <u>G. L. Antipenko, E. S. Beletskaya and Z. L. Koroleva</u>	1498	1462
The Detonating Power of Liquid Explosive Mixtures Based on Nitric Acid. <u>R. Kh. Kurbangalina</u>	1502	1467
Vapor Pressure of Ammonium Chloride Spent Liquors in Soda Production (Solvay Process). <u>L. N. Matusevich and K. N. Shabalin</u>	1506	1470
Investigation of Absorption Rates in Horizontal Mechanical Absorbers with the Aid of the Similarity Principle. <u>S. N. Ganz and M. A. Lokshin</u>	1512	1477
Study of Oxidation-Sulfation Roasting of Sulfide Ores in a Fluidized Bed in a Model Batch Furnace. <u>V. V. Pechkovskii and S. A. Amirova</u>	1519	1484
Mass Transfer on Bubbler Grid and Tube Plates of the Drop-Through (Turbogrid) Type. <u>L. N. Kuz'minykh and A. L. Rodionov</u>	1523	1489
Magnitude of the Interphase Area in Mechanical Agitation of Mutually Insoluble Liquids. <u>L. S. Pavlushenko and A. V. Yanishevskii</u>	1529	1495
Production of Powder Alloys of Nickel with Iron and Molybdenum by Simultaneous Reduction of Mixed Oxides (Diffusion Method). <u>G. A. Semenov</u>	1536	1502
Preparation of Chromium Carbide, Cr_7C_3 . <u>T. Ya. Kosolapov and G. V. Samsonov</u>	1539	1505

CONTENTS (continued)

	PAGE	RUSS. PAGE
Investigation of Local and General Corrosion of Austenitic Chromium-Nickel Steel in Heat Treatment and Descaling. <u>A. V. Shreider, E. M. Kontsevaya and V. P. Gamazov</u> . .	1543	1509
Gas Formation in the Etching of Zinc in Acid Solutions. <u>L. L. Zabolotnyi and A. P. Lizogub</u> .	1549	1515
Investigation of the Porosity and Adsorption Properties of Protective Films Formed on the Heating Surfaces of Corroding Metals. <u>N. G. Chen</u>	1553	1519
Influence of Certain Ions on the Protective Action of Phosphate Inhibitors of Corrosion. <u>N. G. Chen</u>	1556	1523
Density and Conductivity of Certain Melts in the System $\text{Na}_3\text{AlF}_6\text{--Li}_3\text{AlF}_6\text{--Al}_2\text{O}_3$. <u>V. P. Mashovets and V. I. Petrov</u>	1561	1528
Suction Removal of Gases and Liquids Through Porous Electrodes. <u>O. S. Ksenzhek and V. V. Stender</u>	1568	1535
Influence of Electrolysis Conditions on the Roughness and Hardness of Electrolytic Cobalt Deposits. <u>N. P. Fedot'ev, V. B. Aleskovskii, P. M. Vyacheslavov, N. V. Volkhonskii and D. L. Romanova</u>	1575	1542
Rate of Contact Reduction of a Metal from Solution. <u>B. V. Drozdov</u>	1579	1546
Cathodic Reduction of Ferric Oxide. <u>V. P. Galushko, E. F. Zagorodnyaya and L. I. Tishchenko</u>	1583	1551
The Systems Water-Hexamethyleneimine-Sodium Chloride and Water-Hexamethyleneimine-Sodium Hydroxide. <u>E. N. Zil'berman and M. M. Bershtein</u>	1587	1555
The Influence of Dye Concentration on Light Fastness. <u>Ya. A. Legkun</u>	1592	1560
Search for a Method of Estimating the Photoactive Properties of Dyes. <u>N. I. Abramova, V. A. Blinov, N. S. Dokunikhin and V. A. Titkov</u>	1595	1563
Dyeing of Nitron Fibers by Basic Dyes. <u>E. S. Roskin, A. A. Kharkharov and A. L. Shapirov</u> .	1601	1569
Stabilization of Polyvinyl Chloride by Salts of Stearic and Epoxystearic Acids. <u>D. M. Yanovskii, A. A. Berlin, E. N. Zil'berman and N. A. Rybakova</u>	1606	1575
Water-Repellent Treatment of Cellulosic Materials by Organosilicon Compounds. <u>M. G. Voronkov and N. V. Kalugin</u>	1612	1581
Effects of Various Aldehydes on the Behavior of Glucose in Sulfite Cooking. <u>S. A. Sapotnitskii and A. G. Moskaleva</u>	1616	1586
Reactions of Acrichine (Quinacrine Hydrochloride) and Rivanol (Ethoxydiaminoacridine Lactate) with Tannin and Analysis of the Latter. <u>E. O. Turgel'</u>	1620	1590
Hydrochlorination of Divinylacetylene in a Reactor with an Air Lift. <u>A. E. Akopyan and Zh. A. Kosoyan</u>	1625	1595
Catalytic Reduction of Adipic Acid Dinitrile to ϵ -Aminocapronitrile. <u>L. Kh. Freidlin, A. A. Balandin, T. A. Sladkova, D. I. Lainer and L. G. Emel'yanov</u>	1630	1600
Decomposition of Furan by Hot Perhydrol Under Pressure. <u>A. P. Salchinkin</u>	1635	1605
Preparation of Esters of 1-Alkoxypropanediol-2,3. <u>M. S. Malinovskii and V. M. Vvedenskii</u> .	1640	1610

Brief Communications

Reactions of the Tetrachlorides of Tin, Germanium and Titanium with Silicon-Copper Alloy. <u>D. A. Kochkin, M. F. Shostakovskii and L. V. Musatova</u>	1643	1614
Thermal Decomposition of Certain Sulfates in a Current of Steam. <u>A. B. Suchkov, B. A. Borok and Z. I. Morozova</u>	1646	1616
Thermal Decomposition of a Mixture of $MnSO_4 + FeSO_4$ in a Current of Steam. <u>A. B. Suchkov, B. A. Borok and Z. I. Morozova</u>	1649	1618
Reaction of Silicon with Hydrogen Chloride in a Fluidized Bed. <u>K. A. Andrianov, S. A. Golubtsov and L. V. Trofimova</u>	1652	1620
Treatment of Waste Waters by Delayed Precipitation. <u>D. V. Bezuglyi</u>	1656	1624
Voltage Balance of an Electrolytic Cell and Possibilities of Lowering the Specific Power Consumption in the Production of Copper Powder. <u>A. V. Ponomosov</u>	1659	1626
Use of Sodium Thiosulfate for Antiseptic Impregnation of Wood. <u>G. E. Shaltyko, L. L. Pshedetskaya and K. K. Sergeenkova</u>	1662	1629
Methods for Laboratory Synthesis of Polyesters. <u>Zh. S. Sogomonyants</u>	1666	1632
Continuous Method for Preparation of 1,4-Dichlorobutane and Di(4-Chlorobutyl) Ether from Tetrahydrofuran and Phosgene. <u>V. I. Lutkova and N. I. Kutsenko</u>	1670	1635
Investigation of the Chemical Composition of the Fatty Oil from the European Spindle Tree (<i>Euonymus Europaea</i>). <u>N. I. Simonova</u>	1673	1637
Preparation of Monomethyl Ethers of Polypropylene Glycols. <u>S. M. Gurvich, V. R. Likhterov and V. S. Etlis</u>	1676	1640
Oxidative Ammonolysis of γ -Picoline in the Vapor Phase. <u>B. V. Suvorov, S. R. Rafikov, V. S. Kudinova and B. A. Zhubanov</u>	1679	1642
Second International Conference on the Peaceful Uses of Atomic Energy, Geneva, 1958. . .	1681	1644

Book Reviews

Granulated Blast-Furnace Slags and Slag Cements. <u>P. P. Budnikov and L. L. Znachko-Yavorskii</u>	1683	1646
Inhibitors of Metal Corrosion. <u>L. N. Putilova, S. A. Balezin and V. P. Barannik</u>	1685	1647



THE REACTION OF SPODUMENE WITH POTASSIUM SULFATE AT HIGH TEMPERATURES

V. E. Plyushchev

(M. V. Lomonosov Institute of Fine Chemical Technology, Moscow)

It was shown by mineralogical investigations as long ago as the 1880's that double silicates or aluminosilicates containing lithium, found in nature as various minerals, may be decomposed by alkali-metal salts. However, the technological significance of these investigations was not appreciated at the time. Only 20 years later was a method proposed for conversion of lithium into a soluble form for subsequent preparation of various lithium compounds, by sintering of lithium minerals with alkali-metal salts.

Subsequent investigations showed that alkali-metal salts are much more effective for decomposing lithium minerals than are salts of the alkaline-earth metals or of elements of group III of the periodic system, and that alkali sulfates give the best results.

Sintering of lithium minerals with K_2SO_4 attained special significance, as it was found that all lithium minerals react with K_2SO_4 when heated at temperatures up to 1500° (according to the nature of the mineral), with formation of Li_2SO_4 , which is easily leached out by water. It was also shown by Sobolev's detailed investigations [1] in the USSR that the sintering process with K_2SO_4 can be used for all lithium minerals, and can be conducted at $920-1500^\circ$, depending on the quality of the ore, with 98% conversion of Li_2O into a soluble form.

There is an enormous number of published papers and patents on the conversion of lithium minerals by sintering with K_2SO_4 ; investigations relating to lepidolite and to the most important lithium mineral, spodumene ($LiAl[Si_2O_6]$ or $Li_2O \cdot Al_2O_3 \cdot 4SiO_2$) have been particularly numerous.

The reaction between spodumene and K_2SO_4 is almost quantitative at high temperatures, and many workers have suggested that it is a reaction of double decomposition, with formation of potassium aluminosilicate, leucite, ($K[AlSi_2O_6]$ or $K_2O \cdot Al_2O_3 \cdot 4SiO_2$). However, this opinion has not been supported by any investigations of proofs, and was accepted as the most probable and convenient explanation, especially as the formulas of spodumene and leucite have a superficial mineralogical analogy.

As the reaction of spodumene with K_2SO_4 proceeds quite satisfactorily [1-7], there was no urgent necessity for determination of the reaction mechanism, and further studies of the conversion of lithium minerals by sintering with K_2SO_4 were concerned with a search for rational methods for isolation of lithium from sulfate solutions. (Such solutions contain Na_2SO_4 from isomorphous sodium impurities in the spodumene, and K_2SO_4 , used in excess in the sintering process, in addition to Li_2SO_4).

Another trend in research into conversion of lithium minerals by alkali-metal salts consisted of attempts to replace K_2SO_4 (totally or partially) by Na_2SO_4 , which would cheapen the process. However, despite reports [8] that it is possible in principle to replace K_2SO_4 by Na_2SO_4 , the latter is unsuitable for use in the pure form, as at relatively low temperatures ($800-900^\circ$) the conversion of lithium into a water-soluble form is very low (39-49%), while at higher temperatures a semifused and very hard mass is obtained. The results obtained with mixtures of K_2SO_4 and Na_2SO_4 are little better, so that this method has not been adopted in practice.

Many workers who studied the reaction of spodumene with K_2SO_4 did not investigate the nature of the solid phases formed in this reaction.

Nevertheless, the hypothesis that leucite is formed from spodumene is at variance with earlier concepts [2] according to which ion exchange takes place in the interaction of spodumene with K_2SO_4 , similar to the type of exchange in the Permutit method of water treatment. Because of the sharp difference between the ionic radii of lithium (0.78 Å) and potassium (1.33 Å) and the high temperatures needed to effect the process, such analogies cannot be accepted as correct.

The present investigation was a study of the reaction of spodumene with K_2SO_4 at high temperatures [9].

EXPERIMENTAL

Most of the work was performed with thermally-beneficiated spodumene (β -spodumene) of the following composition (wt. %): Li_2O -5.44; Na_2O -3.20; Al_2O_3 -28.33; SiO_2 -62.60; CaO -0.11; K_2O absent, calcination loss 0.20 ($\Sigma = 99.86$). Spectrum analysis showed the spodumene to contain Mg, Mn, Fe, small amounts of Be, Cu, Zr, Ti and Sn and faint traces of Ag.

This spodumene was obtained by roasting of native spodumene (α -spodumene) at 1100° . Comparison of the analytical data with the theoretical composition of pure lithium spodumene shows that the mineral at our disposal was affected by the usual process of partial substitution of lithium by sodium. However, optical analysis showed this spodumene to be quite pure and homogeneous (with average refractive index $n' = 1.520 \pm 0.003$), and it did not contain any other minerals. Its composition corresponded to the formula $(Li, Na)_2O \cdot Al_2O_3 \cdot 4SiO_2$, which represents in general form the process of isomorphous substitution of lithium by sodium. The structural formula of this β -spodumene is $(Li, Na)[AlSi_3O_8]$.

The particle size of the β -spodumene was such that 90% of the particles passed through a 150 mesh screen. (This subdivision occurs in the course of the $\alpha \rightarrow \beta$ conversion of spodumene).

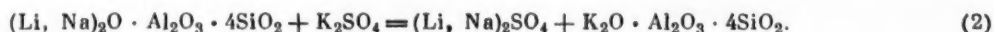
Some of the experiments were performed with spodumene (the α -modification) carefully picked out under the binocular microscope free from extraneous minerals, and then ground for mixing with K_2SO_4 . This spodumene had the following composition (in wt. % of the calcined mineral): Li_2O -6.05, Na_2O -0.12, K_2O -0.12, CaO -0.22, Al_2O_3 -27.58, SiO_2 -66.34, Fe_2O_3 and MgO - traces ($\Sigma = 100.43$). Spectrum analysis showed the presence of Ti, Mn and Cu. The average refractive index n' was 1.665 ± 0.003 . Our earlier investigation, performed jointly with Urazov and Shakhno [10] of this sample of α -spodumene showed that the $\alpha \rightarrow \beta$ transformation occurs in the 990 - 1035° range (at a heating rate of 11 degrees/minute), or in the 995 - 1075° range (at a heating rate of 22 degrees/minute).

METHOD OF INVESTIGATION

The reaction between spodumene and K_2SO_4 was studied for different proportions of the charge components and over a wide temperature range. After preliminary experiments, based on earlier results and on the fact that the sintering time (especially without continuous stirring, which proved impossible to achieve) depends on the mass of the charge (the thickness of the layer), a sintering time of 3 hours was chosen. The amounts of K_2SO_4 taken for the reactions with α - and β -spodumene were 20, 40, 60, 80 and 100% on the weight of mineral, calculated as percentages of the theoretical amounts for the reaction



these amounts, for β -spodumene, corresponded to 62.5, 125, 187.5, 250 and 312.5%. Since Na_2SO_4 as well as Li_2SO_4 is formed in the reaction of spodumene with K_2SO_4 , the reaction should, in general, be represented by the equation



The above amounts of K_2SO_4 then become 50, 100, 150, 200, and 250% of the theoretical.

The charges were prepared by thorough mixing of 10 g of spodumene with the appropriate amount of K_2SO_4 (analytical grade). The sintering was effected in corundum crucibles, which were filled with the charges and placed in a muffle furnace heated to the required temperature. The time required for raising the temperature after the furnace was cooled somewhat by the introduction of the charges was not included in the sintering time.

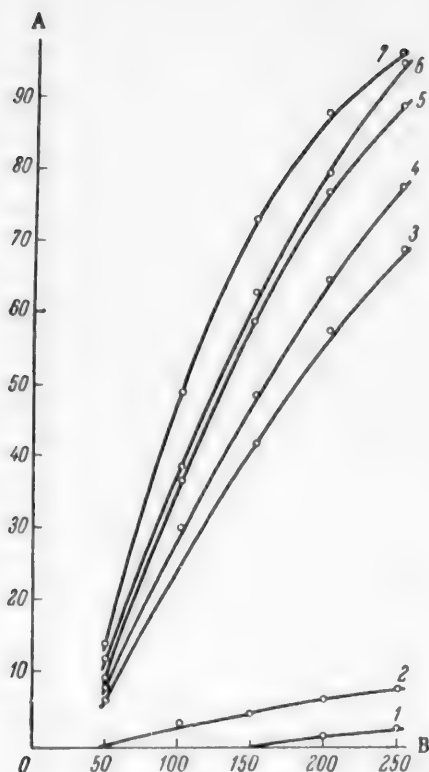


Fig. 1. Effects of sintering temperature and amount of K_2SO_4 taken on the extraction of lithium from β -spodumene: A) extraction of lithium into solution (%); B) K_2SO_4 taken (%); temperature (deg): 1) 700; 2) 800; 3) 900; 4) 950; 5) 1000; 6) 1050; 7) 1100.

sulfates into chlorides), while for determination of sodium, lithium must be completely removed, as in the presence of the latter, sodium cannot be determined in the form of zinc uranyl acetate.

The solutions were also quantitatively analyzed for aluminum (by the alizarin reaction) and soluble SiO_2 (by the reaction with ammonium molybdate [13]). However, negative reactions were obtained in all the experiments.

Results of Experiments on the Reaction of β -Spodumene with Potassium Sulfate

Experiments on the sintering of β -spodumene with K_2SO_4 were undertaken not only to determine the effects of temperature and excess K_2SO_4 on the reaction with spodumene, but also to clarify the behavior of the sodium present in the mineral and to obtain the insoluble phases formed in the reaction of β -spodumene with K_2SO_4 for subsequent investigation.

The results of these experiments are plotted in Fig. 1 and 2. It is seen that some interaction between β -spodumene and K_2SO_4 occurs even at 700°, but it remains slight up to 800°, even with a large amount of K_2SO_4 in the charge. At 900° the interaction of the charge components during sintering increases sharply with increase of the amount of K_2SO_4 taken for the reaction; this is clearly seen in Fig. 1. At 1050-1100° it is possible to obtain the maximum, almost total, conversion of lithium from spodumene into the soluble phase.

Conversion of lithium into the soluble phase is accompanied by similar conversion of sodium, but at 700 and 800° the extent of this conversion is slight; starting with 900° the conversion of sodium into the soluble phase

A platinum/platinum-rhodium thermocouple was used to control constancy of temperature; fluctuations did not exceed $\pm 10^\circ$.

The sintering process was studied in the 700-1100° range.

After the end of the experiments the cooled sinters were carefully and thoroughly removed from the crucibles by treatment with water until soluble salts were leached out completely (as shown by tests for SO_4^{2-}). The solutions and wash waters were combined and collected in measuring flasks.

Lithium, sodium, potassium, and SO_4^{2-} ions were determined in the solutions.

Lithium was determined gravimetrically as Li_2SO_4 after extraction of $LiCl$ from its mixture with other alkali-metal chlorides by means of *n*-propyl alcohol saturated with gaseous HCl . This method was worked out by us jointly with Shakhno [11], and is successfully used not only in technological investigations but in physicochemical analysis.

Sodium was determined by precipitation as sodium zinc uranyl acetate [12]. By this method sodium can be determined without previous separation of potassium, and traces of sodium can be determined quantitatively with a high degree of accuracy; one determination takes about 3 hours.

Potassium was determined by one variant of the chloroplatinate method, whereby potassium can be determined in presence of sulfates, chlorides, and salts of sodium, magnesium, iron, alkaline earths, and a number of other elements. Sulfate was determined as $BaSO_4$.

For determinations of potassium, aliquot portions of the solutions were taken, while lithium, sodium, and SO_4^{2-} were determined in whole solution samples, as for determination of lithium, it is necessary to remove SO_4^{2-} ions (conversion of

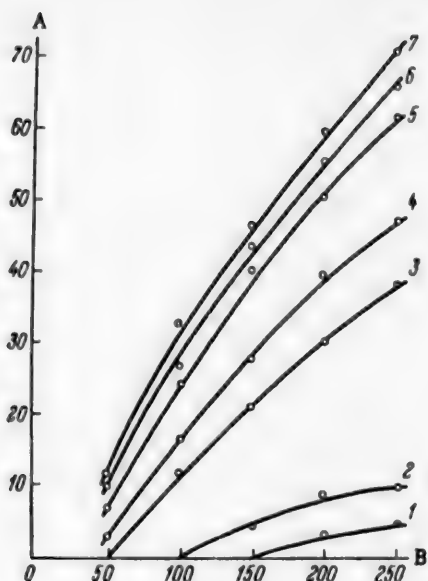


Fig. 2. Effects of sintering temperature and amount of K_2SO_4 taken on the extraction of sodium from β -spodumene: A) extraction of sodium into solution (%); B) K_2SO_4 taken (%); temperature (deg): 1) 700; 2) 800; 3) 900; 4) 950; 5) 1000; 6) 1050; 7) 1100.



Fig. 3. Heating curve of the insoluble residue from a sinter of β -spodumene with K_2SO_4 .

elucidate the influence of the $\alpha \rightarrow \beta$ transformation of spodumene on the mechanism and extent of its sintering reaction with K_2SO_4 .

It was found that up to 900° Li_2SO_4 and Na_2SO_4 are not formed when α -spodumene is sintered with K_2SO_4 , while at 950° and higher the conversion of lithium and sodium into the water-soluble phase reaches the values characteristic for β -spodumene. Evidently, during the prolonged heating used in the sintering process, the $\alpha \rightarrow \beta$ conversion of spodumene occurs at a lower temperature than it does in the pure mineral. It is relevant in this connection that the polymorphous conversion of spodumene depends not only on the rate of heating but also on the nature of the impurities present (K_2SO_4 in the charge) [10].

Thus, the $\alpha \rightarrow \beta$ conversion of spodumene, which was formerly used with success for thermal concentration of spodumene rock and which has partially retained its significance to the present day, is not merely a valuable

also rises sharply, but the relative proportion of sodium extracted into the soluble phase lags increasingly behind the amount of lithium extracted from the spodumene.

Thus, sodium is extracted from spodumene simultaneously with lithium, but the extraction of sodium is incomplete and the insoluble phases formed during the sintering retain sodium as an isomorphous admixture.

It should be noted that determinations of SO_4^{2-} ions in all the solutions formed by aqueous extraction of β -spodumene sinters showed that the sulfate content remains almost unchanged at 99.8–99.6% of the amount initially introduced as K_2SO_4 . At the same time, the potassium contents found in the solution were in good agreement with the calculated amounts which should remain after some K_2SO_4 had been used in the formation of Li_2SO_4 and Na_2SO_4 (these are easily calculated if the conversion of lithium and sodium from spodumene into the soluble phase is known).

All this confirms that the sintering reaction between β -spodumene and K_2SO_4 is formally a reaction between alkali-metal ions, especially as the absence of aluminum and SiO_2 in the aqueous extracts of the sinters confirms that aluminosilicate (β -spodumene) does not undergo decomposition in the reaction. In reality, however, sintering of β -spodumene with K_2SO_4 gives rise, on the one hand, to insoluble phases, which can be regarded only from the purely chemical standpoint as products of substitution or base exchange with unchanged contents of aluminum and silicon, and on the other, to soluble salt phases, the nature of which is determined by the system Li_2SO_4 – Na_2SO_4 – K_2SO_4 .

Thus, the indestructibility of the mineral complex is merely a formal concept, since only the alkali elements are "substituted" in it while the aluminosilicate framework persists, but in fact there is a process of interesting transformations which lead to the disappearance of some groupings and structures and appearance of others.

Results of Experiments on the Reaction of α -Spodumene with Potassium Sulfate

It is well known that lithium can be extracted from α -spodumene (spodumene rock, flotation concentrates) by sintering with potassium sulfate at high temperatures. In the present investigation the purpose of the experiments on sintering of α -spodumene with K_2SO_4 over a wide range of temperatures was to

property used to liberate the metal from extraneous inclusions. This transition is an important intramolecular reaction which, by increasing the lattice parameters of the mineral, prepares it for subsequent molecular transformations at high temperatures. It is through the stage of β -spodumene formation that the complex interaction of α -spodumene with K_2SO_4 is effected.

Identification of Insoluble Residues

The insoluble residues formed in the reactions of α - and β -spodumene with K_2SO_4 , obtained in sintering experiments with maximum excess of K_2SO_4 at all the investigated temperatures, were subjected to X-ray phase analysis. The residues from sinters of α -spodumene with K_2SO_4 formed at 700 and 800° consisted of unchanged α -spodumene, and the residues from sinters of β -spodumene with K_2SO_4 , obtained under the same conditions, did not differ in any respect from the original β -spodumene. Residues from sinters of α - and β -spodumene with K_2SO_4 formed at 900° and over were identical to each other and differed from α - and β -spodumene.

If the reaction product of spodumene and K_2SO_4 is really leucite, then its identification does not present any difficulties, as leucite has been studied in numerous investigations of multicomponent systems of mineralogical interest.

For a detailed study of the insoluble residue of the sinter of spodumene with K_2SO_4 , a certain amount of this substance was specially and carefully prepared by sintering of β -spodumene with K_2SO_4 (in 1:1 ratio by weight) at 1100°. During the sintering process, which lasted 3 hours, the sinter was twice removed from the crucible, ground thoroughly in a mortar, and heated again. The purpose of this was to make the reaction as complete as possible. At the end of the reaction the sinter was washed quite free from soluble salts and the residue was dried and calcined at 200°.

Optical analysis showed that the residue consisted of a single phase, with average $n' = 1.508 \pm 0.003$. It was easily decomposed by hydrochloric acid with liberation of silica. The results of silicate analysis were: found for $K[AlSi_2O_6] - K_2O = 21.40\%$, $Al_2O_3 = 23.51\%$, $SiO_2 = 55.17\%$, calculated for $K[AlSi_2O_6] - K_2O = 21.59\%$, $Al_2O_3 = 23.36\%$, $SiO_2 = 55.05\%$. The potassium content was somewhat low, as the residue contained a certain amount of sodium (leucite also always contains sodium [14]). The X-ray pattern of the insoluble residue was found to be identical with the X-ray pattern of a leucite sample from Vesuvius lava. The heating curve of the insoluble residue shows reversible effects in the 619-640° range. These are characteristic of the polymorphous transition discovered by Bowen and Schairer [15] and studied in detail by Wyart [16, 17]. A heating curve of the insoluble residue is given in Fig. 3.

Thus, the reaction product of spodumene and K_2SO_4 is also identical with leucite by the nature of the polymorphous enantiotropic transition.

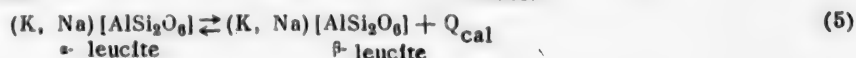
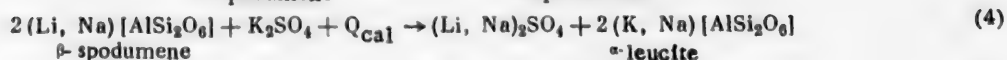
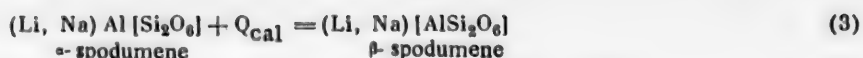
The formation of leucite from β -spodumene in its reaction with K_2SO_4 even at 900° is of exceptional interest as an example of the synthesis of aluminosilicates in solid-phase reactions.

Since the conversion of lithium from spodumene into the soluble phase is determined exclusively by the formation of synthetic leucite, the sharp increase in the conversion of lithium into soluble form at temperatures from 900° becomes understandable. Although it was shown experimentally that a temperature of 900° is high enough for formation of leucite and Li_2SO_4 in the reaction between β -spodumene and K_2SO_4 , in practice a higher temperature is needed for completion of this reaction.

If α -spodumene is used, when the unfavorable stage of preliminary thermal beneficiation of spodumene becomes superfluous, the process temperature should be in the 1050-1100° range. This is because it is necessary to maintain the proper conditions for completion of the $\alpha \rightarrow \beta$ transition as well as the optimum sintering regime.

The sulfate method can be used for extraction of 95-98% of the lithium present in spodumene if the composition of the concentrates which determines the proper charge composition is taken into account, if the heating regime which determines the duration of the sintering stage is correctly chosen, and if the proper temperature conditions are maintained.

In the light of the results of these investigations the mechanism of sintering of spodumene with K_2SO_4 may be represented as a combination of the following reactions:



SUMMARY

1. The reaction between spodumene and potassium sulfate in the 700-1100° range was studied by means of chemical, optical, thermographic, and X-ray phase analysis; it was found that leucite is formed together with lithium and potassium sulfates during sintering of β -spodumene with K_2SO_4 at 900° and over.

2. It was shown by the same methods that leucite is also formed in the reaction of K_2SO_4 and α -spodumene; this emphasizes once again one valuable characteristic of the sulfate process — its universality. However, the mechanism of the process in this case is such that the reaction of α -spodumene with K_2SO_4 proceeds by way of its intermediate conversion into the β -modification, which necessitates an increase of the sintering time and of the heat supply, in view of the conditions for the $\alpha \rightarrow \beta$ transition in spodumene [10].

LITERATURE CITED

- [1] M. N. Sobolev, V. V. Lotov and P. L. Asoskov, *Rare Metals* 3, 47 (1932); 4-5, 41 (1932); 6, 33 (1932).
- [2] J. H. Frydlender, *Rev. produits chim.* 33, 97, 161 (1930).
- [3] E. S. Burkser, R. V. Fel'dman and Z. M. Lisysanskaya, *Rare Metals* 1-2, 52 (1932).
- [4] Z. M. Lisysanskaya and T. V. Ivanova, *Rare Metals* 3, 38 (1933).
- [5] E. S. Burkser, *Rare Metals* 5, 39 (1935).
- [6] E. S. Burkser and A. P. Rutman, *Ukrain. Chem. J.* 9, 446 (1934).
- [7] A. A. Golitsynskii, in the book: *Utilization of Wastes in Heavy Industry* [In Russian] (Moscow, 1936) 3, pp. 307-317.
- [8] G. P. Aleksandrov, *J. Appl. Chem.* 17, 183 (1944).
- [9] B. A. Sakharov, *Chem. Sci. and Ind.* 1, 529 (1956).
- [10] G. G. Urazov, V. E. Plyushchev and L. V. Shakhno, *Proc. Acad. Sci. USSR* 113, 361 (1957).*
- [11] V. E. Plyushchev and L. V. Shakhno, *J. Anal. Chem.* 8, 293 (1953).*
- [12] S. Z. Makarov and V. V. Bukina, *J. Gen. Chem.* 3, 881 (1933).
- [13] F. Feigl, *Spot Tests* (ONTI, Moscow, 1937) [Russian translation].
- [14] P. N. Chirvinskii, *Mem. All-Russian Mineral. Soc.* 66, 124 (1937).
- [15] N. L. Bowen and J. F. Schairer, *Am. J. Sci.* 18, 301 (1929).
- [16] J. Wyart, *Compt. rend.* 203, 938 (1936).
- [17] J. Wyart, *Compt. rend.* 205, 1077 (1937).

Received February 25, 1958

*Original Russian pagination. See C.B. Translation.

THE ROLE OF FILTRATION OF SELENIOUS SULFITE (SELENOSULFATE) SOLUTIONS IN THE PRODUCTION OF PURE SELENIUM

O. V. Al'tshuler, E. A. Subbotina and F. F. Kharakhorin
(A. A. Balkov Institute of Metallurgy, Academy of Sciences USSR)

At the present time the only industrial method used in the USSR for production of selenium for use in semiconductor equipment is the so-called sulfite cyclic process [1]. This process is essentially as follows: technical selenium obtained from anode mud of copper refineries or from lead-chamber mud of the sulfuric acid industry, heavily contaminated with metallic impurities (arsenic, tellurium, and sulfur), is dissolved at about 100° in a solution containing 240 g Na₂SO₃ per liter. The selenium concentration is 90 g/liter. The compound Na₂SSeO₃ [2] is formed in the process. The hot solution is filtered and cooled. On cooling, part of the selenium crystallizes out. The yield at 20° is about 40 g of Se per liter of solution. The selenium is washed, dried, and distilled under vacuum. The mother liquor is used to dissolve another portion of selenium.

As the result of filtration of the selenosulfate solution, crystallization, and distillation, the selenium is freed from most of the impurities, the total content of which falls from 2-2.5% to a few thousandths of one per cent. However, in the industrial production of "pure" (standard) selenium there are considerable variations in the quality of the final product, and batches which do not conform to GOST specifications are sometimes supplied. This is all the more inadmissible in view of the increasingly high standards of purity demanded by the users of selenium.

Our aim was to determine the limiting potentialities of the sulfite process, effected under "pure" laboratory conditions, and to define the role of its individual stages in the purification of selenium. The first stage of the process, filtration of the sulfite solutions of selenium (selenosulfate solutions), is considered in the present investigation.

The impurities were determined spectroscopically and their concentrations were denoted on the following scale: 5, 4, 3, 2, 1, weak lines, traces, faint traces. A rating of 5 corresponds to whole percentages or tenths of 1% and "faint traces" (for most impurities) to decimals of one per cent. The radioactive tracer method was also used. Experiments on the role of filtration in removal of impurities from selenium solutions were performed with samples of technical selenium of various origins, and samples of standard "rectifier" selenium produced by our industry. Thus, the initial impurity contents varied over a wide range. The sodium sulfate used for the experiments contained the following impurities, as shown by spectrum analysis: Mg-2, Al-2, Ca-1, Ti-1, Fe-1, Cu-1. The sulfite solutions were carefully filtered before the selenium was added. Redistilled water was used in all the experiments.

Table 1 contains the results of spectrum analysis of standard selenium and of samples of this selenium recrystallized from sulfite solutions after filtration under different conditions.

The data in Table 1 indicate that without filtration the lines of only two elements, Zn and Pb, were lost as the result of recrystallization, and as far as can be judged from the spectroscopic data the contents of the other impurities remained unchanged after crystallization. Thus, the increased purity of standard selenium after purification by the sulfite method is due mainly to filtration of the selenium solutions.

TABLE 1

Results of Spectrum Analysis of Selenium

Experimental conditions	Impurities											
	Si	Al	Bi	Cd	Tl	Cr	Fe	Cu	Sn	Ca	Zn	Pb
Standard selenium (original)	2	2	Weak lines	Weak lines	Traces	1	2	1	Weak lines	2	Traces	Traces
Crystallization without previous filtration	2	2	Weak lines	Weak lines	—	1	2	Traces	Weak lines	2	—	—
Filtration through one paper filter	Weak lines	Weak lines	—	—	Weak lines	—	Weak lines	Traces	—	2	—	—
Filtration through three paper filters	Traces	Traces	—	—	Traces	—	Traces	Traces	—	Weak lines	—	—

TABLE 2

Results of Spectrum Analysis of Heavily Contaminated Selenium

Selenium	Impurities											
	Ca	Ag	Cr	Cu	Tl	Zn	Si	Mg	Mn	Pb	Fe	Ni
Technical (original)	3	1	—	2	Traces	—	2	2	1	Traces	2	Traces
Recrystallized without filtration	3	1	—	2	Traces	—	2	Traces	1	Traces	2	Traces
Recrystallized and filtered through 30 filters	Weak lines	—	—	—	—	—	Traces	Traces	—	—	Traces	—

Faint traces

2

2

2

2

2

2

2

2

2

2

2

2

2

2

2

The decisive role of filtration in removal of the main bulk of impurities is revealed even more clearly by the results of experiments with heavily contaminated technical selenium. The results of one such experiment are given in Table 2.

To investigate the behavior of individual impurities during filtration, not only the original and final selenium samples but also the deposits on the filters were analyzed. With a large number of consecutive filters the amounts of deposits on the last filters were too small to separate from the paper. In such cases the deposits were analyzed together with the filters. The impurity contents of the filters themselves were estimated at the same time. The results, which refer to solutions of "pure" (standard) selenium, are given in Tables 3 and 4.

The accumulation of impurities on the first filters shows that even when their concentrations in selenium conform to GOST specifications the filtration process is still very effective.

The results of an analogous experiment on a solution of technical selenium are given in Table 5.

Certain conclusions may be drawn about the behavior of different impurities in filtration from the above spectroscopic data for selenium samples and deposits on the filters. Such elements as Cd, Pb, Zn, Ni, As, Ag, Hg, Cr, Te are concentrated on the first filters and are not detected either in the filtrate or in the selenium precipitated from it.

Removal of Sn, Mn, Al, Cu, Fe, Ti from solutions requires a large number of filters, and even then a certain proportion remains in the filtrate and is usually carried down by the selenium during crystallization. It is difficult to judge the behavior of Mg and Ca from analyses of the deposits, as these elements are present in considerable amounts in the filter material itself, but their constant presence in recrystallized selenium indicates that filtration is ineffective with regard to them.

Although these experiments give a fairly clear idea of the role of filtration in the removal of impurities from selenium, it was desirable to supplement it by some quantitative data. For this purpose experiments were carried out with radioactive isotopes— ^{59}Fe , ^{113}Sn , ^{127}Te .

Radioactive tellurium or tin was introduced in the elemental form into melted selenium, and the melt was kept at 400–420° with thorough stirring.

According to the phase diagrams for the Te–Se and Sn–Se systems, tellurium remains in the free state in melts with selenium, but tin forms a selenide under the same conditions. Radioactive iron was dissolved in the minimum amount of hydrochloric acid, the solution was diluted with water, and neutralized with ammonia against methyl red. Fine selenium powder was added to this solution, and a stream of hydrogen sulfide was passed through the suspension. The mixture of selenium and colloidal FeS was dried, and the selenium was remelted with stirring. A similar method was used [3] for introduction of radioactive copper into selenium. The iron could have remained in the selenium as the sulfide, or it could give rise to the corresponding selenide by exchange of sulfur for selenium [4]. To test that the radioactive additives were uniformly distributed, portions of the melts were poured into glass rings placed on a smooth porcelain tile. When cool, the rings with the selenium were placed under the window of an end-type counter so that the lower planes of the casts faced the latter. The γ -activity of selenium samples containing radioactive iron or tin isotopes was measured similarly.

Selenium containing the radioactive additives was dissolved in sodium sulfite solution and the solutions were filtered through a specially designed miniature vacuum filter containing a large number of filter papers about 2 cm in diameter. At the end of the filtration the activity retained on each of the consecutive filter papers was measured.

Figure 1 shows the distribution of tellurium among the filters as a function of the grade of filter paper. Consecutive filter grade numbers are taken along the abscissa axis, and the corresponding activities as percentages of the total activity retained by all the filters are taken along the ordinate axis.

The course of these curves shows that whereas the first layer of ordinary filter paper retains 90% of the tellurium, a closer filter lets through only 2–2.5%, and after the 4th or 5th filter no activity can be detected on the filters. However, this difference in the course of the curves was observed only for freshly prepared selenium solutions. After the solution had stood for several days the first layer of filter paper retained 99% of the total amount of tellurium and from the 4th filter onward the activity coincided with the background (Fig. 2).

TABLE 3

Results of Spectrum Analysis of "Pure" Selenium

Sample	Impurities										
	Al	Fe	Cu	Si	Mg	Mn	Pb	Sn	Zn	Cd	Ti
Original selenium	2	2	Weak lines	2	1	Weak lines	Traces	1	—	1	1
Recrystallized selenium	1	1	Traces	1+	1	—	—	—	—	—	Weak lines
Deposit from 1st filter	2	3	3	3	2	2	2	3	Weak lines	1	2
Deposit from 2nd filter	2	2	Weak lines	2	Traces	1	Traces	1	—	—	1
Deposit from 3rd filter	1	1	Traces	1	—	—	—	—	—	—	Weak lines

TABLE 4

Results of Spectrum Analysis of Deposits on Filters for "Pure" Selenium

Experi- mental conditions	Element												
	Cr	Ag	Ca	Cu	Ti	Hg	Al	Ni	Si	Pb	Mg	Mn	Fe
Filter No. 1	3	Traces	4	1	2	2	2+	1	2	Traces	1	1	3
2	2	—	4	Weak lines	1	2	2+	—	1	—	Weak lines	—	2
3	1	—	4	—	1	—	2	—	Weak lines	—	—	—	1
4	—	—	4	—	1	—	1	—	—	—	—	—	Weak lines
5	—	—	4	—	1	—	1	—	—	—	—	—	
6	—	—	4	—	1	—	1	—	—	—	—	—	
7	—	—	4	Traces	1	—	1	—	Traces	—	Traces	—	Weak lines
8	—	—	4	—	1	—	1	—	—	—	—	—	
9	—	—	4	—	1	—	1	—	—	—	—	—	
10	—	—	4	—	1	—	1	—	—	—	—	—	Traces
Without deposit	—	—	4	Traces	—	—	Weak lines	—	Traces	—	Traces	—	
Original selenium	Traces	Weak lines	3	Traces	Weak lines	—	2	Weak lines	2	Traces	1	1	2

Results of Spectrum Analysis of Deposits on Filters for Technical Selenium

Original
filter with
out de-
posit



Fig. 1. Distribution of tellurium among filters as a function of the filter-paper grade; solution of Se + Te^{127} . A) Activity on filters (%); B) filter grade numbers; filter-paper type: 1) ordinary; 2) white band; 3) blue band.

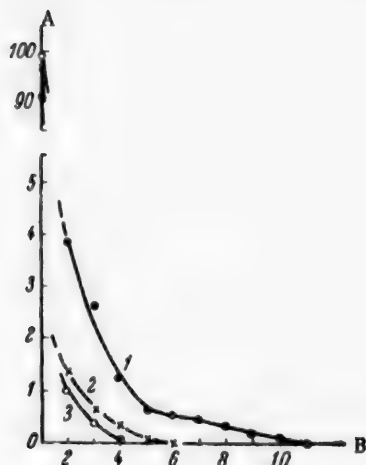


Fig. 2. Effectiveness of tellurium separation as a function of the "age" of Se + Te^{127} solution: A) activity on filters (%); B) filter grade numbers; solutions: 1) freshly prepared; 2) after 24 hours; 3) after 3 days.

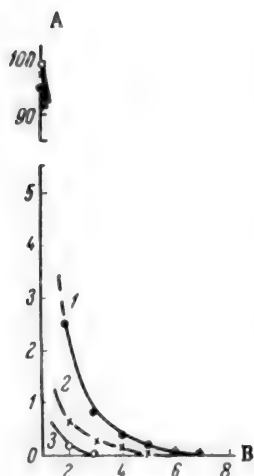


Fig. 3. Effectiveness of tin separation as a function of the "age" of Se + Sn^{114} solution: A) activity on filters (%); B) filter grade numbers; solutions: 1) freshly prepared; 2) after 24 hours; 3) after 3 days.

The concentration of tellurium in the selenium was about 0.1%. Tellurium was not detected in the filtrate at all, so that filtration alone, without the subsequent purification stages (crystallization, distillation), is adequate for complete removal of this impurity from selenium.

The concentration of tin in the selenium was 0.1-1.0%. As in the case of tellurium, the effectiveness of tin removal by filtration increased with the age of the solution; this is shown by the course of the curves in Fig. 3 and by measurements of filtrate activity.

Filtration of a freshly prepared solution lowered its activity 7-fold, filtration of a solution which had stood for 24 hours - 10-fold, and of a solution which had stood for 7 days - 28-fold (the grade and number of filters were the same in each case).

These results suggest that tellurium and tin (not enough data are available on the other impurities) are probably present in a semicolloidal state in selenosulfate solutions. In course of time these impurity particles coagulate and increase in size.

In contrast to tellurium, tin is not extracted completely from solution even when the solution is passed through a large number of the closest filters. This also applies to iron. If the iron content of selenium is 0.1%, a small proportion remains in the filtrate. However, as in the case of tin, the filtration stage is very important - when selenium is crystallized from unfiltered sulfite solution, up to 80% of the activity is concentrated in the forming selenium crystals.

All the foregoing results indicate that in work relating to the production of selenium of high purity a search for more efficient filter materials may be very important if not decisive.

SUMMARY

1. The role of filtration of selenosulfate solutions in removal of metallic impurities and tellurium from selenium was studied.

2. Filtration is of primary importance not only for removal of the main mass of impurities present in technical selenium but also for high purification of standard selenium for rectifiers.

3. Spectrum analysis and radioactive tracer techniques were used to determine the effectiveness of filtration with respect to individual impurities, and its dependence on the type of filter material and the "age" of the selenium solutions. In this connection, a hypothesis is put forward concerning the form in which tellurium and tin impurities are present in the solution.

LITERATURE CITED

[1] S. M. Golyand, *J. Chem. Ind.* 2, 13 (1947); S. M. Golyand and E. I. Tkacheva, Author's certif. No. 64707.

[2] G. W. Mellors, *Comprehensive Treatise on Inorganic and Theoretical Chemistry*, 10, 765 (1952).

[3] L. M. Nijland, *Philips Research Rep.*, 9, 259 (1954).

[4] D. M. Chizhikov, O. V. Al'tshuler and G. N. Zviadadze, *Proceedings of the All-Union Conference on the Use of Radioactive and Stable Isotopes in Science and the National Economy [In Russian]* (1957).

Received April 12, 1958

THERMAL PRODUCTION OF ALKALI METALS FROM THEIR CHLORIDES AND HEAT-TRANSFER CHARACTERISTICS OF BRIQUETTED CHARGES

N. M. Zuev

The alkali metals, and in particular sodium and potassium, are made from their chlorides by the thermal process under vacuum, usually at 800-900°. Under these conditions the chloride is partially reduced to the metal and partially volatilized. Under laboratory conditions the relative amounts of the volatilized and reduced salt depend on the charge temperature or the reaction temperature.

The charge temperature is taken to be the wall temperature of the retort in which the charge is heated. The temperature inside the charge is not measured, and it is assumed that there is no great difference of temperature between the retort walls and the charge. This assumption is generally based on the results obtained in experimental determinations of the thermal conductivity of the charge used in sodium production [1]. Unfortunately, these conductivity determinations were carried out at temperatures below 675° and not under vacuum but at atmospheric pressure, i.e., under conditions which differed considerably from those used in thermal production of alkali metals.

A different view on thermal conductivity was advanced in a paper [2] concerned with a laboratory investigation of potassium production. In this paper it was stated that in the vacuum thermal process the temperature variations in the charge depend on the vacuum maintained and on the presence of salt in the charge.

Investigation of the actual character of heat transfer in the charge is of great importance for theoretical and practical development of the thermal process of alkali-metal production. The purpose of the present paper is to augment the available information on this subject. It is not claimed to be an elucidation of special heat-transfer problems in finely-divided media exemplified by the charges used in the thermal production of alkali metals.

In laboratory investigations the charge, in the form of a small cylindrical briquet, was heated in a massive metallic crucible the internal diameter of which was close to the briquet diameter, so that the charge was heated from all sides. Under these conditions the temperature rises uniformly throughout the briquet volume and becomes equalized over the different regions of the briquet when it is held at constant temperature. However, this continues only up to a certain limit, after which increase of temperature at the crucible walls is no longer accompanied by rise of temperature in the center of the briquet.

Experimental tests show that when the temperature conditions within the briquet are steady, the main physicochemical conversions take place in the surface layers, where active volatilization of the salt and interactions between the charge components take place. A large proportion of the incoming heat is consumed in these conversions. Only a small part of the thermal energy penetrates into the central zone of the briquet to compensate for the loss of heat absorbed in certain endothermal reactions.

The salt is initially volatilized from the briquet surface, and the temperature of its inner zone is determined by the vapor pressure of the salt and the vacuum maintained in the retort.

As the outer layers of the briquet become poorer in salt, their temperature gradually rises, and the zone of active volatilization of the salt shifts into the depth of the briquet. The temperature of the central zone of the

Chloride	p (mm Hg)										T_{in}
	1	5	10	20	40	60	100	200	400	760	
NaCl . . .	865	967	1017	1072	1131	1169	1220	1296	1379	1465	800
KCl	821	915	968	1020	1078	1115	1164	1239	1322	1407	790

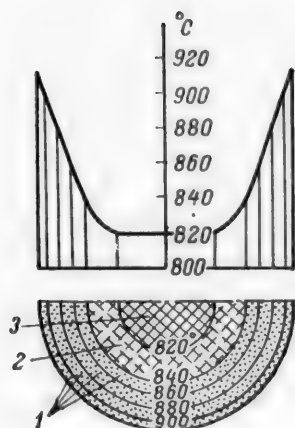


Fig. 1. Temperature variations in a briquet: a) zone poor in salt; 2) intermediate zone; 3) salt-rich zone.

briquet remains constant. The temperature field of the briquet as a whole does not become steady even if a constant temperature is maintained at the crucible walls; the temperature at any point in the briquet is a function of its coordinates, time, and degree of vacuum

$$t = f(x, y, z, \tau, p).$$

Only after all the salt has volatilized does the temperature rise in the center of the briquet, and after a sufficiently long exposure the temperature field becomes steady.

The dependence of the temperature at different points in the briquet on the degree of vacuum is one of the special characteristics of the vacuum thermal process for production of the alkali metals from their chlorides. The existence of this dependence, and the definite laws to which it conforms, have not only been established experimentally, but may be derived by analysis of the physicochemical properties of chlorides.

The vapor pressures of sodium and potassium chlorides vary with the temperature as follows [3].

Since a constant rarefaction is maintained in the working space, as the temperature rises an instant is reached when the vapor pressure of the salt becomes equal to the pressure in the retort. Removal of vapor from the zone of its formation leads to rapid volatilization of the salt, and therefore the temperature does not rise in the zone containing the melted salt.

The volume of the briquet during the thermal process can be divided into three zones in relation to the temperature regime: a) an external zone, poor in chloride, with gradually rising temperature; b) a central zone at constant temperature, with a high chloride content; c) an intermediate zone in which the salt is actively volatilized and which gradually shifts from the surface to the center of the briquet.

This zone distribution and the temperature variations in the zones are shown schematically in Fig. 1.

The distinct differences of salt concentration in the different zones of incompletely-reduced briquets are maintained when the briquets are cooled. In such a briquet the central zone generally forms a dense, distinct core with a high chloride content.

To increase the reduction efficiency of the chloride the temperature of the outer zone of the briquet should be maintained at a higher level. Under these conditions the chloride vapor is reduced more completely to the metal in passing through the heated zone of the charge.

The reduction efficiency can also be raised by an increase of the briquet dimensions, as it is easier to maintain a high temperature in the outer layers of the charge in large briquets. However, access of heat to the central part of the briquet becomes more difficult with increase of briquet size, and the duration of the thermal process increases. This is obvious from the equation for heat transfer by conduction:

$$Q = \frac{\lambda}{\delta} F_s \Delta t \text{ kcal/hour}$$

where λ is the coefficient of thermal conductivity of the outer zone of the briquet, δ is the distance from the briquet surface to the constant-temperature zone, F_x is the calculated surface area of the briquet, and Δt is the temperature difference.

In this equation the temperature difference and the coefficient of thermal conductivity are independent of the briquet size. The values of δ and F_x depend on the external dimensions of the briquet and the volume of the central zone.

Since the quantity of heat entering the central zone is proportional to the ratio of the calculated surface area to the distance from the briquet surface to the constant-temperature zone, F_x/δ , it is evident that the rate of heat flow to the central zone must decrease with increase of the external zone. In this case the time required for reduction of unit amount of charge is considerably greater in the central zone than at the briquet surface.

The variations of the temperature field within a briquet, determined under laboratory conditions, are characteristic in many respects for the vacuum thermal process on the industrial and semiworks scales. In such cases the depth of the heated layer of charge generally extends to some tens of centimeters, while the layer itself consists of individual briquets in different positions relative to the heat-transfer surfaces. Under such conditions heat transfer from the heated walls to the briquets, especially those at a distance from the heating surfaces, is hindered considerably.

At low temperatures at the retort walls, when most of the heat is transferred to the charge by conduction and convection, the heating efficiency is especially low, as under low-pressure conditions there are no convection currents of gas, while heat transfer by conduction is very restricted because of the small areas of contact between the briquets and the walls, and between the briquets themselves.

It is only at temperatures above 700°, when heat transfer by radiation becomes significant, that the charge is heated more effectively. However, because heat is supplied unilaterally to the briquets and the working space is considerable, the temperature is equalized only slowly in the charge. The briquets which are at the retort walls are heated relatively rapidly to the temperature at which intensive volatilization of chloride begins. The succeeding layers of briquets are under less favorable conditions, as heat transfer to them by radiation is impeded, while conduction and convection play an unimportant part. In consequence, there are considerable temperature variations over different regions of the charge.

In this case, as under laboratory conditions, three temperature zones may be distinguished with respect to temperature distribution and reaction characteristics. However, each zone contains a large number of individual briquets, and the isothermal surfaces are not enclosed within individual briquets but cut across them.

The first zone, adjacent to the heating surface, becomes distinct when the thermal process has developed sufficiently, with volatilization of a considerable proportion of the chloride, while the external surface is at a relatively high temperature. This zone is characterized by a gradual increase of temperature and a shift of its boundary from the retort walls into the charge. Thermal energy enters this zone mainly by radiation and to some extent by conduction.

The central zone consists of briquets at some distance from the heating surfaces. It is characterized by constant temperature, low extent of physicochemical conversions, and a high chloride content. Heat transfer to this zone is effected to a considerable extent by convection of the vapors formed in the intermediate zone. Equalization of temperature within the briquets depends on the thermal conductivity of the charge.

The above is a general outline of the temperature characteristics of the thermal processes taking place in the reduction of alkali metals from their chlorides in industrial units. Some of its features must now be considered more closely.

When alkali metals are reduced under laboratory conditions, the temperature of the external surface of the briquet is close to that of the crucible wall. The chloride vapors formed at lower temperatures within the briquet are heated on passing through the external layers, their activity increases, and they react more completely with the other charge components.

The situation is different if the thermal process is effected in an industrial unit. In this case each briquet is heated unilaterally and nonuniformly. Briquets at some distance from the retort walls are under especially unfavorable conditions. Heat transfer to them is hindered by the thermal resistance of the intermediate layer of briquets.

As a result, evacuation of the salt vapor from the charge under industrial conditions differs considerably

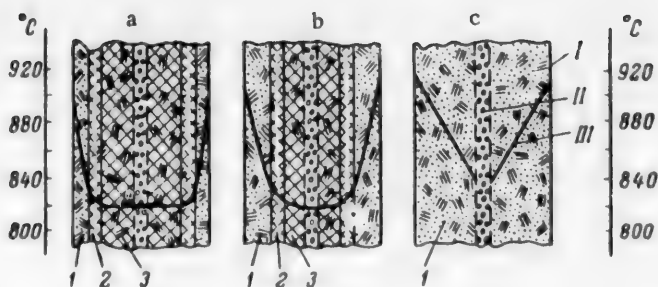


Fig. 2. Temperature variations in a briquetted charge in thermal reduction of alkali metals from their chlorides; a) initial stage of the process; b) volatilization zone shifted into the depth of the charge; c) reduction of metal and volatilization of salt terminated; I) conducting wall of retort; II) central exhaust pipe; III) nature of temperature variations; 1) zone of variable temperatures; 2) zone of chloride volatilization; 3) constant-temperature zone.

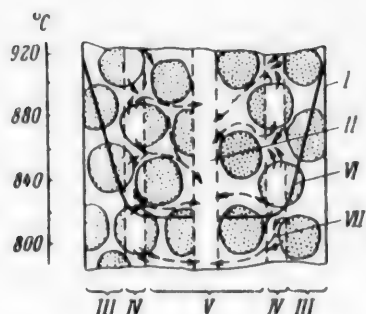


Fig. 3. Evacuation of vapor from briquets; I) conducting wall of retort; II) central exhaust pipe; III) zone poor in salt; IV) volatilization zone; V) constant temperature zone; VI) nature of temperature variations; VII) direction of vapor.

in character from removal of vapor from briquets under laboratory conditions. It is influenced by the multilayer arrangement of the briquets and the great depth of the charge layer. The small temperature difference in each briquet is not sufficient for a substantial increase in the temperature of the chloride vapor as it moves through the briquet pores, and as a result the vapor on leaving the briquet is at a low temperature, differing little from the temperature in the volatilization zone. At such temperatures the activity of the charge is very low, and interaction between chloride vapor and the other charge components is weak.

Further movement of the salt vapor occurs mainly through the voids between the briquets, and depends on the direction of evacuation of the gas. Most of the vapor rapidly leaves the reaction zone. Only a small proportion of the vapor diffuses to the heated briquets which are at the retort walls and are at a high temperature.

Movement of the vapor toward the cold briquets is favored by temperature factors and design characteristics of vacuum thermal plant, where pipes with perforated walls are inserted into the charges for better evacuation of the salt vapor. As a result, the salt vapor is

drawn into the coldest zone immediately on leaving the briquets, and does not come into contact with the charge. Temperature variations in a layer of briquets at different stages on the thermal process are shown schematically in Fig. 2. Figure 3 is a schematic representation of the evacuation of vapor from the briquets if the charge contains a pipe for directed withdrawal of gases through the central zone.

The concept of reaction temperature or reduction temperature must be considered in the light of these characteristics of the thermal process.

In the reduction of alkali chlorides in laboratory apparatus, the crucible-surface temperature may be assumed equal to the surface temperature of the briquet. These temperatures differ significantly only during the initial reduction stages, when the briquet surface is still rich in chloride. As the intermediate zone (volatilization zone) moves inward, the difference between the vapor and crucible-wall temperatures diminishes. Under these conditions most of the salt vapor, after passing through the outer zone of the briquet, leaves the charge at a temperature very close to the temperature of the crucible surface. Therefore under laboratory conditions, when a single briquet is reduced, it is quite justifiable to take the crucible-wall temperature as the reaction temperature.

The situation is different in industrial units. There is a much greater difference between the temperature

of the retort surface and the temperature of the vapor leaving the briquets (the zone of component interaction). The magnitude of this difference depends on the distance of the briquets from the heating walls of the retort, the briquet size, mutual disposition of the briquets, and contact between them. In such cases it would be wrong to assume that the retort-wall temperature is the same as the actual reaction temperature (as has been done in some investigations), because the difference may reach some tens of degrees.

SUMMARY

1. There is a considerable difference between the temperature of the retort walls and the temperature of the zones in which the main interaction of the chloride and its vapor with the other charge components takes place.

2. If the temperature drop in each individual briquet is small, most of the vapor leaves the briquet at a temperature close to the temperature at which it forms.

3. Increase of temperature at the retort walls in practice merely leads to more rapid volatilization of the salt, and is not accompanied by any significant increase of the temperature of the components at the instant of their interaction.

4. With existing methods for charging the briquets the extraction of metal cannot be substantially increased by increase of temperature at the retort walls.

It should be noted, however, that the efficiency of thermal reduction of alkali-metal chlorides under industrial conditions can be raised to the level obtained in laboratory experiments if the thermal process is so conducted that the chloride vapor leaves the briquets at a higher temperature. This may be achieved by increase of the briquet size, use of coated briquets, and in other ways.

LITERATURE CITED

- [1] V. M. Gus'kov and A. I. Voinitskiĭ, *Trans. All-Union Aluminum and Magnesium Inst.* 37 (1955).
- [2] V. M. Gus'kov, N. M. Zuev and A. I. Voinitskiĭ, *Trans. All-Union Aluminum and Magnesium Inst.* 40 (1957).
- [3] D. R. Stull, *Tables of Vapor Pressures of Individual Substances* (Moscow, 1949) [Russian translation].

Received March 5, 1958

EFFECT OF THE COMPOSITION OF GLASS ON DIFFUSION OF COPPER IONS INTO IT

E. A. Ivanova and V. V. Vargin

In surface coloration of glass by the so-called "cementation" process, copper or silver is introduced into the surface layer from compounds in contact with the glass. On heating, ions of these metals [1-4] diffuse from the compounds into the glass to a depth which varies from a few microns (for copper) to tenths of a millimeter (for silver). In the glass the ions are reduced to the metal. Copper colors the glass red (copper ruby), while silver gives a yellow color. The color of the layer is caused by scattering of light by colloidal particles of these metals.

In the development of an industrial method for the production of copper ruby glass in the surface layers, a more detailed study of the process became necessary. The process in which copper ruby is formed in the surface layer of the glass as the result of three consecutive heat treatments was investigated. This process is carried out as follows. The glass is coated with a thin layer of a paste containing a copper compound and a substance which ensures close contact between the glass and the copper compound, and the glass is then heated in air. During the heating the copper ions diffuse into the glass and color it yellow, green, or blue [5-7]. The paste is then removed and the glass is heated in a reducing medium. The color of the glass then changes from yellow to black. The glass is then heated again in air, and its color changes to red.

The information (almost entirely qualitative) available on this process in the literature was not adequate for development of a reproducible technological process for production of a red ruby color in glass surface layers. Our preliminary experiments showed that the glass composition has the greatest influence on the color. A certain amount of information was available on this subject in the literature, but it was contradictory. Thus, while some authors reported that potassium oxide has a favorable influence and recommended the use of potash glasses only [8-10], others stated that soda glasses are preferable [11], and yet others stated that soda-potash glasses should be used [12]. Different effects of calcium oxide, barium oxide, zinc oxide, etc on the color of glass were also reported.

Our results indicated that the quality of the final color is determined to a considerable extent by the first stage of the process, when copper ions diffuse into the glass and the surface layer acquires a yellow, green, or light blue color. It was also found that with appropriate glass compositions it is possible to obtain the yellow coloration equal in intensity to that produced by colloidal silver [12]. This stage of the process was therefore investigated.

METHOD

The diffusion of copper into glass was studied in specimens consisting of plates 1 mm thick and 10 to 50 cm² in area. These plates were coated with a moist paste containing 70% copper sulfate and 30% refractory clay. The dry paste was first ground in a mortar and passed through a sieve with 1600 holes/cm². The coated specimens were dried in a thermostat at 60°, and then heated in a muffle furnace for 20-240 minutes in the 520-600° range. The heating temperature was kept constant within $\pm 5^\circ$. The specimens were introduced into the furnace at the required heating temperature; after the heat treatment they were cooled in air at room temperature and the paste was washed off with water.

As the result of diffusion of copper ions into the glass the specimens increased in weight and the surface

TABLE 1

Composition of Group I Glasses

Glass No.	Composition (molar %)				Softening temperature (deg)	Wt. increase in 30 min at the softening temperature (mg/dm ²)
	SiO ₂	CaO	Na ₂ O	K ₂ O		
1	73.5	9.1	17.4	—	550	66
2	73.5	9.1	8.7	8.7	555	39
3	73.5	9.1	—	17.4	565	5

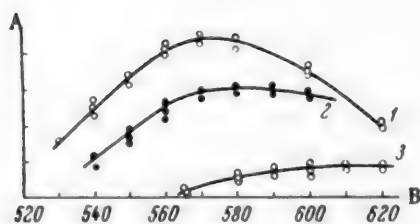


Fig. 1. Effect of heating temperature on weight increase of Group I glasses: A) weight increase in 30 minutes (mg/dm²); B) temperature (deg); the curve numbers correspond to the glass numbers in all the graphs.

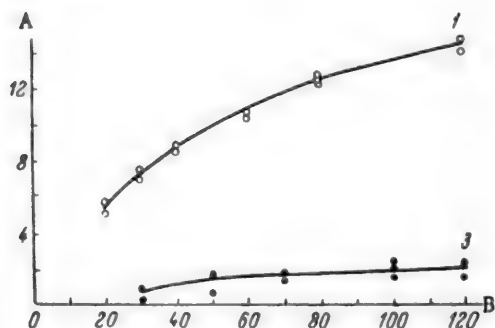


Fig. 3. Effect of heating time on the thickness of the colored layer: A) thickness (μ); B) heating time (minutes).

height of the projection formed as the result of this treatment was measured by means of the MIS-1 microscope to within $\pm 0.5 \mu$.

EXPERIMENTAL

18 glass compositions, divided into 4 groups, were investigated. Group I contained glasses the compositions of which are given in Table 1.

Figure 1 represents the variation of the weight increase with the heating temperature for Group I glasses. At first the weight increase is almost proportional to the temperature rise, then it reaches a maximum and subsequently diminishes. The maximum lies at a temperature 15-40° above the softening point of the glass. At

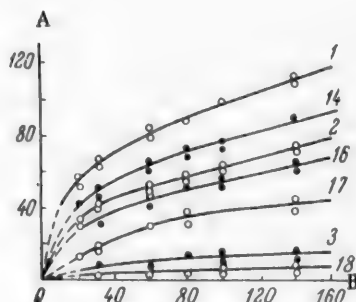


Fig. 2. Effect of heating time on weight increase of Group I and IV glasses: A) weight increase (mg/dm²); B) heating time (minutes).

layer became colored yellow or green. The thickness and color of the layer and the weight increase of the specimen depended on the composition of the glass, the temperature, and the heating time. The absolute weight increases ranged from 3 to 40 mg.

The softening temperature of the glass was taken to be the temperature at which the glass specimen ceased to increase in length in measurements of the expansion coefficient by means of the dilatometer. This temperature was measured to an accuracy of $\pm 5^\circ$.

The thickness of the colored layers on the glass was measured as follows. Part of the specimen surface was coated with paraffin wax, and the specimen was immersed in 4% hydrofluoric acid to remove the colored layer from the unprotected part of the specimen. The

TABLE 2

Chemical Analyses of Glasses

Weight increase (mg)	Copper found by analysis (mg)	α
Soda glass		
7.0	11.0	1.0
7.6	11.0	0.86
12.0	18.0	0.91
12.0	17.2	0.83
33.6	49.4	0.89
Mean		0.9
Potash glass		
2.0	5.0	0.96
2.2	7.8	1.15
2.2	8.4	1.19
2.8	6.0	0.86
5.0	17.0	1.10
6.0	22.2	1.18
12.8	44.4	1.15
Mean		1.07

temperatures above this maximum the paste became fused to the glass surface and the specimens were distorted. Therefore no further determinations were performed in this temperature region.

It is also clear from Fig. 1 that the weight increases at all temperatures are considerably greater for soda than for potash glass. The weight increases of Group I glasses at their softening temperatures were found from these curves; the values are given in Table 1. These results show that the weight increase is greatest for soda glass, the increase for potash glass is about 1/13 of this, while soda-potash glass occupies an intermediate position [14, 15].

The influence of the time of heating at the corresponding softening temperatures on the weight increases of the different glasses is illustrated by the curves in Fig. 3. These curves are parabolic in form; this is consistent with earlier data [16] on the diffusion of silver into glass. It follows from Fig. 3 that the thickness of the colored layer increases with the heating time, tending to a certain limiting value. During 2 hours of heating the thickness of the layer reaches 14 μ on soda glass, and 2 μ on potash glass. In these experiments the glasses were heated at the softening temperatures. Thus both the weight increase and the thickness of the layer are several times larger for soda glass than for potash glass if the specimens are heated under the conditions described.

As the result of diffusion of copper ions into the glass it acquires a color which may be yellow, green, or blue according to the glass composition, temperature, and heating time. Thus, a layer of intense yellow color is formed on soda-potash glass (No. 1) heated for 30 minutes at a temperature close to its softening point. On further increase of the heating temperature the color changes to green, and above 650° to light blue. Increase of the heating time acts in the same direction as increase of temperature, but to a smaller extent. Under the same conditions only a weak yellow color is formed on potash glass.

The spectral curves for layers colored by copper ions are similar to the curves given by Vargin [17] for glasses colored yellow, green, or light blue in the mass by copper oxide.

In the colored layers on soda glass, in contrast to potash glass, light scattering (opacity) readily arises, caused probably by large particles of metallic copper [18]. As sodium oxide is replaced progressively by potassium oxide, the glass properties gradually approach those of potash glasses. The glasses with equal contents of these alkali oxides acquire a fairly intense yellow color, do not show any appreciable light scattering in the layer, and their color remains stable with variations of the heating temperature.

TABLE 3

Results of Chemical Analyses of Pastes*

Heating temperature (deg)	Amount of sodium in paste (mg)			Amount of copper in specimen, by analysis (mg)	α
	after heating	before heating	transferred from glass into paste		
550	7.7	3.2	4.2	13.0	0.89
550	9.4	4.0	5.4	14.2	1.05
570	9.8	3.9	5.9	15.3	1.06
570	10.4	3.1	6.4	15.6	1.11
590	12.1	3.9	8.2	17.1	1.3
590	9.9	3.7	6.2	17.3	0.98
				Mean	1.06

*The method used for chemical analysis of the glasses for determination of the sodium contents of the pastes was developed by K. K. Kolobova and V. A. Gerasimova [22].

In order to find what determines the magnitude of the weight increase, several glass specimens were analyzed chemically for copper, and the pastes were analyzed for sodium. In these experiments the weight increases and the amounts of copper entering the glass from the paste were determined for specimens heated for 30 minutes at the softening temperature [19].

The results of these determinations for soda and potash glasses are given in Table 2.

It is clear from Table 2 that the weight increases for both glasses are less than the corresponding amounts of copper entering the glass. Similar results were obtained by other workers, who studied the diffusion of silver into glass, and who offered the explanation that, for every silver ion entering the glass, one sodium ion leaves it [20, 21]. On the assumption that in our case the difference is also caused by ion exchange, it is possible to calculate the number of alkali-metal atoms lost from the glass for each copper atom entering the glass, from the formula

$$\alpha = \frac{M_{\text{Cu}}}{M_{\text{X}}} \frac{P - Q}{P}, \quad (1)$$

where M_{Cu} is the atomic weight of copper, M_{X} is the atomic weight of the alkali metal, P is the amount of copper in the specimen as found by analysis, Q is the weight increase of the specimen, and α is the number of atoms of alkali metal per atom of copper.

The values found for α are given in the third column of Table 2, from which it is clear that α is close to unity for both soda and potash glass. From these results it can be concluded that an exchange reaction in the 1:1 ratio takes place between the copper ions in the paste and the sodium ions in the glass. With the aid of Eq. (2), in which α is taken to be 1, it is possible to find the coefficient K , which can be used for determining the amount of copper entering the specimen from the weight increase by the equation

$$P = \frac{M_{\text{Cu}}}{M_{\text{Cu}} - M_{\text{X}}} = KQ. \quad (2)$$

The coefficient K is 1.58 for soda glasses, and 2.63 for potash glasses.

The results of determinations of sodium in the pastes before and after heating on soda glass are given in Table 3, which also contains the amounts of copper found by chemical analysis in the specimens. The weight increases of these specimens ranged from 8.2 to 10.9 mg, and the amount of paste on each was ~ 1 g.

The last column of Table 3 contains values of α calculated from the sodium and copper contents found. It is seen that these values of α are close to unity; i.e., they confirm the results in Tables 2 and 3 and the conclusion that the copper and alkali-metal ions enter into an ion-exchange reaction in 1:1 ratio.

TABLE 4

Composition of Group II Glasses

Glass No.	Composition (molar %)				Softening temperature (deg)	Wt. increase in 30 min at the softening temperature (mg/dm ²)	Calculated amount of copper (mg/dm ²)
	SiO ₂	CaO	Na ₂ O	K ₂ O			
4	75.5	9.1	15.5	—	555	55	87
1	73.5	9.1	17.4	—	550	65	104
5	73.0	9.1	17.9	—	550	74	115
6	72.5	9.1	18.4	—	545	74	115
7	71.4	9.1	19.5	—	545	82	130
8	69.5	9.1	21.4	—	540	93	145
9	78.5	9.1	—	12.4	595	2.5	6.6
10	76.5	9.1	—	14.4	585	4	10.5
3	73.5	9.1	—	17.4	565	5	13

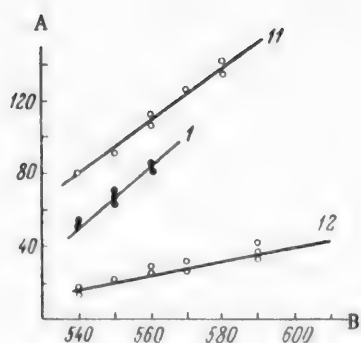


Fig. 4. Effect of heating temperature on weight increase of Group III glasses: A) weight increase in 30 minutes (mg/dm²); B) temperature (deg).

To estimate the relative influence of sodium oxide and potassium oxide on the rate of diffusion of copper ions (Cu^{2+}) into glass, it is necessary to compare the amounts of copper which enter into the soda (No. 1) and potash (No. 3) glasses. We find from equation (2) and the data in Table 1 that the amounts of copper entering soda and potash glasses in the same time are 104.3 mg/dm² and 13.2 mg/dm² respectively, i.e., copper ions diffuse into soda glass 8 times as rapidly as into potash glass. As these rates were compared at equal viscosities of the glasses and similar heating temperatures (550 and 565°), it follows that the observed difference in the rates of diffusion of copper into glass is associated with differences in the nature of the alkali metal present. It is possible that the difference in the rates of diffusion of copper into these glasses is due to the difference between the sizes of the sodium and potassium ions (Na^+ —0.098 Å, K^+ —1.33 Å).

To determine the influence of the amount of alkali oxide present in the glass on this process, glasses of the composition given in Table 4 (Group II) were used. The contents of alkali oxide in both the soda and the potash glasses were varied by replacement of silica. With increase of the sodium oxide content from 15.5 to 21.4 molar % the weight increase rose by a factor of 1.6, and with increase of the potassium oxide content from 12.4 to 17.4 molar % it was doubled.

In addition to the influence of univalent-metal oxides in the glass, the influence of oxides of bivalent metals: ZnO, BaO, PbO, present in the glass on diffusion of copper was studied. For this, calcium oxide in the glass (No. 1) was replaced by equal molar percentages of other bivalent-metal oxides. The composition of this group of glasses is given in Table 5.

Variations of the weight increase of Group III glasses with heating temperature are given in Fig. 4. It follows from Table 5 that the weight increase for zinc glass is greater by a factor of about 1.5, and for barium glass less, by a factor of 13, than it is for calcium glass. It follows that zinc oxide increases the rate of diffusion of copper ions into glass, whereas barium oxide decreases it considerably. Lead oxide also decreases the rate of diffusion of copper ions into glass. The influence of these oxides on the diffusion rate is evidently determined by differences in the mobilities of the alkali-metal ions in the glass, which depend on the nature of the bivalent elements present [23, 24].

Replacement of calcium oxides by oxides of other bivalent metals also influences the color of the surface glass layer. Thus, a pure yellow coloration is obtained in zinc glass, on calcium glass the color has a greenish tinge, and on barium and lead glasses the surface layer is colored green.

TABLE 5

Composition of Group III Glasses

Glass No.	Composition (molar %)						Softening temperature (deg)	Wt. increase in 30 min at the softening temperature (mg/dm ²)	Wt. increase in 30 min at 550° (mg/dm ²)
	SiO ₂	CaO	ZnO	BaO	PbO	Na ₂ O			
1	73.5	9.1	—	—	—	17.4	550	66	66
11	73.5	—	9.1	—	—	17.4	540	80	90
12	74.5	—	—	9.1	—	17.4	510	5 *	25
13	73.5	—	—	—	9.1	17.4	410	—	38

TABLE 6

Composition of Group IV Glasses

Glass No.	Composition (molar %)				Composition (wt. %)				Softening temperature (deg)	Wt. increase in 30 min at the softening temperature (mg/dm ²)
	SiO ₂	CaO	Na ₂ O	K ₂ O	SiO ₂	CaO	Na ₂ O	K ₂ O		
1	73.5	9.1	17.4	—	73.5	8.5	18	—	550	66
4	75.5	9.1	15.5	—	75.5	8.5	16	—	555	55
14	74.2	9.2	14.7	1.9	73.5	8.5	15	3	555	58
15	75.0	9.3	11.8	3.9	73.5	8.5	12	6	560	48
16	75.7	9.4	9.0	5.9	73.5	8.5	9	9	565	35
17	76.5	9.5	6.0	8.0	73.5	8.5	6	12	575	22
18	78.1	9.7	—	12.2	73.5	8.5	—	18	590	3

Introduction of trivalent-metal oxides into the glass, such as 1 to 3% of aluminum oxide or 1 to 4% of boric anhydride in place of silica, diminishes the rate of diffusion of copper into the glass.

Thus, the diffusion rate of copper into glasses of different compositions depends both on the chemical nature and the quantitative proportions of the glass components. In coloration of the surface layer of glass by cupric oxide to a yellow or green color this rate is a factor which determines to a considerable extent the quality of the color. For example, in glasses into which copper ions diffuse at a high rate (weight increase of 60-100 mg/dm² in 30 minutes at the softening temperature), an intense color is produced in the surface layers, but these layers also exhibit considerable light scattering. In glasses in which the rate of diffusion is moderate (weight increase of 30-50 mg/dm²) the layers are colored fairly intensely with slight light scattering, while in glasses in which the diffusion rate is low (weight increase 10-20 mg/dm²) layers of pale color free from scattering are formed. The amount of copper which enters a glass, and therefore the intensity of its surface coloration at a given composition, can be varied within narrow limits only, by variations of temperature and heating time, and therefore choice of the suitable glass composition is of predominant importance.

The glass composition is also of decisive significance in production of copper ruby in the surface glass layer. It was found that the metallic copper particles grow rapidly in glasses in which the diffusion rate of copper ions is high, and slowly where this rate is low. Glass compositions showing weight increases of 10-30 mg/dm² are recommended for production of copper ruby. Opaque layers of metallic copper are easily formed in glasses in which copper ions diffuse at higher rates.

On the basis of these results a series of soda-potash glass compositions, detailed in Table 6, was tested for practical production of yellow and red surface colors on glass.

For production of layers of intense yellow color, glasses No. 4, 14, 15 and 16 should be used; for red color, glasses No. 15, 16 and 17. Glass No. 3 is intended for pink coloration (pale copper ruby), and glass No. 4, for opaque yellow layers.

The influence of heating temperature on the weight increase of specimens of Group IV glasses is similar in character to that for Group I.

It was noticed during melting of the glasses indicated in Table 6 and of the other glasses discussed earlier that homogenization is rapid if the weight increase due to diffusion of copper into the glass is in the range of 60-100 mg/dm², and slow if the weight increase is 10-20 mg/dm².

As stated above, the crystallization rate of metallic copper in glass can be estimated in terms of the diffusion rate of copper ions into the glass. It is found that not only copper, but other substances such as zinc sulfide, cadmium sulfide, or cadmium thioselenide, crystallize rapidly in glasses in which copper crystals grow rapidly [25]. These data suggest that the diffusion rate of copper ions into glass gives an indication of the crystallization rate of a substance introduced into glass in order to obtain it in the crystalline state in the glass.

This provides a possible route to rational selection of glass compositions intended for coloration by colloidal colorants, and also for production of glasses in which the crystallization rates of certain substances must be regulated in order to obtain crystals of definite size (such as opaque or aventurine glasses). The same principle may be applied to selection of rational compositions of light-sensitive glasses.

SUMMARY

1. The diffusion rate of copper (Cu^{2+}) ions into glass depends on the glass composition. This rate is influenced by the nature of the alkaline oxides in the glass. Thus, copper ions diffuse 8 times as rapidly into soda as into potash glass. The diffusion rate of Cu^{2+} into glass decreases with decreasing alkali content and is influenced by the bivalent-metal oxides present. These oxides may be arranged in the following series in order of their effects on the diffusion rate: ZnO , CaO , PbO , BaO . Replacement of silica by alumina or boric anhydride in the glass reduces the rate of diffusion of copper ions into the glass.

2. The quantitative data on the influence of individual glass components on the rate of diffusion of copper ions into it, determined in this investigation, can be used for selection of compositions of glasses in which this diffusion rate has a predetermined value.

3. Diffusion of copper ions into glass proceeds by exchange of alkali-metal ions in the glass with copper ions in 1:1 ratio.

4. Cupric ions introduced into the surface layer of glass by diffusion color it yellow, green, or light blue.

5. Crystallization of metallic copper, zinc sulfide, cadmium sulfide, and cadmium thioselenide is rapid in glasses in which copper ions diffuse at high rates.

6. It is suggested that the rate of diffusion of copper ions into glass gives an indication of the crystallization rates of a number of substances introduced into glass in order to obtain them in the crystalline state in the glass.

LITERATURE CITED

- [1] V. V. Vargin, Production of Colored Glass [In Russian] (State Light Industry Press, 1940) p. 198.
- [2] O. Kubaschewski, Z. Electrochem. 42 (1), 5-7 (1936).
- [3] W. A. Weyl, Colored Glasses (Soc. Glass Technology, Sheffield, 1951).
- [4] J. E. Stanworth, Physical Properties of Glass (Oxford, Clarendon Press, 1950) p. 116-117.
- [5] I. I. Kitaigorodskii, Glass Technology [In Russian] (Industrial Construction Press, Moscow-Leningrad, 1939).
- [6] V. I. Panasyuk, Chemical Treatment of Glass [In Russian] (State Light Industry Press, 1940).
- [7] M. S. Fedorova, Glass Ind. 6, 17-18 (1940).
- [8] A. Lecrinier, P. Gilard and L. Dubrui, Rev. Belge Ind. Verre, 4, 51-57 (1933).
- [9] L. Springer, Sprechsaal, Apr. 5, 83 (7), 121-122 (1950).
- [10] Thorpe's Dictionary of Applied Chemistry, (London, 1951).
- [11] E. E. Mazo, Candidate's Dissertation [In Russian] (Belorussian Polytech. Inst. Minsk, 1940).

- [12] M. S. Fedorova, Collected Scientific Papers on Glass [In Russian] (All-Union Scientific Soc. Engineers and Technicians Press, 1950).
- [13] E. A. Ivanova, Report of the Sci. Res. Laboratory of the Art Glass Works, Theme No. 6, 3, 73 (1952) [In Russian].
- [14] E. A. Ivanova, Report of the Sci. Res. Laboratory of the Art Glass Works, Theme No. 6, 46-74 (1952) [In Russian].
- [15] E. A. Ivanova, Bull. VINSV 1 (1955).
- [16] J. A. Pask and W. Parmelee, J. Am. Cer. Soc. 26, 267 (1943).
- [17] V. V. Vargin, Production of Colored Glass [In Russian] (State Light Industry Press, 1940) pp. 97-103.
- [18] E. A. Ivanova, Report of the Sci. Res. Laboratory of the Art Glass Works, Theme No. 6, 52-54 (1952) [In Russian].
- [19] E. A. Ivanova, Report of the Sci. Res. Laboratory of the Art Glass Works, Theme No. 15, 20 (1955) [In Russian].
- [20] G. Schulze, Ann. Phys. 40, 335 (1913).
- [21] P. LeClerc, Compt. rend. 240, 30 (1955).
- [22] K. K. Kolobova and V. A. Gerasimova, Industrial Lab. 7 (1956).
- [23] E. A. Ivanova, Report of the Sci. Res. Laboratory of the Art Glass Works, Theme No. 6 (1952-55) [In Russian].
- [24] E. A. Ivanova, Bull. VINSV 4 (1956).
- [25] E. A. Ivanova, Report of the Sci. Res. Laboratory of the Art Glass Works, Theme No. 15, 35 (1955).

Received July 22, 1958

A STUDY OF PROCESSES OF MICROSTRUCTURE FORMATION IN INSULATOR PORCELAIN DURING FIRING

N. A. Toropov and A. N. Alekseeva

Processes of microstructure formation in insulator porcelain during firing were studied in detail in transparent sections under the microscope by Norton [1] and Chervinskii [2]. They showed that the original components of the porcelain body undergo changes visible under the microscope during the firing process. Feldspar grains begin to show surface fusion at 1100°, and at 1300° they lose their outline relief [2]. According to Norton, at 1200° all the feldspar grains enter the melt in 1.5 hours. The quartz grains are dissolved peripherally in the glass phase with formation of glassy edges, first observed at 1300° [2] and at 1175° after a heating time of 15 hours [1].

Kaolin fired at 1100° for 1 hour shows only weak mullite formation, and mullite needles are first observed only at 1300° [2]. The formation of the first mullite needles was also observed in samples fired at 1175° for 15 hours, but only in the glass-coated feldspar grains [1]. Chervinskii concluded from his observations that increase of temperature and firing time favors dissolution of quartz in the glass phase and growth of mullite crystals. In Norton's opinion, the decisive factor in the formation of microstructures in porcelain is the firing time.

In view of the effectiveness of simultaneous investigations of porcelain by transmitted and reflected light this method was used for processes of microstructure formation in insulator porcelain fired at 800-1400°. At the same time some samples were investigated by means of X-rays in an ionization unit [3].

EXPERIMENTAL

The material used for the investigation had the following composition (in %): Chasov Yar clay 15, Glukhovets kaolin 30, feldspar 27, Lyubertsy quartz sand 23, porcelain grog (ground) 5.

The body was molded into tablets 12 × 7 mm under a specific pressure of 1500 kg/cm². The specimens were fired in the 800-1400° range. The firing time at the final temperature was from 1 to 15 hours, and in some instances 20 hours. The specimens were cooled in air. Transparent polished sections of the specimens were examined under the microscope at temperature intervals of 100°.

Specimens fired at 800, 900 and 1000° are all similar in phase composition and structure. They consist (Fig. 1, 2) predominantly of clay substance unchanged by firing, with quartz and feldspar grains 0.0015-0.060 mm in size distributed fairly uniformly in it. The clay constituent of the porcelain, which we term the main mass, is seen under crossed nicols to consist mainly of birefringent aggregated grains with dark gray interference colors; in polished sections it is colored pink by Crystal Violet. Quartz and feldspar grains do not differ in color in reflected light; to distinguish between them, the polished section surface is etched deeply with hydrofluoric acid (1:1) for 3-5 minutes. The feldspar grains dissolve completely and disappear from the field of vision, while the quartz grains remain unchanged. The amounts of quartz and feldspar change little (by 2-5% by volume) with increase of the firing time.

At these temperatures, especially at 1000°, some individual grains of feldspar modified by firing are observed, and the first rims, 0.0025 mm wide, appear around some of the quartz grains.

Specimens fired at 1000° (Fig. 3 and 4) consists mainly of clay substance unchanged by firing, containing quartz and feldspar grains. In contrast to the preceding specimens, the main mass is isotropic under crossed nicols, and is colored yellow-pink by Crystal Violet in polished sections.



Fig. 1. Insulator porcelain; firing temperature 900°; time 15 hours; 1) quartz and feldspar grains; 2) main mass; reflected light, $\times 225$.

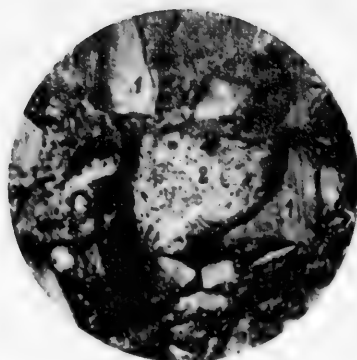


Fig. 2. Insulator porcelain; firing temperature 1000°; time 15 hours: 1) quartz and feldspar; 2) unchanged feldspar grain; 3) main mass; reflected light, $\times 450$.

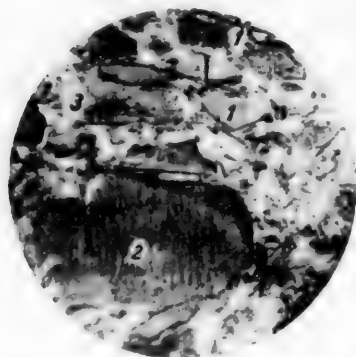


Fig. 3. Insulator porcelain; firing temperature 1100°; time 5 hours: 1) quartz; 2) feldspar; 3) main mass; reflected light, $\times 300$.

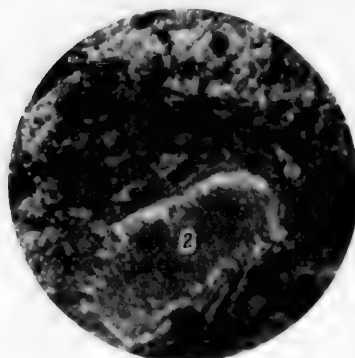


Fig. 4. Same portion of section as in Fig. 3; transmitted light, $\times 300$.

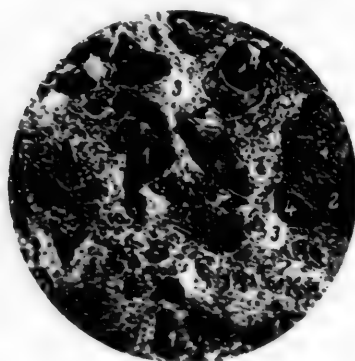


Fig. 5. Insulator porcelain; firing temperature 1200°; time 5 hours: 1) quartz; 2) partially vitrified feldspar grains; 3) main mass; 4) pores; reflected light, $\times 225$.

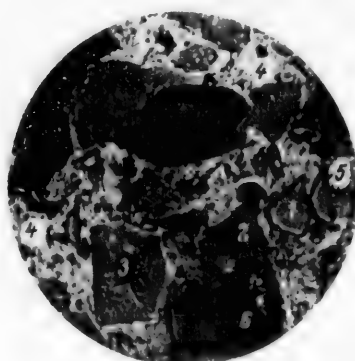


Fig. 6. Insulator porcelain; firing temperature 1200°; time 15 hours: 1) quartz; 2) feldspar (crystalline); 3) vitrified feldspar with mullite; 4) main porcelain mass; 5) meta-cristobalite edges on quartz grains; 6) pores; reflected light, $\times 450$.

Phase Composition of Porcelain

Firing temperature (deg)	Firing time (hours)	Crystal phases in specimen
1000	15	Feldspar, quartz
1200	1	Feldspar, quartz, mullite
1200	20	Quartz, mullite
1400	1	Quartz, mullite
1400	10	Quartz, mullite

The feldspar grains have a deeper gray color than the quartz grains, and only some of the largest feldspar grains do not differ from quartz grains. This change in the color of the feldspar grains is probably the result of homogenization. These specimens are characterized by absence of small grains (of $d = 0.005$ mm) of quartz and feldspar. The quartz content is 13 vol. % after 5 hours of firing, and 10 vol. % after 20 hours. The content of feldspar grains decreases from 12.6 to 10 vol. %. Numerous very fine glassy formations are present in individual feldspar grains. The number of quartz grains with somewhat darker peripheral rims increases appreciably. The structure and phase composition of specimens fired at 1200° (Fig. 5, 6) are similar to those of specimens fired at 1100°. The only difference is that in the former specimens completely vitrified feldspar grains with mullite needles are observed; these are present in considerable amounts in specimens fired for 15 hours. After 5 hours of heating the original feldspar grains, somewhat darker than the quartz grains, predominate; after 10 hours partially vitrified feldspar grains are predominant. The largest single feldspar grains, with d of 0.05-0.06 mm, retain their crystalline structure even after 20 hours. The quartz grains have somewhat darker rims. The number of quartz grains with such edges and the width of these rims increase appreciably with firing time.

Specimens fired at 1300° are composed of a relatively homogeneous mass, which apparently consists of submicroscopic mullite and glass, containing vitrified and considerably fused grains of feldspar with mullite needles and quartz grains with peripheral rims.

The content of vitrified feldspar grains after one hour is 6.5-7.5 vol. %, and the content of quartz grains (including the peripheral rims) is 10 vol. %.

Specimens fired at 1400° are similar in phase composition and structure to specimens fired at 1300°. The only difference is that the vitrified feldspar grains are even more fused and less frequent. The remaining quartz grains have relatively wide peripheral rims (0.03-0.04 mm) which are dissolved rapidly. Only occasional quartz grains are found in specimens fired for 10 hours.

Data on the phase composition of the porcelain, determined from the corresponding X-ray patterns, are given in the table.

It was not possible to detect cristobalite in the X-ray patterns because of the closeness of its strongest lines to the strong quartz and mullite lines.

SUMMARY

The investigations provided some indication of the behavior of the original components of the porcelain body during firing. The dust grains of feldspar, comprising 50% of the initial amount, enter the melt during firing at temperatures up to 1100°. The remaining larger grains are converted into the glassy state on further firing, but retain their external crystal faces. The finer grains pass into the melt while the larger, with mullite inclusions, persist even during subsequent firing.

Before passing into the fused state, feldspar undergoes the following changes during firing: its grains become darker in reflected light than initially, and then become gradually vitrified without morphological changes. The course of these changes is determined more by the duration of heating at a given temperature than by the temperature factor.

About 50 vol. % of the quartz (mainly its dust grains) dissolves during firing up to 1100°. Very narrow peripheral rims are first observed on the quartz grains at 1000°; on further firing the number of quartz grains with peripheral rims and the width of the latter increase.

The peripheral rims, which occupy more than half the area of the original quartz grains, dissolve rapidly at the surface in the surrounding main mass. This behavior of the peripheral rims on quartz during firing (refractive index 1.485) suggests that they consist of cristobalite formed by polymorphic conversion of the original quartz.

The appearance of mullite needles, formed in the porcelain from the kaolinite decomposition products, is first observed under the microscope at 1200°; as on further firing, these needles are observed only in the vitrified feldspar grains. The maximum amount of mullite is observed under the microscope after firing at 1200° for 20 hours. With increase of the firing temperature the vitrified feldspar grains evidently pass into the melt; the mullite present in them dissolves, and its content as shown by the microscope decreases. The mullite needles in the larger vitrified feldspar grains increase appreciably in size and therefore do not undergo any appreciable dissolution even with considerable surface fusion of the feldspar grains themselves.

Clay and kaolin comprise the main porcelain mass, in which quartz and feldspar grains are distributed. When fired at temperatures up to 1100° the main mass, as seen in transparent section, consists chiefly of aggregated grains with dark gray interference colors, separated from each other by interlayers of isotropic substance. Further qualitative changes in the main mass during firing cannot be detected microscopically. The amount of this mass rises sharply with increase of firing temperature, especially at 1300° and over.

It is easy to see that these changes of the original porcelain components take place largely at the same time during porcelain firing. For example, processes of kaolinite formation in the clay component are accompanied by enrichment of this component by a melt formed from the fine particles of feldspar and quartz; evidently this leads to interaction between the kaolinite decomposition products and the melt.

Samples fired at 1200° simultaneously contain mullite needles in vitrified feldspar grains and large crystalline grains of feldspar of $d = 0.05-0.06$ mm. In addition to quartz grains unchanged by firing, there quartz dust grains completely converted to cristobalite (isotropic).

It is therefore evident that, in addition to temperature, firing time, and impurities, the particle-size composition of the porcelain components has a great influence on the processes of microstructure formation in porcelain.

LITERATURE CITED

- [1] Charles L. Norton, J. Am. Cer. Soc. 14, 3, 192 (1931).
- [2] N. M. Chervinskii, Ceramic Collection 13, 21-28 (1941).
- [3] N. A. Toropov, P. F. Konovalov, A. I. Efremov and G. V. Anan'eva, Cement 3, 17 (1954).

Received April 26, 1958

THE RELATIONSHIP BETWEEN THE STRESSED STATE OF PORCELAIN AND DAMPING OF VIBRATIONS INDUCED IN IT

V. Z. Petrova and A. I. Avgustinik

When vibrations are induced in any real body, part of the elastic energy is converted into heat. This effect is associated with internal friction. The possibility of determining internal friction, especially at elevated temperatures, is of great importance for investigation of reactions in solids. For example, in metal science it is possible by determination of the coefficient of internal friction to investigate diffusion effects and sintering processes, and to determine the maximum solubility limits of individual alloy components. However, as yet there is no comprehensive theory covering all the phenomena associated with internal friction in solids.

The coefficient of internal friction may be found by calculation of the ratio $\Delta W/W$, where ΔW is the energy dissipated in one vibration cycle and W is the elastic energy of the specimen at the instant of maximum deformation. Here it is assumed that the restoring forces are proportional to the vibration amplitude, and the dissipating forces are proportional to the vibration velocity. Then the ratio of two consecutive amplitudes A_n/A_{n+1} is constant. The natural logarithm of this ratio (the logarithmic decrement) is taken as a measure of internal friction

$$\delta = \ln \frac{A_n}{A_{n+1}}.$$

Another method for determination of the damping decrement is based on measurement of the width of the resonance peak. Kolsky [1] gives the following expressions for determination of the damping decrement by the second method:

$$\frac{\Delta W}{W} = 2\delta; \quad \frac{\Delta f}{f_0} = \frac{\sqrt{3}}{\pi} \delta; \quad \delta = \frac{\pi \Delta f}{\sqrt{3} f_0},$$

where Δf is the change of frequency on either side of the resonance peak when the amplitude is halved, and f_0 is the fundamental vibration frequency of the specimen (the maximum amplitude is a_{\max} at frequency f_0) (Fig. 1). The latter method was used in our investigation.

The logarithmic damping decrement is determined fairly rarely for silicate materials. Deeg [2] used this method for porcelain bodies, and Latyshenko [3] for concretes. In their opinion, the logarithmic decrement is a characteristic which gives an indication of the stressed state and mechanical strength of a material. It must be pointed out in this connection that, in contrast to the elasticity modulus (E), the value of the logarithmic decrement characterizes the plastic properties of a material. It is therefore necessary to determine E and δ jointly, as these values characterize the physicomaterial properties [1-4].

The following are the main difficulties in determination of the damping decrement: first, the double-peak effect, or the appearance of a double amplitude peak (f_1 and f_2) at amplitudes A_1 and A_2 (Fig. 2); second, inaccuracy in the determination of resonance characteristics of these substances because of the very small values of the logarithmic damping decrement for porcelain ($\delta = 0.001-0.005$); third, the value of the damping decrement is influenced by the magnitude of the inducing stress, support, and the needle pressure.

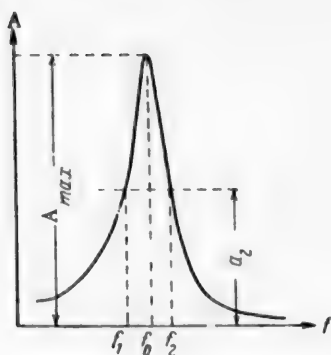


Fig. 1. Resonance-frequency characteristics: A) vibration amplitude; f) frequency.

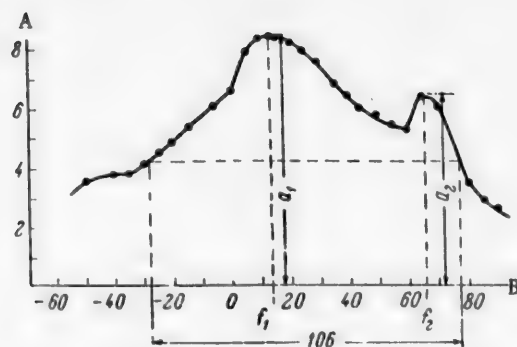


Fig. 2. Resonance-frequency characteristics of an unfired specimen of square cross section: A) volt-meter readings (v); B) frequency of applied vibrations (cps).

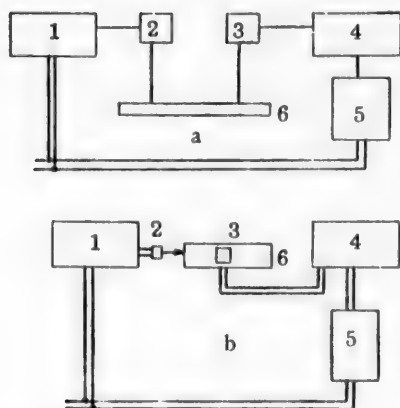


Fig. 3. Block diagram of apparatus for determination of the logarithmic damping decrement: a) suspended specimen; b) on panel; 1) ZG-2A audio-frequency oscillator; 2) transducer; 3) receiver; 4) amplifier (IChMK-2 instrument); 5) cathode-ray voltmeter; 6) specimen.

To eliminate these effects, we used two methods for determination of the damping decrement: 1) vibrations were induced by means of a needle with a rubber pad, and 2) the vibrations were induced through threads.

Block diagrams of the test units are shown in Fig. 3.

In both cases the IChMK-2 instrument was used; this can be used for fairly accurate determinations ($\pm 7\%$) of the vibration frequencies of a body at 5000 cps and over. In our case, when the damping frequency of unfired porcelain is only 10-20 cps, this instrument is very inaccurate. Therefore the ZG-2A audio-frequency oscillator was used, and a cathode-ray voltmeter was used for determination of $A_{max}/2$. Thus, the IChMK-2 instrument was used in our scheme merely as an amplifier (amplification $\times 100,000$).

In the apparatus for determination of the logarithmic decrement in specimens in rod form, the transducer was a dynamic source, the diffuser of which contained an ebonite holder for the needle. The receiver was an ordinary adapter head. The specimen was suspended from Nichrome wire of $d = 0.05$ mm, or asbestos cord.

Specimens which had been used for determination of the elasticity modulus (E) by the resonance method (vibrations induced by means of a needle) were used for determination of δ . The specimen dimensions were: fired, $l = 140$ mm, $b \times h = 2.85 \times 2.85$; unfired, $l = 170-200$ mm, $b \times h = 2.9 (30) \times 30 (29)$. Here l is the specimen length, b is the width, and h is the height. All the specimens were made from insulator porcelain body from the "Proletarii" factory, by drawing through the mouthpiece of a laboratory press. The specimens were fired in the tunnel kiln of the "Proletarii" factory. Some of the specimens were placed in a perforated fireclay box, fired in a Silit furnace at 1320° , and then cooled rapidly in a stream of air ($T = 25^\circ$, $V_{air} = 7-8$ meters/second) in order to produce stress in the specimens.

RESULTS

For unfired material, the damping decrement was determined for the same specimens which were then dried, in order to investigate the effect of moisture content on the decrement. The unfired specimens have a high damping decrement (0.07-0.1) in comparison with fired, and therefore the accuracy of Δf determination is fairly high.

TABLE 1

Determination of δ for an Unfired Specimen

Determination No.	Fundamental frequency (cps)	$f_1 - f_0$ (cps) (-)	$f_2 - f_0$ (cps) (+)	Δf	Logarithmic damping decrement (δ)	Reading error	Deviation (%)
1	1530	39	28	67	0.0790	0.0077	0.09
2	1530	38.5	27.5	66	0.0785	0.0012	1.50
3	1530	34	35	69	0.0820	0.0023	2.89
4	1530	39	31	70	0.0830	0.0033	4.13
5	1530	38	29	67	0.0790	0.00077	0.96
$\delta_{av} \dots$					0.07976		

TABLE 2

Logarithmic Damping Decrements for Specimens of the Same Moisture Content

Specimen No.	Fundamental frequency (cps)	Logarithmic damping decrement (δ)	Deviations from mean	Deviations (%)
1	1530	0.0797	+0.0031	+4.04
5	1450	0.0745	-0.0021	-2.70
6	1514	0.0750	-0.0016	-2.01
18	1585	0.0710	-0.0056	-7.31
21	1554	0.0820	+0.0054	+7.06
25	1509	0.0781	+0.0015	+2.00
		$\delta_{av} 0.0766$		

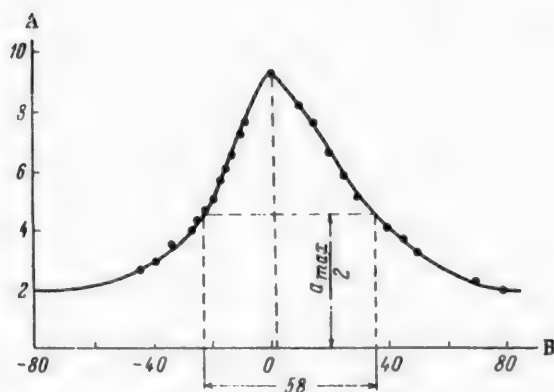
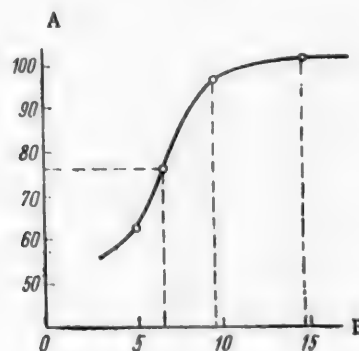


Fig. 4. Resonance-frequency characteristics of an unfired specimen of rectangular section: A) volt-meter readings (v); B) frequency (cps).

Fig. 5. Effect of moisture content on the logarithmic damping decrement: A) values of $\delta \cdot 10^{-3}$; B) moisture content (%).

In developing the method, we encountered the double-peak effect (the appearance of two amplitude peaks). The nature of this effect can be seen in the resonance characteristics of unfired specimens (Fig. 2). The appearance of a double amplitude peak complicates determination of δ , and in some instances makes it quite impossible.

There is no full explanation of this effect. Latyshenko and Thomson [3, 5], who studied the front resistance

TABLE 3

Logarithmic Damping Decrements for Fired Specimens

Specimen No.	Fundamental frequency (cps)	Logarithmic damping decrement (δ)	Deviation (%)
1	3684	0.00179	+24.3
2	4600	0.00163	+13.1
3	4314	0.00149	+3.4
4	4540	0.00126	-12.5
5	4754	0.00126	-12.5
		δ_{av} 0.00144	

TABLE 4

Logarithmic Damping Decrement for Fired Specimen No. 1 with Fundamental Frequency of 3864 cps

$f_2 - f_1$ (cps)	$f_0 - f_1$ (cps)	Δf (cps)	Logarithmic damping decrement (δ)	Deviation (%)
21	14	35	0.00175	2.205
20	16	36	0.00181	1.10
26	10	36	0.00181	1.10
20	15	35	0.00175	2.20
20	17	37	0.00186	3.91
			δ_{av} 0.00179	

of concretes, refer in their papers to difficulties in determining δ for concrete specimens because of the appearance of a double amplitude (resonance) peak, and suggested that the effect is associated with the cross-sectional shape of the specimen and the formation of microcracks in it during tests of frost resistance.

To test the hypothesis that the shape of the cross section influences the resonance-frequency characteristics, we ground down specimens of square cross section to a 20 x 30 cm rectangular section. This resulted in disappearance of the twinning of the amplitude peak for unfired specimens (Fig. 4). For each specimen 5-6 determinations were performed; the deviations of the values of δ for each specimen were slight (Table 1).

The equation $\delta = \pi \Delta f / \sqrt{3} f_0$ was used to calculate δ .

Table 2 contains the results of determinations of δ_{av} for 6 specimens from a batch of 30. The most divergent values of δ were chosen; this gives an indication of the deviations for determinations on a single batch.

The other 24 specimens gave $\pm 2\%$ deviation, and therefore specimens No. 18 and 21, which showed large deviations from the mean value of δ , were tested again; the resonance-frequency characteristics of these specimens are somewhat diffuse owing to the double amplitude peak.

Vibrations could not be induced in porcelain-body specimens containing over 20% moisture. The first value of δ was obtained at $\sim 15\%$ moisture. The results are plotted in Fig. 5. The determinations were performed with the same specimen, which was dried before each successive determination of δ ; each time a piece of the material was split off for moisture determination, and the specimen was ground flat before the measurement.

TABLE 5

Effect of Cooling Conditions on the Logarithmic Damping Decrements of Fired Specimens

Conditions		Logarithmic damping decrement (δ)
firing	cooling	
Factory kiln	Normal	0.00353
Silt furnace	Normal	0.00184
Air blast at temperatures (deg):		
Silt furnace	1000	0.00449
	700	0.00288
	800	0.00305
	500	0.00183

Deeg's method [2] gives $\delta = 0.066$ at $W = 5\%$ for porcelain body; this is in agreement with our results for unfired material. The curve for δ as a function of moisture content shows that δ decreases with decreasing moisture content; this may be attributed to increase of the mechanical strength and E of the specimen.

Determination of the damping decrement for fired specimens was difficult because of the low values of δ (of the order of 0.001-0.008). It was therefore necessary to perform the experiments at a single excitation stress and to determine the resonance characteristics, from which δ was calculated, for each specimen.

The results obtained for porcelain specimens of square cross section, fired at 1320° , are given in Table 3.

The results in Table 4 show that the deviations between the values obtained for the same specimen are small (from 1.1 to 3.9%). For determinations on different specimens from the same batch the deviations are fairly considerable ($\pm 13\%$); the value for specimen No. 1 (Table 3) is high because of the diffuse resonance characteristics (double peak), and values for the other 15 specimens are not given in the table, as the deviations between their values of δ are within $\pm 5\%$.

Since, according to the authors cited above, twinning of the resonance peak depends on the cross-sectional shape of the specimen and its stressed state, the experiments were repeated with specimens of definite rectangular section, but cooled by the old procedure. As the section was rectangular (20×30), twinning due to the shape was eliminated. If the effect persisted, this would show that the double-peak effect is caused by stresses in the specimen. The determinations showed that the effect persisted in a number of specimens. Therefore there is some connection between δ and structural disturbance due to stress.

To verify this, several determinations were performed on specimens fired at 1320° in a Silt furnace, which were cooled down from 1000, 700, and 500° (in cold air) under a stream of air from a fan. The values of δ so found were compared with δ for factory-fired specimens; the results are presented in Table 5. Between 10 and 15 specimens were taken for each cycle.

It follows from Table 5 that the logarithmic damping decrement is a sensitive measure of changes in the stressed state of ceramics. The highest value of δ was observed in a specimen cooled down from 1000° .

SUMMARY

1. The logarithmic damping decrement can be used in investigations of either fired or unfired ceramics. The variations of δ with moisture content can be used for control of moisture content.
2. The stresses set up in a ceramic material during cooling after firing can be characterized qualitatively and quantitatively by determinations of δ .
3. The apparatus used in our experiments gives a fairly good degree of accuracy ($\pm 13\%$); for more accurate frequency determinations it is necessary to design a new type of audio-frequency oscillator and to develop a method for inducing vibrations which eliminates the experimental error factors.

LITERATURE CITED

- [1] H. Kolsky, *Stress Waves in Solids* (IL, 1955) [Russian translation].
- [2] E. Deeg, *Silicate Chemistry and Technology* 4 (1956).
- [3] V. A. Latyshenko, in the book: *Collected Research Papers on Concrete and Reinforced Concrete*, 1 [In Russian] (Acad. Sci. Latvian SSR Press, 1957).
- [4] A. S. Gurvich, *Trans. Sci. Res. Inst. Constructional Ceramics* 12 (1957).
- [5] W. T. Thomson, *ASTM Proceedings* 40 (1940).

Received September 19, 1958

A STUDY OF THE STABILIZATION CONDITIONS AND STABILITY OF ZrO_2

L. P. Kachalova and A. I. Avgustinik

Stability of solid solutions in the system ZrO_2 -CaO was studied by Duwez and his associates [1]. They found that, in contrast to zirconium-magnesium compositions, solid solutions of cubic structure in the system ZrO_2 -CaO were stable at all temperatures.

In 1956 Weber and co-workers [2] confirmed the phase stability of zirconium oxide-calcium oxide solid solutions at all temperatures. On the other hand, Keler and Andreeva [3], in 1957, showed by a dilatometric method that solid solutions of the composition 90% ZrO_2 + 10% CaO decompose as the result of prolonged heat treatment at 1200-1300°.

In our studies of the stabilization conditions of zirconium dioxide for production of wares of high thermal endurance, considerable attention was devoted to the question of stability of solid solutions in the system ZrO_2 -CaO.

The investigation was carried out on compositions in the limited region of the phase diagram for ZrO_2 -CaO:

Composition code mark	C-20	C-16	C-14	C-12	C-10	C-08
Zirconium dioxide (molar %)	80	84	86	88	90	92
Calcium oxide (molar %)	20	16	14	12	10	8

The starting materials were ZrO_2 and $CaCO_3$. The chemical composition of the zirconium dioxide, by analysis, was (in %): ZrO_2 - 97.53, Al_2O_3 - 0.70, SiO_2 - 1.20, Fe_2O_3 - 0.40, calcination loss 0.17; the $CaCO_3$ was of analytical reagent grade. The zirconium dioxide was ground in a vibratory mill for 5 hours down to a content of 74% of particles smaller than 10 μ .

The specimens were formed into rods (8 x 8 x 65 mm) by dry pressing under a pressure of 1000 kg/cm². Firing at temperatures up to 1500° was performed in a Silit furnace, and at 1700-1900° in a high-temperature TVV-2M vacuum furnace with a tungsten heating element.

It is known that the first stage in the formation of solid solutions in the system ZrO_2 -CaO is formation of zirconate which interacts at high temperatures with the remaining ZrO_2 and passes into solid solution [4].

It was found by x-ray analysis that after firing at 1500° the principal phase in all the compositions was a solid solution of the cubic form. In addition, small amounts of monoclinic zirconium oxide remained in C-14 and C-08 specimens.

Chemical phase analysis showed that at least 5% of another phase, calcium zirconate, was present in all the compositions. The results of phase analysis are given in Table 1; it is seen that with increase of the stabilization temperature the amount of calcium zirconate diminishes, and at 1900° $CaZrO_3$ passes completely into the solid solution. As soon as the formation of solid solutions is complete, the surface energy is utilized in the recrystallization process. Microscopic investigations of sections from the C-10 composition fired at 1500 and 1900° revealed an increase of grain size from 1 to 50 μ respectively.

Complete conversion of monoclinic zirconium dioxide into solid solutions of the cubic form, in conjunction with recrystallization, occurs at 1900° and results in a sharp lowering of the thermal stability of the

TABLE 1

Formation of Solid Solutions at Different Stabilization Temperatures

Composition code mark	Composition of original mixture				Amount of original mixture in g	Amount of residue insoluble in HCl*					
	ZrO ₂	CaO	ZrO ₂	CaO		1500°		1700°		1900°	
	molar %		wt. %			in g	in %	in g	in %	in g	in %
C-20	80	20	89.7	10.3	0.5000	0.4732	94.64	0.4755	95.10	0.4944	98.88
C-10	90	10	95.2	4.9	0.5000	0.4745	94.90	0.4818	96.36	0.4940	98.80

TABLE 2

Behavior of Solid Solutions in Relation to Time of Heat Treatment

Composition	Composition of original mixture				Amount of original mixture in g	Amount of residue insoluble in HCl					
	ZrO ₂	CaO	ZrO ₂	CaO		1500°		1700°		1900°	
	molar %		wt. %			in g	in %	in g	in %	in g	in %
C-20	80	20	89.7	10.3	0.5000	0.4730	94.60	0.4750	95.00	0.4939	98.78
C-10	90	10	95.2	4.8	0.5000	0.4660	93.20	0.4830	96.60	0.4940	98.80
C-20	80	20	89.7	10.3	0.5000	0.4712	94.24	0.4750	95.00	0.4935	98.70
C-10	90	10	95.2	4.8	0.5000	0.4625	92.50	0.4814	96.28	0.4910	98.20

*The amount of ZrO₂ dissolved in HCl is disregarded; according to analytical data, it is 0.5-0.7%

specimens. It was found in course of the investigation that this lowering is due not only to the fact that the linear coefficient of thermal expansion for compositions with a cubic structure is double that of specimens consisting of mixtures of cubic solid solutions with monoclinic ZrO₂, but also to considerable changes in the elastic properties. Variations of the elastic characteristics of the specimens with the stabilization temperature and phase composition are given in Table 3,

It follows from these data that for production of zirconia ceramics of high thermal stability the starting material should be previously-stabilized zirconium dioxide mixed with raw monoclinic ZrO₂. The amount of monoclinic zirconium dioxide added and the subsequent firing temperature depend on the amount of calcium zirconate present in the previously-stabilized ZrO₂. It is necessary to take into account the possible formation of solid solutions of cubic structure by the interaction of calcium zirconate with monoclinic ZrO₂ at high temperatures, and to prevent this reaction from taking place. This leads to certain important technological conclusions.

1. Preliminary stabilization should be effected at high temperatures (1900°) which ensure conversion of calcium zirconate into solid solution. In such cases the amount of raw monoclinic zirconium dioxide should not exceed 10-15% by weight. The final firing temperature depends only on the degree of porosity required.

Amount of CaZrO_3 passing into solution						Amount of free CaO		Maximum theoretical amount of CaZrO_3	
stabilization temperature (deg)									
1500°		1700°		1900°		1500°	1900°		
in g	in %	in g	in %	in g	in %	in g	in g	in g	in %
0.0268	5.36	0.0245	4.90	0.0056	1.12	not detected	not detected	0.1500	30
0.0255	5.10	0.0182	3.64	0.0060	1.20			0.077	15.4

Amount of calcium zirconate passing into solution						Amount of free CaO		Maximum theoretical amount of CaZrO ₃	
stabilization temperature (deg)									
1500°		1700°		1900°		1500°	1900°		
in g	in %	in g	in %	in g	in %	in g	in %	in g	in %

50 hours of heat treatment

0.0270	5.40	0.0250	5.00	0.0061	1.22	Not detected	Not detected	0.1500	30.0
0.034	6.80	0.017	3.40	0.0060	1.20			0.0770	15.4

300 hours of heat treatment

0.0288	5.76	0.0250	5.00	0.0065	1.30	Not detected	Not detected	0.1500	30.0
0.0375	7.50	0.0186	3.72	0.0081	1.62			0.0770	15.4

2. When zirconium dioxide previously stabilized at 1500-1700° is used, the best thermomechanical characteristics are obtained if not more than 10% by weight of monoclinic zirconium dioxide is added if the wares are subsequently fired at 1500°, and not more than 30% for a firing temperature of 1900°. Such specimens had high thermal stability under rapid changes of temperature from 1400° to room temperature, and withstood more than 30 cycles.

Study of the Stability of Solid Solutions in the System $\text{CaO} - \text{ZrO}_2$

In addition to the compositions described above, specimens C-10, C-20 and C-30 of the following composition were investigated:

90% of cubic solid solution of	$\text{ZrO}_2 - \text{CaO} + 10\%$ monoclinic	ZrO_2
80%	+ 20%	"
70%	+ 30%	"

After being fired at 1500, 1700 and 1900° the specimens were given prolonged heat treatment at 1200°. Specimens after 50, 100, 150 and 300 hours of heat treatment were investigated by physicochemical methods and their properties were studied.

The curves in Fig. 1 represent porosity variations of the specimens with the stabilization temperature and duration of heat treatment. It is seen that the greatest increase of porosity (3-4%) after 50 hours of heating was

TABLE 3

Elastic Properties of Specimens

Composition	Poisson's ratio			Shear modulus $G \cdot 10^5$ (kg/cm ²)			Elasticity modulus $E \cdot 10^5$ (kg/cm ²)		
	stabilization temperature (deg)								
	1500°	1700°	1900°	1500°	1700°	1900°	1500°	1800°	1900°
C-20	0.257	0.268	0.303	4.37	4.41	4.87	10.99	11.55	15.50
C-14	0.232	—	0.290	2.57	—	4.77	6.33	—	14.60
C-12	0.225	—	0.232	2.55	—	4.67	6.30	—	14.25
C-10	0.180	0.257	0.265	2.41	2.38	4.30	6.25	5.95	13.50

found for specimens C-10 and C-12. The porosity increase diminished with increase of calcium oxide content, and there was almost no change in the region of the C-20 composition. Specimens stabilized at 1900° showed almost no change of porosity. The behavior of the specimens was not changed much by increases of the heat treatment time to 100 or 300 hours. It is interesting to note that the stability of the C-20 composition was also reflected by its elasticity characteristics (the elasticity and shear moduli remained unchanged even after 300 hours of heat treatment).

Specimens prepared from previously-stabilized ZrO_2 mixed with raw monoclinic ZrO_2 showed larger changes as the result of heat treatment.

These differences in behavior of the different compositions as the result of prolonged heat treatment are clarified by means of dilatometric investigations. Figure 2 shows curves for the expansion of C-10 composition stabilized at 1500° as a function of the time of heat treatment. The loop representing reversible conversion of monoclinic ZrO_2 into the tetragonal form changes its shape even after 50 hours of treatment. After 300 hours of treatment the loop increases sharply in size, which indicates an increased content of monoclinic ZrO_2 in the specimen. Monoclinic ZrO_2 can appear only by decomposition of the solid solution.

No such effect is found for the C-10 composition stabilized at 1900°. The expansion curve for the specimen was almost unchanged. In this case the solid solutions are more stable. This stability is apparently due to the absence of monoclinic ZrO_2 , in contrast to the C-10 composition stabilized at 1500°. This hypothesis was confirmed by subsequent observations. It was found that the thermal expansion of the C-20 composition, irrespectively of the stabilization temperature, is entirely unchanged as the result of heat treatment at 1200° for up to 300 hours.

Good confirmation of the dilatometric data is provided by the results of chemical phase analysis. Variations of the behavior of solid solutions in relation to the time of heat treatment are given in Table 2.

The fact that calcium oxide was not detected shows that it is combined as calcium zirconate as soon as liberated by decomposition of the solid solution. This is confirmed by the 2.5% increase of the calcium zirconate content in C-10 (stabilization temperature 1500°) as the result of heat treatment for 300 hours.

The results of X-ray investigations also confirm that the stabilization effect depends on the phase composition, and stability can be ensured if only the cubic structure is present in the specimens. Structural changes were detected only in specimens which consisted of mixtures of the cubic and monoclinic structures before heat treatment. For example, the X-ray pattern of the C-10 composition stabilized at 1500° was primarily indicative of monoclinic ZrO_2 after heat treatment (Fig. 3a).

It was found in the investigation that if destabilized specimens are again subjected to high temperatures (1800-1900°) solid solutions are formed again. The X-ray pattern corresponds to a cubic structure of the ZrO_2 -CaO solid solution (Fig. 3b).

SUMMARY

1. Stability of solid solutions of the cubic form in the system ZrO_2 -CaO depends on the phase composition.
2. If only the cubic structure is present in the specimens the solid solutions do not decompose.

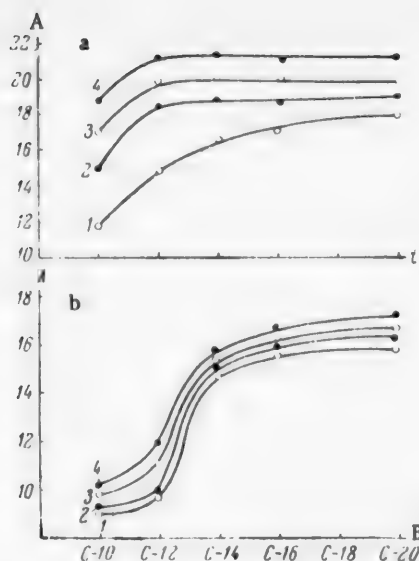


Fig. 1. Variations in the porosity of the specimens with the stabilization temperature, composition, and duration of heat treatment at 1200°: A) apparent porosity (%); B) composition; treatment times (hours): 1) 0; 2) 50; 3) 100; 4) 300; temperature (deg): a) 1500; b) 1900.

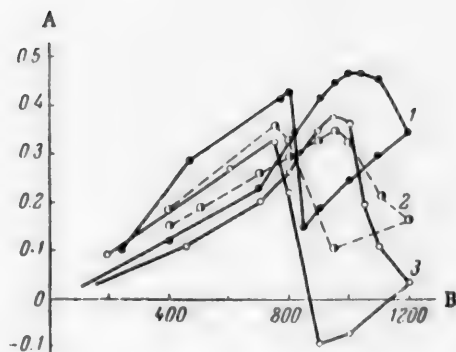


Fig. 2. Dilatometric curves for stabilized ZrO_2 for different times of heat treatment at 1200°; composition: 90% ZrO_2 + 10% CaO: A) expansion Δl (mm/cm); B) temperature (deg); treatment times (hours): 1) 0; 2) 50; 3) 300.

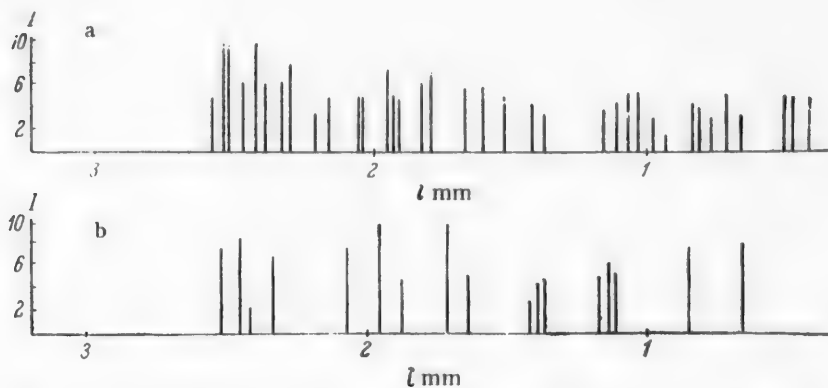


Fig. 3. X-ray patterns of C-10 composition stabilized at 1500°: a) after 300 hours of heat treatment at 1200°; b) for destabilized specimen fired at 1800°.

3. Partial decomposition of solid solutions takes place in specimens containing some monoclinic ZrO_2 in addition to the cubic structure. The monoclinic form apparently causes destabilization of the inversion temperature of ZrO_2 .

4. The solid solutions are decomposed into the free oxides, and calcium oxide is combined as calcium zirconate as soon as liberated.

5. Decomposition of the solid solutions is accompanied by changes in the properties of the specimens.

6. When destabilized specimens are subjected to high temperatures (1800-1900°) solid ZrO_2 -CaO solutions of the cubic form are again formed.

LITERATURE CITED

- [1] P. Duwez, F. Brown and F. Odell, J. Amer. Cer. Soc. 35, 5, 107-113 (1952).
- [2] B. Weber, H. Garrett, F. Mauer and U. Schwartz, J. Amer. Cer. Soc. 39, 6, 197-206 (1956).
- [3] E. K. Keler and A. B. Andreeva, Refractories 2, 65-70 (1957).
- [4] E. K. Keler and N. A. Godina, Proc. Acad. Sci. USSR 103, 2, 247-249 (1955).

Received July 1, 1958

EFFECTS OF ADDED ORGANOSILICON COMPOUNDS ON THE ACID RESISTANCE AND OTHER TECHNICAL CHARACTERISTICS OF CERAMIC MATERIALS

V. A. Bork and I. I. Kornblit

(D. I. Mendeleev Institute of Chemical Technology, Moscow)

The increasingly stringent demands with respect to the purity of reagents make it necessary to search for new anti-corrosion materials, of greater resistance than those known at present. This fact prompted the present investigation, the aim of which was to find suitable acid-resisting materials and to study the influence of organosilicon compounds on the acid resistance and certain other characteristics of ceramic products made from these materials. It is known that ceramic materials based on refractory metal oxides such as alumina have exceptional resistance to the action of various agents. However, the sintering of such oxides requires a great amount of heat energy. Various binders such as quartz powder are used to lower the sintering temperature. The choice of organosilicon compounds as binders is guided by the following considerations [1, 2]: 1) during firing of the wares the organic portion of the organosilicon compound is completely volatilized as the result of pyrolysis, while the polymer which remains after certain complex processes, close to $(\text{SiO}_2)_n$ in composition, is chemically resistant; 2) after removal of the organic radicals chemically-active centers arise, capable of interacting with active molecules of other components, and this assists sintering and aging of the fired body; 3) if SiO_2 is used as a binder in the form of organosilicon compounds it is possible to distribute SiO_2 uniformly in a state of molecular dispersion, so that a material of uniform properties is formed after firing; 4) organosilicon compounds act as plasticizers, which is significant in molding of the wares.

EXPERIMENTAL

Alumina of G₀ grade was used, of the following chemical composition:

Al_2O_3	SiO_2	Fe_2O_3	Na_2O	Calcination loss	Σ
98.5	0.07	0.02	0.54	1.1	100.23

Experiments were carried out in order to determine the firing temperature which confers the highest corrosion resistance to alumina. The alumina was divided into several portions, each of which was heated at a definite temperature: 830, 900, 1000, 1200, 1450 and 1730°. The reagents tested were acids: 10, 20 and 35% HCl, 10, 20 and 50% HNO_3 , and 10, 50 and 85% H_2SO_4 , and also 10 and 50% KOH and NaOH. The action of these agents on the powders was tested during 24 hours in the cold and 1 hour at boiling.

The data obtained on the solubility of alumina, heated at different temperatures, in acids and alkalies confirm earlier published results according to which the acid resistance of alumina increases with the firing temperature.

A similar relationship between chemical resistance and firing temperature was found for the action of alkalies on alumina heated at various temperatures; in general, alkalies are the more corrosive (Fig. 1).

For a final decision with regard to the choice of raw material for the present investigation, tests were performed on white artificial corundum close to alumina in grain size (150-400 μ). The corundum powder was

TABLE 1

Solubility of α - Al_2O_3 in Acids (%)

Acid and concentration (%)	Solubility of α - Al_2O_3 (in %)			
	alumina fired at 1730°		artificial corundum	
	24 hours in the cold	1 hour at the boil	24 hours in the cold	1 hour at the boil
HNO_3 { 40 20 50	0.23 0.24 0.29	0.46 0.49 0.30	0.09 0.11 0.13	0.14 0.21 0.18
H_2SO_4 { 10 50 85	0.11 0.17 0.31	0.19 0.19 0.91	0.05 0.12 0.21	0.07 0.14 0.70

TABLE 2

Solubility of Kaolin in Acids

Kaolin firing temperature (deg)	Sieve No.	Solubility (%) in			
		HNO_3		H_2SO_4	
		10%	35%	10%	85%
Unfired	06	2.51	12.32	9.31	31.74
1100		0.99	3.05	5.63	22.48
1250		0.69	1.42	2.37	13.28
1600		0.21	1.22	1.29	6.60
Unfired	02	3.21	13.48	10.42	46.41
1100		1.93	4.25	7.39	27.68
1250		0.94	1.94	4.51	17.50
1600		0.44	0.72	1.12	8.92
Unfired	015	3.89	15.06	12.72	30.11
1100		2.51	5.53	8.49	32.84
1250		1.23	2.23	6.35	20.70
1600		0.278	0.81	1.16	10.07

treated with nitric and sulfuric acids under the same conditions as the alumina. The results, compared with data for alumina fired at 1730°, are summarized in Table 1, which shows that white artificial corundum is more resistant to acids than alumina. This may be ascribed to the smoother surface of the corundum grains.

We also determined the solubility of kaolin of different grain sizes, unfired and fired at 1100, 1200 and 1600°, in HNO_3 and H_2SO_4 .

The results of these tests are given in Table 2; it follows that the solubility of kaolin in acids decreases with increase of firing temperature.

The acid resistance increases with decrease of grain size, owing to the decreasing specific surface.

It follows from these experiments that the acid resistance of alumina and kaolin can be raised considerably by the use of high-temperature firing (Fig. 1, 2).

The main raw material used in the present investigation was white artificial corundum of No. 100 granulation, containing 0.59% impurities, and having the following composition (%):

Al_2O_3	Fe_2O_3	SiO_2	CaO	Na_2O	Σ
99.41	0.12	0.27	0.09	0.24	100.13

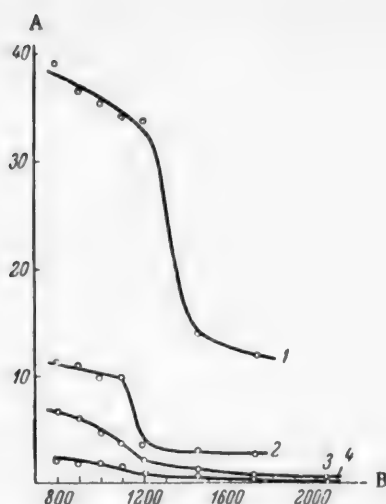


Fig. 1. Effect of firing temperature on the solubility of alumina: A) solubility (%); B) firing temperature (deg); the corrosive media were 50% solutions of: 1) NaOH; 2) KOH; 3) H_2SO_4 ; 4) HNO_3 .

TABLE 3

Solubility of Specimens Fired at 1250° in Concentrated Sulfuric Acid After 72 Hours of Treatment

Body No.	Binder	Solubility (%)
1	Polymer A	3.82
2	Polymer B	Destroyed
3	Polymer C	4.51
4	Quartz powder	2.71
5	Silicic acid	1.1

TABLE 5

Solubility of Specimens in Concentrated Sulfuric Acid After 216 Hours of Treatment

Body No.	Solubility (%)
1	3.67
2	0.62
3	1.98
4	3.19
5	1.33

the mortar rose and the mixture was stirred. When a temperature of 130-150° had been reached, the mass was additionally plasticized by addition of paraffin wax. The plasticized mass was then cast into specimens which were subsequently fired. The firing was performed in a flame furnace (up to 1600°) or in a Silit furnace (up to 1250°), with an exposure time of 2 hours.

Five types of specimens were prepared, containing the following binders: 1) mixture of polyethoxy

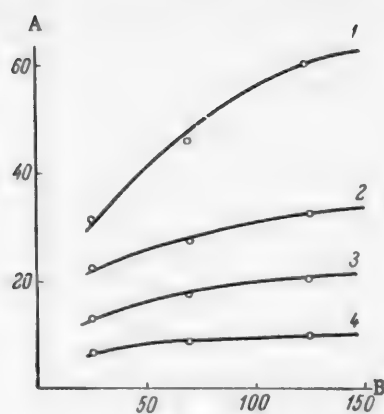


Fig. 2. Effect of particle size on the solubility of kaolin fired at different temperatures: A) solubility (%); B) specific surface (cm^2); 1) unfired kaolin; 2) fired at (deg): 2) 1100; 3) 1250; 4) 1600.

TABLE 4

Solubility of Specimens Fired at 1600° in Concentrated Sulfuric Acid After 72 Hours of Treatment

Body No. *	Solubility (%)
1	0.73
2	0.03
3	0.47
4	0.03
5	0.01

*Here and subsequently the body numbers refer to the same five types of specimens made with different binders (see Table 3).

Concentrated sulfuric acid, which is the most corrosive of the media, was used for tests of acid resistance.

The standard specimens used for tests on the experimental materials were cylinders 20 mm in diameter and height. They were made by the process used in the production of "sinoksal" refractories [3].

The corundum was treated with organosilicon compounds in a heated metal mortar with continuous stirring. Solvents were used to distribute the polymers more uniformly over the grain surfaces. The solvent evaporated as the temperature in

TABLE 6

Properties of Materials Made with Different Binders

Body No.	Firing temperature								
	1250°					1600°			
	σ_{cm} (kg/cm ²)	γ (g/cc)	w (%)	B (%)	Δh (%)	σ_{cm} (kg/cm ²)	γ (g/cc)	w (%)	B (%)
1	411	2.1	20.8	45.2	1.6	712	2.15	20.2	44.7
2	327	2.07	22.4	45.5	0.5	662	2.12	22.0	45.6
3	310	2.11	22.7	45.8	4.5	796	2.16	21.2	44.6
4	294	2.37	21.4	44.3	0.3	732	2.18	17.9	42.4
5	412	2.88	23.7	45.4	3.4	756	2.24	19.4	43.5

TABLE 7

Mechanical Strength of Specimens Before and After Treatment with Concentrated H₂SO₄ (216 Hours)

Body No.	σ_{cm} (kg/cm ²)		Loss of mechanical strength (%)
	before treatment	after treatment	
1	712	646	9.3
2	662	659	2.1
3	696	656	4.3
4	732	691	5.6
5	756	684	9.5

polysiloxanes (still residues) containing 14.2% SiO₂ (Polymer A); 2) hydrolyzed ethyl silicate 40 containing 21.9% SiO₂ (Polymer B); 3) solution of FG-9 alkyd silicone resin in benzene containing 11.3% SiO₂ (Polymer C); 4) silica in the form of finely-ground quartz sand; 5) aqueous silicic acid containing 76% SiO₂.

The amounts of binder added to the mixes in all five types corresponded to 5% SiO₂.

The following determinations were performed on the specimens: 1) acid resistance R (%); 2) bulk density γ (g/cc), water absorption w (%), and porosity B (%); 3) firing shrinkage Δh (%); 4) compressive strength σ_{cm} before and after acid treatment.

Water absorption, porosity, and bulk density were determined by hydrostatic weighing of water-saturated specimens from which air had been removed [3]. Shrinkage was determined by measurements of the specimens before and after firing. Mechanical strength was determined by means of compressive tests in a hydraulic press. The acid resistance was investigated as follows. The specimens were dried to constant weight at 110°, weighed on an analytical balance, placed in a 500 ml flask fitted with a reflux condenser, and covered with sulfuric acid of sp. gr. 1.84. The first test cycle consisted of alternate heating and cooling of the specimens during 72 hours; the total heating time was 24 hours at 300°. After 72 hours the specimens were taken out of the acid, washed thoroughly, covered with distilled water, left for 24 hours, and then boiled for 1 hour. They were dried at 110° and heated strongly to remove all sulfuric acid from the pores and weighed; the relative loss of weight R₁ (%) after the first treatment was calculated.

The same cycle of treatments was then performed twice more and R₂ and R₃ after the second and third treatments were calculated.

Thus, the materials were subjected to the corrosive medium for a total time of 216 hours.

It follows from Table 3 that, after firing at 1250°, specimens containing organosilicon polymers were less resistant than specimens with quartz powder of silicic acid to the action of acid for 72 hours.

Therefore, in the subsequent investigations specimens made from the same mixes were fired at 1600° and then treated with acid as before. It was found that organosilicon compounds do not confer any advantage even when the firing is performed at a high temperature; this follows from the data in Table 4.

Materials containing aqueous silicic acid as binder proved to be the most resistant to attack; this is of undoubted practical significance in a number of cases. As Table 4 shows, specimens made with quartz powder and with Polymer B had equal resistance to the same reagent, close to that of specimens made with silicic acid.

Hydrolyzed ethyl silicate showed considerable advantages as binder for corundum compositions only in prolonged action of the corrosive medium (216 hours, with three treatment cycles) on specimens fired at 1600° (Table 5).

It should be noted that with this prolonged acid treatment the specimens made with aqueous silicic acid again have the lowest solubility (with the exception of Polymer B).

Since, under given conditions, the behavior of a material in the corrosive medium depends on the nature of the binder, other properties of the experimental materials were studied. The results of these tests are given in Table 6.

It follows from the data in Table 6 that of the specimens fired at 1250° compositions containing Polymer A or aqueous silicic acid as binders have the greatest mechanical strength. The density and strength of the specimens increase considerably if the firing temperature is raised to 1600°. The specimen containing silicic acid as binder was found to have the highest density (2.24 g/cc). However, there was no correlation between acid resistance and the other properties of the specimens. The mechanical strength, determined by compressive tests, changes little under the influence of acid treatment (Table 7).

Specimens made with Polymer B showed the greatest stability of compressive strength.

It follows that Polymer B (hydrolyzed ethyl silicate 40) proved to be the best binder with regard to stability of mechanical strength as well as corrosion resistance.

SUMMARY

1. Materials containing hydrolyzed ethyl silicate 40 (Polymer B) have 5 times the acid resistance of materials containing silica, and double the acid resistance of materials made with aqueous silicic acid.

2. Specimens containing ethyl silicate 40 show little change in mechanical strength after treatment with concentrated sulfuric acid for 216 hours.

3. With increase of the firing temperature from 1100 to 1600° for kaolin, and from 880 to 1730° for alumina, the resistance of these powders to the action of acids and alkalis increases.

LITERATURE CITED

- [1] A. P. Kreshkov, *Organosilicon Compounds in Technology* [In Russian] (Industrial Construction Press, 1956).
- [2] A. P. Kreshkov and I. D. Abramson, *Trans. Mendeleev Inst. Chem. Technol.*, Moscow 13, 142 (1948).
- [3] K. K. Strellov, *Technical Control in the Production of Refractories* [In Russian] (Metallurgy Press, 1952).

Received November 4, 1957

DENSITY OF SOLUTIONS OF N_2O_4 IN STRONG NITRIC ACID

G. L. Antipenko, E. S. Beletskaya and Z. I. Koroleva

Up to now there has been a lack of detailed data in the literature on densities in the system $\text{HNO}_3\text{--N}_2\text{O}_4\text{--H}_2\text{O}$ in the region of low water concentrations (up to 5% by weight).

A survey of the literature showed that by 1950 only four papers [1-4] had been published on density in the binary system $\text{HNO}_3\text{--N}_2\text{O}_4$. Of the information presented in these publications, the data of Klemenc [4] are the most reliable. The results obtained by the other three workers [1-4] are not in satisfactory agreement with those of Klemenc, probably because they used less pure materials.

In recent years several new publications [5-9] have appeared, containing the results of density determinations in the region of low water concentrations (up to 5%) in the ternary system $\text{HNO}_3\text{--N}_2\text{O}_4\text{--H}_2\text{O}$ at temperatures from 0 to 65°.

The data available in the literature are inadequate, in particular in the low-temperature region. An attempt was therefore made to determine experimentally the densities of solutions in the concentration region of practical interest, over a wide range of temperatures.

EXPERIMENTAL PROCEDURE

Nitric acid was prepared by twofold vacuum distillation of a mixture of concentrated nitric and sulfuric acids at room temperature. The product, which contained traces of water and nitrogen oxides, was stored at temperatures below -40°.

Nitrogen tetroxide was prepared from the technical product by distillation in a current of oxygen through a tube containing phosphorus pentoxide.

The $\text{HNO}_3\text{--H}_2\text{O}$ and $\text{HNO}_3\text{--H}_2\text{O}_4\text{--H}_2\text{O}$ solutions were prepared by addition of small portions of distilled water to the acid cooled to -30°. The amounts of water and nitrogen tetroxide added were determined gravimetrically.

Densities were determined by means of a glass dilatometer about 7 ml in capacity. The dilatometer was calibrated against mercury by the weighing method. The cathetometer used in the experiments ensured an accuracy of 0.0005 ml in the volume determinations. The temperature in the thermostat was maintained to an accuracy of $\pm 0.05^\circ$ in the 0-50° range, and to an accuracy of $\pm 0.15^\circ$ at lower temperatures (between 0 and -60°).

EXPERIMENTAL DATA

The densities of solutions of nitrogen tetroxide in strong nitric acid were determined in the concentration range of 10-27% N_2O_4 and 0-5% H_2O , between -60 and +50°. The determinations were started at the lowest temperature, and the temperature was then raised to the highest value by 10° steps.

The total time taken for each series of determinations was about 7 hours; of this, not more than 2 hours was required at room and higher temperatures. Therefore the thermal decomposition of nitric acid which occurs in almost anhydrous solutions could not have a significant effect on the density values found, as it is known [8] that the rate of this process is relatively low. This was confirmed by the results of a special experimental check.

TABLE 1

Comparison of Experimental and Literature Data on Densities in the System HNO_3 - N_2O_4 - H_2O

Component contents (wt. %)		Density (g/cc) from data of				
N ₂ O ₄	H ₂ O	this paper	Masson [5]		Sprague [6]	
			ρ	Δρ	ρ	Δρ
Temperature 0°						
4.80	5.18	1.545	1.549	-0.004	—	—
4.97	1.73	1.561	1.559	+0.002	—	—
11.21	5.63	1.565	1.570	-0.005	—	—
11.63	2.11	1.584	1.584	0.000	—	—
19.02	5.14	1.594	1.593	+0.001	—	—
19.70	1.74	1.615	1.614	+0.001	—	—
Temperature 25°						
4.80	5.18	1.505	1.506	-0.001	1.508	-0.003
4.97	1.73	1.521	1.517	+0.004	1.520	+0.001
11.21	5.63	1.525	1.527	-0.002	1.530	-0.005
11.63	2.11	1.544	1.542	+0.002	1.545	-0.001
19.02	5.14	1.554	1.550	+0.004	1.551	+0.003
19.70	1.74	1.575	1.572	+0.003	1.575	0.000
Temperature 40°						
4.80	5.18	1.479	1.479	0.000	1.481	-0.002
4.97	1.73	1.495	1.488	+0.007	1.494	+0.001
11.21	5.63	1.499	1.500	-0.001	1.503	-0.004
11.63	2.11	1.518	1.516	+0.002	1.518	0.000
19.02	5.14	1.528	1.521	+0.007	1.523	+0.005
19.70	1.74	1.549	1.543	+0.006	1.547	-0.002

The probable maximum error in the determinations was estimated on the following considerations: a) inaccuracy of volume determination (about 0.0005 ml) led to an error of 0.0001 unit in the density determinations; b) weighing to the nearest 0.0002 g gave an error of about 0.00005 unit of density; c) temperature measurements in the ranges of 0 to 50° and 0 to -60° to within 0.1 and 0.3° respectively could give errors of about 0.0002 and 0.0005 density units; d) the maximum error in determinations of the concentrations of nitrogen oxides (0.2%) and water (0.1%) could give rise to errors of 0.0007 and 0.0005 density units respectively.

It follows that the probable maximum error in the experimental determinations did not exceed 0.002 density units.

The results of experimental density (ρ_t) determinations are in quite satisfactory agreement with the empirical formula

$$\rho_t = 1.593 + 0.37 \left(\frac{C_2}{C_1 + C_2} - 0.2 \right) - a \cdot C_3 - b(t - 20), \quad (1)$$

where C_1 is the HNO_3 concentration in solution (wt. %), C_2 is the N_2O_4 concentration (wt. %), C_3 is the H_2O concentration (wt. %), and t is the temperature (deg).

The coefficient a in Eq. (1) is a function of the concentration ratio of nitrogen tetroxide and nitric acid in solution, and is given by the equation

$$a = 0.00536 + 0.0072 \left(\frac{C_2}{C_1} - 0.15 \right). \quad (2)$$

The coefficient b is the temperature coefficient of density; its average values were found to be: in the

TABLE 2

Densities in the System $\text{HNO}_3\text{--N}_2\text{O}_4\text{--H}_2\text{O}$

t (°C)	Density (g/cc) at water content (wt. %) in solution					
	0	1	2	3	4	5

	Concentration of			N_2O_4 5%		
-60	1.666	1.661	1.657	1.652	1.648	1.643
-50	1.650	1.645	1.641	1.636	1.632	1.627
-40	1.634	1.629	1.625	1.620	1.616	1.611
-30	1.618	1.613	1.609	1.604	1.600	1.595
-20	1.602	1.597	1.693	1.588	1.584	1.579
-10	1.586	1.581	1.577	1.572	1.568	1.563
0	1.570	1.565	1.561	1.556	1.552	1.547
+10	1.554	1.549	1.545	1.540	1.536	1.531
+20	1.538	1.533	1.529	1.524	1.520	1.515
+30	1.521	1.516	1.512	1.507	1.503	1.498
+40	1.504	1.499	1.495	1.490	1.486	1.491
+50	1.487	1.482	1.478	1.473	1.469	1.464

	Concentration of			N_2O_4 10%		
-60	1.684	1.679	1.675	1.670	1.665	1.660
-50	1.668	1.663	1.659	1.654	1.649	1.644
-40	1.652	1.647	1.643	1.638	1.633	1.628
-30	1.636	1.631	1.627	1.622	1.617	1.612
-20	1.620	1.615	1.611	1.606	1.601	1.596
-10	1.604	1.599	1.595	1.590	1.585	1.580
0	1.588	1.583	1.579	1.574	1.569	1.564
+10	1.572	1.567	1.563	1.558	1.553	1.548
+20	1.556	1.551	1.547	1.542	1.537	1.532
+30	1.539	1.534	1.530	1.525	1.520	1.515
+40	1.522	1.517	1.513	1.508	1.503	1.498
+50	1.505	1.500	1.496	1.491	1.486	1.481

	Concentration of			N_2O_4 20%		
-60	1.721	1.716	1.711	1.706	1.701	1.696
-50	1.705	1.700	1.695	1.690	1.685	1.680
-40	1.689	1.684	1.679	1.674	1.669	1.664
-30	1.673	1.668	1.663	1.658	1.653	1.648
-20	1.657	1.652	1.647	1.642	1.637	1.632
-10	1.641	1.636	1.631	1.626	1.621	1.616
0	1.625	1.620	1.615	1.610	1.605	1.600
+10	1.609	1.604	1.599	1.594	1.589	1.584
+20	1.593	1.588	1.583	1.578	1.573	1.568
+30	1.576	1.571	1.566	1.561	1.556	1.551
+40	1.559	1.554	1.549	1.544	1.539	1.534
+50	1.542	1.537	1.532	1.527	1.522	1.517

temperature range of +20 to -60° $\Delta\rho/\Delta t = 0.0016$ g/cc·degree; in the temperature range of 20-50°, $\Delta\rho/\Delta t = 0.0017$.

The above empirical formula cannot be used for extrapolation into regions of higher N_2O_4 concentrations (> 26%), as in these regions the curvature of the $\rho = f(C_2)$ curves at $C_3 = \text{const.}$ and $t = \text{const.}$, and of $\Delta\rho/C_3 = f(C_2/C_1)$ curves at $t = \text{const.}$ becomes appreciable.

To determine the lower limit of concentrations of nitrogen tetroxide in strong nitric acid down to which extrapolation is permissible, density data available in the literature were compared with values calculated from the formula (Table 1). Data published since 1950 by Masson [5] and Sprague [6] were used. It may be concluded from the results of the comparison that 5% N_2O_4 is the lower concentration limit of nitrogen tetroxide permissible for extrapolation by means of formula (1).

TABLE 2 (Continued)

t (°C)	Density (g/cc) at water content (wt. %) in solution					
	0	1	2	3	4	5
Concentration of N ₂ O ₄ 25%						
-60	1.740	1.734	1.728	1.720	1.716	1.710
-50	1.724	1.718	1.712	1.704	1.700	1.694
-40	1.708	1.702	1.696	1.688	1.684	1.678
-30	1.692	1.686	1.680	1.672	1.668	1.662
-20	1.676	1.670	1.664	1.656	1.652	1.646
-10	1.660	1.654	1.648	1.640	1.636	1.630
0	1.644	1.638	1.632	1.624	1.620	1.614
+10	1.628	1.622	1.616	1.608	1.604	1.598
+20	1.612	1.606	1.600	1.592	1.588	1.582
+30	1.595	1.589	1.589	1.575	1.567	1.561
+40	1.578	1.572	1.566	1.558	1.550	1.544
+50	1.561	1.555	1.549	1.541	1.533	1.527
Concentration of N ₂ O ₄ 26%						
-60	1.743	1.737	1.731	1.725	1.719	1.713
-50	1.727	1.721	1.715	1.709	1.703	1.697
-40	1.711	1.705	1.699	1.693	1.687	1.681
-30	1.695	1.689	1.683	1.677	1.671	1.665
-20	1.679	1.673	1.667	1.661	1.655	1.649
-10	1.663	1.657	1.651	1.645	1.639	1.633
0	1.647	1.641	1.635	1.629	1.623	1.617
+10	1.631	1.625	1.619	1.613	1.607	1.601
+20	1.615	1.609	1.603	1.597	1.591	1.585
+30	1.598	1.592	1.586	1.580	1.574	1.568
+40	1.581	1.575	1.569	1.563	1.557	1.551
+50	1.564	1.558	1.552	1.546	1.530	1.524

The empirical formula (1) was used to calculate solution densities at different component concentrations and temperatures; these values are recommended for use in technical calculations (Table 2).

SUMMARY

1. Densities in the system HNO₃-N₂O₄-H₂O were determined in the concentration regions of 0-5% H₂O and 10-27% N₂O₄ between -60 and +50°.

2. An empirical formula is given for calculation of solution densities; this can be used for extrapolation down to 5% N₂O₄.

LITERATURE CITED

- [1] G. Lunge and Marchlewsky, Z. Angew. Chem. 5, 12, 330 (1892).
- [2] P. Pascal and M. Garnier, Bull. Soc. Chim. (4), 25, 143, 309 (1919).
- [3] W. R. Bousfield, J. Chem. Soc. 115, 45 (1919).
- [4] A. Klemenc and J. Rupp, Z. Anorg. Chem. 194, 54 (1930).
- [5] D. M. Masson, J. Petker and S. P. Vango, J. Phys. Chem. 59, 6, 511 (1955).
- [6] R. W. Sprague and E. Kaufmann, Ind. Eng. Chem. 47, 3, 458 (1955).
- [7] Technical Encyclopedia, Handbook of Physicochemical and Technical Data [In Russian] (Soviet Encyclopedia Press, Moscow, 1927-1933).
- [8] G. D. Robertson, D. M. Masson and W. H. Corcoran, J. Phys. Chem. 59, 8, 683 (1955).
- [9] O. P. Kharbanda, Ind. Chem. 32, 380, 412 (1956).

Received February 24, 1958

THE DETONATING POWER OF LIQUID EXPLOSIVE MIXTURES BASED ON NITRIC ACID

R. Kh. Kurbangalina

Nitric acid is widely used in chemical industry, and in recent years it has also been used in rocket technology. Nitric acid is not explosive in itself, but it forms explosive mixtures with combustible materials.

We determined the detonating power of mixtures of nitric acid with certain fuels; the detonating power was estimated from the critical diameter. The critical diameter [1] is usually taken to be the minimum diameter of an explosive (ES) charge which, under given conditions (these are: charge density and the ES particle size in the case of powdered ES [2], the initial temperature [3] for liquid ES, and the material and wall thickness of the charge container for all ES), ensures steady propagation of the detonation through the ES charge to a distance greater than ten charge diameters. The critical diameter is to a certain extent associated with the sensitivity of the ES. It is found in a number of instances that the more sensitive the ES, the less is the critical diameter. For example, nitrate esters (nitroglycerin, nitroglycol, methyl nitrate) are more sensitive than liquid trotyl, and their critical diameters are fractions of the critical diameter of liquid trotyl. The critical diameter of lead azide, etc., is very small.

In our experiments the charge containers were thin-walled glass tubes with funnel-shaped widened ends for the initiator. The tubes were from 20 to 70 cm long. The explosions were initiated either by a compressed charge of PETN or hexogen 17 mm in diameter, density 1.4-1.6 g/cc, weight 4-10 g, or directly by means of a No. 8 detonator capsule in an aluminum cartridge. In some cases (for small critical diameters) the initiation was effected by small amounts of lead azide.

The nitric acid used for preparation of the explosive mixtures had density of 1.51 g/cc, and the fuels were of chemically pure grade.

The components were mixed several minutes before the explosion, and cooled in water or snow. The temperature in the explosion chamber was in the 5-15° range. The course of the detonation wave through the ES charge was investigated in two ways: by photographic recording of the luminescence of the detonating charge, and by deformation of an iron plate placed under the ES charge.

The results of the tests are given in Table 1, which also contains approximate calculated values for the heat of explosion.

It follows from these results that mixtures of nitric acid with nitrobenzene, m-nitrotoluene, and dichloroethane detonate stably even at very small charge diameters, of the order of a few millimeters or less. A mixture consisting of 72% nitric acid and 28% nitrobenzene, which has zero oxygen balance, detonates stably in thin-walled glass tubes of 0.6 mm internal diameter, whereas such sensitive explosive liquids as nitroglycerin, nitroglycol, and methyl nitrate no longer detonate stably when the tube diameter is less than 2-2.5 mm. It should be pointed out that a charge diameter of 0.6 mm is not yet critical for a mixture of nitric acid and nitrobenzene (72:28). Apparently the critical diameter for this mixture is even smaller. This is also partially indicated by the fact that the thickness of the container wall has an influence on stable propagation of detonation in this mixture. For example, a mixture of nitric acid + nitrobenzene (72:28) detonated stably in a thermometer tube 0.25 mm in internal diameter with walls 3 mm thick (the length was 75 cm), whereas detonation was not propagated through a thin-walled tube (0.07 mm) of the same internal diameter. This effect of wall thickness can only occur when the critical diameter is small and the thickness of the container wall is very much greater than the critical diameter.

TABLE 1

Test Results

Composition of explosive mixture	Calc. heat explosion (kcal/kg), water as steam	Tube diameter (mm)	Thickness of glass wall (mm)	Propagation of detonation	Critical diameter (mm) d_{cr}
Nitric acid + nitrobenzene (72:28)	1465	1.7 0.95 0.6 0.25 0.25	0.1 0.2 0.4 0.07 3.0	Passed Died down Passed	< 0.6
Nitric acid + m-nitrotoluene (48:52)	1000	4.4 3.6	0.7 0.65	Passed Died down	$3.6 < d_{cr} < 4.4$
Nitric acid + dichloroethane (56:44)	1000	3.6 2.6	0.6 0.6	Passed Died down	$2.6 < d_{cr} < 3.6$
Nitric acid + glycol (67:33)	1420	25 20	1.5 1.3	Passed Died down	$20 < d_{cr} < 25$
Nitric acid + methyl alcohol (70:30)	1280	10	1.0	Did not pass	> 10
Liquid trotyl	1000		2		> 32 (at $+100^\circ$)
Nitrate ester (nitroglycerin, etc)	1500		0.7		2-2.5

The investigated mixture of 48% nitric acid + 52% m-nitrotoluene has a negative oxygen balance and is close to trotyl in elementary chemical composition. A comparison of the critical diameters of this mixture and liquid trotyl is of interest. The critical diameter of the mixture of nitric acid and m-nitrotoluene (48:52), determined at 10° , is about 4 mm, whereas the critical diameter of liquid trotyl [2], determined at 100° , is over 32 mm,* i.e., the limiting diameter for the mixture is 1/8 of that for trotyl. Such a comparison of these values of the critical diameters is not valid, as they were determined at different initial temperatures, and the critical diameter of liquid ES depends very much on the initial temperature: increase of the initial temperature diminishes the critical diameter [3]. It is impossible in practice to determine the critical diameter of the mixture at 100° , and of trotyl below its melting point. The critical diameter of the mixture HNO_3 + m-nitrotoluene, determined at 100° , would be much less than 4 mm, and therefore the critical diameters of the mixture and trotyl should differ by much more than a factor of 8. It follows that a mixture of nitric acid and m-nitrotoluene is much more sensitive to detonation than liquid trotyl. The critical diameter of the mixture of nitric acid and m-nitrotoluene, which has zero oxygen balance, was not determined. We consider that it should be close to the critical diameter of a mixture of nitric acid and nitrobenzene (72:28).

It follows from the above results that mixtures of nitric acid with fuels of the nitrobenzene or m-nitrotoluene type (apparently, with compounds of this structure in general) have exceptionally high detonating power. The small values of the critical diameter suggest that these ES are highly sensitive, and carry a risk of explosion under impact, friction, and heat. Moreover, these mixtures, especially mixtures with oxygen balances close to zero, are very sensitive to initiating impulses. For example, a mixture of nitric acid + nitrobenzene (72:28) was detonated under our experimental conditions by 80 mg of pressed azide, whereas more than 300 mg/mg of lead azide of the same density was required to induce detonation at a high velocity in nitroglycerin.

Table 1 also shows that a mixture of nitric acid with such an inert substance as dichloroethane is explosive. Our value for the critical diameter of a mixture consisting of 56% nitric acid and 44% dichloroethane (a mixture of this composition has zero oxygen balance in formation of HCl) is about 3 mm, which is very close

*According to more accurate determinations the critical diameter of liquid trotyl at 100° is 40-45 mm.

TABLE 2

Detonation Velocities of Mixtures

Composition of explosive mixture	Heat of explosion (cal/g)	Density (g/cc)	Charge diameter (mm)	Detonation velocity (m/sec)
Nitric acid + nitrobenzene (72:28)	1465	1.41	0.25 10.0	6200 6800
Nitric acid + dichloroethane (56:44)	1000	1.39	6.0	6100
Nitric acid + glycol (67:33)	1420	1.36	25.0	6200
Nitric acid + m-nitrotoluene (48:52)	1000	1.31	5.3	5200
Liquid trotyl*	1000	1.45	27.0	6500

* At 130°.

to the critical diameters of such dangerous ES as nitrate esters, even despite the fact that the heat of explosion of this mixture is 2/3 of the heat of explosion of nitrate esters. Experimental work with mixtures of nitric acid and alcohols is more difficult, because when alcohols (methyl alcohol and glycol in our experiments) are mixed with nitric acid, reactions of partial nitration and oxidation take place, and the mixtures are therefore not homogeneous. In our experiments alcohols were mixed with nitric acid, with cooling in snow and water, literally a few minutes before the detonation. Few experiments were performed, but they were sufficient to estimate the order of magnitude of the critical diameter. The critical diameter of mixtures of nitric acid with alcohols proved to be relatively large, of the order of 20 mm, or 8 to 10 times the critical diameter of the corresponding nitrate esters.

The detonation velocities of the investigated mixtures were also determined; the results are given in Table 2.

The maximum velocities were not determined specially for these mixtures. The values given for the detonation velocities were determined incidentally during determinations of the critical diameters. In studies of the influence of tube diameter on the detonation velocities of liquid nitrate esters it was found that the detonation velocity near the limit is only about 10% lower than the maximum velocity [4], i.e., detonation in liquid ES, in contrast to explosive powders, dies down with a small decrease of velocity. This rule can be applied to the mixtures studied. The maximum detonation velocities for these mixtures should be about 10% above the values given in Table 2. This is clearly illustrated in the case of the mixture nitric acid + nitrobenzene (72:28), for which the detonation velocity away from the limit is known. The accuracy of determination of the detonation velocities was $\pm 4-5\%$.

It should be noted that the detonation velocities given in Stettbacher's book [5] for liquid ES are much too high (by 1200-1500 m/second), evidently because of the inaccurate method of determination.

SUMMARY

The detonating power of mixtures of nitric acid with nitrobenzene, m-nitrotoluene, dichloroethane, and glycol was investigated and it was found that all these mixtures are explosive, detonation-sensitive substances with detonation velocities of the order of 6000-7000 m/second, corresponding to their heats of explosion, densities, and compositions of the explosion products. The critical diameters of most of the mixtures are very small; this suggests that mixtures of nitric acid with fuels can easily be exploded by a blow, impact, or heat. Such mixtures require careful handling.

LITERATURE CITED

- [1] Yu. B. Khariton, Theory of Explosive Substances, Collection of the Institute of Chemical Physics [In Russian] (Acad. Sci. USSR Press, 1947) p. 7-28.
- [2] A. Ya. Apin and V. K. Bobolev, J. Phys. Chem., 22, 1367 (1946).

- [3] A. W. Campbell, M. F. Malin and T. E. Holland, J. Appl. Phys. 27, 963 (1956).*
- [4] R. Kh. Kurbangalina, Candidate's Dissertation [In Russian] (Inst. Chem. Phys. Acad. Sci. USSR, Moscow, 1947).
- [5] A. Stettbacher, Gunpowders and Explosives (ONTI, Moscow, 1936) p. 104 [Russian translation].

Received April 24, 1958

*Original Russian pagination. See C.B. Translation.

VAPOR PRESSURE OF AMMONIUM CHLORIDE SPENT LIQUORS IN SODA PRODUCTION (SOLVAY PROCESS)

L. N. Matusevich and K. N. Shabalín

(S. M. Kírov Polytechnic Institute of the Urals)

The literature contains a number of publications dealing with measures for preventing the formation of calcium sulfate deposits in distillation equipment. Many of these publications [1-3] agree in the view that incrustations can be prevented or eliminated by maintenance of appropriate temperature conditions in the mixer and the ammonia still.

In accordance with the temperature conditions, calcium sulfate may crystallize in different forms: as the dihydrate $\text{CaSO}_4 \cdot 2\text{H}_2\text{O}$, the hemihydrate $\text{CaSO}_4 \cdot 0.5\text{H}_2\text{O}$ and anhydrite, CaSO_4 . Each form has its own temperature region and its own solubility curve. When the liquors pass through the distillation equipment the temperature changes. The temperature is lower in the mixer than in the still, and the dihydrate is usually formed in the mixer; at temperatures above 93-95° this is converted into the hemihydrate and anhydrite in the still [4]. Some authors consider that the sole cause of calcium sulfate deposition on the equipment walls is the decrease in its solubility on increase of temperature owing to formation of the less soluble form. We believe that in this case general recrystallization of the deposit is of even greater significance, as in the course of this process even all the salt precipitated earlier has the tendency and opportunity to grow onto the walls in the course of this recrystallization.

The foregoing considerations lead to certain recommendations with regard to operating procedure, according to which the liquors treated in the distillation unit do not pass through the 93-95° range. This result may be achieved in two ways. The mixing procedure may be so organized that the temperature of the liquor in the mixer does not fall below 95° — this is the "hot" distillation regime. On the other hand, the liquor temperature can be maintained below 95° even at the bottom of the still — this is the "cold" regime.

In fact, work experience of many years, both here and abroad [2, 5], shows that both with the "hot" and the "cold" distillation regimes there is always less incrustation in the still caused by deposited calcium sulfate than is found under operating conditions in which the liquors pass through the 93-95° temperature range.

It is quite evident that with any temperature regime it is necessary to maintain definite pressure conditions in the still and mixer, because the liquid there is at the boil, and the vapor pressure of a solution of given composition is a definite function of the temperature.

Therefore for selection of a temperature regime for distillation it is necessary to know what pressure should be maintained in the distillation equipment.

The monograph by Mikulín and Polyakov [3] contains a review of publications dealing with determinations of vapor pressures in distillation equipment. However, the data presented there are very restricted; vapor pressures of solutions of different compositions are given only for one or two temperatures.

The purpose of the present investigation was to determine the vapor pressures of liquors in the distillation equipment in relation to their composition in the relevant temperature range.

It was decided to use the static method for the vapor pressure determinations. Of the many types of apparatus recommended for this purpose we selected the "manometric" type [6, 7]. The apparatus shown schematically in Fig. 1a was designed as the result of certain modifications and improvements.

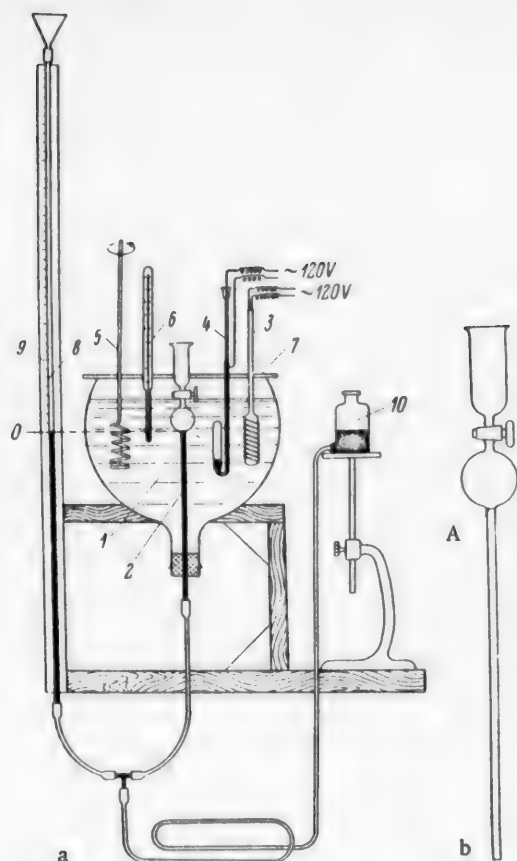


Fig. 1. Apparatus for determination of vapor pressures of solutions: a) general view of apparatus; b) glass buret; 1) thermostat; 2) buret; 3) heater; 4) thermoregulator; 5) stirrer; 6) thermometer; 7) lid; 8) manometer tube; 9) scale; 10) leveling vessel.

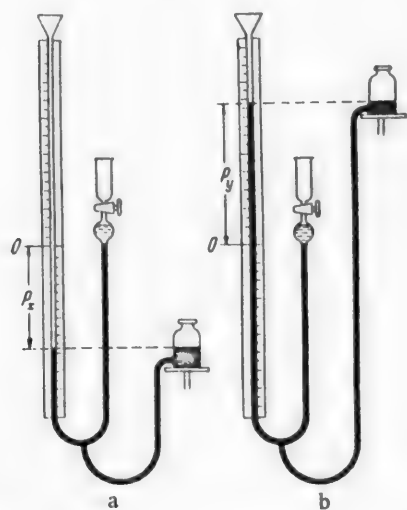


Fig. 2. Measurement of vapor pressures of solutions.

The main part of the apparatus is the thermostat 1 made from heat-resisting glass. A glass buret 2 is fixed in the thermostat from below by means of a rubber bung. The thermostat is equipped with a heater 3, a thermoregulator 4, a stirrer 5, and an accurate thermometer 6. The thermostatic liquid was glycerol, which made it possible to operate at temperatures up to 120° . The thermostat is covered by a cardboard lid 7, cut in half, to reduce evaporation of glycerol at high temperatures and to protect the buret stopcock from cooling. The lower end of the buret is connected by rubber tubes to a manometer tube 8 attached to the scale 9, and a leveling vessel 10 placed on a stand with a moving stage and filled with mercury purified by distillation under vacuum.

The glass buret (Fig. 1b) is a tube with a spherical bulb at the top, above which it is connected through a stopcock to a cylindrical beaker. Below the spherical bulb on the buret there is a mark A, clearly visible through glycerol, which coincides exactly with the zero mark on the scale 9 (Fig. 1a).

The procedure for determination of the vapor pressures of solutions was as follows. The leveling vessel was raised with the buret stopcock open, and the spherical bulb of the buret was filled with mercury, the air from it being displaced upward. The solution to be tested was then poured into the cylindrical beaker of the buret onto the raised mercury level. The leveling vessel was then lowered to draw a suitable portion of the solution into the bulb; about $4/5$ of the bulb volume, or about 15 cc, was filled with the solution. The buret stopcock was closed and the apparatus was ready for the experiment. The heater and stirrer were switched on and the thermoregulator was set to a definite temperature.

As the required temperature became established in the thermostat and the vapor pressure increased, the operator moved the leveling vessel so that a bubble of vapor formed over the solution, and then the position of the leveling vessel was adjusted so that the mercury level in the buret was exactly opposite the mark A. The mercury displaced from the buret passed into the leveling vessel, and the vapor bubble over the solution then occupied about $1/5$ of the volume of the spherical bulb. Since the manometer bulb is connected to the leveling vessel, the mercury levels in them were the same and could be read off on the scale 9.

The solution was held at each fixed temperature until the mercury level in the manometer tube became constant, showing that equilibrium had been attained. This usually required no more than 30-40 minutes. To check the accuracy of the manometer-tube readings, equilibrium was approached both from lower pressures (with gradual raising of the leveling vessel) and from

TABLE 1

Composition of Distillation Liquors

Solution No.	Solution composition					
	CaCl ₂		NaCl		NH ₃	
	g/liter	n.d.	g/liter	n.d.	g/liter	n.d.
1	134.5	48.5	61.1	20.9	39.2	46.0
2	115.2	41.5	54.9	18.8	35.3	41.5
3	147.9	53.3	67.2	23.0	43.1	50.6
4	134.5	48.5	61.1	20.9	25.6	30.0
5	134.5	48.5	61.1	20.9	34.1	40.0
6	134.5	48.5	61.1	20.9	42.6	50.0
7	134.5	48.5	61.1	20.9	51.1	60.0
8	138.8	50.0	58.5	20.0	—	—
9	119.3	43.0	49.7	17.0	—	—

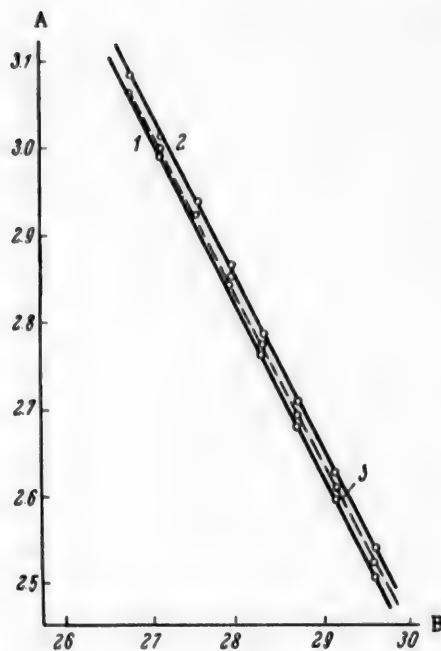


Fig. 3. Vapor pressure-temperature relationships for solutions No. 1-3: A) $\log p$; B) $1/T \cdot 10^4$; solutions: 1) No. 1; 2) No. 2; 3) No. 3.

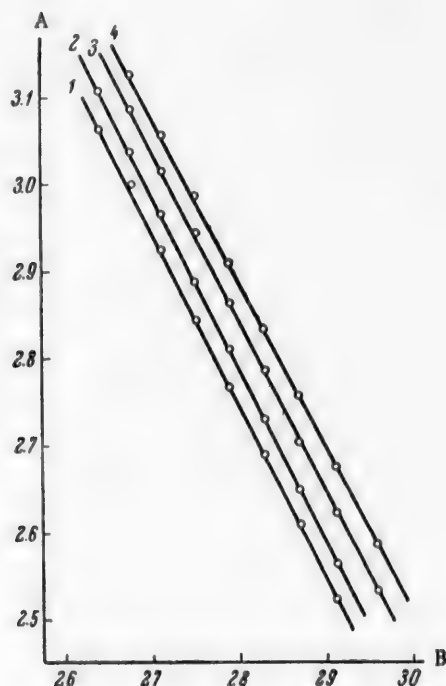


Fig. 4. Vapor pressure-temperature relationships for solutions No. 4-7: A) $\log p$; B) $1/T \cdot 10^4$; solutions: 1) No. 4; 2) No. 5; 3) No. 6; 4) No. 7.

higher pressures (with gradual lowering of the leveling vessel). When the manometer-tube readings coincided for the two procedures the experiment at the given temperature was taken to be completed, and the total equilibrium vapor pressure over the solution was found from the position of the mercury in the manometer tube and the barometric pressure.

At vapor pressures below atmospheric, the mercury in the measuring tube is below the scale zero (Fig. 2a) and the vapor pressure of the solution p_s is expressed as the difference:

$$p_s = P_{\text{atm}} - (p_x + \Delta p),$$

TABLE 2

Composition of Absorber Liquors

Solution No.	Solution composition							
	Na ₂ CO ₃		NaCl		NH ₄ Cl		NH ₄ OH	
	g/liter	n.d.	g/liter	n.d.	g/liter	n.d.	g/liter	n.d.
10	95.4	36	157.8	54	96.3	36	103.4	95
11	95.4	36	157.8	54	96.3	36	120.9	105

where P_{atm} is the barometric pressure (in mm Hg); p_x is the scale reading from 0 to the mercury level (mm Hg), and Δp is the hydrostatic pressure of the solution itself in the buret, which depends on the height of the solution column and its density (mm Hg).

In the region of higher pressures the mercury level in the measuring tube becomes established above the scale zero (Fig. 2b) and the vapor pressure of the solution is expressed as the sum:

$$p_s = P_{\text{atm}} + (p_y - \Delta p).$$

With this apparatus it is possible to determine the equilibrium vapor pressures of a given solution at different temperatures without recharging of the apparatus with the solution. It proved to be convenient to perform the first determination at the lowest temperature, and then to pass gradually to higher temperatures.

To test the accuracy of the results obtained with this apparatus, the vapor pressures of pure water were determined. It was found that in the low-temperature region (40–60°) the results are accurate to within ± 1 mm Hg, and at higher temperatures (100–120°) and therefore higher pressures, within ± 10 mm Hg, or $\pm 1\%$.

The compositions of the solutions used for the vapor-pressure determinations are given in Tables 1 and 2. The contents of the components of each solution are given in grams per liter and also in normal divisions* (n.d.) as is usual in the soda industry.

The first solutions to be tested were No. 1–7, which corresponded in composition to the liquors at the top of the still and in the mixer. Solution No. 1, containing 69.4 n.d. Cl[−] and 46 n.d. NH₃, corresponds in composition to the average concentration of the distillation liquors in soda plants. The concentrations of all the components in solutions No. 2 and 3 were respectively weaker and stronger by 10% than this main solution. Solutions No. 4–7 did not differ from the main solution in their CaCl₂ and NaCl contents, but had different NH₃ concentrations.

The temperature range of the investigation was chosen to include temperatures above and below the transition temperatures of calcium sulfate modifications – 93–95°.

Our results are in good agreement with the individual data found in the literature. For example, Terashkevich, Danil'chenko and Babkina [8] determined the vapor pressures at 85 and 95° of solutions No. I and II, similar in composition to two of our solutions (No. 3 and 4 respectively). The numbers of our solutions, their composition, and our results are indicated in parentheses below.

Solution No.	Solution composition (n.d.)			Pressure (mm Hg)	
	NH ₃	CaCl ₂	NaCl	85°	95°
I	50.9	41.0	14.2	721	1019
(3)	(50.6)	(53.3)	(23.0)	(731)	(1027)
II	30.8	41.7	14.5	581	835
(4)	(30.0)	(48.5)	(20.9)	(588)	(838)

*A normal division (n.d.) corresponds to 1/20 g-equiv of substance per liter of solution.

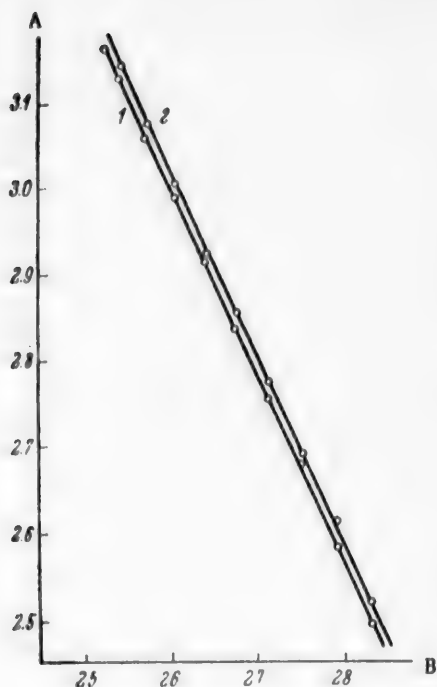


Fig. 5. Vapor pressure-temperature relationships for solutions No. 8 and 9: A) $\log p$; B) $1/T \cdot 10^4$; solutions: 1) No. 8; 2) No. 9.

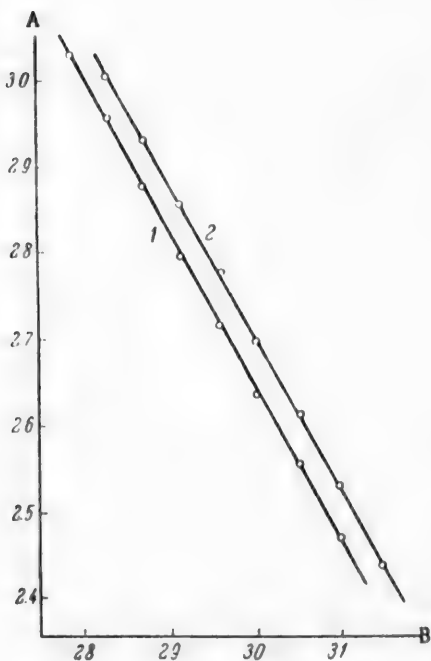


Fig. 6. Vapor pressure-temperature relationships for solutions No. 10 and 11: A) $\log p$; B) $1/T \cdot 10^4$; solutions: 1) No. 10; 2) No. 11.

It is known [9] that the relationship between vapor pressure and temperature over a narrow temperature range may be represented by the equation

$$\log p = A - \frac{B}{T},$$

where A and B are constants for the given solution.

Our experimental data were plotted in $\log p - 1/T$ coordinates as shown in Fig. 3 and 4. It is seen that the results are very satisfactorily linear. This confirms the validity of our determinations. It is especially important that by extrapolation of these straight lines it is possible to find p for temperatures outside the experimental temperature range.

It follows that in order to have a temperature above 93-95° in the mixer and the upper container of the still the pressure must be maintained at about 1000 mm Hg (absolute), with permissible variations between 900 and 1100 mm.

For selection of the temperature conditions in the still the pressure at the lower end of the apparatus as well as at the top is of interest. The latter pressure must be equal to the pressure at the top of the still, i.e., the vapor pressure of the liquor at the temperature of the top, plus the total resistance of the still, i.e., the total hydrostatic pressure of the liquid on all the plates. According to production data [3], the average value of this pressure is 200-300 mm, and depends on the still design and operating conditions.

For determination of the equilibrium vapor pressure of the liquid at the bottom of the still, solutions No. 8 and 9 (Table 1) were tested; these correspond in composition to the varying liquor concentrations at the still exit [10]. The temperature range investigated again included the transition temperatures, i.e., 93-95°. The maximum temperature in the determinations was so chosen that the pressure difference between the top of the still (as found in the previous determinations for temperatures above 95°) and the bottom was not less than the resistance indicated above, 300 mm Hg.

The experimental results for solutions No. 8 and 9 were again plotted in $\log p - 1/T$ coordinates (Fig. 5). It is seen that the experimental points again fit exactly on a straight line. The pressure over the solution in this case is due only to the water-vapor pressure.

The results of this part of the investigation show that if the "hot" distillation regime is required, with the temperature of the liquid in the upper part of the still not below 95°, the temperature at the bottom of the still must be not less than 117-118°, for which a pressure of about 1300 mm must be maintained there. Under the "cold" regime the temperature of the exit liquor must not exceed 95°, which corresponds to a pressure of about 600 mm at the bottom. The pressure at the top of the still and in the mixer must be 600-300 = 300 mm Hg (absolute), which is a very considerable degree of vacuum.

The above results can also be used for correct choice of the characteristics of the steam fed into the still.

Any change in the temperature regime in the still results in corresponding changes of pressure, not only in the still and mixer, but also in the absorber, the operation of which is interconnected with that of the still.

Solutions No. 10 and 11, the compositions of which are given in Table 2, were prepared for determinations of vapor pressure of the liquid at the bottom of the absorber.

These solutions, which differed only in their NH_3 concentrations, corresponded in composition to the usual solutions leaving the absorber [10]. In these experiments the temperature range was so chosen that the pressure difference between the top of the still (from our earlier experiments on "hot" and "cold" distillation regimes) and the lower part of the absorber where the gas from the still enters was not less than 150-200 mm, which corresponds to the resistance of the intermediate equipment (heat exchanger and condenser), in accordance with production data [3].

The results of this part of the investigation are plotted in Fig. 6. In this case the pressure over the solution is the sum of the partial pressures of NH_3 , CO_2 , and water vapor.

Figure 6 shows that a plot of the experimental points $\ln p = f(1/T)$ coordinates is again satisfactorily linear.

The data in Fig. 6, in conjunction with the data in Fig. 3 and 4, show that under the "hot" distillation regime the pressure at the bottom of the absorber should be maintained at about 800-850 mm, which corresponds to a liquor temperature of about 75° . Under the "cold" regime there should be a considerable degree of vacuum at the bottom of the absorber. Even if the resistance of the intermediate equipment is reduced (by the use of heat exchangers of the scrubber type) its value would be 100-150 mm, changing further at the point of entry to the absorber to 300-100 = 200 mm (absolute). The temperature at the bottom of the absorber must then be maintained at 40° .

SUMMARY

1. A manometric apparatus was designed and used to determine vapor pressures of ammonium chloride Solvay liquors over a wide temperature range.
2. The experimental data give satisfactory linear plots $\ln p - 1/T$ coordinates; this confirms their accuracy and allows extrapolation.
3. The results can be used for predetermination of pressures in distillation equipment in order to establish given temperature conditions intended to diminish incrustation of the equipment walls.

LITERATURE CITED

- [1] V. E. Voronchikhin, J. Chem. Ind. 13, 24, 1486 (1936).
- [2] Ya. R. Gol'dshtein, Trans. All-Union Inst. Soda Industry 5, 163 (1949).
- [3] G. I. Mikulin and L. K. Polyakov, Distillation in the Soda Industry [In Russian] (Goskhimizdat, 1956).
- [4] V. R. Terashkevich, S. S. Urazovskii, R. E. Shtok and É. M. Éidelman, J. Chem. Ind. 16, 8, 12 (1939).
- [5] G. I. Mikulin, Trans. All-Union Inst. Soda Industry 6, 91 (1952).
- [6] K. N. Shabalín and V. S. Udintseva, J. Chem. Ind. 3, 2, 165 (1930).
- [7] N. D. Litvinov, Industrial Lab. 9, 5-6, 583 (1940).
- [8] V. R. Terashkevich, E. M. Danil'chenko and V. Yu. Babkina, Trans. Ukrainian State Sci. Res. Inst. Appl. Chem. 3, 1, 31 (1937).
- [9] A. V. Rakovskii, Introduction to Physical Chemistry [In Russian] (ONTI, Moscow, 1938).
- [10] V. F. Chernov, Production of Soda Ash [In Russian] (Goskhimizdat, Moscow, 1956).

Received April 2, 1958

INVESTIGATION OF ABSORPTION RATES IN HORIZONTAL MECHANICAL ABSORBERS WITH THE AID OF THE SIMILARITY PRINCIPLE

S. N. Ganz and M. A. Lokshin

(Dnepropetrovsk Institute of Chemical Technology)

Mass-transfer processes under conditions of high turbulence take place under the combined influence of numerous physicochemical and hydrodynamic factors which determine the process kinetics.

In view of the great diversity of the conditions which influence absorption processes in high-speed mechanical absorbers [1-4], investigation of such processes is very complicated.

The mutual influence of these conditions may be investigated with the aid of the similarity principle; the rate of mass transfer in mechanical absorbers is determined by the following functional relationship:

$$\varphi(\rho_L, \rho_G, \mu_L, \mu_G, D_L, D_G, V_L, V_G, n_s, g, x_G, c_L, D_a, L_a, d_d, b, H, a, K_g) = 0, \quad (1)$$

where d_d is the disk diameter (m), D is the internal diameter of the absorber (m), b is the vane width (measure of the vane projection area (m)), a is the vane height (m), H is the height of the liquid level in the absorber (m), ρ_L is the density of the liquid ($\text{kg} \cdot \text{sec}^2/\text{m}^4$), ρ_G is the density of the gaseous medium ($\text{kg} \cdot \text{sec}^2/\text{m}^4$), μ_L is the dynamic viscosity coefficient of the liquid ($\text{kg} \cdot \text{sec}/\text{m}^2$), μ_G is the dynamic viscosity coefficient of the gaseous medium ($\text{kg} \cdot \text{sec}/\text{m}^2$), D_L is the coefficient of molecular diffusion in the liquid (m^2/second), D_G is the coefficient of molecular diffusion in the gas (m^2/second), V_G is the linear velocity of the gaseous mixture (m/second), V_L is the linear velocity of the liquid (m/second), n_s is the number of revolutions of the disks per second (1/sec), g is the acceleration due to gravity (m/sec^2), x_G is the concentration of the absorbed component in the gas (kg/m^3), c_L is the concentration of the absorbent (kg/m^3), and K_g is the coefficient of absorption ($\text{kg}/\text{m}^3 \cdot \text{sec} \cdot \text{kg}/\text{m}^3 = 1/\text{m} \cdot \text{sec}$).

The number of disks z_d in the absorber was 4, and the number of vanes z_v on each disk was 12-16.

The method of dimensional analysis [5-8] was used, after transformation of Eq. (1), to derive the functional expression for the diffusional criterion, which incorporates the similarity criteria for the hydrodynamic and physicochemical conditions of mass transfer in mechanical absorbers:

$$K_i' = K_g \frac{d_d^3}{D_G} = A \cdot \text{Re}_G^{\alpha} \cdot \text{Re}_L^{\beta} \cdot (\text{Pr}_G')^{\gamma} \cdot (\text{Pr}_L')^{\delta} \cdot \left(\frac{n_s d_d^2}{D_L} \right)^{\omega} \cdot \text{Ga}^{\epsilon} \cdot \left(\frac{x_G}{\rho_L g d_d} \right)^{\phi} \times \\ \times \left(\frac{c_L}{\rho_L g} \right)^{\delta} \cdot S_{\text{diff}}^{\eta} \cdot \Gamma_L^{\alpha} \cdot \Gamma_b^{\beta} \cdot \Gamma_H^{\gamma}, \quad (2)$$

where $\text{Re}_G = V_G d_d \rho_G / \mu_G$ is the Reynolds number for the gas; $\text{Re}_L = V_L d_d \rho_L / \mu_L$ is the Reynolds number for the liquid; $\text{Pr}_G' = \mu_G / \rho_G D_G$ is the analog of the Prandtl number for the gas; $\text{Pr}_L' = \mu_L / \rho_L D_L$ is the analog of the Prandtl number for the liquid; $n_s d_d^2 / D_L$ is a criterion characterizing the action of centrifugal force; $\text{Ga} = g d_d^3 / \nu_L$ is the Galileo criterion; $x_G / \rho_L g d_d$ is the criterion of proportionality of the concentration fields

ν_L is the kinematic coefficient of viscosity of the liquid (in m^2/second).

In the gas phase; $c_L/\rho_L g$ is the criterion of proportionality of the concentration fields in the liquid phase; $Ki^* = K_g d_d^3/D_G$ is the Kirpichev diffusional criterion; $S_{dif} = D_G/D_L$ is the diffusion ratio; $G_L = L_a/d_d$, $G_b = b/d_d$, $G_H = H/d_d$ are geometrical similarity ratios.

To determine the values of the indices and of the dimensionless coefficient A in the above expression, Eq. (2) was reduced to the form:

$$K_g = A \cdot \frac{36 \cdot 10^6 D_G}{d_d^3} \cdot Re_G^x \cdot Re_L^y \cdot (Pr_G^*)^z \cdot (Pr_L^*)^\beta \cdot \left(\frac{\eta_s d_d^2}{D_L} \right)^\omega \cdot \left(\frac{r G}{\rho_L g d_d} \right)^\psi \times \\ \times \left(\frac{r L}{\rho_L g} \right)^\delta \cdot Ga^s \cdot S_{dif}^q \cdot \Gamma_L^a \cdot \Gamma_b^p \cdot \Gamma_H^r \left[\frac{kg}{m^3 \cdot hr \cdot atmos} \right]. \quad (3)$$

Equation (3) represents the rate of absorption of a moderately-soluble gas, when the process is determined by diffusional resistance of both the gas and the liquid films. If the gas is very soluble or sparingly soluble, the process is determined by only one film resistance. Therefore in the absorption of a very soluble gas, the term Pr_L^* vanishes from Eq. (3). In the absorption of a sparingly-soluble gas the terms Pr_G^* and Re_G vanish.

The influence of characteristic equipment dimensions and hydrodynamic and physicochemical process factors on the rate of absorption of nitrogen oxides by aqueous nitric acid solutions was studied, and the results were correlated with the aid of Eq. (3).

The effect of the linear velocity of the liquid on the rates of absorption of NO_2 by water and 5% HNO_3 was studied at 10% concentration of $(NO + NO_2)$ in the gas, at $t = 20^\circ$; the fraction of the absorber volume filled with liquid, φ , was 0.209, $n = 2900$ rpm, $b/d_d = 0.147$, and the gas flow rate $W_G = 100-2100 \text{ m}^3/\text{m}^3 \cdot \text{hour}$. The linear velocity of the liquid was varied in the range of 0.012-0.327 m/second. The results are plotted in Fig. 1. It follows from these results that the linear liquid velocity has less influence than other hydrodynamic factors on the absorption coefficient, as the velocity of the liquid transported by the disks at right angles to its flow along the apparatus is many times greater than its horizontal velocity. The ratio between the amounts of liquid and gas in the apparatus, determined by the ratio H/d_d , is more significant in the absorption process.

To determine the relationship between K_g and H/d_d a series of experiments was performed in which H/d_d was varied in the range of 0.159 to 0.294, which corresponded to 0.088-0.209 for the fraction of absorber volume filled. Apart from the factors already indicated, $V_L = 0.025$ m/second and $b/d_d = 0.147$ were also kept constant in this series. The results are plotted in Fig. 2. It is seen that the absorption coefficient also increases with increase of the amount of liquid in the apparatus. However, the higher the curves lie the less is the distance between them, and there is an optimum value of H/d_d above which further filling of the apparatus is not only useless but even harmful [9].

The next series of experiments was concerned with a study of the effect of angle of set of the disk vanes on the absorption coefficient at different W_G . The angle of set of the vanes determines their frontal area, and therefore the degree of agitation and pulverization of the liquid, frictional forces, and power consumption. With the initial factors kept constant, we varied b/d_d in the range of 0.05-0.18 at $W_G = 300-2100 \text{ m}^3/\text{m}^3 \cdot \text{hour}$ and $V_L = 0.025$ m/second. The results of this series of experiments are presented in Fig. 3, which shows that the angle of set of the vanes has a significant influence on the process rate. The greater the frontal area, the more the amount of liquid actively taking part in the absorption process, and the higher the value of K_g .

The dependence of K_g on the ratio L_a/d_d was next studied. This study was performed at gas rates from 300 to 2100 $\text{m}^3/\text{m}^3 \cdot \text{hour}$. In this series of experiments the volume of liquid in the apparatus was kept constant ($\varphi = 0.196$) in addition to the other constant factors indicated above. The results are plotted in Fig. 4. It is seen that the curves for L_a/d_d as a function of the gas rate first ascend steeply, then their slope diminishes, and finally they tend to become parallel to the abscissa axis. There is therefore an optimum L_a/d_d ratio which, in relation to the design features of the apparatus, should be taken as 2.5-2.6.

It was stated earlier that the experiments were performed in absorbers with four disks. The choice of a

*In the range of $W_G = 300-1300$, the curves in logarithmic coordinates are linear.

**At $W_G > 1300$.

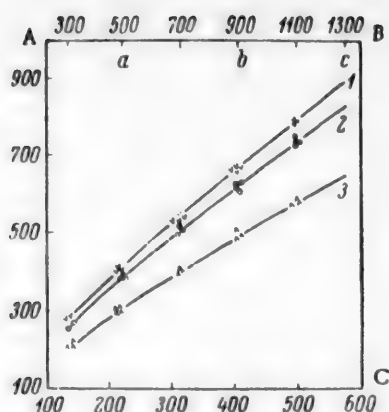


Fig. 1. Variations of the absorption coefficient of nitrogen oxides K_g with the gas rate W_g and the liquid velocity V_L : $t = 20^\circ$, $n = 2900$ rpm, absorbent 5% HNO_3 , $\varphi = 0.209$ [$NO + NO_2$] = 10%, $b/d_d = 0.147$; A) absorption coefficient K_g ($kg/m^3 \cdot hr \cdot atm$); B) gas rate W_g ($m^3/m^3 \cdot hour$); C) Re_G ; liquid velocity (m/sec): 1) 0.0327; 2) 0.025; 3) 0.012.

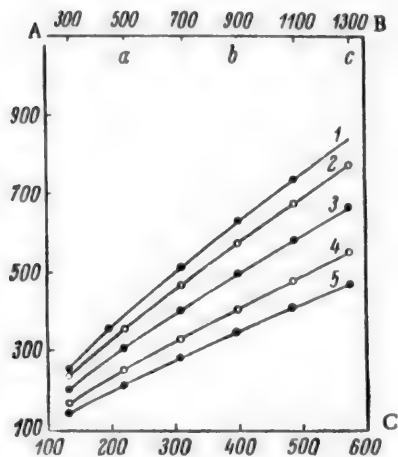


Fig. 3. Variations of the absorption coefficient with the gas rate W_g and the ratio b/d_d : $t = 20^\circ$, $n = 2900$ rpm, absorbent 5% HNO_3 , $\varphi = 0.196$, [$NO + NO_2$] = 10%, $H/d_d = 0.278$, $V_L = 0.025$ m/sec; A) absorption coefficient K_g ($kg/m^3 \cdot hr \cdot atm$); B) gas rate W_g ($m^3/m^3 \cdot hr$); C) Re_G ; ratio b/d_d : 1) 0.180; 2) 0.147; 3) 0.107; 4) 0.070; 5) 0.050.

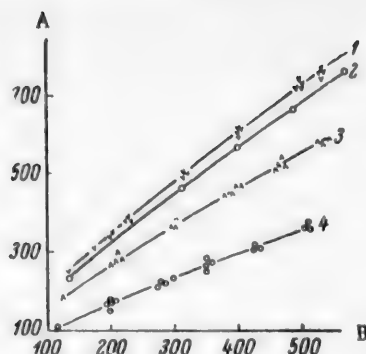


Fig. 2. Variations of the absorption coefficient with the H/d_d ratio and the gas rate W_g : $t = 20^\circ$, $n = 2900$ rpm, absorbent 5% HNO_3 , [$NO + NO_2$] = 10%, $b/d_d = 0.147$, $V_L = 0.025$ m/sec; A) absorption coefficient K_g ($kg/m^3 \cdot hr \cdot atm$); B) $Re_G \approx W_g$; values of H/d_d and φ respectively: 1) 0.294, 0.209; 2) 0.278, 0.0196; 3) 0.233, 0.153; 4) 0.159, 0.088.

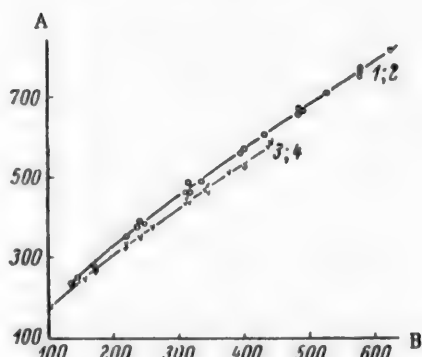


Fig. 4. Variations of the absorption coefficient with the ratio L/d_d and gas rate W_g : $t = 20^\circ$, $n = 2900$ rpm, absorbent 5% HNO_3 , $\varphi = 0.196$, [$NO + NO_2$] = 10%, $b/d_d = 0.147$, $V_L = 0.025$ m/sec; A) absorption coefficient K_g ($kg/m^3 \cdot hr \cdot atm$); B) $Re_G \approx W_g$; ratio L/d_d : 1) 5.950; 2) 4.762; 3) 2.235; 4) 1.635.

four-disk absorber was based on the results of earlier experiments with five-disk apparatus, in which samples of gas and liquid were taken after each disk for analysis, and the analytical results were used for calculating the degree of conversion of nitrogen oxides in each disk zone. The same method was used in a pilot unit in absorption of nitrogen oxides by water and $Ca(OH)_2$ solution, and also in an experimental production unit in absorption of nitrogen oxides by $Ca(OH)_2$ solution.

TABLE 1

Zone	Concentration of HNO_3 in solution (%)	Exponents and coefficient					
		δ	s	β	q	$\log A$	
I	5-20%	-0.011	0.062	0.835 c_L	-0.467 c_L	-15.46	-0.5133 c_L
II	20-30%	-0.300	0.058	0.24 c_L	4.56 c_L	-11.7773	-18.927 c_L

* c_L is the concentration of absorbent (in hundredths).

TABLE 2

Exponents and coefficient	Exponents and coefficient at HNO_3 concentrations of								
	5%	10%	15%	20%	25%	30%	35%	40%	
δ	-0.011	-0.011	-0.011	-0.011	-0.300	-0.300	-0.300	-0.300	-0.300
s	0.062	0.062	0.062	0.062	0.058	0.058	0.058	0.058	0.058
β	-0.266	-0.225	-0.183	-0.141	-0.144	-0.132	-0.120	-0.108	-0.108
q	1.01	0.986	0.963	0.940	0.137	1.365	1.593	1.82	1.82
A	32685 $\cdot 10^{-20}$	31194 $\cdot 10^{-20}$	29040 $\cdot 10^{-20}$	27370 $\cdot 10^{-20}$	3097 $\cdot 10^{-20}$	354.3 $\cdot 10^{-20}$	39.66 $\cdot 10^{-20}$	4.485 $\cdot 10^{-20}$	

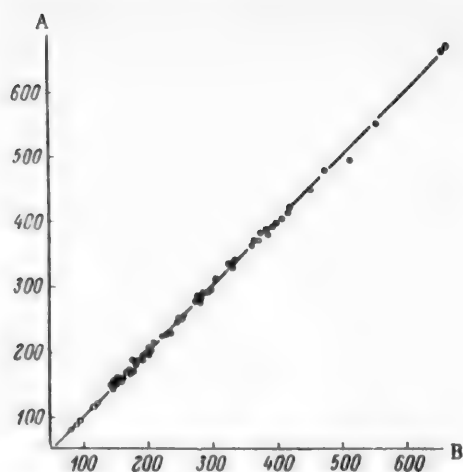


Fig. 5. Correlation graph for the system $\text{NO}_2\text{--HNO}_3$: A) experimental value of $Ki_e \cdot 10^6$; B) theoretical value of $Kl_T \cdot 10^6$, calculated by Eq. (4).

All these experiments showed that the most complete absorption of nitrogen oxides with the least power consumption is attained with the use of four disks. Average experimental data on the absorption of nitrogen oxides by water at $W_G = 700 \text{ m}^3/\text{m}^2 \cdot \text{hour}$, initial HNO_3 concentration = 20%, $V_g = 15 \text{ m/sec}$, concentration of $(\text{NO} + \text{NO}_2) = 8\%$ (degree of oxidation of $\text{NO} = 82\%$), at $t = 26\text{--}27^\circ$ are given below.

Disk zones	0—1	0—2	2—3	3—4	4—5
Absorption	20—24.8	24.8—48	48—62	62—64.5	64.5—65

$(\text{NO} + \text{NO}_2) = 8\%$.

It follows from the above data that the degree of conversion of nitrogen oxides in the fifth disk zone is very low, and does not justify the power consumption for the fifth disk. Therefore all the subsequent experiments were performed in four-disk absorbers.

In accordance with the experimental data detailed in earlier papers [1-4], the analytical method [10] was used for determining the values of the indices in Eq. (3) for the ab-

sorption of nitrogen oxides by water and aqueous nitric acid solutions.

The general critical mass-transfer equation for the system nitrogen oxides-nitric acid in horizontal absorbers is of the form:

$$Ki' = A \cdot Re_G^{0.81} \cdot Re_L^{0.315} \cdot \left(\frac{n_3 d_d^2}{D_L} \right)^{0.736} \cdot Ga^{\delta} \cdot Pr_G^{0.436} \cdot Pr_L^{\beta} \cdot \left(\frac{x_G}{\rho_L g d} \right)^{0.236} \cdot \left(\frac{c_L}{\rho_L} \right)^{\gamma} \cdot S_{dif}^q \cdot \Gamma_L^{-0.36} \cdot \Gamma_b^{0.462} \cdot \Gamma_H^{1.16}, \quad (4)$$

where δ , β , γ and q are indices, and A is the coefficient. Their values for different concentrations of HNO_3 in solution are given in Table 1.

The coefficient A was found from the general criterial equation, when

$$Ki' = \frac{K_g \cdot d_d^3}{D_G \cdot 36 \cdot 10^6}. \quad (5)^*$$

The agreement between experimental values and values calculated by Eq. (4) is illustrated by the correlation graph in Fig. 5.

The applicability of Equation (4) was verified in numerous experiments under the following conditions:

$$\begin{aligned} t &= 20\text{--}60^\circ, & c_L &= 2\text{--}40\% \text{ HNO}_3 \\ x_G &= 0.6\text{--}10\%, & W_G &= 400\text{--}1300 \text{ m}^3/\text{m}^2 \cdot \text{hr} \\ V_L &= 0.012\text{--}0.4 \text{ m/sec. and over}, & n &= 800\text{--}2900 \text{ rpm} \\ L_a/d_d &= 1.6\text{--}6.0, & b/d_d &= 0.07\text{--}0.18, & H/d_d &= 0.16\text{--}0.3. \\ & & \text{at } \varphi &= 0.08\text{--}0.22). \end{aligned}$$

*Any experimental value of K_g in $\text{kg}/\text{m}^2 \cdot \text{hour} \cdot \text{atmos}$ was taken.

SUMMARY

1. The derived criterial Equation (2) represents with adequate accuracy the process of absorption in mechanical (rotary) high-speed absorbers.
2. Experimental and calculated values of KI' lie very close together on the linear correlation graph, which shows that Eq. (4) represents fairly accurately the absorption of NO_2 by aqueous solutions of HNO_3 in mechanical absorbers.

LITERATURE CITED

- [1] S. N. Ganz and S. L. Kapturova, J. Appl. Chem. 28, No. 6 (1955).*
- [2] S. N. Ganz, M. A. Lokshin and S. L. Kapturova, J. Appl. Chem. 28, No. 8 (1955).*
- [3] S. N. Ganz, J. Appl. Chem. 28, No. 10 (1955).*
- [4] S. N. Ganz, J. Appl. Chem. 30, No. 6 (1957).*
- [5] M. V. Kirpichev, Proc. Acad. Sci. USSR, OTN, No. 4-5 (1945).
- [6] P. G. Romankov, Hydraulic Processes in Chemical Technology [In Russian] (Goskhimizdat, 1948).
- [7] L. S. Élgenson, Modeling [In Russian] (Soviet Science Press, 1952).
- [8] G. K. D'yakonov, The Similarity Principle in Physicochemical Processes [In Russian] (Acad. Sci. USSR Press, 1956).
- [9] S. N. Ganz, J. Appl. Chem. 30, No. 9 (1957).*
- [10] M. D. Kuznetsov, J. Appl. Chem. 21, No. 1, 48 (1948).

Received February 7, 1958

*See C.B. Translation.

STUDY OF OXIDATION-SULFATION ROASTING OF SULFIDE ORES IN A FLUIDIZED BED IN A MODEL BATCH FURNACE

V. V. Pechkovskii and S. A. Amirova

(A. M. Gor'kii State University, Perm')

Sulfation roasting of sulfide ores in fluidized beds is now used fairly often in chemical industry and non-ferrous metallurgy [1-3]. Sulfation roasting is a complex process, some aspects of which are still obscure. The hypothesis according to which sulfates may be formed by two routes [4] is prominent at the present time among the numerous views concerning the mechanism of sulfate formation during oxidative roasting of sulfides. According to this hypothesis, the conversions which jointly result in the formation of sulfates by the oxidation of bivalent-metal sulfides may be schematically represented as follows:



It has now been proved experimentally that sulfates in presence of sulfides have reduced thermal stability and decompose more rapidly [4, 5]. It is therefore believed that the final roasting products contain mainly sulfates formed by reactions (3) and (4).

The purpose of the present investigation was to study the formation of cobalt sulfate in the roasting of flotation pyrite in a fluidized bed in a laboratory furnace. The aspects studied were loss of material in dust form from the furnace, and the effect of temperature on the degree of sulfation of cobalt and combustion of sulfur, the roasting time, the particle size of the roasted material, and the sample weight.

EXPERIMENTAL •

The material used was flotation pyrite containing Fe 36.0%, S 38.5%, Co 0.7% and other components, and cinders obtained from this pyrite by oxidative roasting at 800-850°. Flotation pyrite containing over 0.5% Co is usually called cobalt concentrate [6].

The apparatus consisted of a furnace, cyclone, rheometer, and a compressed-air cylinder. The furnace was a quartz tube with a drawn-out lower end. The principal dimensions of the reaction tube were (in mm): internal diameter of wide part, 23, of narrow part, 7.3; length of wide part, 500, of narrow part, 235. The transition from the wide to the narrow part of the tube was in the shape of a smoothly narrowing cone.

The material was fed in from above through a special feed device with the air turned on. To terminate an experiment the air was turned off, when the material immediately fell through the narrow end of the reaction tube into a quartz tray. The gaseous roasting products passed through the cyclone into the atmosphere. Pure cobalt concentrate and mixtures of concentrate with cinders were roasted. The furnace was fed with nongranulated material, or with material in the form of granules of definite size. Sulfite waste liquor was used as binder for granulation of the cinders and concentrate. Small (4-6 g) and large (40-50 g) samples were used. The height

•V. V. Parkacheva took part in the experimental work.

TABLE 1

Effect of Granule Size on Bulk Density of Cobalt Concentrate and Cinders

	Bulk density (g/cc) at granule size (mm)		
	0.25-0.5	0.1-0.25	non-gran
Concentrate	1.42	1.84	1.56
Cinders	0.87	1.14	1.10

TABLE 2

Effects of Temperature and Duration of Roasting on the Degree of Sulfur Combustion and Sulfation of Cobalt. Sample: 5.0 g concentrate + 1.0 g cinders; granule size > 0.1 to < 0.25 mm; air velocity 0.12 m/second

Duration of experiment (min)	Temperature				
	425°	475°	525°	575°	675°
Degree of sulfur combustion (%)					
5.0	26.2	48.5	60.5	85.0	95.5
10.0	30.4	59.5	76.0	97.1	98.6
15.0	33.1	68.9	84.3	98.7	99.2
30.0	40.0	79.4	91.1	98.8	99.2
Degree of cobalt sulfation (%)					
5.0	31.2	51.7	60.9	48.2	0
10.0	39.8	55.2	66.7	51.7	0
15.0	44.2	60.4	68.1	53.4	0
30.0	45.3	60.4	67.9	53.0	0

temperature the tip of a thermocouple in a quartz sheath was immersed directly in the center of the fluidized bed. After each experiment the sulfur, and total and water-soluble cobalt in the cinders and cyclone dust were determined [7].

Finally, it must be pointed out that the laboratory model batch furnace used in our experiments is now used fairly extensively for studying the kinetics of oxidative roasting of various sulfides and sulfide ores in the fluidized state [8, 9].

The principal experimental results are presented in Tables 1-4.

First, it was established that dust loss depends on the linear air velocity, temperature, grain size, and physicochemical properties of the material. Dust loss in the roasting of nongranulated concentrate and cinders reaches 50-60% of the amount of material charged into the furnace. Dust loss is reduced sharply by granulation of the cinders and concentrate. With granulated cinders the dust loss does not exceed 10%, and is almost independent of the temperature. Somewhat different results are observed in the roasting of granulated cobalt concentrate. When granulated cobalt concentrate is roasted at 425-450° the dust loss does not exceed 2-3%, but it increases with temperature and at 700-725° it is about 18-22%. The increase of dust loss with increase of the roasting temperature of granulated cobalt concentrate is caused by cracking of the pyrite particles during conversion into ferrous sulfide [10].

of the fluidized material in the reaction tube was about 2 cm with the small samples, and 17-19 cm with the large samples.

The uniform fluidization regime depended on the linear velocity of the air passed through the reaction tube. This velocity was determined experimentally for each sample in a cold model of the furnace. The optimum linear velocity at which the material formed a dense and uniform fluidized layer without slugging or falling through to the tray depended on the weight of the sample and its particle size; it varied in our experiments from 0.111 to 0.165 m/second. It was found that the agitation intensity of the material varies with the air velocity, particle size of the material, and the fluidization height. It was also noticed that when a mixture of cinders and concentrate is fluidized, under certain conditions the material tends to separate out: the upper part of the layer becomes richer in cinders, and the lower, in concentrate. For studying the composition of the material along the height of the fluidized bed, the material was lowered into the lower drawn-out end of the tube, and the whole sample was then divided along its height into four roughly equal parts. It was found that the separation of the material along the height of the fluidized bed depends on the agitation intensity. The separation effect diminishes or becomes negligible at high agitation intensities. The actual effect of separation of the cinders and concentrate in the fluidized bed is due to differences in the true and bulk densities of these substances. The bulk densities of cinders and concentrate are given in Table 1.

To maintain a definite temperature in the furnace, the quartz tube was wound around with a Nichrome coil and covered with a thin layer of asbestos insulation. The voltage in the furnace winding was regulated by means of an autotransformer. For measurements of

TABLE 3

Effects of Duration of Roasting on the Degree of Sulfur Combustion and Sulfation of Cobalt. Sample: 42.1 g of concentrate; granule size > 0.25 to < 0.5 mm; temperature 475°

Duration of expt. (min)	No. of sample downward from top	Degree of sulfur combustion (%)	Sulfur content of sample (%)	Degree of cobalt sulfation (%)
15.0	1	48.2	19.6	21.5
	2	49.2	19.3	21.5
	3	49.2	19.3	21.5
	4	40.0	22.8	19.7
30.0	1	87.0	5.0	66.0
	2	83.1	6.4	66.0
	3	83.1	6.4	66.0
	4	81.4	7.1	54.0
40.0	1	91.0	3.0	70.0
	2	89.0	4.2	70.0
	3	86.2	5.2	70.0
	4	85.8	5.4	70.0

TABLE 4

Effects of Granule Size on the Degree of Sulfur Combustion and Sulfation of Cobalt. Duration of experiment 15 minutes, sample: 21.0 g of concentrate + 12.7 g of cinders

Temperature (deg)	No. of sample downward from top	Sulfur content of sample (%)			Degree of cobalt sulfation (%)		
		> 0.1 to < 0.25 mm	> 0.25 to < 0.5 mm	> 0.5 mm	> 0.1 to < 0.25 mm	> 0.25 to < 0.5 mm	> 0.5 mm
475	1	15.9	6.8	46.3	62.4		
	2	17.0	8.0	45.6	58.0		
	3	17.0	8.8	45.6	59.0		
	4	17.3	12.0	43.2	59.0		
580	1	6.8	0.6	16.8	27.3		
	2	7.6	0.8	16.8	27.3		
	3	8.0	1.0	16.8	27.3		
	4	10.4	1.6	14.9	23.6		

Note: > 0.1 to < 0.25 mm and > 0.25 to < 0.5 mm are the granule size ranges.

than with large samples. Moreover, there is some decrease in the rate of sulfur combustion at the initial stage because of a decrease in the agitation intensity. It was found that the agitation intensity is greater in large than in small samples. In particular, this is indicated by the fact that when a small sample is roasted there is no separation of the material along the height of the bed, whereas with large samples, as Tables 3 and 4 show, there is a fairly distinct variation in the composition of the material up the bed. The material is somewhat richer in sulfide sulfur at the lower end.

Data on the degree of sulfation of cobalt during roasting of cobalt concentrate in a fluidized bed are

It was found that the combustion rate of sulfur and the degree of sulfation of cobalt when cobalt concentrate is roasted in a fluidized bed depend on the temperature, roasting time, grain size, and agitation intensity.

Results obtained for 6.0 g samples of concentrate and cinders are given in Table 2. It follows from Table 2 that the sulfur combustion rate increases sharply with temperature up to 550°, changes little in the 550-650° range, and is almost independent of temperature above 650°. These results indicate that up to 550° the roasting of cobalt concentrate is a process determined by kinetics, and with increase of temperature above 650° diffusion becomes the determining factor.

It must be noted that when small samples are roasted the combustion of sulfur is very rapid. At temperatures above 600° the combustion of sulfur in roasting of cobalt concentrate in a fluidized bed is almost quantitative within 3-4 minutes.

It is clear from the data in Table 4 that the amount of sulfur burned out increases appreciably with granule size. This is because the linear velocity of the air passed through the reaction tube increases with granule size.

It was found further that the weight of the sample taken for roasting influences the burning out of sulfur from cobalt concentrate. With samples of 4-6 g the amount of sulfur burned out varies little with the sulfur content of the original material. Thus, at 580°, with a roasting time of 10 minutes and with 37.0 and 17.6% of sulfur respectively in the material, the degree of combustion is 95.5 and 97.1% respectively for small samples. With 40-50 g samples, as is evident from the data in Tables 3 and 4, the degree of combustion decreases appreciably with increasing sulfur content in the original mixture. Increase of the sample weight also influences to some extent the relationship between the rate of sulfur combustion and the roasting time.

It can be concluded from the data in Tables 2 and 3 that the rate of sulfur combustion falls somewhat with increase of sample weight, especially during the initial stages of roasting. Thus, at 475° with a roasting time of 15 minutes, the degree of sulfur combustion was 68.9 and 48.3% for samples of 6.0 and 42.0 g respectively.

This lowering of the sulfur combustion rate is due partly to the fact that there is a larger excess of air, especially during the first stages of roasting, with small

presented in Tables 2-4. It may be concluded from the data in Table 2 that the relationship between the degree of sulfation of cobalt and the temperature is represented by a curve with a maximum. In our experiments the maximum degree of cobalt sulfation was reached at 525-550°. It was established as the result of numerous experiments that when small samples (4-6 g) are roasted under batch conditions a degree of sulfation of cobalt greater than 65-68% cannot be achieved, whereas with samples of 40-50 g it is fairly easy to reach 70% and even higher. This fact is explained as follows. The data in Tables 2 and 3 indicate that a fairly high degree of sulfation of cobalt is attained only after most of the sulfide sulfur has been burned out of the material. However, under batch roasting conditions, near the end of the process, when most of the sulfide sulfur has been burned out of the material, and the conditions are suitable for sulfation of cobalt, the sulfur dioxide content of the gas phase falls sharply so that the rates of reactions (3) and (4) are diminished.

The relatively low degree of sulfation of cobalt during intensive roasting indicates that the rate of sulfation of cobalt by reactions (3) and (4) is slower than the rate of sulfide oxidation by reaction (2).

It follows that when, by increase of the sample size in batch roasting, oxidation of sulfides and sulfation of oxides are effected at more or less comparable rates, the degree of sulfation of cobalt is increased.

The data in Tables 3 and 4 also indicate that with less intensive agitation the degree of sulfation of cobalt is greater in the upper than in the lower layers of the fluidized material. This is because with less intensive agitation the upper layers of the fluidized material contain less sulfide sulfur than the lower layers.

From these experimental results it may be concluded that the extent and rate of sulfating roasting of cobalt concentrates are determined mainly by the extent and rate of the oxidative roasting of sulfides and of sulfation of oxides in accordance with Eqs. (3) and (4). It must be noted that a given factor has different effects on the rate and extent respectively of the above-named principal stages of sulfating roasting of cobalt concentrates.

Thus, the rate of oxidation of sulfides and the extent of sulfur combustion during roasting in a fluidized bed increase with increase of temperature, granule size, and agitation intensity, and decrease with increase of the sulfur dioxide concentration in the gas phase.

At the same time, the degree of cobalt sulfation falls with rise of temperature above 525-500°, with increased content of sulfide sulfur in the roasted material and agitation intensity, and with decrease of the sulfur dioxide concentration in the gas phase.

This suggests that it may be necessary to effect these main stages in sulfating roasting of sulfides and sulfide ores as separate operations.

The results of these experiments indicate that under certain conditions the stages of sulfide oxidation and oxide sulfation may be effected separately during roasting of cobalt concentrates in fluidized beds by the natural separation of the cobalt concentrate from its roasting products along the height of the fluidized bed.

In such cases sulfide oxidation would take place mainly at the top, and oxide sulfation below.

A more correct name for this would probably be oxidation-sulfation roasting.

LITERATURE CITED

- [1] F. M. Stephens, Chem. Eng. Progr. 49, 455 (1953).
- [2] G. Ya. Leizerovich, I. S. Lonskii and V. Z. Chamyi, Nonferrous Metals 9, 19 (1957).
- [3] G. Ya. Leizerovich, Roasting in a Fluidized Bed [In Russian] (Metallurgy Press, 1956).
- [4] V. I. Smimov, Hydrometallurgy of Copper [In Russian] (Metallurgy Press, 1954).
- [5] M. E. Pozin, A. M. Ginstling and V. V. Pechkovskii, J. Appl. Chem. 27, 1237 (1954).*
- [6] R. M. Perel'man, A. Ya. Zvorykin and N. V. Gudima, Cobalt [In Russian] (Acad. Sci. USSR Press, 1949).
- [7] S. A. Fainberg, Analysis of Nonferrous Metal Ores [In Russian] (Metallurgy Press, 1953).
- [8] D. M. Chizhikov, Trans. A. A. Baikov Inst. Metallurgy 2 (1957).

*Original Russian pagination. See C.B. Translation.

- [9] A. M. Malets, Chem. Sci. and Ind. 4, 530 (1957).
- [10] K. M. Malin et al., Sulfuric Acid Technology [In Russian] (Goskhimizdat, 1950).

Received February 5, 1958

MASS TRANSFER ON BUBBLER GRID AND TUBE PLATES OF THE DROP-THROUGH (TURBOGRID) TYPE*

I. N. Kuz'minykh and A. I. Rodionov

(D. I. Mendeleev Institute of Chemical Technology, Moscow)

During recent years absorption and rectification towers with sieve and grid trays of the drop-through type have become widely adopted in industry [1-4]. The design and advantages of equipment with such trays have been described in detail [5]. Several publications deal with hydrodynamical tests of such trays [6-8], and some data on their efficiency in rectification are available [9].

The literature contains no data on mass-transfer rates in absorption-desorption processes on grid trays of this type, and we therefore carried out experiments on desorption of oxygen from water on grid and tubular plates over a wide range of gas and liquid rates.

The apparatus used for the tests was described previously [9]. The dimensions of the test plates were $0.1 \cdot 0.7 = 0.07 \text{ m}^2$. The grids used differed in slot width (3, 4 or 5 mm) with an open area of 15-33%. Tubular grids, assembled from tubes 10 and 22 mm in diameter, had an open area of 12-23% with the same slot width. The gas velocity in the experiments was varied from 0.39 to 2.65 m/second, and the liquid rate from 5 to 50 $\text{m}^3/\text{m}^2 \cdot \text{hour}$.

The degree of desorption, plate efficiencies, and mass-transfer coefficients were determined in relation to the influence of various factors. The plate efficiencies were determined as the ratio of the difference between the oxygen concentrations in the liquid before and after the grid to the difference between the oxygen concentration of the liquid before the grid and the equilibrium concentration:

$$\eta = \frac{c_1 - c_2}{c_1 - c_e}$$

The mass-transfer coefficients were determined per unit grid area and unit volume of the foam formed on the grid, and were calculated from the following equations:

$$K_{La} = \frac{l \cdot (c_1 - c_2)}{S \cdot \Delta c} \text{ and } K_V = \frac{l \cdot (c_1 - c_2)}{S \cdot H \cdot \Delta c},$$

where K_{La} is the mass-transfer coefficient per unit grid area (in m/hour); K_V is the mass-transfer coefficient per unit foam volume (in hours^{-1}); S is the grid area (in m^2); H is the height of the foam layer (in m); l is the liquid flow rate (in m^3/hour); c_e is the equilibrium oxygen concentration in water (kg/m^3); c_1 and c_2 are the oxygen concentrations in the water before and after the tray (in kg/m^3).

As in our previous investigations [10-13], the average driving force of the process Δc was determined for conditions of complete mixing of the liquid on the plates.

For all the grids tested the degree of oxygen desorption varied in the range of 33-67%. As was to be expected, the degree of desorption increases with increase of the gas velocity and with decrease of the flow rate per unit cross section.

*Ya. Kulanbaev and A. Mel'nikov assisted in the experiments.

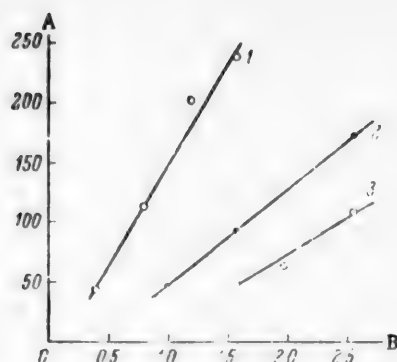


Fig. 1. Variations of mass-transfer coefficient with gas velocity for grids of different open area at $L = 20 \text{ m}^3/\text{m}^2 \cdot \text{hour}$: A) mass-transfer coefficient K_La (m/hour); B) gas velocity (m/second); 1) grid 3-18, $f = 15.3\%$; 2) grid 3-11.5, $f = 23.2\%$; 3) grid 3-9, $f = 33.4\%$.

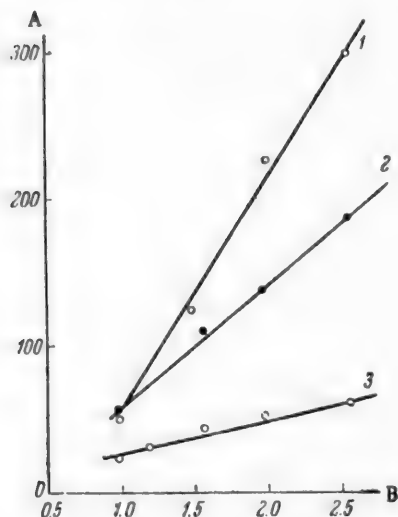


Fig. 3. Variations of foam height, mass-transfer coefficient, and resistance of grid 3-11.5, $f = 23.2\%$ with the gas velocity at $L = 30 \text{ m}^3/\text{m}^2 \cdot \text{hour}$: A) values of H , K_La and P ; B) gas velocity (m/second); 1) foam height H (mm); 2) mass-transfer coefficient K_La (m/hour); 3) grid resistance P (mm H_2O).

The experimental data obtained in the present investigation showed that the relationship between K_La and the gas velocity is not the same as it is on sieve plates with cross flow of gas and liquid. In the present instance increase of the gas velocity over the column cross section (w_c), both in grid and in tubular trays, leads to a continuous increase of the liquid-phase mass transfer coefficient (K_La). This is clear from Fig. 1, which represents variations of K_La with the gas velocity for grids with open areas of 15.3, 23.2 and 33.4%, for the same liquid rate

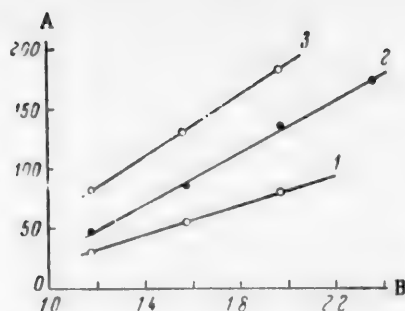


Fig. 2. Variations of mass-transfer coefficient with the gas velocity and liquid rate for a 3-25 tubular grid: A) mass-transfer coefficient K_La (m/hour); B) gas velocity (m/second); liquid rate L ($\text{m}^3/\text{m}^2 \cdot \text{hour}$): 1) 10, 2) 20; 3) 50.

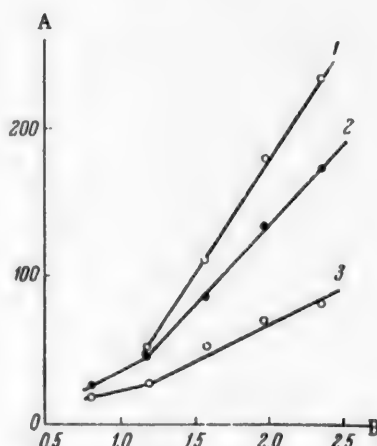


Fig. 4. Variations of foam height, mass-transfer coefficient, and resistance of tubular grid 3-25 with the gas velocity at $L = 20 \text{ m}^3/\text{m}^2 \cdot \text{hour}$: A) values of H , K_La , and P ; B) gas velocity (m/second); remaining designations as in Fig. 3.

It follows from earlier publications [11-13] that in desorption on sieve plates with cross flow of gas and liquid the mass-transfer coefficient (K_La) first increases to a maximum with increase of gas velocity, then decreases, and beyond $w_c \approx 1.2 \text{ m/second}$ it depends little on the gas rate. The maximum K_La is found at roughly the same gas velocity as the maximum height of the cellular-foam layer.

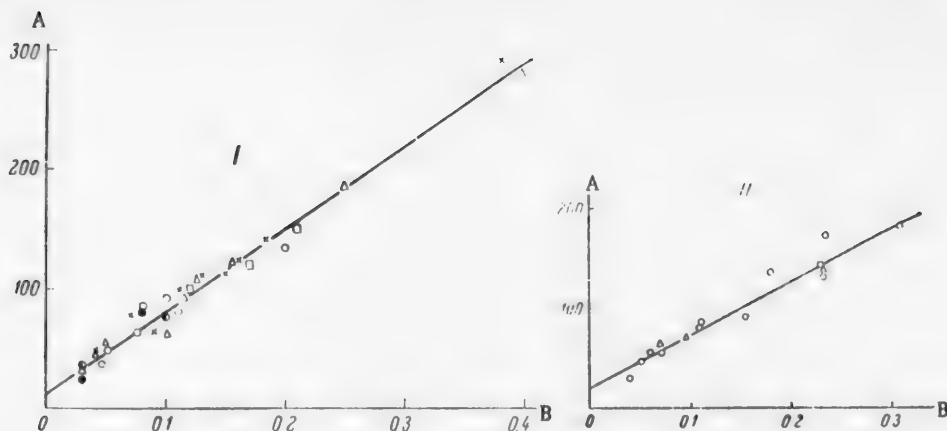


Fig. 5. Variations of mass-transfer coefficient with the height of the foam layer for grid trays (I) and tubular trays (II): A) mass-transfer coefficient $K_L a$ (m/hour); B) height of foam layer (m); the different points correspond to different grids (from 3-9 to 5-17), with different values of f (from 15.3 to 33.4%).

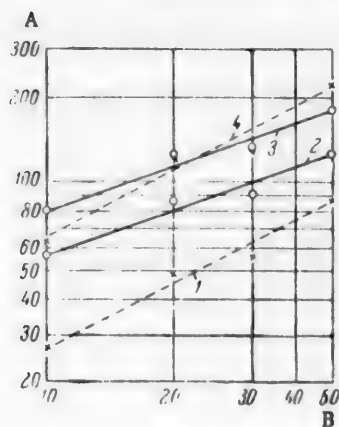


Fig. 6. Variation of the mass-transfer coefficient with the liquid rate: A) mass-transfer coefficient $K_L a$ (m/hour); B) liquid rate L ($\text{m}^3/\text{m}^2 \cdot \text{hour}$); 1) grid plate 3-9, $w_c = 1.57$ m/sec; 2) grid plate 3-25, $w_c = 1.57$ m/sec; 3) tubular plate 3-25, $w_c = 1.97$ m/sec; 4) grid plate 3-11.5, $w_c = 1.97$ m/sec.

($L = 20 \text{ m}^3/\text{m}^2 \cdot \text{hour}$). A similar relationship between $K_L a$ and gas velocity at three liquid rates ($L = 10, 20$ and $50 \text{ m}^3/\text{m}^2 \cdot \text{hour}$) is found for a grid assembled from tubes 22 mm in external diameter (Fig. 2). For both types of grids the relationship between $K_L a$ and the gas velocity may be represented by the following general linear equation

$$K_L a = A + Bw_g.$$

The coefficients A and B depend not only on the grid design and perforation, but also on the liquid rate per unit cross section. It follows from Fig. 1 that the less the open area of the grid the greater the mass-transfer coefficient and the greater its increase with increase of the gas rate. For example, at a gas velocity (w_g) of 1.5 m/second for a grid of open area (f) of 15.3%, $K_L a$ is approximately 230 m/hour, for a plate with $f = 23.2\%$, $K_L a \approx 86$ m/hour, and for a grid with $f = 33.4\%$, $K_L a \approx 45$ m/hour. Thus, if the open area of the grid is increased a little more than twofold the coefficient $K_L a$ is reduced fivefold.

This variation of $K_L a$ with the gas velocity is determined by the hydrodynamics of the bubbling process. The value of the coefficient ($K_L a$) depends on the height of the gas-liquid layer (foam) on the grid, and this layer grows continuously with increase of the gas velocity in the column (Fig. 3 and 4). The same diagrams show variations of grid resistance and the coefficient $K_L a$. It follows from these data that these three characteristics (H , $K_L a$, and P) increase unequally with the gas

velocity. The foam layer increases to the greatest extent, and the plate resistance to the least. Thus, for a grid with 23.2% open area, at a liquid rate (L) of $30 \text{ m}^3/\text{m}^2 \cdot \text{hour}$ (Fig. 3), increase of the gas velocity from 1.2 to 2.4 m/second (i.e., by a factor of 2) produces a 3.2-fold increase in the height of the foam layer. The mass-transfer coefficient ($K_L a$) is increased 2.3-fold, and the grid resistance is doubled. The experimental results show that the less the open area of the grid, the greater the increases of H , P , and $K_L a$. For example, for a tubular grid of 12.4% open section (Fig. 4) if the gas velocity is changed over the same range the height of the foam layer is increased 4.8-fold, the desorption coefficient 4-fold, and the grid resistance 3.4-fold. The fact that H and $K_L a$ change unequally with increase of the gas rate shows that the ratio $K_L a/H$ decreases. This ratio represents the efficiency of unit height of the foam layer, and is equal to the volume coefficient of mass transfer K_v . The expenditure of energy, indicated by the value of P/H , also decreases. The decrease in the efficiency

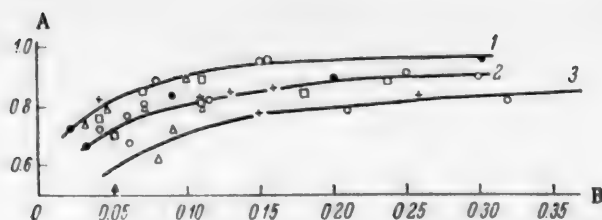


Fig. 7. Variation of tray efficiency with height of foam layer: A) tray efficiency η ; B) height of foam layer (in m); the different points correspond to grid and tubular trays with different values of f (from 12.4 to 33.4%); liquid rate L ($\text{m}^3/\text{m}^2 \cdot \text{hour}$): 1) 10; 2) 20; 3) 50.

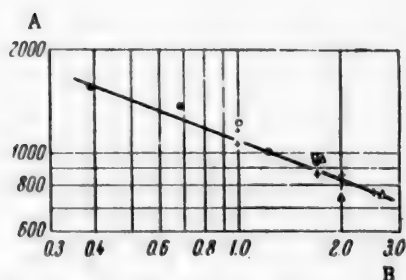


Fig. 8. Variation of K_V with gas velocity: A) mass-transfer coefficient K_V (hr^{-1}); B) gas velocity in column (m/second); the different points correspond to trays with different values of f (from 15.3 to 33.4%).

of unit height of foam layer, despite the growth of the layer, indicates that its turbulence diminishes.

On a tubular grid of $f = 12.4\%$ at liquid rate $L = 20 \text{ m}^3/\text{m}^2 \cdot \text{hour}$, a foam layer is formed at a gas velocity (w_c) of approximately 1.2 m/second , which corresponds to the lower limit of grid operation. Below this velocity it operates unevenly, and gas does not pass through some of the openings. Under these conditions another regime prevails; this may be described as the regime of uneven operation of the grid. The $K_L a$ and P curves (Fig. 4) have breaks at the gas velocity corresponding to transition from this regime to the foaming regime. In the region of uneven operation, $K_L a$ increases continuously with the gas velocity, but not at the same rate as under the foaming regime. The influence of various factors on $K_L a$ under conditions of uneven operation of the grid is not considered in the present communication.

Trays assembled from tubes have lower retaining power for liquid, and therefore the foam layer formed on tubular trays is smaller by a factor of 2 or 3 than the layer formed at the same gas and liquid rates on grids of the same open section. This decrease of the foam layer produces a 2 to 3-fold decrease of the mass-transfer coefficient, as can be seen from a comparison of Fig. 1 and 2.

Figure 5 (I) represents variations of the mass-transfer coefficient with the height of the foam layer for six different grid trays. The experimental points fit satisfactorily on a straight line for all the investigated gas and liquid rates, irrespective of the grid performance. It is therefore possible to represent the relationship between $K_L a$ and the foam height (H) by the following equation:

$$K_L a = 12 + 675H.$$

It follows from the data in Fig. 5 (II) that an analogous relationship holds for two grids assembled from tubes 22 mm in diameter:

$$K_L a = 20 + 535H.$$

The effect of slot width on the coefficient $K_L a$ was determined in tests on grids with slot widths of 3, 4 and 5 mm, all with approximately the same open section of 23%. These experiments were performed at liquid rates of 20 and 50 $\text{m}^3/\text{m}^2 \cdot \text{hour}$ and gas velocities of 1.5 and 2 m/second . Hydrodynamic tests showed that increase of slot width under otherwise constant conditions results in a decrease of the foam height on the grid, and this in turn leads to decrease of $K_G a$. Analysis of the experimental data gave the following relationship between $K_L a$ and slot width:

$$K_L a = C_1 \cdot b^{-0.75},$$

where C_1 is a proportionality factor.

The effect of liquid rate on the coefficient of mass transfer ($K_L a$) was studied with four grid plates and one tubular plate with 12.4% open section. Figure 6 shows the results of experiments with the tubular plate and two grid plates at gas velocities of 1.5 and 2 m/second. The experimental points gave approximately linear plots in logarithmic coordinates. The slopes of the lines are different for tubular and grid plates; the slope factor is 0.7 for grid plates and 0.5 for tubular plates. The relationship between $K_L a$ and the liquid rate can therefore be expressed as follows:

$$K_L a = C_2 L^{0.7},$$

$$K_L a = C_3 L^{0.5},$$

where C_2 and C_3 are proportionality factors which incorporate the influence of all the other factors.

It follows from these results that the coefficient $K_L a$ increases with the liquid rate to a greater extent on grid plates than on tubular plates. This is because under equivalent conditions more liquid drops through tubular plates, and less remains on the plates.

When a layer of foam is present on the plates (in the gas-velocity range of 0.39–2.56 m/second and at liquid rates of 5–50 m³/m²·hour) the efficiency of grid trays varies between 0.53 and 0.95. For trays assembled from pipes the efficiency varies from 0.44 to 0.88 at the same gas and liquid flow rates. As expected, the tray efficiency increases with increasing gas velocity and decreases of the open area and slot width. The efficiency decrease is most prominent with increase of liquid rate. A similar result was obtained for sieve plates with cross flow of gas and liquid [14].

Figure 7 represents variations of efficiency with the height of the foam layer for four grid trays and one tubular tray. The points for three different liquid rates fit fairly accurately onto three almost parallel curves. These results show that the greatest increase in efficiency takes place as the foam height rises to 100 cm; the efficiency continues to increase beyond this, but at a lower rate. The tray efficiency decreases with increase of the liquid rate, despite the equal heights of the foam layer. This occurs because the higher the liquid rate the lower the gas velocity required for formation of a given foam height. It follows that at constant H the foam density increases and its turbulence diminishes with increase of the liquid rate, and this influences the degree of oxygen removal from water.

For a given foam height the efficiencies of grid and tubular plates are equal but, as already stated, more liquid tends to fall through the tubular plates and therefore they require roughly double the gas velocity for formation of a foam layer of the same height as on grid plates of the same open area.

The mass-transfer coefficient per unit foam volume is independent of the liquid rate and the grid perforation, but decreases with increase of gas velocity (Fig. 8). In logarithmic coordinates the experimental points fit around a straight line. The relationship between the mass-transfer coefficient and the gas velocity can therefore be expressed as follows:

$$K_V = C_4 w^{-0.4}.$$

The relationship between the volume mass-transfer coefficient and the gas velocity in the column (w_c), for grid and tubular trays, can be represented with reasonable accuracy by the equation:

$$\eta = (0.2 + 0.05 w_c) \log K_V.$$

SUMMARY

1. In tests of grid and tubular plates for desorption of oxygen from water it was found that the efficiency increases with increasing gas velocity and foam height and decreasing liquid rate. The efficiency varies in the range of 0.53–0.95 for grid plates and 0.44–0.88 for tubular plates. The relationship between efficiency and mass-transfer coefficient (K_V) was determined.

2. The mass-transfer coefficient ($K_L a$) increases with increasing gas velocity, foam height, and liquid rate. Empirical formulas are derived for determination of $K_L a$ as a function of the foam height, liquid rate, and grid slot width.

3. The mass-transfer coefficient (K_v) is independent of the liquid rate and the grid perforation, but decreases with the gas velocity to the power -0.4 .

LITERATURE CITED

- [1] Ch. Eng. Progr. 50, 2, 57 (1954).
- [2] J. A. Samaniego, Oil and Gas, J. 52, 51, 161 (1954).
- [3] L. N. Kuz'minykh and M. D. Babushkina, Paper Ind. 22 (1955); 3 (1956).
- [4] L. N. Kuz'minykh and V. N. Kochetkov, Trans. MKhTI 24, 441 (1957).
- [5] L. N. Kuz'minykh, Chem. Ind. 4, 234 (1956).
- [6] V. V. Dil'man, B. P. Darovskikh, M. É. Aéroov and L. S. Aksel'rod, Chem. Ind. 3, 1956 (1956).
- [7] M. Cervinka and O. Cerny, Chem. Prom. 5, 232 (1955).
- [8] L. N. Kuz'minykh and E. V. Babaev, Trans. MKhTI 24, 432 (1957).
- [9] M. É. Aéroov and E. P. Darovskikh, Chem. Ind. 2, 92 (1957).
- [10] L. N. Kuz'minykh and Zh. A. Koval', Trans. MKhTI 18, 101 (1954).
- [11] L. N. Kuz'minykh, L. S. Aksel'rod, Zh. A. Koval' and A. I. Rodionov, Chem. Ind. 2, 86 (1954).
- [12] L. N. Kuz'minykh and Zh. A. Koval', J. Appl. Chem. 28, No. 1, 21 (1955).*
- [13] L. N. Kuz'minykh and A. I. Rodionov, J. Appl. Chem. 29, No. 9, 1330 (1956).*
- [14] A. S. Foss and I. A. Gerster, Ch. Eng. Progr. 52, 1, 28 (1956).

Received February 15, 1958

*Original Russian pagination. See C.B. Translation.

MAGNITUDE OF THE INTERPHASE AREA IN MECHANICAL AGITATION OF MUTUALLY INSOLUBLE LIQUIDS

I. S. Pavlushenko and A. V. Yanishevskii

(Leningrad Technological Institute, Leningrad)

The effectiveness of mechanical agitation of two mutually insoluble liquids is determined by the uniformity of distribution of the disperse phase throughout the agitated volume on the one hand, and by the dispersity of the disperse phase on the other.

An earlier paper [1] contains an expression for the relationship between the "determining" stirrer speed (i.e., the speed which ensures uniform phase distribution), the physicochemical properties of the stirred liquids, and certain geometrical factors, for four cases of mechanical stirring.

There has been a considerable number of publications dealing with the dispersity of the disperse phase in agitation of two mutually insoluble liquids. The reason is that dispersity is a most important qualitative characteristic of a mixture of two mutually insoluble liquids.

Pollard [2] in 1909, and Newman [3] in 1914 came to the conclusion that each type of mixer design has its own optimum emulsification conditions, determined by the stirrer speed and the geometrical characteristics of the system. The same conclusion was reached by Herschel [4] in 1917. Moore [5] found in 1919 that when two mutually insoluble liquids are agitated the diameter of the disperse-phase droplets depends on the time of stirring. Stamm [6], and later Harkins and Beeman [7], investigated the relationship between the dispersity of the disperse phase and stirrer speed, but did not obtain any calculation formulas.

As the result of a study of the performance of propeller mixers, Bissell [8] formulated in 1938 the general requirements for mechanical emulsification.

The most thorough investigations are these of Vermeulen et al. [9] and Rodger et al. [10]. By analysis of the experimental data with the aid of dimensionless groups these authors derived somewhat different equations relating the interphase area to the physicochemical properties of the stirred liquids, stirrer speed, and the main geometrical factors. These equations take the different conditions determining the process fairly fully into account, but, in our view, they suffer from the important defect that owing to some lack of stringency in the derivation they contain artificially composed dimensional groups which are difficult to determine in practice.

As shown earlier [1], the average diameter of the disperse-phase droplets formed in this process should depend on the physicochemical properties of the stirred liquids, the main geometrical factors, stirrer speed, and possibly also on the acceleration of free motion.

This relationship can be expressed in the following general form:

$$d_d = \varphi(\rho_m, \rho_p, \mu_m, \mu_p, \sigma, d_s, D, H_0, h, V_m, V_p, n, g). \quad (1)$$

The following notation is used: ρ_m, ρ_p , the densities of the dispersion medium and the disperse phase ($\text{kg} \cdot \text{sec}^2 / \text{m}^4$); μ_m, μ_p , the viscosities of the dispersion medium and the disperse phase ($\text{kg} \cdot \text{sec} / \text{m}^2$); σ , the interfacial tension (kg / m); V_m, V_p , the volumes of the dispersion medium and the disperse phase (m^3); d_s , the stirrer diameter (m); d_d , the average diameter of a disperse-phase droplet (m); D , the vessel diameter (m); H_0 , the total height of the liquid layer (m); h , the distance between the medium line of the stirrer and the bottom of the vessel (m); n , the stirrer speed (revolutions/second); g , the acceleration due to gravity ($\text{m} / \text{second}^2$).

System No.	System	ρ_p ($\frac{\text{kg} \cdot \text{sec}^2}{\text{m}^3}$)	ρ_m ($\frac{\text{kg} \cdot \text{sec}^2}{\text{m}^3}$)	μ_p ($\frac{\text{kg} \cdot \text{sec}}{\text{m}^2}$)	μ_m ($\frac{\text{kg} \cdot \text{sec}}{\text{m}^2}$)	σ ($\frac{\text{kg}}{\text{m}}$)
Group 1						
I	Octane in water	71.8	102.0	$8.56 \cdot 10^{-5}$	$1.02 \cdot 10^{-4}$	49.0
II	Toluene in water	88.5	102.0	$6.42 \cdot 10^{-5}$	$1.02 \cdot 10^{-4}$	45.4
III	Octane with carbon tetrachloride in water	104.0	102.0	$6.7 \cdot 10^{-5}$	$1.02 \cdot 10^{-4}$	49.5
IV	Toluene in aqueous glycerol (a)	88.5	115.0	$6.42 \cdot 10^{-5}$	$6.9 \cdot 10^{-4}$	31.4
V	Medicinal petrolatum in water	92.0	102.0	$1.83 \cdot 10^{-2}$	$1.02 \cdot 10^{-4}$	26.0
Group 2						
VI	Machine oil in aqueous glycerol (b)	93.5	119.2	$2.53 \cdot 10^{-2}$	$1.54 \cdot 10^{-3}$	1.77
VII	(c)	93.5	122.6	$2.53 \cdot 10^{-2}$	$4.7 \cdot 10^{-3}$	1.77
VIII	(d)	93.5	126.0	$2.53 \cdot 10^{-2}$	$1.94 \cdot 10^{-2}$	1.63
IX	Technical petrolatum in aqueous glycerol (d)	89.0	126.0	$1.89 \cdot 10^{-3}$	$1.94 \cdot 10^{-2}$	5.41
X	Water in technical petrolatum	102.0	89.0	$1.02 \cdot 10^{-4}$	$1.89 \cdot 10^{-3}$	22.9
XI	Water in machine oil	102.0	93.5	$1.02 \cdot 10^{-4}$	$2.53 \cdot 10^{-2}$	24.5
XII	Machine oil in water	93.5	102.0	$2.53 \cdot 10^{-2}$	$1.02 \cdot 10^{-4}$	24.5

Note: Solution a was prepared from glycerol used for dynamite production; solutions b, c and d were made with different batches of technical glycerol.

Expansion of the functional relationship (1) by the method of dimensional analysis, with the aid of the practical methods described earlier [11], readily gives twenty criterial equations expressing the relationships between the variables. The process is most conveniently represented by an expression of the form:

$$\frac{d}{d_s} = C \cdot \left(\frac{\rho_m d_s^2}{\mu_m} \right)^a \cdot \left(\frac{\rho_m d_s}{\mu_m} \right)^b \cdot \left(\frac{\rho_m d_s^3}{\mu_m^2} \right)^p \cdot \left(\frac{\rho_p}{\rho_m} \right)^f \cdot \left(\frac{\mu_r}{\mu_m} \right)^e \cdot \left(\frac{D}{d_s} \right)^i \cdot \left(\frac{H_0}{d_s} \right)^m \cdot \left(\frac{h}{d_s} \right)^k \cdot \left(\frac{V_p}{d_s^3} \right)^r \cdot \left(\frac{V_m}{d_s^3} \right)^t \quad (2)$$

or, in abbreviated form

$$\frac{d}{d_s} = C \cdot Re_c^a \left(\frac{Re_c^2}{We_c} \right)^b \cdot Ga^p \cdot S_p^f \cdot S_\mu^e \cdot \Gamma_D^i \cdot \Gamma_{H_0}^m \cdot \Gamma_h^k \cdot K_p^r \cdot K_m^t \quad (3)$$

It is obvious that the stirring time has a significant influence both on uniformity of distribution of the phases in the whole volume, and on the dispersity of the disperse phase.

Equation (3) is derived on the assumption that the time of stirring is sufficient for a steady state to be reached.

The general analysis and mathematical derivations were confirmed by appropriate experiments.

EXPERIMENTAL

The experiments were performed in special installations described in previous papers [1, 11]. The liquids were stirred in cylindrical vessels 200 and 300 mm in diameter, with standardized spherical bottoms, by means of 3-blade NMP4-298-49 screws of pitch 1 and 50, 75, 100 and 150 mm in diameter. The vessels and screws were made from stainless steel in conformity with the specifications of the Scientific Research Institute of Chemical Machinery Construction [2].

The vessel was always filled with the liquid mixture to a height equal to its diameter, i.e., so that $H_0 = D$, and the ratio of the distance between the bottom of the vessel and the stirrer to the vessel diameter was constant at $h/d_S = 1/5$ [1].

All the experiments were performed at $20^\circ (\pm 0.5^\circ)$ with systems, details of which are given in the table. The concentration of the disperse phase was varied between 7.5 and 40%. The dispersity of Systems I-V, formed from transparent colorless liquids, was determined with the aid of the "light probe" designed by the authors [13], from the scattering of a parallel beam of light. The dispersity of Systems VI-XII, formed from technical liquids, was found by measurement of the diameters of disperse-phase droplets photographed under high magnification. In most of the systems of the second group the viscosity of the dispersion medium was high enough to ensure adequate stability of emulsion samples withdrawn from the agitated mixtures, so that they could be photographed under an ordinary microscope. The emulsion samples were withdrawn and photographed within 5-8 seconds.*

For greater accuracy, several emulsion samples were taken and photographed in each determination. Photographs of two emulsions are shown in Fig. 1 and 2.

The value taken for the diameter of a disperse-phase droplet was the average for the volume. For example, the average droplet diameter in the disperse phase of the emulsion shown in Fig. 1 determined in this way is 18μ . The system was agitated at constant stirrer speed in each experiment. The stirrer speeds used for each system were within the range from the determining value to the speed at which air began to be drawn into the system (when the vortex reached the stirrer hub). The stirring was continued until the dispersity of the disperse phase ceased to increase. During this time the dispersity became virtually constant throughout the stirred volume, in conformity with the earlier conclusions of Bissell [9] and Rebinder [14].

Photographic examination of the emulsion droplets showed that when systems with a viscous dispersion medium are stirred, such as machine oil in aqueous glycerol (System VIII), ordinary O/W or W/O emulsions are always formed (Fig. 1). When a system with a viscous disperse phase and a medium of low viscosity is stirred, such as machine oil in water (System XII), a "multiple" emulsion is formed (Fig. 2).

In such an emulsion each disperse-phase droplet contains minute droplets of liquid consisting of the dispersion medium. In such cases the concept of the interface becomes much more complicated, as in fact there are two interfaces differing greatly from the hydrodynamic standpoint. This is evidently why our earlier investigation of the system medicinal petrolatum-water (System V) with the aid of the light probe did not produce definite results giving an indication of the interfacial area. For this reason the experimental data for these systems were not used in subsequent analysis.

*Photographs taken at different time intervals (within the above limits) did not reveal any appreciable breakdown of the emulsions in the samples.

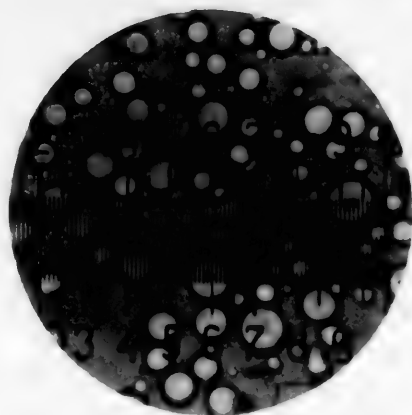


Fig. 1. System VIII, $V_p/V_p + V_m = 0.2$, division = 2.9μ .



Fig. 2. System XII, $V_p/V_p + V_m = 0.5$, 1 division = 11.1μ .

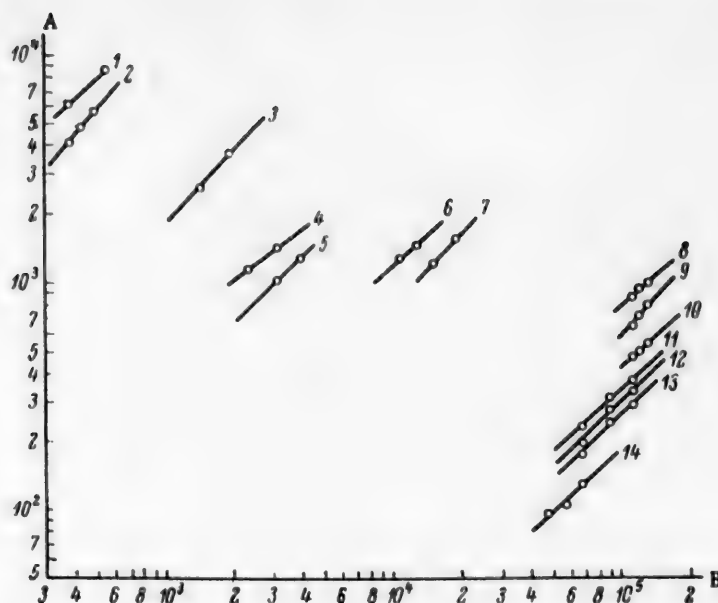


Fig. 3. Variations of interfacial area with Re_c : A) experimental values of Ad_S ; B) values of Re_c .

Line No. in diagram	System No. (see table)	$\frac{D}{d_s}$	$\frac{v_p}{v_p + v_m}$
1	IX	2	0.2
2	VIII	2.67	0.2
3	VII	2	0.2
4	X	2	0.1
5	X	3	0.1
6	IV	2	0.2
7	IV	2	0.2
8	I	2	0.4
9	I	2	0.15
10	I	2	0.075
11	III	2	0.1
12	III	2	0.2
13	III	2	0.3
14	III	4	0.1

It must be pointed out that in Systems VI and VII some minute droplets of aqueous glycerol were present in the droplets of machine oil. However, in these cases their total surface area was very small and the error introduced into the final results was not large.

It is important to note that this effect could be detected photographically in the emulsions. From this point of view the photographic method is preferable to others, including the sedimentometric [15].

DISCUSSION OF RESULTS

The general expression (2) was simplified somewhat for derivation of the final equation.

The ratio h/d_s , which is constant, and the ratio H_0/d_s , which is equal to D/d_s , can be eliminated from the equation. The ratios V_p/d_s^3 and V_m/d_s^3 which represent the concentrations of the liquids constituting the system are more conveniently expressed as $V_p/V_p + V_m$. Analogously, ρ_p/ρ_m is conveniently replaced by $\Delta\rho/\rho_m$.

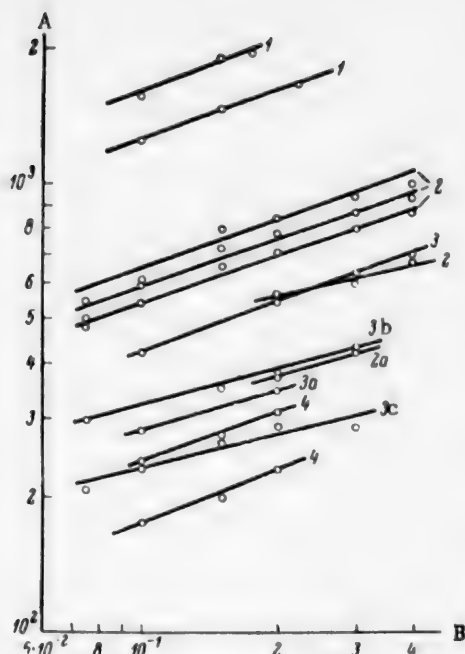


Fig. 4. Influence of the concentration of the disperse phase on interfacial area: A) experimental values of Ad_s ; B) concentration of disperse phase $V_p/V_p + V_m$;

Line No. in diagram	System No. (see table)	$\frac{D}{d_m}$
1	IV	2
2	I	2
2a	I	2.67
3	II	2
3a	II	2.67
3b	II	3
3c	II	4
4	III	2

These simplifications give

$$Ad_s = C \cdot \left(\frac{\rho_m d_s^2}{\mu_m} \right)^a \cdot \left(\frac{\rho_m d_s}{\mu_m^2} \right)^b \cdot \left(\frac{\rho_m^2 s}{\mu_m^2} \right)^p \cdot \left(\frac{\Delta \rho}{\rho} \right)^f \cdot \left(\frac{\mu_p}{\mu_c} \right)^g \cdot \left(\frac{D}{d_s} \right)^t \cdot \left(\frac{V_p}{V_p + V_m} \right)^{q*} \quad (6)$$

or, in abbreviated form,

$$Ad_s = C \cdot Re_c^a \cdot \left(\frac{Re_c^2}{We_c} \right) \cdot Ga^p \cdot S_{\Delta p}' \cdot S_{\mu}^g \cdot \Gamma_D^t \cdot K_e^q \quad (7)$$

* $1/Ad_s$, which is always less than unity, is replaced by its reciprocal.

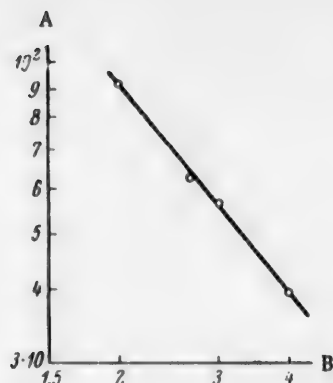


Fig. 5. Variation of the interfacial area with the ratio D/d_s ; A) experimental values of

$$\frac{Ad_s}{Re_c} \cdot \left(\frac{Re_c^2}{We_c} \right)^{0.56} \cdot S_{\Delta p}^{-0.25} S_{\mu}^{0.27} \cdot \left(\frac{V_p}{V_p + V_m} \right)^{-0.32} \quad \text{B) values of } D/d_s.$$

The dispersity of the emulsion formed is more correctly [13] expressed not in terms of the average diameter of the disperse-phase droplets but in terms of the interfacial area per unit volume of the disperse phase (S) or per unit volume of emulsion (A). These quantities are expressed as

$$S = \frac{6}{d_d} \quad (4)$$

$$A = S \left(\frac{V_p}{V_p + V_m} \right) \quad (5)$$

Here the dimensions of S and A are determined by the dimensions of d_d .

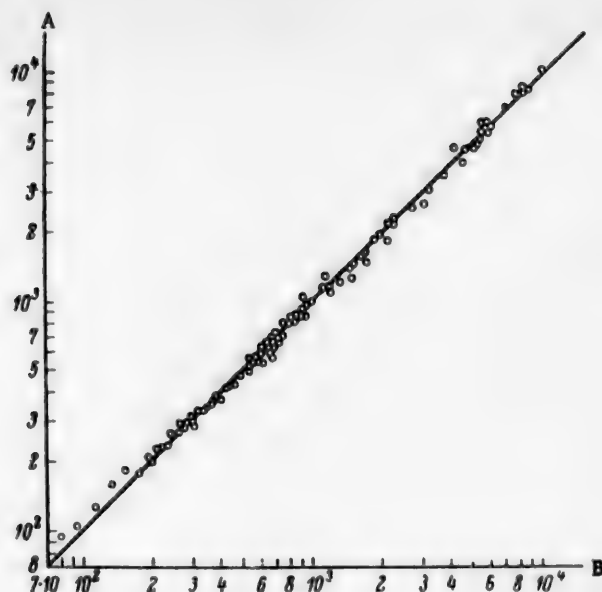


Fig. 6. Correlation of experimental and calculated data:
A) experimental values of Ad_s ; B) calculated values of Ad_s .

The numerical values of the indices of the dimensionless groups in Eq. (7) and of the coefficient in this equation were determined as follows. The values of the indices of Re_C ($a = 1$, Fig. 3*) and K_e ($n = 0.32$, Fig. 4**) were found by the usual method of graphical analysis. Then, with known values of a and n , and at a constant value of $\Gamma_D = 2$, the indices of (Re_C^2/We_C) , Ga , $S_{\Delta p}$ and S_μ ($b = -0.56$, $p = 0$, $f = 0.25$, $e = -0.27$) are found by trial and error.

Since the index of the Galileo criterion is found to be zero, it follows that acceleration due to gravity does not influence the value of the interfacial area.

The index of Γ_D ($l = -1.21$, Fig. 5) was then found graphically, and the coefficient ($C = 2.12 \cdot 10^2$) was determined analytically. Substitution of these values finally gives

$$Ad_s = 2.12 \cdot 10^2 \cdot Re_C \cdot \left(\frac{Re_C^2}{We_C} \right)^{-0.56} \cdot S_{\Delta p}^{0.25} \cdot S_\mu^{-0.27} \cdot \Gamma_D^{-1.21} \cdot K_e^{0.32} \quad (8)$$

or, in a form suitable for calculations

$$A = 2.12 \cdot 10^2 \frac{\rho_m^{0.10} \mu_m^{0.39} \Delta p^{0.25} n d^{1.85}}{\sigma^{0.56} \mu_p^{0.27} D^{1.21}} \left(\frac{V_p}{V_p + V_m} \right)^{0.32} \left[\frac{m^2}{m^3} \right] \quad (9)$$

Experimental values of Ad_s are correlated with values calculated by Eq. (8) in Fig. 6, which includes data from 99 determinations.

The average deviation is in the range of 2-10%. The equation is valid within the following limits:

$$\begin{aligned} Re_C &= 3.15 \cdot 10^2 \text{ to } 1.32 \cdot 10^5, & S_{\Delta p} &= 0.02 \text{ to } 0.296, \\ \left(\frac{Re_C^2}{We_C} \right) &= 4.1 \text{ to } 7.35 \cdot 10^6, & \Gamma_D &= 2 \text{ to } 4, \\ S_\mu &= 0.004 \text{ to } 16.4, & K_e &= 0.075 \text{ to } 0.4. \end{aligned}$$

*The experimental data refer to vessels of different diameters (200 and 300 mm).

**Experimental data determined at different stirrer speeds.

SUMMARY

1. A general equation is derived for correlating the interfacial area in mechanical stirring of two mutually insoluble phases with their physicochemical properties, certain geometrical factors, and the stirrer speed, with the system in a steady state.

2. Within the limits studied the specific interfacial area: a) is directly proportional to the stirrer speed; b) increases with increasing density and viscosity of the medium, density difference between the disperse phase and the medium, the concentration of the disperse phase, and the stirrer diameter; c) decreases with increase of the disperse-phase viscosity, interfacial tension, and vessel diameter.

3. With the differences in experimental conditions taken into account, the results are fairly close to those of Vermeulen, Rodger and their co-workers.

4. A calculation formula is recommended for practical calculation of the interfacial area when two mutually insoluble liquids are agitated by means of a propeller stirrer.

LITERATURE CITED

- [1] I. S. Pavlushenko and A. V. Yanishevskii, *J. Appl. Chem.* XXXI, No. 9, 1348 (1958).*
- [2] E. W. Pollard, *Pharm. J.* 83, 135 (1909).
- [3] F. R. Newman, *J. Phys. Chem.* 18, 38 (1914).
- [4] W. Herschel, *U.S. Bureau of Standards Technological Papers*, 86, 1-37 (1917).
- [5] W. C. Moore, *J. Am. Chem. Soc.* 41, 944 (1919).
- [6] A. J. Stamm, *Coll. Symp. Monograph*, 3, 251 (1925).
- [7] W. D. Harkins and N. Beeman, *Proc. Nat. Acad. Sci.* 11, 635 (1925).
- [8] E. S. Bissell, *Ind. Eng. Ch.* 30, 493 (1938).
- [9] T. Vermeulen, G. M. Williams, and G. Langlois, *Chem. Eng. Progr.* 51, 2, F85 (1955).
- [10] W. A. Rodger, V. G. Trice and J. H. Rushton, *Chem. Eng. Progr.* 52, 12, 515 (1956).
- [11] I. S. Pavlushenko and N. M. Kostin, *J. Appl. Chem.* 30, 1160 (1957).*
- [12] *Standards for Chemical Equipment Construction*, 1 [In Russian] *Sci. Res. Inst. Chem. Machinery*, (Mashgiz, 1950).
- [13] A. V. Yanishevskii and I. S. Pavlushenko, *J. Appl. Chem.* 31, No. 8, 1215 (1958). *
- [14] P. A. Rebinder, *Colloid J.* 8, No. 3, 157 (1946).
- [15] B. M. Babanov and V. V. Kafarov, *Colloid J.* 20, No. 1, 121 (1958).*

Received February 28, 1958

*Original Russian pagination. See C.B. Translation.

PRODUCTION OF POWDER ALLOYS OF NICKEL WITH IRON AND MOLYBDENUM BY SIMULTANEOUS REDUCTION OF MIXED OXIDES (DIFFUSION METHOD)

G. A. Semenov

In the production of powder alloys by the diffusion method, powdered metals which are to form the alloy components are often used. The constituents of an alloy may include powdered components, the melting points of which are considerably above the diffusion temperature, or the melting points of one or more of the components may be below the diffusion temperature. The first case includes formation of copper-nickel alloy powders, and the second, formation of powdered alloys of copper with tin, zinc, and other metals.

The temperature and time of heating of the powder mixture in the furnace are very important for diffusion in the solid state (when the diffusion temperature is below the melting points of the powdered components), as the most favorable conditions for any given case are regarded to be those which result in the formation of a powder in the form of a spongy product which is easily subdivided. A factor of no less importance is the medium (gaseous or solid) which surrounds the powder particles and prevents formation of oxide films on the particles or reduces them; the presence of oxide films hinders diffusional processes, especially in the case of powders of such easily-oxidized metals as manganese or chromium.

The purpose of the present work was production of nickel-based powder alloys by simultaneous reduction of nickel and iron oxides and molybdenum trioxide, and determination of the factors which influence the course of simultaneous reduction of the oxides, mutual diffusion of the metals, the grain size of the powders, and their oxygen contents.

EXPERIMENTAL

Preparation of alloys. The starting materials were nickel oxide, iron oxide, and molybdenum trioxide. The oxides of iron and nickel were prepared by decomposition of the corresponding oxalates at 600° in air. The first stage of the preparation was mixing of iron and nickel oxalates and molybdenum trioxide in a ball mill for 8 hours (without addition of moisture). The powder mixtures were poured onto nickel trays and decomposed under various conditions. The resultant oxide mixtures were again ground in a ball mill for 8 hours. The mixtures were then poured into boats and reduced in hydrogen (dew point - 30°) at various temperatures (600, 750, 900°) for 2 hours.

The investigated alloys were of the following composition (%): 1) NIMO-20-Ni 60, Mo 20, Fe 20; 2) NIMO-30-Ni 65, Mo 30, Fe 5.

Data on the effects of reduction conditions on some properties of NIMO-20 and NIMO-30 alloys are given in the table.

It follows from the data in the table that powders reduced under different conditions differ in particle-size distribution and bulk density. One probable reason for these differences is that interdiffusion of metal particles formed as the result of reduction takes place at various reduction temperatures in addition to reduction of the oxides in the mixture (these processes apparently take place simultaneously during a certain period). For confirmation of this, powders made from oxide mixtures by reduction under the conditions indicated were investigated by X-ray diffraction.*

*The X-ray investigations were performed in the X-ray department of the Stalin Institute of Steel by E. I. Onishchik under the guidance of Professor Ya. S. Umanskii.

	Alloy					
	NIMO-20			NIMO-30		
Reduction temperature (deg)	600	750	900	600	750	900
Oxygen content (wt. %)	1.35	0.89	0.82	1.5	0.74	0.7
Particle-size distribution (in μ , %)						
0.5—1	30.5	17.45	1.3	53.4	25.8	8.2
1.0—2	40.3	33.0	26.6	23.0	36.5	22.8
2.0—4	27.1	47.0	52.0	23.6	37.7	48.0
4.0—8	2.1	2.25	3.0	—	—	18.2
8.0—12	—	—	2.0	—	—	16.8
Bulk density (g/cc)	0.618	0.664	1.552	0.46	0.48	1.69

X-Ray Investigation of NIMO-30 Alloy Powders Made by Reduction of Oxide

Mixtures Under Various Conditions

Sample 1. The oxide mixture was reduced in hydrogen at 600° for two hours; the metallic nickel, molybdenum, and iron phases did not form solid solutions, as indicated, in particular, by the unchanged lattice constant for nickel ($a = 3.518$ kX).

Sample 2. The oxide mixture was reduced in hydrogen at 750° for two hours; the sample consisted mainly of a solid solution in nickel ($a = 3.58 \pm 0.005$ kX) and a solid solution in molybdenum ($a = 3.135 \pm 0.005$ kX). In addition a phase was detected close in its parameters to the Fe_7Mo_8 phase with a rhombic lattice, but differing somewhat from it in the lattice constant (its composition may be therefore expressed by the formula Ni_7Mo_8), and a small amount of free molybdenum.

Sample 3. The oxide mixture was reduced in hydrogen at 900° for two hours. Analysis revealed the presence of a principal phase consisting of a nickel-based solid solution ($a = 3.587$ kX), a small amount of the compound Ni_7Mo_8 , and a small amount of free molybdenum.

X-Ray Investigation of NIMO-20 Alloy Powders Made by Reduction of Oxide

Mixtures Under Various Conditions

Sample 4. The oxide mixture was reduced in hydrogen at 600° for two hours. Interaction between the metallic phases was very weak, as indicated by the slight increase in the lattice constant of nickel ($a = 3.524 \pm 0.005$ kX).

Sample 5. The oxide mixture was reduced in hydrogen at 750° for two hours. In this case there was vigorous interaction between the metals in the mixture; the principal phase was a nickel-based solid solution with lattice constant $a = 3.585$ kX, lines for the intermetallic compound were detected, free iron was also absent; a small amount of free molybdenum was found.

Sample 6. The oxide mixture was reduced in hydrogen at 900° for two hours. The same phases as in the previous case were found by X-ray analysis.

SUMMARY

1. Powdered NIMO-30 and NIMO-20 alloys are formed by reduction of mixtures of nickel, iron, and molybdenum oxides in hydrogen under various conditions even at a relatively low temperature (900°).

2. In reduction at the lowest temperature (600°) the first stage merely consists of reduction of oxides, mainly to the metals, in both alloy mixtures. At a higher temperature (750°) interdiffusion of the metals takes

place; in the case of NIMO-30 alloy, with a higher molybdenum content, four phases are formed: a solid solution in nickel, a solid solution in molybdenum, the compound Ni_7Mo_8 , and a small amount of free molybdenum. If the molybdenum content is decreased and the composition modified somewhat (alloy NIMO-20) two phases are formed under the same reduction conditions: a solid solution in nickel and a small amount of free molybdenum. On increase of the reduction temperature to 900° three phases are formed in the case of NIMO-30 alloy: a solid solution in nickel, the compound Ni_7Mo_8 , and a small amount of free molybdenum. In the case of NIMO-20 alloy there is no change in phase composition.

3. Powder alloys containing different phases are likely to be more active in sintering (NIMO-30 alloy).

Received November 15, 1957

PREPARATION OF CHROMIUM CARBIDE, Cr_7C_3

T. Ya. Kosolapov and G. V. Samsonov

(Kiev Institute of Powder Metallurgy and Special Alloys,
Academy of Sciences, Ukrainian SSR)

Chromium carbide of the formula Cr_7C_3 was first prepared by Ruff and Foehr [1] by the action of heat on chromium with carbon in magnesite crucibles at 1800-1850°. They attributed the formula Cr_8C_2 (8.45% C) to this carbide. Subsequent investigations [2-4] showed that the more probable formula of this carbide is Cr_7C_3 (9.01% C). Some workers [5] prepared Cr_7C_3 by the action of heat on a mixture of chromium oxide and carbon in 27:7 molar ratio at 1200-1500°, with removal of the CO formed by a system of pumps. In view of the fact that the low-carbon chromium carbides Cr_7C_3 and Cr_{23}C_6 dissolve readily in the binding metal, which increases brittleness of the alloys, and that they are less resistant to oxidation than Cr_3C_2 , their applications are limited [6, 7].

The purpose of the present work was to study the conditions for formation of the pure single-phase carbide Cr_7C_3 .

EXPERIMENTAL

The formation conditions of Cr_7C_3 were studied by means of the reduction of chromic oxide by carbon



A mixture of the theoretical composition was moistened with dextrin solution, added in the proportion of 0.5 g per 100 g of mixture, stirred thoroughly, and dried. The mixture was then molded into briquets 20 mm in height and diameter. The briquets were placed in graphite cartridges and heated in a Tammann furnace at temperatures from 1000 to 1600° (at 100° intervals) in a hydrogen atmosphere. The exposure time at each temperature was 1 hour.

The extent of reaction was estimated from the weight ratio of the products obtained to the products which should have been obtained if the reaction was complete.

All the products were also analyzed chemically for chromium and total and free carbon.

The results, which are given in Table 1, show that at 1000 and 1100° the reduction is not complete and the ratio A/B > 1; the amount of bound carbon is low, and of free, high. The sum of the chromium and total carbon contents is less than 100%.

At 1200° the degree of reduction increases; the extent of reaction reaches the value of 1 and remains close to this at temperatures up to 1600°. The contents of bound carbon at 1200 and 1300° are close to the theoretical value (9.01%), and at higher temperatures they increase somewhat. The content of free carbon begins to fall at 1200° and remains negligible over the entire temperature range.

Increase of the bound-carbon content of temperatures of 1400° and over is the consequence of carburization by carbon from the gas phase with formation of a higher chromium carbide, Cr_3C_2 .

This hypothesis is confirmed by the content of residue insoluble in hydrochloric acid, which is characteristic of the presence of the higher chromium carbide [8].

TABLE 1

Results of Experiments on Preparation of Chromium Carbide Cr_7C_3 , Carbon Content of Mixture 23.3%, Exposure Time 1 Hour

Temperature (deg)	Briquet weight (g)		Loss of briquet weight (%)	Calculated weight of carbide (g) B	A/B	Contents of (%)					
	before heating	after heating, A				Cr	C _{tot}	C _{free}	C _{bound} *	C _r + C _{tot}	insoluble residue
1000	11.70	10.91	6.9	6.75	1.61	55.76	19.54	18.50	1.29	75.3	—
1100	11.40	7.98	30.0	6.58	1.21	75.11	14.09	11.97	2.41	89.2	—
1200	11.69	6.77	42.1	6.74	1.00	90.84	9.28	0.09	9.18	100.12	3.2
1300	11.65	6.64	43.0	6.72	0.98	90.93	9.33	0.04	9.29	100.26	3.8
1400	11.84	6.72	43.2	6.83	0.98	90.31	9.83	0.13	9.71	100.14	14.7
1500	8.59	4.91	42.9	4.96	0.99	88.47	10.98	Not found	10.98	99.45	44.7
1600	9.18	5.10	44.4	5.30	0.96	—	10.76	Same	10.76	—	—

*C_{bound} is calculated for the Cr_7C_3 phase: $C_{\text{bound}} = C_{\text{tot}} - C_{\text{free}}/100 - C_{\text{free}} \cdot 100\%$

TABLE 2

Calculated Data on the Carbon Contents of Parts of the Reduction Products Soluble and Insoluble in HCl

Temperature (deg)	Weights of products formed (g)	C contents of products (g)	Weight of insoluble residue (g)	C content of insoluble residue		Weight of soluble carbides (g)	C contents of soluble carbides	
				in g	in %		in g	in %
1400	6.72	0.66	0.99	0.13	13.1	5.73	0.53	9.24
1500	4.91	0.54	2.19	0.29	13.2	2.72	0.25	9.19

TABLE 3

Chemical Composition of Products Formed at Different Heating-Up Rates
Carbon content of mixture 23.0%,
temperature 200°, exposure time 1 hour

Heating-up time (min)	C content (%)	
	C _{bound}	C _{free}
20	9.14	} Traces
40	9.02	
80	9.17	

The presence of Cr_7C_3 in the reduction products formed at 1400 and 1500° is confirmed by the calculations in Table 2, based on determinations of C_{tot}, C_{free}, and insoluble residue in the samples, and of carbon in the insoluble residue.

It follows that the optimum temperature for preparation of the carbide Cr_7C_3 of the calculated composition is 1200-1300°.

To determine the influence of the time taken to raise the temperature to the optimum, experiments were carried out in which the temperature was raised from 800 to 1200-1300° during 20, 40 and 80 minutes, with a subsequent exposure of 1 hour at the optimum temperature. The results in Table 3 show that the rate of temperature rise has no practical effect on the composition of the reduction products, and that a heating-up time of 20 minutes is sufficient from the technological aspect.

In addition, in order to determine the exposure time at the optimum temperature, the briquets were heated up from 800 to 1200-1300° with the following exposure times at the optimum temperature: 0 (the cartridge was pushed through into the cooling chamber immediately 1200-1300° was reached), 30, 60, 120 and 180 minutes.

The results are given in Table 4.

TABLE 4

Chemical Composition of Products Formed During Different Exposure Times, Carbon content of mixture 23.0%, temperature 1200°, heating-up time 20 minutes

Exposure time (min)									
0		30		60		120		180	
C _{bound}	C _{free}	C _{bound}	C _{free}	C _{bound}	C _{free}	C _{bound}	C _{free}	C _{bound}	C _{free}
2.20	15.97	2.22	10.02	9.02	Not detected	9.36	Not detected	9.55	Not detected

TABLE 5

Chemical Composition of Products Formed from Mixtures of Different C Contents

C content of mixture (%)	C content of final product (%)	
	C _{bound}	C _{free}
23.3	9.89	0.09
23.3	10.28	0.17
23.0	9.66	0.13
22.8	8.94	0.03
22.8	9.09	0.08

According to the data in Table 4, the product formed after exposures of 0 and 30 minutes has a high content of free carbon, with insufficient bound carbon, which may be possible as the result of carbide formation with a deficiency of carbon. On increase of the exposure time to 1 hour, the vacant sites are filled, and the carbide Cr_7C_3 of the calculated composition is formed.

Further increase of the exposure time leads to formation of a certain amount of the higher carbide Cr_3C_2 , from carbon in the gas phase. Thus, the optimum conditions for formation of the carbide Cr_7C_3 are: raising of temperature from 800 to 1200-1300° over a period of 20 minutes, and exposure at 1200-1300° for 1 hour.

For production of larger amounts of Cr_7C_3 (from 300 g of mixture) the most effective procedure is to use a mixture containing 2-3% less than the calculated amount of carbon, because of the ready formation of Cr_3C_2 in the Tamman furnace (Table 5).

For the same reason, the best results are obtained if the mixture is used in the form of small lumps rather than powder, as the total hydrocarbon-vapor pressure is higher over a finely-divided powdered mixture than over lumps, and the possibility of carburization of the mixture with formation of Cr_3C_2 is greater.

The carbide Cr_7C_3 formed from 300 g of mixture with a heating-up time of 20 minutes from 800 to 1300° and an exposure of 1.5 hours at the final temperature often contains insufficient bound carbon and a large amount of free carbon.

If the exposure time is increased to 2 or more hours, the products contain more carbon than corresponds to the composition Cr_7C_3 .

TABLE 6

Analytical Data on the Carbide Cr_7C_3 Formed by the Two-Stage Process

C contents (%)			
Cr ₇ O ₃ formed by heating in a Tamman furnace, with 20 minutes heating-up time to 1300° and 1.5 hours exposure (A)		Cr ₇ C ₃ formed from powdered product A additionally heated in a Tamman furnace at 1300° for 20 minutes	
C _{bound}	C _{free}	C _{bound}	C _{free}
8.38	1.00	9.02	0.07
8.06	1.04	9.06	0.03

If the products formed as described above are ground and additionally heated in powder form in a graphite cartridge at 1200-1300° in a hydrogen atmosphere in a Tammann furnace, the products obtained contain up to 0.2% of free carbon and of carbon corresponding to the carbide Cr_7C_3 .

This two-stage process is effective because as the reduction proceeds the hydrocarbon-vapor pressure over the mixture decreases and the reduction slows down somewhat. Grinding of the product and subsequent heating increase the surface activity of the particles and reduction to Cr_7C_3 is rapidly completed.

Comparative analytical data on products formed by the two-stage process are presented in Table 6.

SUMMARY

The conditions for formation of chromium carbide Cr_7C_3 of the calculated composition, with the minimum free-carbon content were studied; it was found that the two-stage process is the most suitable for production of the carbide Cr_7C_3 . In this process a mixture containing 2-4% less than the calculated amount of carbon is heated in a Tammann furnace in a hydrogen atmosphere; the temperature is raised from 800 to 1200-1300° during 20 minutes, the mixture is held at the final temperature for 1.5 hours, powered, and heated again at 1200-1300° in a graphite cartridge in a hydrogen atmosphere for 15-20 minutes.

LITERATURE CITED

- [1] O. Ruff and T. Foehr, Z. anorg. Ch. 104, 27 (1918).
- [2] M. Hansen, Structure of Binary Alloys, 1 (1941) p. 345 [Russian translation].
- [3] H. Goldschmidt, J. Iron a. Steel Inst. 160, 345 (1948).
- [4] E. Friemann and F. Sauerwald, Z. anorg. Ch. 203, 64 (1932).
- [5] K. Kelly, F. S. Boerliche, G. S. Moore, E. H. Huffman and W. N. Bangert, Techn. Reports Bureau of Mines, Technical Paper, 662 (1944).
- [6] G. V. Samsonov and Ya. S. Umanskii, Solid Compounds of High-Melting Metals [In Russian] (Metallurgy Press, 1957) p. 136.
- [7] R. Kieffer and P. Schwarzkopf, Hard Alloys (Metallurgy Press, 1957) p. 120 [Russian translation].
- [8] T. Ya. Kosolapova and G. V. Samsonov, J. Appl. Chem. 32, No. 1, 55 (1959).*

Received February 28, 1958

*Original Russian pagination. See C.B. Translation.

INVESTIGATION OF LOCAL AND GENERAL CORROSION OF AUSTENITIC CHROMIUM-NICKEL STEEL IN HEAT TREATMENT AND DESCALING*

A. V. Shreider, E. M. Kontsevaya and V. P. Gamazov

The production of stainless sheet steel and nickel-based heat-resisting alloys includes an operation in which the hot-rolled steel is rolled cold after being heat-treated and cleaned by means of emery wheels. The cold rolling is carried out with the use of a lubricant which facilitates plastic deformation. After homogenizing heat treatment of the cold-rolled metal, the scale is removed by a combined alkaline-acid process and the surface quality is checked.

Only fine ripples, dents, and small scratches not exceeding half the sheet-thickness tolerance are permitted [1, 2] on the surface of the finished sheet metal. However, a number of defects are found in production which undoubtedly owe their origin to corrosion, and the presence of which leads to rejection of the metal, as their removal by mechanical cleaning exceeds the thickness tolerance. Among the possible causes suggested for these faults were silicate particles (from the furnace crown), sand, alkali, or water splashes on the lubricated surface, a high sulfur content (1.0-1.5%) in fuel oil, and uneven application of lubricant before the rolling. Deviations from the normal descaling procedure are also likely causes of metal corrosion [3]. This is due both to the general corrosiveness of the media used and to the possible action of "unremoved scale-metal" galvanic cells during the pickling process [4].

These suggestions were tentative and had not been confirmed by direct experiment. The aims of the present investigation included determination of the causes of local and general corrosion of the metal during heat treatment and pickling.

EXPERIMENTAL

Method of investigation. The samples used for the investigation included the austenitic stainless steels OKh18N9 (0.06 C, 0.20 Mn, 0.80 Si, 0.020 S, 0.035 P, 17.0 Cr, 8.5 Ni), 1Kh18N9 (0.15 C, 0.2 Mn, 0.8 Si, 0.025 S, 0.030 P, 18.3 Cr, 8.8 Ni), 1Kh13N4G9 (0.25 C, 7.4 Mn, 0.33 Si, 0.025 S, 0.03 P, 16.7 Cr, 4.3 Ni), and a heat-resisting nickel-chromium alloy of the Nichrome type (0.11 C, 0.8 Mn, 0.81 Si, 0.010 S, 0.015 P, 20.0 Cr, 78.0 Ni, 0.15 Ti, 0.45 Fe). These types of sheet metal, widely used in various branches of technology, have often been rejected in works practice owing to corrosion. All the test specimens of each metal type were cut from a single sheet. The specimen dimensions were 50 × 45 × 1.5 mm. In order to simulate production conditions, lubricant with or without admixtures was applied to the specimen surfaces by means of a rubber roller. The lubricants used (in conformity with the cold-rolling technology used in production of sheet steel) were machine oil, soap emulsion, and kerosene. As it has been found in works practice that the lubricated surface may become contaminated with various impurities, the following admixtures were introduced into the lubricants: carbon black, silica (quartz dust), sulfur, emery dust, alkali (NaOH), and 10, 25 and 50% of water.

High-temperature oxidation (simulating heat treatment after cold rolling) was effected in an electrically heated air furnace with exposures of 2, 5, 7 and 10 minutes at 800, 900, 1000 and 1100° (in the technological process the exposure time for metal not greater than 2 mm thick is 2 minutes, and the following furnace

*Communication II on high-temperature oxidation of stainless sheet steel.

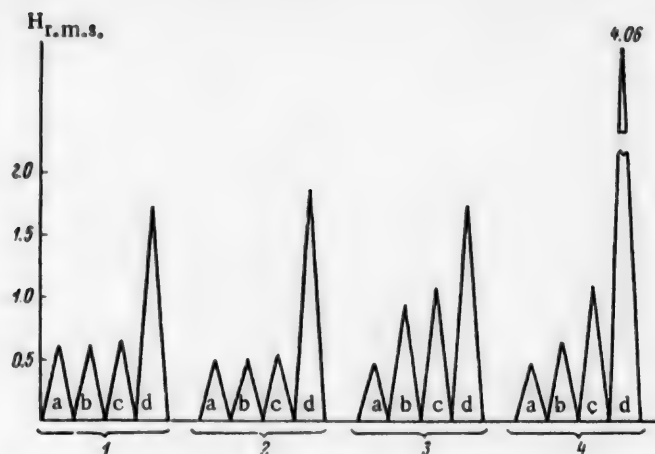


Fig. 1. Variations of the surface smoothness H_{rms} (in μ) of test specimens: specimens: 1) OKh18N9; 2) 1Kh18N9; 3) 1Kh13N4G9; 4) Nichrome: a) original specimen; b) after oxidation for 2 minutes at 1100°; c) after oxidation under lubricant; d) after oxidation under lubricant with added sulfur.

temperatures are used: for OKh18N9 and 1Kh18N9, 1070-1100°; for 1Kh13N4G9, 1130-1150°; for Nichrome, 1040-1060°).

Scale was removed [5] by consecutive treatments in an alkaline melt, an acid bath, and a brightening and passivating solution. The caustic treatment (in a melt of 80% caustic soda and 20% sodium nitrate) was carried out at 300, 400, 450 and 500° with exposures of 10, 20, 40 and 80 minutes (20 minutes at 500° in the technological process). The acid pickling (18% sulfuric acid and 5% sodium chloride) was effected at 40, 60, 70 and 80° with exposure times of 5, 10, 15 and 20 minutes (15 minutes at 70° in the technological process). The brightening (in 6-8% nitric acid) was carried out by the works procedure (5 minutes at 45°), as preliminary experiments showed that no corrosion effects or weight losses are observed at this stage of the process even with considerable deviations from the specified conditions. Changes of surface quality were estimated by means of an Abbott profilometer.

Electrochemical effects during scale removal in the alkaline melt were studied by means of a very simple apparatus in which a microammeter was used to determine the polarity and current generated by a couple consisting of two electrodes, one covered with scale and one with an unoxidized surface.

If the specimens were coated with noncontaminated lubricants, the high-temperature oxidation was decreased in the case of 1Kh14N4G9 (105 instead of 280 g/m²), and increased very slightly in the cases of OKh18N9 (29 instead of 28 g/m²), 1Kh18N9 (27 instead of 19 g/m²), and Nichrome (21 instead of 20 g/m²), in all cases in 2 minutes at 1100°. This result is associated with the decrease in the oxidizing power of the atmosphere in the furnace caused by combustion of the lubricant, and can be explained by the decrease of gaseous corrosion of the manganese-rich 1Kh13N4G9 steel and its increase in the cases of OKh18N9, 1Kh18N9, and Nichrome with decrease of the excess air ratio [6].

No differences could be detected between the oxidation rates of specimens coated with different kinds of lubricant; evidently all the lubricants are oxidized under these experimental conditions without formation of thermally unstable (but corrosive) organic acids. Similarly, application of the pure lubricants in the form of individual drops was not accompanied by formation of spots or local surface defects, visible after heat treatment and pickling.

In experiments on the application of lubricants containing various impurities onto the metal surface it was found that the presence of sulfur results in a serious increase of metal corrosion in heat treatment and pickling. For example, when 50% of sulfur was added to machine oil the corrosion loss of OKh18N9 was 170 g/m² (after oxidation for 2 minutes at 1100° and scale removal), whereas with equal amounts of the other additives (silica,

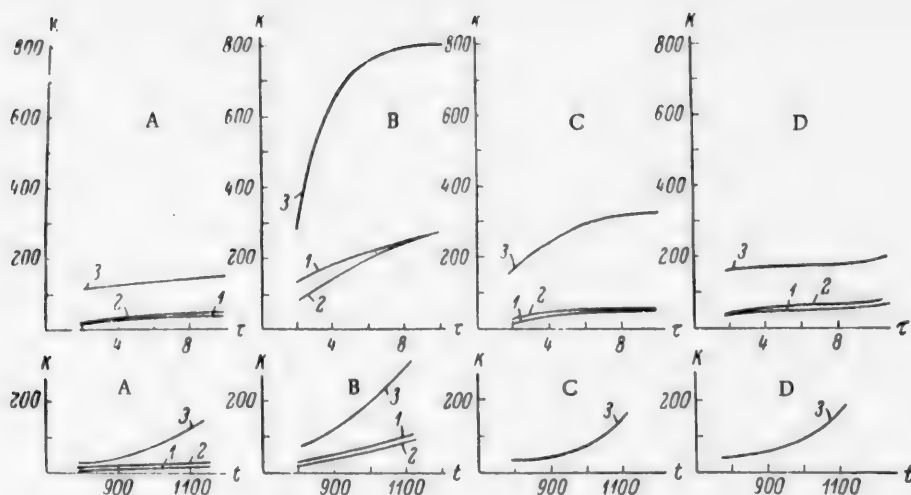


Fig. 2. Corrosion losses caused by heat treatment and scale removal; effects of variations in the high-temperature oxidation conditions: K) corrosion (g/m^2); τ) exposure time at 1100° (minutes); t) temperature at exposure time of 2 minutes (deg); A) Nichrome; B) 1Kh13N4G9; C) 1Kh18N9; D) OKh18N9; heat treatment: 1) without lubricant; 2) with pure lubricant; 3) with lubricant containing sulfur.

carbon black, alkali, emery dust) it was $28 \text{ g}/\text{m}^2$; the corresponding results for 1Kh18N9 were 160 and $26 \text{ g}/\text{m}^2$, for 1Kh13N4G9, 380 and $106 \text{ g}/\text{m}^2$, and for Nichrome, 136 and $40 \text{ g}/\text{m}^2$. These results were confirmed by measurements of surface smoothness (Fig. 1).

Application of drops of lubricant containing carbon black or alkali resulted in the appearance of dark spots after heat treatment and pickling. Microscopic investigation of polished sections showed that the corrosion in the formation of these spots was of a purely surface character. After application of lubricant with addition of quartz or emery dusts the metal surface remained smooth.

The fact that SiO_2 (quartz dust) and Al_2O_3 (emery dust) have no appreciable effect is attributable to the high melting points of silica (above 2500°) and alumina (2200°) and the relatively short exposure during heat treatment.

The effect of carbon black is slight because of the rapid combustion of carbon at the experimental temperatures. Slight corrosion (in effect, a mere change of surface color) in presence of added alkali is due to local variations in the composition and structure of the oxide film under the action of Na_2O at high temperature. Because the exposure is brief, the corrosion does not penetrate to any significant depth into the metal, only the nature of the oxide film and a thin surface layer of metal are changed in practice. The high experimental temperature accounts for the absence of any effect of water added to the lubricant.

However, when sulfur was added to the lubricant there was strong local corrosion, revealed after removal of scale, and accounted for by the characteristics of high-temperature oxidation of chromium-nickel steels and nickel-chromium alloys by sulfur dioxide [7, 8]. The sulfide (and sulfide-oxide) films formed in the process are less firmly attached to the basis metal than the corresponding oxide films. This is due to the very high molecular-volume ratios (over 2.5) for sulfide films consisting of FeS , NiS , MnS and Cr_2S_3 , so that these films crack under the action of the large internal stresses developing in them and the oxidizing agents have better access to the metal.

In addition, nickel sulfides can form a eutectic with metallic nickel; the melting point of this (640°) is considerably lower than that of the material constituting the oxide film on nickel and on nickel-based alloys (such as Nichrome).

Figure 2 shows that when sulfur is added to the lubricant the parabolic curves representing corrosion kinetics at 1100° become steeper (especially in the case of the low-chromium alloy 1Kh13N4G9), and indicate that the

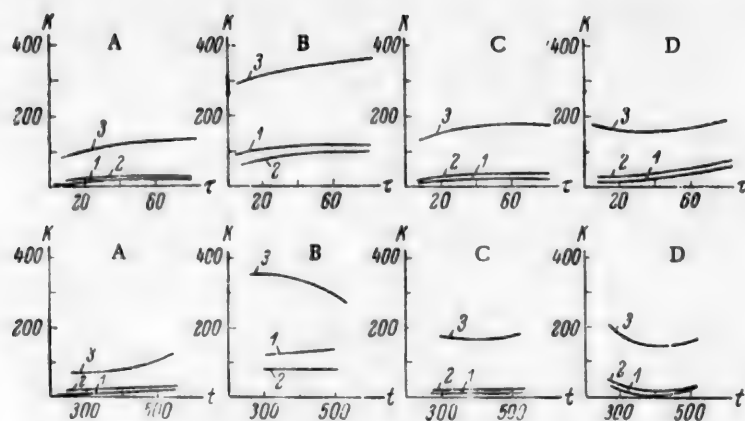


Fig. 3. Corrosion losses caused by heat treatment and scale removal; effects of variations in alkaline treatment conditions: K) corrosion (g/m^2); τ) exposure time at 500° (minutes); t) temperature at exposure time of 20 minutes (deg); specimens: A) Nichrome; B) 1Kh13N4G9; C) 1Kh18N9; D) OKh18N9; heat treatment: 1) without lubricant; 2) with pure lubricant; 3) with lubricant containing sulfur.

corrosion losses are considerably greater for all the alloys. The presence of a high chromium content (for example, 20.0% in Nichrome) accounts for the smaller increase of the rate of gas-phase corrosion in presence of SO_2 in the atmosphere [7].

After exposures (of up to 20 minutes) under lubricant containing sulfur, at 600, 900 and 1000° , it was found (by examination of polished sections under the microscope) that no intercrystalline corrosion took place in any of the metals investigated. This is especially important in evaluation of the quality of metal rejected because of surface defects caused by corrosion; metal with signs of local corrosion due to the action of sulfur, which can be removed mechanically without loss of metal to a depth exceeding half the sheet-thickness tolerance, can be supplied to the consumer without objections.

Intercrystalline corrosion cannot occur in this case in Nichrome, which is particularly susceptible to the corrosive action of sulfur, because of the brevity of the exposure and fairly complete combustion of sulfur; the high-temperature intercrystalline corrosion of nickel-chromium alloys (by formation of nickel sulfide at the grain boundaries) which has been described [7] occurs during fairly prolonged action of a medium formed with incomplete combustion of sulfur.

In order to determine the possible causes of corrosion, a study was made of the effects of varying the exposure times and temperatures in high-temperature oxidation (heat treatment), alkaline pickling, and removal of residual scale in acid solution. The corrosion was estimated from the weight losses of specimens after treatment in accordance with the works procedure at all stages except one. The weight losses were determined for specimens oxidized without lubricant and coated with uniform layers of pure lubricant and lubricant with added sulfur. The results of these experiments are given in Fig. 2-4.

The graphs indicate that OKh18N9 is attacked more vigorously than 1Kh18N9; this is due to the different chromium contents of the two steels (17.0 and 18.3% respectively).

As the result of combustion of sulfur during the experiments the kinetic curves for high-temperature oxidation of specimens coated with lubricant containing sulfur show a gradual decrease of the corrosion rate.

The increase of the temperature coefficient caused by addition of sulfur to the lubricant is due to a change of the corrosion mechanism when sulfide instead of oxide films are formed; as the result of rapid cracking and peeling of sulfide films the high-temperature oxidation is determined not by diffusion (as in coating of the surface by a continuous oxide film) but by chemical combination with sulfur on the metal surface.

The effect of the temperature of the caustic melt on corrosion differs for the different metals investigated;

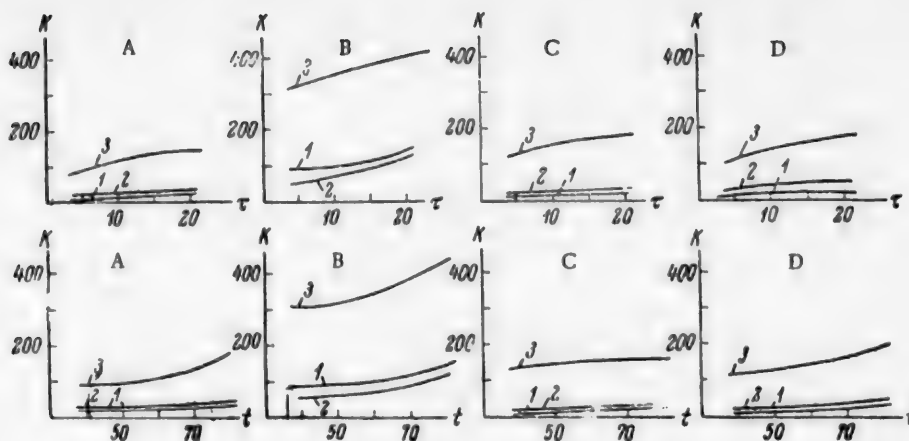


Fig. 4. Corrosion losses caused by heat treatment and scale removal; effects of variations in acid pickling conditions: K) corrosion (g/m^2); τ) exposure time at 70° (minutes); t) temperature at exposure time of 15 minutes ($^\circ\text{C}$); specimens: A) Nichrome; B) 1Kh13N4G9; C) 1Kh18N9; D) OKh18N9; heat treatment: 1) without lubricant; 2) with pure lubricant; 3) with lubricant containing sulfur.

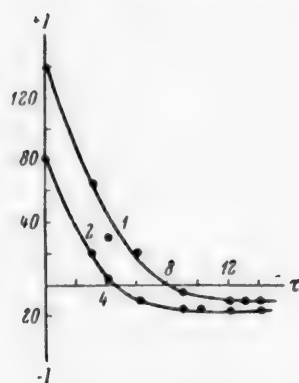


Fig. 5. Variations of the current of corrosion cells with time: τ) time (minutes); I) current strength (microamp); electrodes of unoxidized Nichrome and Nichrome oxidized for 2 minutes at 1100° : 1) under pure lubricant; 2) without lubricant; electrolyte - melt of 80% caustic soda and 20% sodium nitrate at 500° .

this is because of differences in their composition and in the chemical and phase composition of films formed by high-temperature oxidation of their surfaces. The stronger corrosion of OKh18N9 and 1Kh18N9 at lower melt temperatures (300°) is attributable to incomplete removal of scale. The "scale-metal" couples which arise as a result of this during the subsequent acid pickling lead to intensified local corrosion. Otherwise, variations of temperature and exposure time in the caustic melt only influence the extent of general (uniform) corrosion.

Variations of the technological procedure by increases of the exposure time and temperature (within limits likely in practice) during acid treatment result in considerably increased corrosion of the metal. The kinetic and temperature curves determined in a study of the acid pickling process were steeper for specimens coated with a lubricant containing sulfur before the high-temperature oxidation. The explanation is that as a result of the specific action of sulfur such specimens have a rougher surface than specimens oxidized without lubricant or coated with pure lubricant. Increase of the true surface area leads to more intensive corrosion in the acid liquor. Deviations of temperature and exposure time from those used in the technological pickling process result only in intensification of general corrosion of the metal.

Electrochemical tests showed that the current is considerably greater in a couple containing a Nichrome electrode previously subjected to high-temperature oxidation under a lubricant (Fig. 5). This may be ascribed to the formation of a rougher surface when Nichrome is oxidized under the lubricant (Fig. 1); such a surface traps air mechanically much easier when

immersed in the melt. The oxygen in this air acts as depolarizer in the corrosion process.

The observed reversal of electrode polarity (the unoxidized metal changed from an anode to a cathode) is associated with gradual exposure of regions of pure metal under the scale on the specimen originally oxidized cathodically, with expenditure of the mechanically-trapped oxygen, and with a possible passivating effect of the nitrate.

These experiments demonstrate the electrochemical character of descaling in caustic nitrate melts.

LITERATURE CITED

- [1] GOST 5582-50 [In Russian].
- [2] Ferrous Metals Technical Specification 3162-52 [In Russian].
- [3] J. Lomas, Machinery Lloyd 23, 11 (1951).
- [4] V. O. Krenig and E. M. Zaretskii, Corrosion and Its Prevention 3-4, 9-18 (1939).
- [5] N. P. Zhetvin, F. S. Rakhovskaya and A. N. Ushakov, New Methods of Steel Pickling [In Russian] (Metallurgy Press, 1957).
- [6] N. P. Zhetvin, F. A. Prokopovich, E. M. Kontsevaya and B. S. Brusilovskii, Steel 8, 723 (1952).
- [7] K. Hauffe, Oxydation von Metallen und Metallegierungen, Springer-Verlag (1956).
- [8] V. V. Ipat'ev and D. V. Zheltukhin, J. Appl. Chem. 30, No. 9, 1281 (1957). *

Received December 13, 1957

*Original Russian pagination. See C.B. Translation.

GAS FORMATION IN THE ETCHING OF ZINC IN ACID SOLUTIONS

I. I. Zabolotnyi and A. P. Lizogub

Our method for studying gas formation in the acid corrosion of zinc [1] was applied in the present investigation to determination of the sizes of gas bubbles liberated by the action of hydrochloric acid on zinc in presence of surface-active agents and during the etching of zinc in mixtures of hydrochloric and nitric acids of different concentrations. This investigation was initiated in an attempt to determine the variations of gas formation with changes in the conditions of acid corrosion of zinc; this is significant in relation to investigation of the etching of zinc printing blocks.

EXPERIMENTAL

Diagrams were first obtained showing the distribution by radius of the hydrogen bubbles liberated during etching of zinc in 5 and 10% hydrochloric acid solutions in presence of such surface-active agents as amyl alcohol, Nekal (sodium dibutylnaphthalene sulfonate), gelatin, and caproic acid. Each of the investigated solutions contained one of these substances in 0.06% concentration. The experimental results presented in the table show that all these agents decrease the most probable bubble radius.

Surface-active agent	Most probable bubble radius (in μ) in etching in HCl solution (%)	
	5%	10%
Without addition	55	190
Caproic acid	35	70
Amyl alcohol	40	80
Gelatin	40	—
Nekal	50	85

It is significant that the influence of surface-active agents is more pronounced in the more highly concentrated acid solution.

Before dealing with the corrosion of zinc in acid mixtures, we studied the kinetics of gas formation during etching of zinc in pure aqueous solutions of nitric acid at different concentrations. It follows from Fig. 1 that in the corrosion of zinc in 16, 20, 25 and 30% HNO_3 solutions during 25 minutes the bubble size either remains unchanged or decreases slightly; the decrease is almost within the limits of experimental error. For comparison, a curve for 8% hydrochloric acid (Curve V) is given in the same diagram.

The most probable bubble radii in the range of nitric acid concentrations from 6 to 30% are represented by Curve I (Fig. 2). The same diagram also shows the influence of additions of 5% HNO_3 (Curve II) and 2% HNO_3 (Curve III) to HCl solutions of different concentrations on the bubble size. It is clear from a comparison of these results with Curve IV for HCl solutions without additives that nitric acid reduces the most probable bubble radius, and the decrease may be either slight or very considerable.

However, subsequent experiments showed that with certain proportions of hydrochloric to nitric acid in the

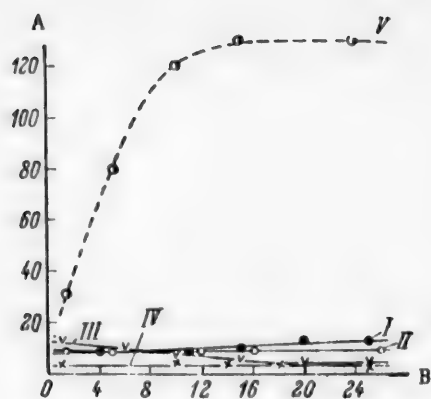


Fig. 1. Kinetics of gas formation during etching of zinc in nitric acid solutions of different concentrations: A) most probable bubble radius (μ); B) time (minutes); HNO_3 concentrations (%): I) 16; II) 20; III) 25; IV) 30; V) 8% HCl solution.

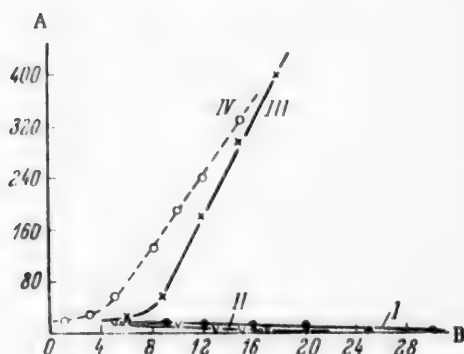


Fig. 2. Effects of nitric and hydrochloric acid concentrations on the most probable bubble radius: A) most probable bubble radius (μ); B) acid concentration (%); I) $R = f(C_{\text{HNO}_3})$; II) $R = f(C_{\text{HCl}} + 5\% \text{HNO}_3)$; III) $R = f(C_{\text{HCl}} + 2\% \text{HNO}_3)$; IV) $R = f(C_{\text{HCl}})$.

mixtures nitric acid may have a different and opposite influence on gas formation. For example, the most probable bubble radius in the corrosion of zinc in 10% hydrochloric acid is 180μ , but if this solution additionally contains about 10% of nitric acid the most probable radius reaches 280μ (point on Curve I, Fig. 3, corresponding to a mixture of 40 ml 20% HCl and 50 ml 20% HNO_3). The curves in Fig. 3 clearly show that the bubble size depends very strongly on the relative proportions of hydrochloric and nitric, or sulfuric nitric (Curve II) acids in the mixture.

The decrease of bubble size found for a mixture containing about 15% HCl and 5% HNO_3 interested us, and experiments were therefore carried out to find whether this effect occurs at other concentrations of HCl and HNO_3 , if the ratio of these concentrations is kept constant at 3:1. It is clear from Fig. 4 that the bubble size remains unchanged at hydrochloric acid concentrations from 6 to 21%, with corresponding nitric acid concentrations from 2 to 7%. With a more highly concentrated solution, containing 27% HCl and 9% HNO_3 , the bubble size increases somewhat.

The dual influence of nitric acid on the most probable bubble radius was detected in studies of the kinetics of gas formation in the corrosion of zinc in acid mixtures recommended in the production instructions for etching of zinc blocks [2] (Fig. 5). The opposing effects of HNO_3 on gas formation are all the more evident in this case as the solutions differ relatively little in composition.

DISCUSSION OF RESULTS

The similar influence of the surface-active agents used, differing from each other in their molecular state, on the size of hydrogen bubbles formed during corrosion of zinc in hydrochloric acid is determined by the adsorption of these substances on the zinc surface. These substances form a layer on the zinc surface, which inhibits the discharge of hydrogen ions. This leads to increased hydrogen overvoltage and greater microcathodic polarization, and this probably leads, in accordance with the data in the table, to a decrease in the most probable size of the hydrogen bubbles.

The more pronounced decrease of bubble size observed with the use of more concentrated acid solutions containing surface-active agents can be explained by the overvoltage theory of Frumkin and his school [3], according to which hydrogen-ion concentration has less influence than the presence of surface-active agents and of high-valence ions on the overvoltage.

It should be pointed out that the decrease in the size of hydrogen bubbles formed in acid corrosion of zinc in presence of surface-active agents is caused not only by electrochemical changes but also by adsorption of these substances on the surfaces of the forming hydrogen bubbles. This is confirmed by the fact that the bubble size did not change appreciably with the distance from the zinc surface undergoing direct corrosion. As has been noted by one of us [4], this stabilization of gas evolution corresponds to more uniform etching of zinc surfaces in sulfuric and hydrochloric acid solutions containing surface-active substances. It follows that the gas evolution which occurs during acid corrosion of metals can give an indication of the state of surface etching.

Our consideration of the experimental data presented in Fig. 1-5 was based on the assumptions that all the corrosion processes in which large gas bubbles ($R > 20\text{-}30 \mu$) are liberated involve hydrogen depolarization

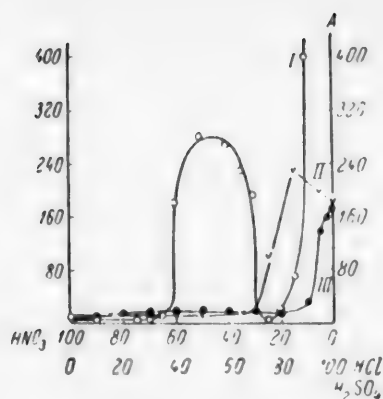


Fig. 3. Most probable radii of gas bubbles liberated during corrosion of zinc in mixtures of different acid solutions: A) most probable bubble radius (μ); acid solution (%): I) 20 HCl and 20 HNO₃; II) 10 HCl and 10 HNO₃; III) 20 H₂SO₄ and 20 HNO₃.

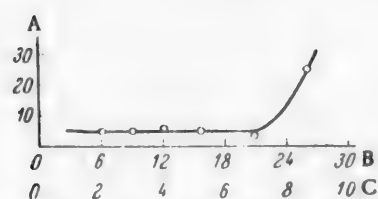


Fig. 4. Sizes of gas bubbles liberated in the etching of zinc in mixtures of hydrochloric and nitric acids in 3:1 concentration ratio: A) most probable bubble radius (μ); B) HCl concentration (%); C) HNO₃ concentration (%).

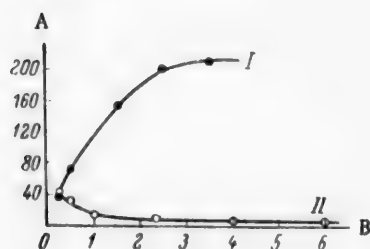
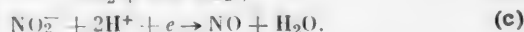


Fig. 5. Variations of the most probable bubble radius during corrosion of zinc in different solutions: A) most probable bubble radius (μ); B) time (minutes); respective contents of HNO₃ (d = 1.4); HCl (d = 1.2) and H₂O in solutions (in ml): I) 270, 270 and 1000; II) 150, 200 and 1000.

(hydrogen was detected by the flash test), while corrosion processes accompanied by formation of small bubbles involve oxidative depolarization according to the scheme [5]:



It is possible that in some instances when zinc was etched in these acid mixtures hydrogen and oxides of nitrogen were evolved simultaneously. We now consider which factor has the predominant influence on the most probable bubble radius. It may be assumed that the size of gas bubbles liberated during corrosion of a metal depends on the nature of the metal, its surface roughness, temperature to which the specimen is heated in the course of corrosion, solution composition and, finally, the microelectrode potentials of the acting local cells where the bubbles are formed. The first three factors were relatively constant in all the experiments; the following observation is of value in determining the factor which has the greatest influence on bubble size. When zinc is etched in some mixtures of nitric and hydrochloric acids, the composition of which corresponds to the abrupt transition from oxidative to hydrogen depolarization (for example, two points on Curve I, Fig. 3 correspond to such a composition), small bubbles are formed at first. However, 10–20 minutes after the start of corrosion the bubbles suddenly increase to a radius of 200 μ and over, evidently because of a slight decrease of the nitric acid concentration at the corroding surface; it appears that at this point oxidative depolarization is abruptly replaced by hydrogen depolarization.

In our view, this effect justifies the conclusion that the sharp transition from small to large bubbles is the consequence of an abrupt changes in the microelectrode potentials, as obviously the other factors listed above cannot change instantaneously.

It is from this standpoint and in accordance with Frumkin's electrocapillary theory [3], which successfully explains the relationship between the bubble size of gases liberated during electrolysis and the electrode potential, that we interpret our observations of gas formation in corrosion processes accompanied by oxidative depolarization.

The small size of the bubbles liberated in the action of nitric acid on zinc is evidently the consequence of the high overvoltage for liberation of nitrogen oxides, i.e., of retardation of one of the processes of electron acceptance. As a result, the microcathodes acquire far larger negative values than is the case in processes with hydrogen depolarization, so that the contact angle at the metal-solution-bubble boundary is small, and small bubbles are released.

Apparently concentrational polarization does not occur here, and therefore the bubble size does not depend on the nitric acid concentration.

In our opinion, the bubble size remains constant during the corrosion process because impurities dissolve in nitric acid together with zinc, so that the area of the microcathode regions remains

unchanged. Accordingly, their potentials also remain unchanged, and the most probable bubble radius is likewise constant. Absence of impurities on the zinc surface was demonstrated by the mirror-bright surface observed in all corrosion processes with oxidative depolarization.

SUMMARY

1. Surface-active agents decrease the most probable radius of the gas bubbles liberated when zinc is etched in hydrochloric acid solutions.

2. Gas formation during acid corrosion of zinc conforms to the following rules: a) corrosion of zinc in nitric acid solutions of different concentrations is accompanied by liberation of gas bubbles the size of which remains approximately constant during the process; b) addition of nitric to hydrochloric acid produces a considerable decrease or increase of bubble size as compared with that observed in corrosion in pure hydrochloric acid solutions; the nature of this change depends on the amounts of nitric and hydrochloric acid in the mixture.

LITERATURE CITED

- [1] I. I. Zabolotnyi and A. P. Lizogub, *J. Appl. Chem.* 31, 730 (1958). *
- [2] Etching of Zincographic Printing Blocks (Technical production instructions edited by S. P. Miklashevskii, 1948) [In Russian].
- [3] B. N. Kabanov and A. I. Frumkin, *J. Phys. Chem.* 4, 539 (1933); B. N. Kabanov and E. Zh. Faingluz, *J. Phys. Chem.* 8, 795 (1936).
- [4] I. I. Zabolotnyi, *Proc. Sci. Session of the Fedorov Polygraphic Inst. of the Ukraine* 10, 65 (1952).
- [5] G. V. Akimov and O. T. Deryagina, *J. Phys. Chem.* 26, 282 (1952).

Received July 15, 1957

*Original Russian pagination. See C.B. Translation.

INVESTIGATION OF THE POROSITY AND ADSORPTION PROPERTIES OF PROTECTIVE FILMS FORMED ON THE HEATING SURFACES OF CORRODING METALS

N. G. Chen

In corrosion processes one of the main factors in retardation of chemical and electrochemical breakdown of a metal is the protective film. Such films may be produced on metal surfaces either under natural or under artificial conditions.

The problem of porosity and adsorption properties of these films is very important and has been studied little as yet.

Recent papers dealing with this problem are concerned mainly with studies of the porosity of anodic oxide films on aluminum and its alloys [1] and adsorption of electrolyte ions on anodic Al_2O_3 films [2]. The protective films formed by the action of certain ions on heating surfaces of corroding steel have been studied very little. Therefore studies of ion adsorption on various films, and investigations of their porosity, which is one of the determining factors in the protective action of such films, are of great interest, because they should reveal the influence of the adsorption of certain ions on the porosity of protective films.

EXPERIMENTAL

The adsorption properties of protective films formed on corroding metal surfaces were studied with the aid of the radioactive isotopes S^{35} and P^{32} in the form of the compounds $Na_2S^{35}O_4$, $Na_2HP^{32}O_4$ and $Na_3P^{32}O_4$, which were added to solutions containing the corresponding stable salts at different concentrations (Tables 1-3).

Porosity was determined by the Tomashov method [1] and calculated from the formula

$$\beta = \frac{p \cdot 10^6}{\gamma \cdot b \cdot s},$$

where β is the porosity (%); p is the weight of oil taken up by the film pores (g); γ is the density of the oil (g/cc); b is the film thickness (μ); s is the film area (cm^2).

Metal corrosion was determined gravimetrically from the weight loss of the test specimens. The specimen was weighed on an analytical balance before the experiment and after, the corrosion products being removed by means of hydrochloric acid containing inhibitor. The specimens were dried for 24 hours over concentrated sulfuric acid in a desiccator before each weighing.

The experiments were performed at pH of about 9; in view of the fact that under industrial conditions corrosion of metal equipment often occurs in a boiling corrosive medium with continuous formation of corrosion products, a steel experimental unit with a reflux condenser was used in this investigation. Specimens of steel (3) were inserted into this apparatus so that on one side the specimen was in contact with a boiling solution and on the other it was heated electrically. Thus, the specimen acted as a heating surface during the experiment. Each experiment was continued for 10 hours. After the experiment the specimen was removed from the apparatus and washed repeatedly in running tap water until the activity became constant. The specimen was then dried and the activity of the surface which had been in contact with the boiling solution containing a radioactive trace

TABLE 1

Corrosion Rate and Adsorption of HPO_4^{2-} and SO_4^{2-} Ions

Solution concentration (mg/liter)	Na_2SO_4		Na_2HPO_4	
	Corrosion rate (mg/m ² ·hr)	Ion adsorption (pulses/cm ² ·min)	Corrosion rate (mg/m ² ·hr)	Ion adsorption (pulses/cm ² ·min)
800	691.7	7.6	325.0	241.7
1000	691.7	5.4	275.0	177.0
2500	608.3	4.2	283.0	185.2
5000	625.0	3.5	308.3	204.9

TABLE 2

Correlation of Porosity and Adsorption of Protective Films

Substance	Film porosity (%)	Ion adsorption (pulses/cm ² ·min)	Corrosion rate (mg/m ² ·hr)
Na_2HPO_4	30.3	65.7	208.3
Na_3PO_4	25.8	23.3	333.3
Na_2SO_4	60.4	3.7	650.0
$\text{Na}_3\text{PO}_4 + 35 \text{ mg/l NaCl}$	40.5	57.8	441.0
$\text{Na}_3\text{PO}_4 + 35 \text{ mg/l Na}_2\text{SO}_4$	49.2	74.6	416.0

TABLE 3

Effects of Concentration of Na_3PO_4 Solution on Adsorption of PO_4^{3-} Ions on Protective Films and on Film Porosity

Solution concentration (mg/liter)	Na_3PO_4	
	film porosity (%)	ion adsorption (pulses/cm ² ·min)
50	46.2	11.4
200	33.8	22.8
400	25.8	22.7
800	25.0	26.0

was measured by means of a type B unit. The ion adsorption was expressed in pulses per cm² per minute. The results of our experiments are presented in Tables 1-3.

DISCUSSION OF RESULTS

It follows from Table 1 that under given conditions, at all the solution concentrations tested, the corroding metal surface adsorbs much more HPO_4^{2-} ions than SO_4^{2-} ions.* On the other hand, metal corrosion is much slower in Na_2HPO_4 solutions than in sulfate solutions.

Correlation of the porosity and adsorption properties of protective films with the corrosion rates of the metal in different corrosive media, but of the same concentration (400 mg/liter), reveals the following facts (Table 2).

First, the porosity of protective films formed on corroding metal surfaces in sodium sulfate solution is approximately double that of films formed in phosphate solution, and the corrosion rate of the metal in the medium containing Na_2SO_4 is greater in roughly the same proportion.

Second, whereas adsorption of anions from solutions of Na_2HPO_4 , Na_3PO_4 and Na_2SO_4 , free from chloride ions, decreases in the sequence of HPO_4^{2-} , PO_4^{3-} and SO_4^{2-} , the corrosion rate increases in the same sequence under the same conditions.

Third, addition of either NaCl or Na_2SO_4 to Na_3PO_4 solution sharply increases film porosity, adsorption of PO_4^{3-} ions, and the corrosion rate.

*In comparison of the adsorptions, the difference between the radiation energies of S^{35} and P^{32} isotopes was taken into account.

Experiments on adsorption of PO_4^{3-} ions on protective films and determinations of the film porosity in relation to the concentration of the Na_3PO_4 solution (Table 3) show that with increase of sodium phosphate concentration the adsorption of PO_4^{3-} increases and the porosity of the phosphate films decreases.

Locomotive boilers are often subject to strong sulfate corrosion in use. In the light of our experimental data the explanation of this effect is that the protective film formed by the action of SO_4^{2-} ions on the metal surface is highly porous. The porosity is 60.4%. There is no doubt that such a porous film cannot have an adequate protecting effect.

Moreover, our experiments show that chloride anions greatly increase the porosity of phosphate films. Their protective effect is thereby diminished considerably, but the adsorptive capacity of the films becomes much greater, probably owing to the increase of their total area (Table 2). Thus, Cl^- ions break down the continuity of the protective films and thereby favor corrosive destruction of the metal.

The literature contains diverse views on the corrosive action of chloride ions. The most likely of these views, in our opinion, is that in the corrosion process the chloride ions are adsorbed on the film and displace oxygen anions. As a result, the metal chloride is formed, which is readily soluble in the medium, so that pores are formed over different regions of the film [3, 4], whereas if the anions give insoluble compounds such as phosphates with the metal, the protective films formed on the metal surface have low porosity and protect the metal quite reliably against corrosion (Table 2).

The radioactivity acquired by a metal surface covered by an oxide film and placed in contact with a solution containing radioactive ions may be due to the following factors.

First, it is known that corrosive breakdown of a metal coated with an oxide film occurs in consequence of rupture of this film and formation of anodic regions at the exposed places, with formation of cathodic regions at places coated with the electronically-conducting film. The radioactive cations are deposited at the latter after neutralization of their charges, and confer radioactivity on the metal surface [5].

Second, radioactive cations become directly incorporated in the protective film formed on the surface of a corroding metal during the corrosion process [6]. Radioactive ions may become included in the protective film either by chemical interaction between the anions and the metal with formation of insoluble compounds, or as the result of adsorption.

In our experiments phosphate and sulfate anions were incorporated into the protective film formed on the metal surface. This shows that a film formed on the surface of a corroding metal probably always contains anions from the corrosive medium, and the contents of these anions in a particular film depend on the concentration (Table 3) and nature (Table 2) of these anions.

According to our results, the anion content of the passivating layer has a definite influence on the passive state of the metal.

SUMMARY

1. Tomashev's oil-filling method for determination of the porosity of protective films can be used with sufficient accuracy for determining the relationship between film porosity and corrosion rate.
2. The adsorption properties and porosities of protective films formed by the action of SO_4^{2-} , PO_4^{3-} , HPO_4^{2-} and Cl^- ions on heating surfaces of corroding metals were studied; the results explain the corrosive action of Cl^- , SO_4^{2-} ions and the inhibiting action of HPO_4^{2-} and PO_4^{3-} ions.

LITERATURE CITED

- [1] N. D. Tomashev and A. V. Byalobzhetskii, Trans. Inst. Phys. Chem. Acad. Sci. USSR 3, 2 (1951).
- [2] A. V. Bogoyavlenskii and A. P. Vedernikov, J. Appl. Chem. 30, No. 2, 1868 (1957). *
- [3] N. D. Tomashev, Theory of Metal Corrosion [In Russian] (Metallurgy Press, 1952).
- [4] L. Vanyukova and B. Kabanov, Proc. Acad. Sci. USSR 59, No. 5 (1948).
- [5] M. T. Simnad and R. C. Ruder, J. Electroch. Soc. 98, 301 LIX, 5 (1948).
- [6] D. M. Brasher and E. K. Stove, Chem. Ind. 23, 171 (1952).

*Original Russian pagination. See C.B. Translation.

INFLUENCE OF CERTAIN IONS ON THE PROTECTIVE ACTION OF PHOSPHATE INHIBITORS OF CORROSION

N. G. Chen

Corrosion inhibitors are widely used in practice for protecting metals against the destructive effects of corrosive media. Therefore studies of the influence of certain ions on the protective action of corrosion inhibitors, including sodium phosphates, are of definite practical importance. The experiments were performed by the radioactive-tracer method described in the preceding paper.*

The protective action of the corrosion inhibitors was calculated by means of the formula

$$Z = \frac{(\rho_0 - \rho) \cdot 100}{\rho_0}, \quad (1)$$

where Z is the protective action, ρ_0 is the rate of corrosion without inhibitor, and ρ is the rate of corrosion in presence of inhibitor.

RESULTS AND DISCUSSION

The feed waters of steam boilers and of cooling and heating systems are usually natural waters containing various ions from dissolved salts; these have a very strong corrosive action on iron. Sodium phosphates are widely used for protecting metals against the electrochemical action of corrosive media; the inhibiting effect of phosphates is due to adsorption of phosphate ions on the metal surface with formation of a protective film consisting of $\gamma\text{-Fe}_2\text{O}_3$ and $\text{FePO}_4 \cdot 2\text{H}_2\text{O}$ [1].

This interpretation of the inhibiting action of sodium phosphates is also confirmed by our experiments, which show that 20-30 times as much sodium phosphate as sodium sulfate is adsorbed on the corroding metal surface, but sodium sulfate attacks the metal 2-3 times as rapidly. This shows, on the one hand, that adsorption of PO_4^{3-} ions is of predominant significance in inhibition of metal corrosion, and on the other, that slight adsorption of negatively-charged ions such as SO_4^{2-} on the surface of a corroding metal not only fails to protect the metal but favors the corrosion of iron.

To account for this fact, we first consider Table 1, which shows that the salts Na_2SO_4 , NaCl and CaSO_4 have different corrosive effects. Two facts are revealed by a comparison of their corrosiveness. First, the salts and NaCl have the same cation but different anions (SO_4^{2-} and Cl^-). Thus, the difference between their corrosive effects depends only on the presence of dissimilar anions. At solution concentrations below 0.6 g/liter the SO_4^{2-} anion is more corrosive than the chloride ion, which is smaller and has greater penetrating power. Second, the compounds Na_2SO_4 and CaSO_4 have the same anion but different cations (Na^+ and Ca^{2+}). This greatly influences their corrosive properties. In presence of Ca^{2+} ions the activating effect of the anions is sharply decreased (Table 1).

Determinations of the adsorption of the same ions from boiling solutions containing the radioactive traces S^{35} and Ca^{45} show that the adsorption of SO_4^{2-} anions by the corroding metal surface reaches 38.7%, and that of Ca^{2+} ions, 189.9%**. In the light of these results we attribute the corrosive action of the SO_4^{2-} ion to the fact

*See p. 1553.

**In the case of Ca^{2+} ions adsorption may be accompanied by precipitation of double salts.

TABLE 1

Corrosive Effects of Different Salts

Solution concentration (g/liter)	Corrosion rate (g/m ² · hr)		
	NaCl	Na ₂ SO ₄	CaSO ₄
0.025	0.408	0.475	0.2708
0.05	0.400	0.5417	0.2708
0.10	0.525	0.8583	0.3460
0.20	0.480	0.8333	0.2700
0.40	0.425	0.6500	0.3460
0.60	0.509	0.7083	0.3460

TABLE 2

Effect of Chloride Ions on the Protective Action of Na₃PO₄

Na ₂ SO ₄ con- centration (g/ liter)	Na ₂ SO ₄	Na ₂ SO ₄ + + Na ₃ PO ₄	Protective action of Na ₃ PO ₄ in Na ₂ SO ₄ solution (%)	Na ₂ SO ₄ + Na ₃ PO ₄ + NaCl	Protective action of Na ₃ PO ₄ in Na ₂ SO ₄ solution in presence of chloride (%)
	Corrosion rate (g/ m ² · hr)			Corrosion rate (g/ m ² · hr)	
0.025	0.475	0.3500	26.3	0.5166	0.09
0.05	0.5417	0.3910	27.7	0.5250	3.8
0.10	0.8583	0.4166	51.4	0.5750	33.2
0.20	0.8333	0.3910	53.7	0.4580	45.3
0.80	0.6917	0.3333	51.9	0.3666	47.0
1.00	0.6917	0.3333	51.9	0.4333	37.3
2.50	0.6083	0.3750	38.3	0.4333	29.8
5.00	0.6250	0.3833	22.6	0.4083	34.6

that adsorption of SO₄²⁻ ions, which are negatively charged, accelerates release of positively charged iron ions from the metal into solution, and thereby favors the anode process. Adsorption of Ca²⁺ cations, which are positively charged, prevents the release of the similarly-charged iron ions from the metal, and the anode process is therefore retarded [2].

Thus, one of the causes of the influence of different ions on metal corrosion is their tendency to be adsorbed on the corroding metal surface. The adsorption of sodium phosphates is particularly high. This no doubt accounts for their protective action, and in this case the accelerating effect of the adsorption layer, saturated with negative charges, on the release of positive iron ions from the metal is inhibited sharply by the shielding effect of the phosphate film and electrophoretic blocking of the anodic regions of the metal. However, the protective action of sodium phosphates is diminished by the influence of extraneous ions, especially chloride anions (Table 2).

It follows from Table 2 that chloride ions diminish the protective effect of sodium triphosphate, especially at Na₂SO₄ concentrations below 0.10 g/liter.

This factor probably accounts for the considerable corrosion, often observed in southern railroad practice, when phosphate is used in boilers fed with water containing a mixture of sodium sulfate and chloride. With increase of the Na₂SO₄ concentration the protective effect of Na₃PO₄ increases at first, and then falls sharply at high Na₂SO₄ concentrations; the phosphate inhibitor is most effective at sodium sulfate concentrations between 0.1 and 1 g of sodium sulfate per liter.

The literature contains various explanations of the adverse effect of chloride ions on the action of corrosion inhibitors.

To clarify this problem, we studied metal corrosion with simultaneous determination of the adsorption of phosphate ions on the metal surface in presence of different ions in the corrosive medium. The relationship

TABLE 3

Protective Action of Na_3PO_4 in Relation to Adsorption

Concentration of NaCl solution (g/liter)	NaCl	NaCl + Na_3PO_4			Protective action of Na_3PO_4 (%)
	corrosion rate (g/m ² ·hr)	equilibrium concentration (g/liter)	corrosion rate (g/m ² ·hr)	equilibrium concentration (g/m ² ·hr)	
0.05	0.40	0.0026	0.325	36.666	18.7
0.10	0.525	0.0080	0.400	49.500	23.8
0.80	0.583	0.0120	0.425	158.200	27.1
1.00	1.041	0.0164	0.350	84.347	66.3
2.50	1.054	0.0473	0.388	134.347	63.1
5.00	0.7666	0.0500	0.388	188.09	49.3

between the protective effect of sodium triphosphate and the adsorption of PO_4^{3-} was first studied. The experiments were performed as follows. First the rate of corrosion of the metal was determined in NaCl solutions with concentrations increasing from 0.05 to 5 g/liter. The corrosion rate and adsorption of PO_4^{3-} were then determined in sodium phosphate solution containing the radioactive P^{32} isotope. The protective effect of the phosphate inhibitor was calculated by means of Eq. (1). The results of these experiments (Table 3) show that the protective effect of sodium phosphate increases with adsorption of PO_4^{3-} on the corroding metal surface. However, at higher NaCl concentrations in the corrosive medium the protective effect of Na_3PO_4 diminishes slightly.

The analogous variations of these two values indicate that there is a direct relationship between adsorption and the inhibiting effect of sodium triphosphate. Having thus established the relationship between adsorption of the corrosion inhibitor and its protective action, we directed our subsequent experiments mainly toward studies of the influence of chloride anions on the adsorption of phosphate ions during metal corrosion in presence of extraneous ions in the corrosive medium. Table 4 contains the experimental results, which represent the relationship between adsorption and the concentrations of solutions of different salts and salt mixtures. It is clear from Table 4 that at high solution concentrations the adsorption of disodium hydrogen phosphate by the corroding metal surface is considerably greater than that of Na_3PO_4 . Therefore at high solution concentrations Na_2HPO_4 should be a more effective corrosion inhibitor than trisodium phosphate. This is confirmed by the results of our experiments, which show that at a solution concentration of 1 g/liter the inhibiting effect of disodium hydrogen phosphate is 1.2 times that of Na_3PO_4 .

To determine the influence of chloride ions on the adsorption of PO_4^{3-} and HPO_4^{2-} during metal corrosion, we added 0.035 g of NaCl per liter to the investigated solutions at all concentrations.

The results of these experiments proved unexpected (Table 4). The chloride ion, which is a very active corrosive agent, increases adsorption of PO_4^{3-} and HPO_4^{2-} to a considerable extent. This was confirmed by further experiments in presence of other ions in the corrosive medium (Table 4). The metal corrosion rate in sodium sulfate solutions containing Na_3PO_4 first only rises slightly with increase of the sulfate concentration, and then falls with further increase of Na_2SO_4 concentration. In the region of sodium sulfate concentrations where the corrosion rate falls there is an increase in the adsorption of sodium phosphate on the surface of the corroding metal. Addition of sodium chloride to these solutions in the proportion of 0.4 g/liter increases considerably both the corrosion rate and the adsorption of PO_4^{3-} .

In the light of these experimental data it is of interest to study the effect of chloride ions on adsorption of PO_4^{3-} and metal corrosion in presence of noncorrosive ions, such as SiO_3^{2-} which has an inhibiting effect, in the solutions. The results of these experiments are presented in Table 5; they show that as the Na_2SiO_3 concentration increases the corrosion rate and adsorption of PO_4^{3-} on the metal surface gradually diminish, whereas in presence of the corrosive ions Cl^- or SO_4^{2-} in the solutions the adsorption of PO_4^{3-} increases up to a definite limit with increasing concentration.

The presence of 0.4 g per liter of sodium chloride in Na_2SiO_3 solution, irrespectively of the concentration of the latter, also increases the corrosion rate and adsorption of PO_4^{3-} on the metal surface.

TABLE 4

Variations of the Adsorption Coefficient with Concentrations of Various Salt Solutions

Concentration of stable phosphates (g/liter)	Adsorption coefficient				Sulfate concentration (g/liter)	Na ₂ SO ₄ + Na ₃ PO ₄			Na ₂ SO ₄ + Na ₃ PO ₄ + NaCl		
	Na ₃ PO ₄	Na ₂ HPO ₄	Na ₃ PO ₄ + NaCl	Na ₂ HPO ₄ + NaCl		equilibrium phosphate concentration (g/l)	Adsorption coefficient	corrosion (g/m ² · hr)	equilibrium phosphate concentration (g/l)	Adsorption coefficient	corrosion (g/m ² · hr)
0.025	1.5	2.00	3.42	3.67	0.025	0.0023	14.81	0.3500	0.0033	71.75	0.5166
0.05	6.33	3.41	8.12	7.24	0.050	0.0024	15.89	0.3910	0.0025	81.53	0.5250
0.200	7.47	5.70	11.95	15.64	0.200	0.0049	32.65	0.4166	0.0080	151.33	0.5750
0.400	6.44	8.52	15.76	24.13	0.400	0.0061	31.72	0.3910	0.0151	160.11	0.5250
0.800	7.50	12.00	14.38	26.34	0.800	0.0160	103.18	0.3330	0.0187	143.2	0.5166
2.500	7.52	15.18	14.62	26.97	1.000	0.0310	87.75	0.3330	0.0310	153.17	0.4333
5.000	5.75	14.94	16.6	24.80	2.500	0.0500	105.67	0.3750	0.0500	173.40	0.4333

TABLE 5

Effects of Na₂SiO₃ Concentration on Corrosion Rate and Adsorption of PO₄³⁻

Na ₂ SiO ₃ concentration (g/liter)	Na ₂ SiO ₃ + Na ₃ PO ₄			Na ₂ SiO ₃ + Na ₃ PO ₄ + NaCl		
	equilibrium concentration (g/liter)	adsorption coefficient	corrosion rate (g/m ² · hr)	equilibrium concentration (g/liter)	adsorption coefficient	corrosion rate (g/m ² · hr)
0.025	0.0055	30.43	0.2250	0.0047	159.91	0.4750
0.05	0.0094	24.05	0.2750	0.0083	99.05	0.5166
0.10	0.0206	1.45	0.1916	0.0189	36.76	0.4912
0.15	0.0445	1.40	0.2166	0.0330	33.68	0.4000
0.20	0.0500	2.81	0.2166	0.0431	26.28	0.3250

Thus, in all cases chloride ions increase both adsorption of phosphate ions and the corrosion rate of the metal. This may be explained as follows. The protective film formed by phosphate inhibitors on the metal surface prevents access of the corrosive agent to the metal and inhibits further development of the corrosion process. If chloride ions are present in the corrosive medium they are adsorbed on the film and displace oxygen ions [3]. This results in the formation of the metal chloride, which dissolves readily in the medium so that pores are formed at various regions of the film [4]. This effect, on the one hand, increases the total film area, which accounts for the considerable increase in the adsorption of PO₄³⁻ and HPO₄²⁻ on the metal surface under the influence of chloride ions, and on the other, it sharply lowers the protective effect of the film because the porosity is increased. The presence of pores in the film makes the metal more vulnerable to the corrosive agent.

However, the experiments show that the protective action of the phosphate film on the metal surface is not eliminated completely by the corrosive action of chloride ions; its shielding effect is merely diminished to some extent.

Our explanation of the diminishing effect of sodium silicate on adsorption of Na₃PO₄ with increase of the Na₂SiO₃ concentration is that in a boiling solution sodium silicate is present, as the result of hydrolysis, mainly in the form of colloidal particles of silicic acid which, being negatively charged, become concentrated at the regions of the metal surface where positive iron ions formed in the course of corrosion accumulate [1]. The colloidal particles undoubtedly prevent adsorption of PO₄³⁻, so that the degree of adsorption decreases.

The fall of the corrosion rate as PO₄³⁻ ions are displaced from the adsorption layer by colloidal silicic acid shows that Na₂SiO₃ has a greater inhibiting effect than sodium phosphate. However, the presence of sodium silicate in boiler water is most undesirable because of its relatively easy solubility in high-pressure steam.

SUMMARY

The protective action of sodium phosphate in presence of various ions in the corrosive medium and the influence of chloride ions on adsorption of phosphate inhibitors were studied by the radioactive tracer method; the results demonstrated, in the case of sodium phosphates, the predominant significance of adsorption in the protective action of corrosion inhibitors.

LITERATURE CITED

- [1] L. L. Rozenfel'd, Inhibitors of Corrosion in Neutral Media [In Russian] (Izd. AN SSSR, 1953).
- [2] L. I. Antropov, Influence of Additives on Metal Corrosion in Oxidizing Media. Problems of Corrosion and Metal Protection [In Russian] (Izd. AN SSSR, 1956).
- [3] L. Vanyukova and B. Kabanov, Proc. Acad. Sci. USSR 59, No. 5 (1948).
- [4] N. D. Tomashov, Theory of Metal Corrosion [In Russian] (Metallurgy Press, 1942).

Received December 25, 1957

DENSITY AND CONDUCTIVITY OF CERTAIN MELTS IN THE SYSTEM $\text{Na}_3\text{AlF}_6 - \text{Li}_3\text{AlF}_6 - \text{Al}_2\text{O}_3$

V. P. Mashovets and V. I. Petrov

It was shown in our previous communication [1] that partial replacement of sodium cryolite by the lithium compound in aluminum electrolytes should lower the electrolysis temperature by 70–80°. In view of the properties of lithium salts, it is to be expected that a mixed electrolyte of this type should also have certain advantages with regard to a lower density and higher conductivity of the melt.

EXPERIMENTAL

Melt densities. Sodium and lithium cryolites made synthetically from chemically-pure fluorides of sodium, lithium, and aluminum were used in the experiments. Their stoichiometric composition was checked by chemical analysis, hot titration, and optical crystallography. Density was determined by the hydrostatic weighing method with a hollow platinum float suspended on an analytical balance; the weighings were to an accuracy of 1 mg. A 100 g sample of the material was put in a platinum crucible with a lid with two openings, one for the float thread and the other for the thermocouple. The exposed junction of a platinum-platinum/rhodium thermocouple was immersed directly in the melt. The crucible was contained in a vertical tubular furnace. The float was weighed at 40 mg intervals at different melt temperatures; the temperature varied at the rate of 2–3° per minute. The change of the float volume was calculated from the coefficient of linear expansion of platinum.

In illustration, Table 1 contains the directly determined densities of the two pure cryolites and one binary mixture. The density found for sodium cryolite is in good agreement with literature data; this confirms that the determinations were sufficiently accurate and sensitive.

The density of each melt was determined over a temperature range of 150–200°; it was found to be a linear function of the temperature in all cases:

$$d_t = d_{1000} - \alpha (t - 1000) \text{ g/cm}^3.$$

Therefore Table 2 contains only inter- or extrapolated values of d_{1000} and the temperature coefficients α for all the investigated binary and ternary melts (the latter containing alumina).

Figure 1 represents the density isotherms of binary $\text{Na}_3\text{AlF}_6 - \text{Li}_3\text{AlF}_6$ mixtures; there is a distinct minimum at about 70 wt. % of Li_3AlF_6 .

Figure 2 shows that if the compositions are expressed in molar percentages the molar volumes of the mixtures at 1000° vary almost linearly with composition. The additivity of the molar volumes indicates that there is no interaction between the two cryolites.

The results obtained for three compositions in the binary system $\text{Na}_3\text{AlF}_6 - \text{Al}_2\text{O}_3$ are in good agreement with the data of Abramov [2] and Vayna [3].

The ternary system $\text{Na}_3\text{AlF}_6 - \text{Li}_3\text{AlF}_6 - \text{Al}_2\text{O}_3$ was investigated only between 0 and 50 wt. % of Li_3AlF_6 , as the region of higher contents of lithium cryolite is of no practical interest because of the low solubility of alumina.

The points within the triangular diagram were chosen at the intersections of the paths leading from the

TABLE 1

Densities of Some Melts at Different Temperatures

Na ₃ AlF ₆		50% Na ₃ AlF ₆ + 50% Li ₃ AlF ₆ (wt. %)		Li ₃ AlF ₆	
tempera- ture (deg)	density (g/cc)	temperature (deg)	density (g/cc)	temperature (deg)	density (g/cc)
1016	2.088	762	2.266	788	2.237
1034	2.070	792	2.237	879	2.143
1064	2.043	815	2.218	917	2.107
1084	2.025	860	2.182	958	2.071
1107	2.007	890	2.147	990	2.040
1124	1.995	936	2.110	1029	2.001

TABLE 2

Densities at 1000° and Temperature Coefficients

Melt No.	Composition (wt. %)			Density (g/cc), d ₁₀₀₀	Temperature coefficient α · 10 ³
	Na ₃ AlF ₆	Li ₃ AlF ₆	Al ₂ O ₃		
1	100	0	—	2.103	0.89
2	80	20	—	2.076	0.90
3	70	30	—	2.064	0.90
4	60	40	—	2.052	0.92
5	50	50	—	2.045	0.92
6	40	60	—	2.022	0.93
7	30	70	—	2.016	0.92
8	20	80	—	2.018	0.92
9	0	100	—	2.032	0.93
10	95	—	5	2.063	0.80
11	90	—	10	2.043	0.77
12	88	—	12	2.035	0.77
13	76.6	19.2	4.2	2.045	0.84
14	72.2	18.0	9.8	2.014	0.77
15	67.6	28.8	3.6	2.037	0.88
16	64.0	27.2	8.8	2.012	0.80
17	58.2	38.6	3.2	2.027	0.86
18	55.6	36.8	7.6	2.010	0.84
19	48.7	48.7	2.6	2.012	0.88
20	46.8	46.8	6.4	2.002	0.78

Al₂O₃ corner at Na₃AlF₆ : Li₃AlF₆ weight ratios of 8 : 2, 7 : 3, 6 : 4 and 5 : 5 with the paths leading from the Li₃AlF₆ at Na₃AlF₆ : Al₂O₃ ratios of 95 : 5 and 88 : 12. The melt compositions and principal results are given in Table 2, while Fig. 3 is a ternary diagram with lines of equal densities at 1000°; this shows that the melt densities decrease considerably with increase of the alumina content and on replacement of part of the sodium cryolite by the lithium compound. As an example, we consider the electrolyte containing 7% Al₂O₃ by weight. The density of sodium cryolite containing this amount of alumina is 2.053 at 1000°. For an electrolyte of the composition 68% Na₃AlF₆, 25% Li₃AlF₆ and 7% Al₂O₃ d₁₀₀₀ = 2.021. The decrease of 0.032 does not seem large. It must be remembered, however, that the density of aluminum at the same temperature is 2.290; the difference between the densities of the pure sodium electrolyte and the metal is 0.237. On addition of 25% of lithium cryolite the difference increases to 0.269, an increase of 13.5%, which is, of course, advantageous for separation of the metal from the electrolyte. It was reported earlier [1] that the electrolysis can be conducted at 880° with an electrolyte containing 25% Li₃AlF₆ and 7% Al₂O₃. The density of this electrolyte at that temperature is d₈₈₀ = 2.118, and the density of aluminum is 2.321. Thus, even at this low temperature the density difference is enough to ensure that the metal remains under the electrolyte.

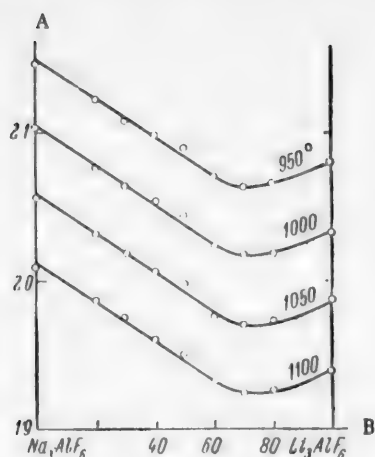


Fig. 1. Density isotherms for the system Na_3AlF_6 - Li_3AlF_6 : A) density d of binary mixtures (g/cc); B) melt composition (wt. %).

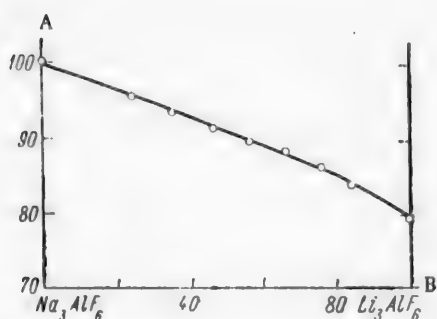


Fig. 2. Isotherm for the molar volumes of melts in the system Na_3AlF_6 - Li_3AlF_6 at 1000° : A) molar volume of melt (cc); B) melt composition (molar %).

Electrical conductivity. Conductivities were determined with the aid of a bridge circuit with an audiofrequency electronic oscillator type GZ-1 and a piezoelectric telephone connected through a tube amplifier. A distinct sound minimum and good reproducibility could be obtained at a frequency of 5.5 kilocycles/second. Two of the bridge arms were in the form of an ordinary rheochord. The third arm contained a resistance box in parallel with a capacitor box with regulation steps of 10 μF . All the circuit connections were shielded by grounded armor.

The measuring cell consisted of two hemispherical concentric platinum electrodes; the internal diameter of the external electrode was 40 mm, and the external diameter of the internal electrode was 9 mm. The current was fed to the electrodes by platinum wires 2 mm in diameter welded to the electrodes; the upper ends of the wires were fixed in a special stand fitted with micrometer screws for precise vertical and horizontal positioning of the electrodes. 200 g of electrolyte was fused in a platinum crucible and the electrodes were immersed in the melt; the immersion depth was kept constant, the constancy being checked by means of a special platinum contact connected to the regulating stand through an electric lamp. The resistance of the current leads and contacts was measured, with the electrodes short-circuited, over a wide temperature range, and the appropriate corrections were applied to the final results. The temperature was measured by means of a platinum-platinum/rhodium thermocouple, the exposed junction of which was immersed in the melt.

The cell constant c was determined before each experiment with the aid of 0.1 N KCl solution at $18 \pm 0.1^\circ$, and the value for high temperatures was calculated with a correction for the linear expansion of platinum from the formula

$$C_2 = C_1 \frac{1 + 8868 \cdot 10^{-9} t_1 + 1324 \cdot 10^{-12} t_1^2}{1 + 8868 \cdot 10^{-9} t_2 + 1324 \cdot 10^{-12} t_2^2}.$$

The cell constant was also checked against 1 N KCl solution and 30% H_2SO_4 solution; its value was about 0.27 cm^{-1} .

In experiments with melts a capacity of about 1 μF had to be connected in the resistance-box arm; the sound minimum in the telephone at a frequency of 5.5 kilocycles/second was determined over a 1-3 mm length of the rheochord wire, which corresponds to a measurement accuracy of ± 0.2 -0.6%. With possible errors in determinations of the cell constant and temperature, errors of melt composition, etc., take into account, the estimated error of our determinations was $\pm 3\%$.

The methods of melt preparation and composition control were the same as in the density measurements.

Figure 4 shows conductivity polytherms for the two cryolites and their mixtures. It is seen that in all cases the conductivity varies linearly with the temperature; the temperature coefficient for Na_3AlF_6 was 0.0043, and for Li_3AlF_6 and the binary melts it was $0.0048 \text{ ohm}^{-1} \text{ cm}^{-1} \text{ degree}^{-1}$. Inter- and extrapolated values for the conductivities at 1000° are given in Table 3.

In Table 4 the results of our determinations for Na_3AlF_6 are compared with the data of other authors. It is seen that all the results differ considerably between themselves, but our result agrees exactly with the value given by Abramov, Kostyukov, and Nordvik [10].

In the case of lithium cryolite the only available value is that of Abramov, Kostyukov, and Nordvik [10],

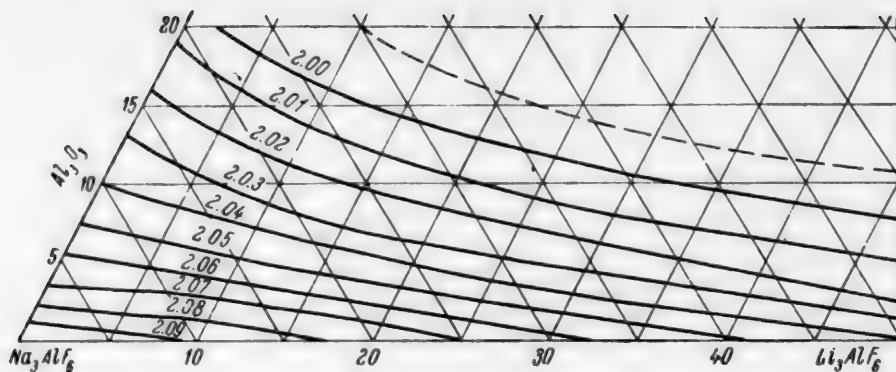


Fig. 3. Lines of equal density for the system $\text{Na}_3\text{AlF}_6\text{-Li}_3\text{AlF}_6\text{-Al}_2\text{O}_3$ at 1000° .

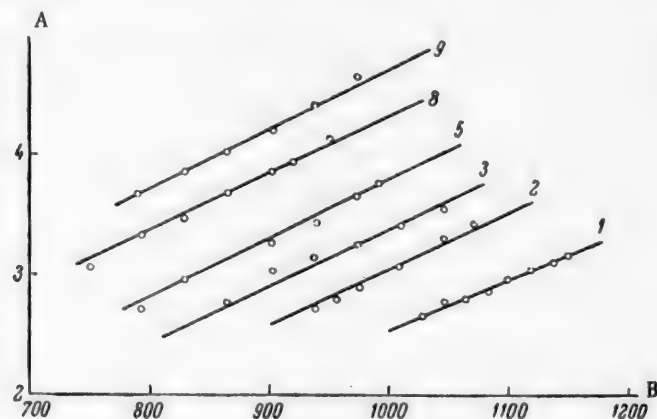


Fig. 4. Conductivities of melts in the system $\text{Na}_3\text{AlF}_6\text{-Li}_3\text{AlF}_6$ as functions of the temperature: A) conductivity κ ($\text{ohms}^{-1} \cdot \text{cm}^{-1}$); B) temperature (deg); the curve numbers correspond to the melt numbers (Table 2).

TABLE 3

Conductivity κ at 1000°

Melt No.	Composition (wt. %)		
	Na_3AlF_6	Li_3AlF_6	($\text{ohms}^{-1} \cdot \text{cm}^{-1}$)
1	100	0	2.53
2	80	20	3.05
3	70	30	3.38
5	50	50	3.80
8	20	80	4.33
9	0	100	4.71

who found $\kappa_{1000} = 4.00 \text{ ohms}^{-1} \cdot \text{cm}^{-1}$, which is lower than our value by nearly 18%. The cause of this discrepancy is not clear.

The conductivity isotherms for binary melts (Fig. 5) show that κ increases very steeply with increase

TABLE 4

Conductivity κ of Na_3AlF_6 at 1000° from the Data of Different Authors

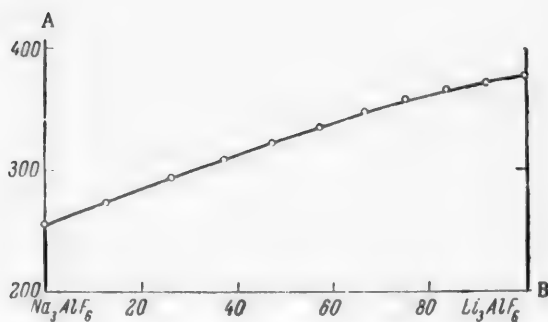
Authors	κ_{1000} ($\text{ohms}^{-1} \cdot \text{cm}^{-1}$)
Arndt and Kalass [4]	2.23
Cuthbertson and Waddington [5]	2.84*
Batashev [6]	3.23
Belyaev [7]	2.29
Vayna [8]	2.36
Edwards [9]	2.72
Abramov, Kostyuk and Nordvik [10]	2.52
Our data	2.53

*At 1025° .

TABLE 5

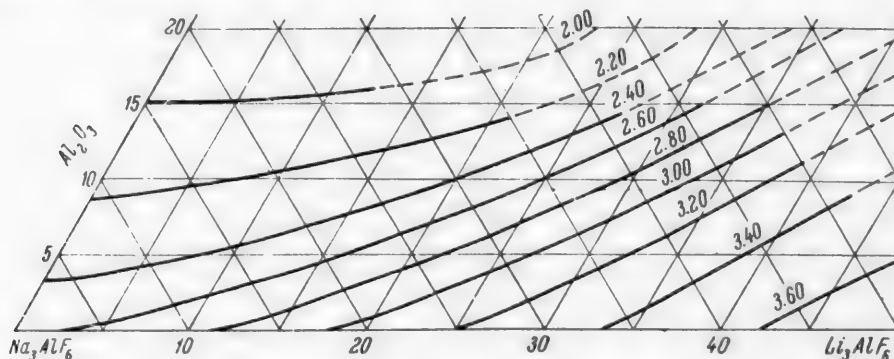
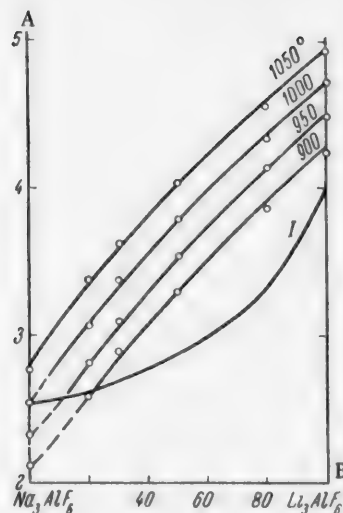
Conductivity κ of Melts Containing Alumina, at 1000°

Melt No.	(ohms ⁻¹ cm ⁻¹)	(ohm ⁻¹ cm ⁻¹ degree ⁻¹)
10	2.35	0.0042
12	1.97	0.0051
13	2.67	0.0054
14	2.43	0.0055
15	3.24	0.0048
16	3.10	0.0047
19	3.73	0.0050
20	3.44	0.0052

Fig. 6. Molar conductivity of melts in the system $\text{Na}_3\text{AlF}_6\text{-Li}_3\text{AlF}_6$ at 1000°: A) molar conductivity ($\mu\text{ohm}^{-1}\cdot\text{cm}^2$); B) melt composition (molar %).

positions are expressed in molar percentages the deviation from linearity is only slight, which again confirms that there is no significant interaction between the two cryolites.

The conductivities of 8 melts containing alumina were also determined. The conductivity was a linear function of temperature in each instance. Without giving the direct determination results, we present merely the summarized data (Table 5) on conductivities of melts containing alumina (the melt numbers and corresponding compositions are the same as in Table 2).

Fig. 7. Conductivities of melts in the system $\text{Na}_3\text{AlF}_6\text{-Li}_3\text{AlF}_6\text{-Al}_2\text{O}_3$ at 1000°: the numbers on the curves in Fig. 7 and 8 represent values of the conductivity κ ($\text{ohms}^{-1}\cdot\text{cm}^{-1}$).Fig. 5. Conductivity isotherms for melts in the system $\text{Na}_3\text{AlF}_6\text{-Li}_3\text{AlF}_6$: A) conductivity κ ($\text{ohms}^{-1}\cdot\text{cm}^{-1}$); B) melt composition (wt. %); Curve 1) conductivity isotherm at 1000° from Abramov's data [2].

of the lithium content. The same diagram also contains the isotherm at 1000° based on the data of Abramov et al.; it differs sharply from ours both in absolute values and in the shape of the curve.

The molar volumes (Fig. 2) and conductivities were used for calculating the molar conductivities of mixtures of the two cryolites (Fig. 6); if the com-

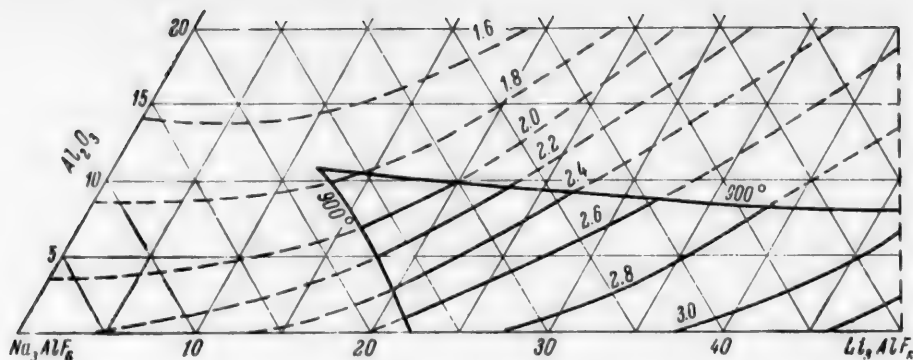


Fig. 8. Conductivities of melts in the system Na_3AlF_6 - Li_3AlF_6 - Al_2O_3 at 900° : the "900°" line represents the start of crystallization.

The portions of the triangular diagram at 1000° and 900° , presented in Fig. 7 and 8, show that the conductivity falls sharply with increase of Al_2O_3 content and rises with increase of Li_3AlF_6 content. For example, the pure sodium electrolyte containing 7 wt. % Al_2O_3 has a conductivity of $2.27 \text{ ohms}^{-1} \cdot \text{cm}^{-1}$; an electrolyte containing 68% Na_3AlF_6 , 25% Li_3AlF_6 and 7% Al_2O_3 as before has $\kappa_{1000} = 2.80$, which is 23% higher.

As already stated, the electrolyte of this last composition can be used for electrolysis at 880° . Even at that low temperature its conductivity is $2.32 \text{ ohms}^{-1} \cdot \text{cm}^{-1}$, which is virtually the same as that of a pure sodium electrolyte containing 7% Al_2O_3 , at 1000° .

Therefore by the use of a mixed sodium-lithium cryolite the electrolysis temperature can be lowered to about 880° without fall of conductivity and with a very slight increase of the electrolyte density, with a permissible alumina content of 7-8% by weight and 25% Li_3AlF_6 .

SUMMARY

1. The density of melts of the binary system Na_3AlF_6 - Li_3AlF_6 decreases as sodium cryllite is replaced by the lithium compound, and passes through a minimum at 70 wt. % Li_3AlF_6 . The molar volumes of the binary mixtures vary additively. In the ternary system Na_3AlF_6 - Li_3AlF_6 (up to 50%)- Al_2O_3 (up to 20%) the density decreases with increase of Li_3AlF_6 content, and even more so with increase of Al_2O_3 content.
2. The conductivity of binary melts rises sharply in the transition to lithium cryolite; the molar conductivity increases with a slight deviation from additivity. In the ternary system lithium cryolite increases and alumina lowers the conductivity.
3. In a definite range of the ternary melts it is possible to carry out electrolysis at temperatures of the order of 880° without decrease of conductivity and with a permissible increase of density, as compared with the conditions used at present in the industrial production of aluminum.

LITERATURE CITED

- [1] V. Mashovets and V. Petrov, J. Appl. Chem. 30, 1695 (1957).*
- [2] G. Abramov, Light Metals 11, 27 (1936).
- [3] A. Vayna, Alluminio, 19, 540 (1950).
- [4] K. Arndt and W. Kalass, Z. Elektroch. 30, 12 (1924).
- [5] J. Cuthbertson and J. Waddington, Trans. Farad. Soc. 32, 745 (1936).
- [6] K. Batashev, Light Metals 10, 48 (1936).
- [7] A. Belyaev, Electrochemical Processes in the Electrolytic Production of Aluminum [In Russian] (Metallurgy Press, Moscow, 1947).

*Original Russian pagination. See C.B. Translation.

- [8] A. Vayna, *Alluminio*, 19, 215 (1950).
- [9] J. Edwards, *J. Electrochem. Soc.* 100, 508 (1953).
- [10] G. Abramov, A. Kostyukov and L. Nordvik, *Trans. Leningrad Polytech. Inst.* 188, 40 (1957).

Received March 19, 1958

SUCTION REMOVAL OF GASES AND LIQUIDS THROUGH POROUS ELECTRODES

O. S. Ksenzhek and V. V. Stender

(Dnepropetrovsk Institute of Chemical Technology)

Nearly all electrochemical processes differ from ordinary chemical reactions in one important respect — the over-all reaction effected in the cell is divided spatially into two interconnected reactions taking place at the respective electrodes. On the one hand, this is an important advantage of electrochemical methods, whereby valuable products can be obtained. On the other hand, spatial separation of the electrode reactions leads to certain technological and design difficulties because of the need to use various diaphragms or other devices for separation of the products formed at the electrodes. Permeable porous electrodes can be used with success instead of diaphragms in some cases for separation of the electrode products. The products formed at the electrode surfaces must then be drawn off through the pores.

Heise [1] and Janes [2] have described a number of electrochemical processes in which porous electrodes operating on this principle are used. For example, by the use of porous electrodes with removal of the electrolysis products by suction through the pores, it is possible to effect relatively simply the anodic oxidation of manganate to permanganate, ferrous to ferric iron, arsenite to arsenate, etc.

If the system undergoing electrolysis is homogeneous and no new phases (such as solid or gas) are formed in the process, the action of a permeable electrode reduces in the hydraulic sense to simple filtration. Conditions of filtration through a permeable electrode become considerably more complicated if gaseous electrolysis products are drawn off through the pores together with the electrolyte. However, this case is extremely interesting from the practical standpoint.

Suction of air bubbles through porous electrodes can be arbitrarily separated into two stages: 1) removal of bubbles by the stream of electrolyte from the electrode surface, where they were held by capillary forces, and 2) filtration of the aerated liquid through the electrode pores.

The course of the first stage of this process is determined by a very complex combination of different factors which cannot be taken into account in advance. The second stage has been studied in greater detail. For example, Khristianovich [3] and Lapuk [4] have shown that filtration of an aerated liquid conforms to Darcy's law, but the liquid and gas have a retarding effect on each other. Certain preliminary experiments for study of the conditions of gas evacuation through porous electrodes were carried out in our laboratory [5]. The present communication contains the results of experiments on evacuation of insoluble and soluble gases formed at porous graphite electrodes of various structures.

EXPERIMENTAL PROCEDURE

The apparatus used for investigating the performance of porous electrodes with evacuation of the electrode products is shown schematically in Fig. 1. In these experiments sulfuric acid solution (concentration $C = 2N$) was drawn through a porous graphite electrode (a disk 36 mm in diameter and 8 mm thick). The electrode was cathodically polarized, and the hydrogen formed on it was partly drawn downward by the electrolyte stream and partly collected in the measuring buret. The results were used for plotting curves for variations of the degree of evacuation and pressure drop at the electrode (Δp) with the flow rate of the electrolyte (v) at different current

Electrode type	Density	Porosity	Pore con- volution coef- ficient*	Permea- bility coef- ficient (cm/hr)**	Number of pores*** per cm ²	Mean pore dia- meter*** (μ)
PT	1.18	46	2.02	53.2	6800	65.2
Ts	1.27	42	1.82	12.9	32000	30.3
SS	1.18	46	2.98	5.3	21300	30.4
ChEZ-30	1.01	54	2.34	7.6	42000	26.4
ChEZ-40	0.884	50.5	2.06	27.0	21000	41.7

*Determined by the conductivity method [6].

**For 1 cm specimen thickness, liquid viscosity 1 centipoise, and hydrostatic pressure 1 cm H₂O.

***Calculated by the method described in the literature [7].

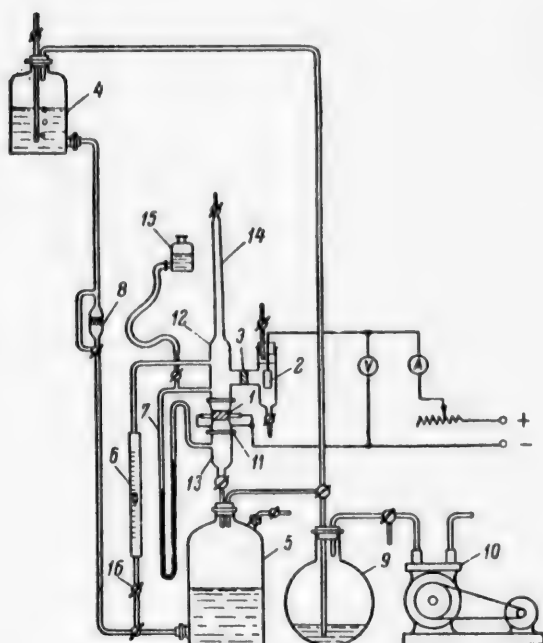


Fig. 1. Apparatus for investigating the performance of porous graphite electrodes with suction removal of the electrode products: 1) test electrode; 2) anode; 3) diaphragm; 4) header vessel; 5) receiver; 6) rotameter; 7) differential manometer; 8) filter; 9) buffer vessel; 10) vacuum pump; 11) connection; 12) upper part of cell; 13) lower part of cell; 14) measuring buret; 15) leveling vessel.

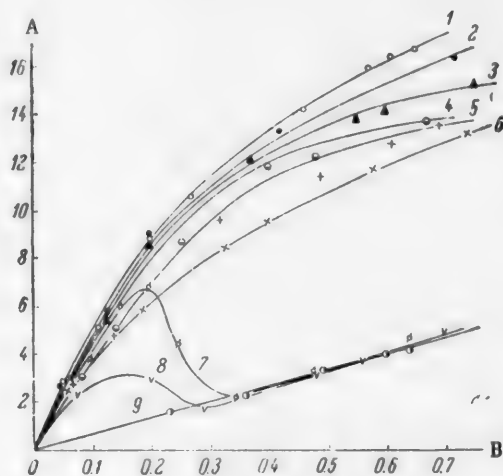


Fig. 2. Variation of the pressure drop in a porous electrode type PT with the electrolyte flow rate: A) pressure drop Δp (cm Hg/cm); B) electrolyte flow rate (ml/cm²·second); current density (amp/cm²): 1) 0.5; 2) 0.4; 3) 0.3; 4) 0.2; 5) 0.1; 6) 0.05; 7) 0.03; 8) 0.02; 9) 0.

densities. The degree of evacuation was defined as the ratio of the volume of the gas drawn off to the total volume of liberated gas.

The specimens investigated consisted of experimental porous graphite made at the Chelyabinsk Electrode Factory (ChEZ-30 and ChEZ-40). Brief details of the physical properties

of these electrodes are given in the table.

RESULTS AND DISCUSSION

The experimental results are presented in Fig. 2-9 (results for electrodes of the ChEZ-30 type are not given; these electrodes are similar in properties to electrodes of the PT type).

It follows from the graphs for the pressure drop at the electrode as a function of the electrolyte flow rate

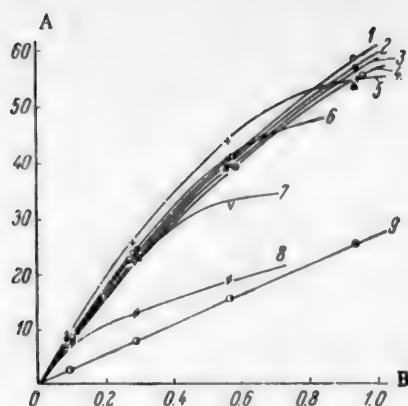


Fig. 3. Variation of the pressure drop in a porous electrode type ChEZ-40 with the electrolyte flow rate: designations as in Fig. 2.

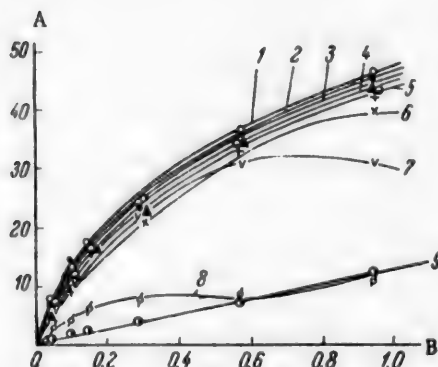


Fig. 5. Variation of the pressure drop in a porous electrode type Ts with the electrolyte flow rate: designations as in Fig. 2.

the electrode falls to a value which corresponds to absence of current.

The form of the $\Delta p-v$ curves indicates that the ratio of the gas and liquid volumes in the electrode pores is highest at low flow rates. The gas then exerts a strong retarding effect on the liquid. As the flow rate increases the pores become less saturated with gas and its retarding effect diminishes accordingly. If the current density is low, then at a sufficiently high flow rate the saturation of the pores with gas diminishes to such an extent that it no longer has any appreciable retarding effect on the liquid.

The close similarity of the curves for different current densities seems to indicate that the gas: liquid ratio at a given flow rate depends little on the current density.

The curves for the degree of evacuation as a function of the electrolyte flow rate are similar in general character for different electrodes, but they have appreciable quantitative differences from each other. Electrode type Ts has the best properties (with regard to degree of evacuation). With these electrodes, at a flow rate of 1 ml/second \cdot cm², the degree of evacuation reaches 90% even at a current density of 0.5 amp/cm². At current densities below 0.2 amp/cm² evacuation is almost complete.

With other electrodes, such as ChEZ-40, PT, or ChEZ-20, the degree of evacuation at 0.5 amp/cm² and $v = 1.0$ ml/second \cdot cm² is about 25-50%, and complete evacuation is observed only at current densities of

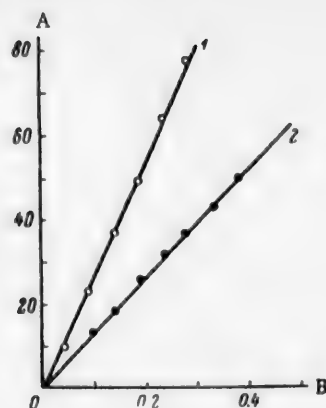


Fig. 4. Variation of the pressure drop in a porous electrode type SS with the electrolyte flow rate: A) pressure drop Δp (cm Hg/cm); B) electrolyte flow rate (ml/cm² \cdot second); current density (amp/cm²): 1) 0.5-0.02; 2) 0.

that in absence of current the filtration of electrolytes through porous electrodes conforms to the Darcy law in all the cases studied, showing that the flow of liquid in the pores is streamline (Werking [8] observed a gradual transition from streamline to turbulent flow at high flow rates through electrodes with coarse pores).

When the current is switched on the electrode permeability falls sharply, and the filtration rate ceases to be a linear function of the pressure difference.

The current density has relatively little influence on permeability. It is only at very low current densities at electrodes with the coarsest pores (PT, Ts, and ChEZ-40) that the $\Delta p-v$ relationship is of a peculiar character—when a definite flow rate is reached the hydraulic resistance of

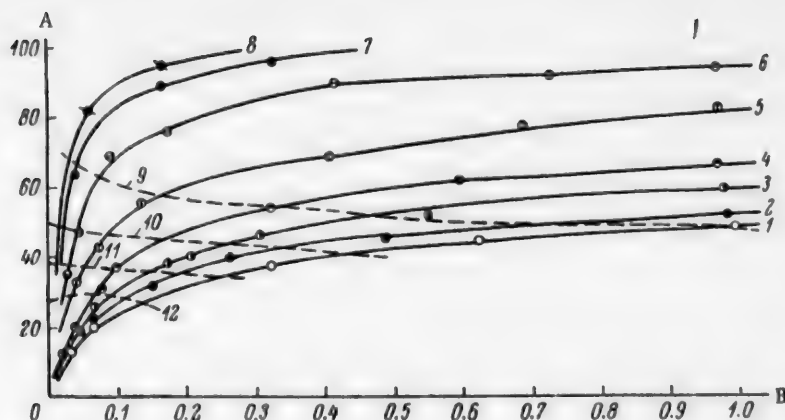


Fig. 6. Variations of the degree of evacuation of the gas with the liquid flow rate and current density for electrode type PT: A) degree of evacuation (%); B) electrolyte flow rate (ml/cm²·second); current density (amp/cm²): 1) 0.5; 2) 0.4; 3) 0.3; 4) 0.2; 5) 0.1; 6) 0.05; 7) 0.03; 8) 0.02; solubility of chlorine (g/liter): 9) 0.1; 10) 0.25; 11) 0.5; 12) 1.

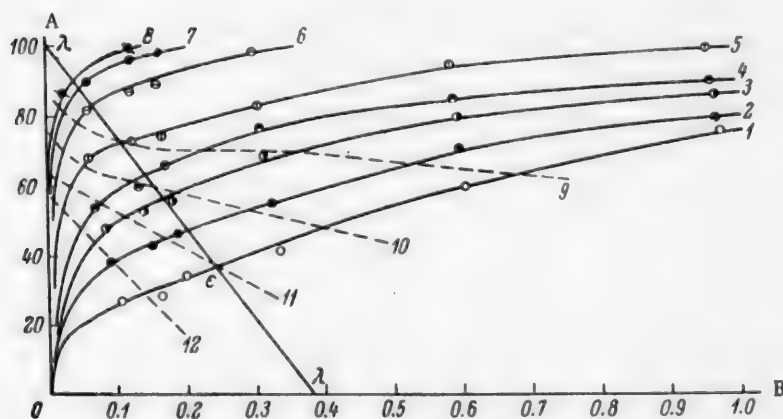


Fig. 7. Variations of the degree of evacuation of the gas with the liquid flow rate and current density for ChEZ-40 electrode: designations as in Fig. 6.

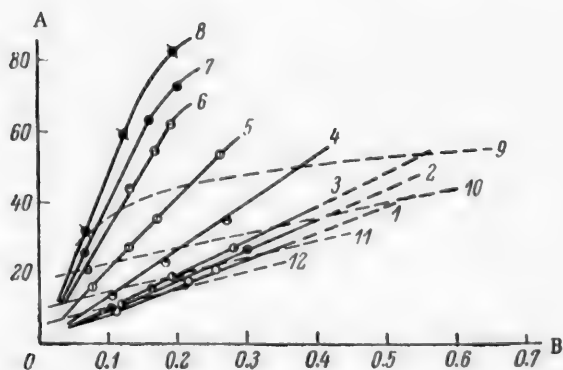


Fig. 8. Variations of the degree of evacuation of the gas with the liquid flow rate and current density for electrode type SS: designations as in Fig. 6.

0.02-0.03 amp/cm². The evacuation conditions are even worse with SS type electrodes. This type of electrode was studied only up to flow rates of about 0.3 ml/second·cm², as its hydraulic resistance is very high. For the investigated region the flow rate-degree of evacuation curves are much flatter than for the other electrodes.

Therefore virtually complete evacuation of an insoluble gas through the electrode pores is possible in principle even at relatively high current densities, but the quantity of electrolyte required for this is very large. For example, to remove hydrogen from the surface of a type T's electrode (the best with respect to evacuation conditions of all the electrodes studied) at a current density of

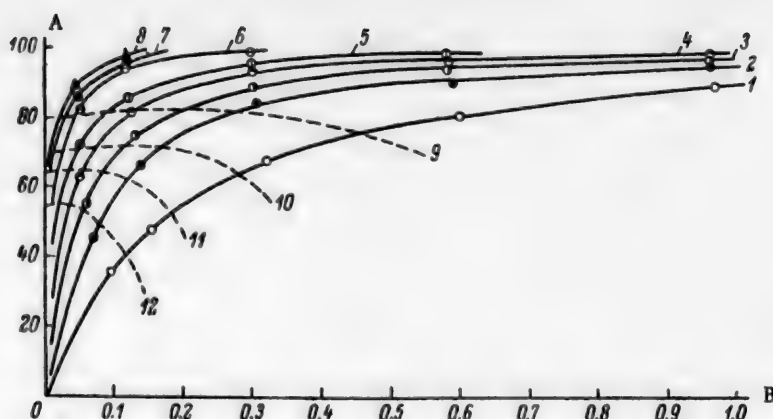


Fig. 9. Variations of the degree of evacuation of the gas with the liquid flow rate and current density for electrode type Ts: designations as in Fig. 6.

0.1 amp/cm² about 0.7 ml of electrolyte per cm² electrode area per second is required. This fact restricts the possibility of technical application of processes involving the use of porous electrodes with suction removal of gaseous products at the electrodes.

The spatial position of the electrode surface (horizontal facing upward, vertical, horizontal facing downward, etc.) should not have any significant effect on the evacuation conditions. It is clear from the pressure drop-flow rate graphs that when an aerated liquid is drawn off the pressure drop required to produce a given flow rate is greater by 10-40 mm Hg than that required for a pure liquid. This excess pressure drop is required for removal of the gas bubbles. The force acting on a bubble in a pore is approximately equal to the pressure drop multiplied by the cross-sectional area of the bubble. The force of hydrostatic upthrust is proportional to the bubble volume. For a bubble 1 mm in diameter the first of these forces is roughly two orders of magnitude greater than the second, and even greater than this for smaller bubbles. It follows that the role of hydrostatic forces is small in this case.

If the gas liberated at the electrode is soluble in the electrolyte, it is removed in two ways from the active electrode surface — by dissolution and by entrainment of the bubbles in the liquid stream. The amount of liquid required for evacuation of the gas should be correspondingly less. The influence of gas solubility on the conditions of its removal by suction can be determined, with some degree of approximation, from data on evacuation of an insoluble gas.

The amount W_d of gas carried away in the dissolved state by the electrolyte may be assumed proportional to the flow rate v and the solubility C of the gas:

$$W_d = v \cdot C. \quad (1)$$

The total quantity of gas liberated at the electrode in unit time at current density D is:

$$W = \frac{M \cdot D}{n \cdot F}, \quad (2)$$

where M is the molecular weight.

The quantity of gas remaining undissolved is therefore

$$W_r = W - W_d = \frac{M \cdot D}{n \cdot F} - v \cdot C. \quad (3)$$

Or, as a percentage of the total quantity:

$$\frac{W_r}{W} = \left(1 - \frac{v \cdot C \cdot n \cdot F}{M \cdot D}\right) \cdot 100. \quad (4)$$

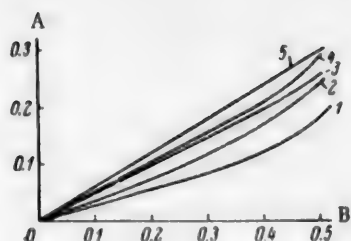


Fig. 10. Variation of the electrolyte flow rate with current density when the solubility of chlorine in the electrolyte is 0.5 g/liter: A) electrolyte flow rate ($\text{ml}/\text{cm}^2 \cdot \text{second}$); B) current density (amp/cm^2); electrodes: 1) Ts; 2) ChEZ-40; 3) PT; 4) ChEZ-30; 5) SS.

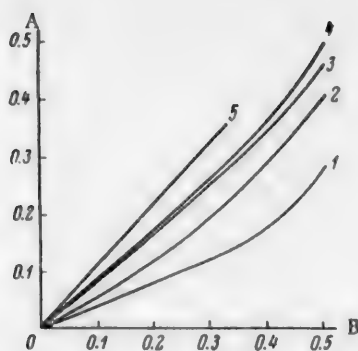


Fig. 11. Variation of the electrolyte flow rate with current density when the solubility of chlorine in the electrolyte is 0.25 g/liter: designations as in Fig. 10.

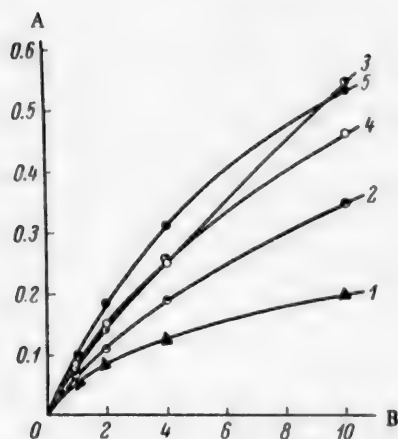


Fig. 12. Variation of flow rate with the solubility of the evacuated gas at current density of $0.3 \text{ amp}/\text{cm}^2$: A) electrolyte flow rate ($\text{ml}/\text{cm}^2 \cdot \text{second}$); B) $(\text{solubility})^{-1}$ (in liters of solution per g chlorine); curve numbers as in Fig. 10.

If this expression is plotted in flow rate-degree of evacuation coordinates, a sloping line is obtained which runs from the point $y = 100\%$, $x = 0$ to its intersection with the abscissa axis at a point corresponding to dissolution of all the gas liberated at the electrode.

Consider a concrete example. Suppose that chlorine ($M = 71$, $n = 2$) is liberated at the electrode. Its solubility is taken as 0.5 g/liter ($C = 0.5 \cdot 10^{-3} \text{ g/ml}$). Then at current density $0.5 \text{ amp}/\text{cm}^2$ equation (4) is represented by the line $\lambda - \lambda$ (Fig. 7). The point of intersection of this line with the evacuation line for the same current density (ϵ) evidently corresponds to complete removal of chlorine from the electrode surface. In this case 63% of the chlorine is removed by dissolution and 37% by entrainment of bubbles in the liquid stream.

Points of complete evacuation for other current densities and solubilities were determined similarly. In Fig. 6-9 the geometrical positions of these points are represented by dash lines, which we shall term, for brevity, lines of complete evacuation. Lines of complete evacuation are drawn for the following chlorine solubilities (in g/liter): 0.1, 0.25, 0.5 and 1.

The position of the lines of complete evacuation on the graph gives a direct indication of the relative proportions of chlorine removed by dissolution and mechanical entrainment respectively under given conditions.

It is evident from the graphs that evacuation conditions are much more favorable for soluble than insoluble gases. For example, with an electrode type Ts at current density $0.1 \text{ amp}/\text{cm}^2$ removal of an insoluble gas required an electrolyte velocity of about 0.7 cm/sec . If the solubility of the gas (chlorine) is 1 g/liter , a velocity of about $1/30$ of this, approximately 0.03 cm/second , is sufficient for complete evacuation. The fraction of chlorine removed by dissolution is then only about 45%. Gases of high enough solubility can be removed completely even at very high current densities.

The evacuation conditions are somewhat worse with electrodes of other types, but the difference between them is less pronounced than it is in the removal of an insoluble gas. This is illustrated more clearly by the curves in Fig. 10 and 11, which represent the flow rate at which complete evacuation is obtained, as a function of current density. It is seen that this function is approximately linear, at least for current densities up to $0.4 \text{ amp}/\text{cm}^2$. For the least permeable of the electrodes studied (type SS) the flow rate necessary for complete

evacuation is approximately double the rate for specimen Ts, which shows the best evacuation conditions. The electrodes of the other types are intermediate in properties between the Ts and SS types.

The ratio between the amounts of gas in the dissolved state and in bubble form differs for different electrodes. Thus, when the solubility is 0.5 g/liter and the current density is 0.1 amp/cm² this ratio is approximately 1:2 for electrode type Ts. This ratio increases with increasing solubility and current density. The same rule holds for other electrodes apart from SS, but the ratio between the amounts of dissolved and mechanically entrained gas is somewhat greater, from 1:1 to 2:1. For the SS electrode this ratio reaches 8:1 under the same conditions. In this last case up to 80-90% of the gas is removed by dissolution.

The electrolyte flow rate necessary for complete evacuation of the gas rises rapidly with decreasing solubility of the gas. Figure 12 represents the variation of the required flow rate with the solubility of the gas (chlorine), reciprocal solubility being taken along the abscissa axis. The curves for the different electrodes are approximately of the same general form.

SUMMARY

1. Total evacuation of an insoluble gas through a porous electrode is possible only at very high liquid flow rates and relatively low current densities, i.e., with a very low degree of utilization of the electrolyte.
2. The conditions for evacuation of a soluble gas are considerably more favorable. In the case of chlorine, when its solubility in the electrolyte is 1 g/liter and at a current density of 0.1 amp/cm² a liquid velocity of about 0.03 cm/second is sufficient; this is about 1/30 of the velocity required for removal of an insoluble gas at the same current density.
3. The best results are obtained with electrodes of homogeneous structure and a low degree of pore convolution (type Ts).

LITERATURE CITED

- [1] G. W. Heise, *Trans. Electroch. Soc.* 75, 147 (1939).
- [2] M. Janes, *Trans. Electroch. Soc.* 77, 13 (1940).
- [3] S. A. Khristianovich, *Appl. Math. and Mech.* 5, 2 (1941).
- [4] B. B. Lapuk, *Petroleum Ind. USSR* 5 (1941).
- [5] O. S. Ksenzhek and A. B. Livshits, *Trans. Dnepropetrovsk Inst. Chem. Technol.* 5, 263 (1956).
- [6] V. V. Stender and O. S. Ksenzhek, *J. Appl. Chem.* 32, No. 1, 110 (1959).*
- [7] I. É. Bauslīt, T. Z. Kir'yanov and V. V. Stender, *J. Appl. Chem.* 28, 127 (1945).
- [8] L. C. Werking, *Trans. Electroch. Soc.* 74, 365 (1938).

Received January 20, 1958

*Original Russian pagination. See C.B. Translation.

INFLUENCE OF ELECTROLYSIS CONDITIONS ON THE ROUGHNESS AND HARDNESS OF ELECTROLYTIC COBALT DEPOSITS

N. P. Fedot'ev, V. B. Aleskovskii, P. M.
Vyacheslavov, N. V. Volkhonskii and
D. L. Romanova

Metallic cobalt is known to have high catalytic activity, which depends on the surface area of the metal.

One of the most suitable methods for production of active cobalt is by electrolytic deposition of rough coatings of the metal on steel, copper, etc.

It is known from the literature [1] that the structure of electrolytic deposits greatly depends on the electrolysis conditions. The degree of roughness of a coating reflects its crystalline structure and therefore it is to be expected that the roughness of a cobalt deposit should also depend on the electrolyte composition and electrolysis conditions.

Numerous investigations [2-5] have shown that mechanical properties of electrolytic deposits, such as hardness, are very closely associated with their structure. Therefore in the present investigation determinations of the degree of roughness of cobalt coatings were accompanied by microhardness measurements. The surface roughness of the deposits was measured by means of the IZP-17M profilograph with a vertical enlargement of 4000. The measure of the degree of surface roughness is the arithmetic average of the heights of the microirregularities, expressed in microns. Brass was the basis metal. The roughness of the basis surface correspond to class 12 of GOST 2789-51. Microhardness was measured by means of the PMT-3 instrument at a constant coating thickness of 50 μ and a constant load of 100 g. The specimens were mechanically polished before the determinations. Under such conditions the hardness of the basis metal does not affect the hardness of the coating, and the effects of cold working may be ignored [6]. The electrolyte used in our experiments was cobalt sulfate solution ($\text{CoSO}_4 \cdot 7\text{H}_2\text{O}$, 200 g/liter). The anodes were made of platinum. The possibility of using nickel and lead as insoluble anodes was also investigated.

EXPERIMENTAL

Effect of coating thickness. The experimental conditions in this series were: electrolyte $\text{CoSO}_4 \cdot 7\text{H}_2\text{O}$, 200 g/liter, pH from 1.5 to 2.5, temperature $50 \pm 1^\circ$, cathode current density 5 amp/dm². The results are plotted in Fig. 1.

It is clear from Fig. 1 that the roughness of a cobalt deposit increases almost linearly with its thickness; this is because the grain size of the deposit increases with thickness. On the other hand, the microhardness decreases with increasing thickness; this decrease is relatively rapid at first and then slows down, which is quite consistent with the relationship between roughness, grain size, and coating thickness described in the literature [5].

Effect of electrolyte pH. The electrolyte acidity was varied in the pH range from 2 to 5. The remaining conditions were as in the preceding series of experiments. The results are plotted in Fig. 2. At first the roughness of the cobalt deposits increases while the microhardness decreases with increase of electrolyte pH. At pH values from 3.5 to 4.0 the reverse effects are observed.

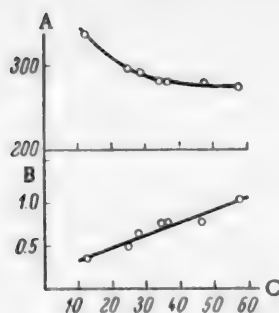


Fig. 1. Variations of roughness and microhardness with the thickness of cobalt coatings: A) H (in kg/mm^2); B) h_{av} (in μ); C) coating thickness (in μ).

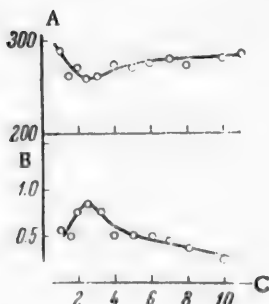


Fig. 3. Effect of cathodic current density on roughness and microhardness of cobalt coatings: A) H (in kg/mm^2); B) h_{av} (in μ); C) current density (in amp/dm^2).

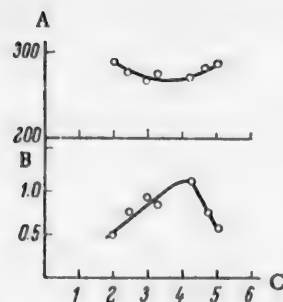


Fig. 2. Effects of electrolyte pH on roughness and microhardness of cobalt coatings: A) H (in kg/mm^2); B) h_{av} (in μ); C) electrolyte pH.

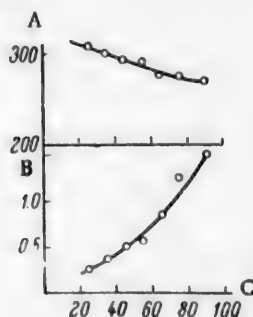


Fig. 4. Effect of electrolyte temperature on roughness and microhardness of cobalt coatings: A) H (in kg/mm^2); B) h_{av} (in μ); C) temperature (deg).

The decrease of surface roughness and increase of microhardness as the pH rises from 3.5 to 5.0 can be explained, by analogy with nickel [7], by the influence of cobalt hydroxides forming in the catholyte layer, where the pH is higher than in the main volume of the electrolyte. Cobalt hydroxides may be incorporated in the deposit and thereby hinder crystal formation. It is likely that at lower pH values the deposition of cobalt is greatly influenced by the simultaneous discharge of hydrogen ions (the current efficiency at electrolyte pH of 1-2.5 and 30° is in the 25-35% range), which hinders crystal growth.

Effect of cathodic current density. The electrolyte pH was maintained in the range of 1.5 to 2.5. The solution temperature was $50 \pm 1^\circ$. The cathodic current density was varied over a wide range. The roughness of the deposit increases with current density and passes through a maximum at cathodic current density $D_c = 2.5 \text{ amp}/\text{dm}^2$. This effect of current density on the structure of deposits has been reported in the literature [1]. The explanation is that, with increase of current density, initially the linear rate of crystal growth increases and predominates over the rate of formation of new crystallization centers. At a definite current density (at $D_c = 2.5 \text{ amp}/\text{dm}^2$ under the conditions in question) the cathode potential reaches a value at which the formation rate of new crystallization centers begins to prevail over the growth rate of individual crystals, the deposit becomes more finely crystalline, and therefore the degree of roughness decreases. Further increase of current density (above 10-12 amp/dm^2) again leads to an increase of surface roughness, but the nature of the deposit (individual large crystals) is indicative of the start of dendrite formation. The microhardness of the deposits varies in the reverse sequence, with a maximum at a current density of $2.5 \text{ amp}/\text{dm}^2$.

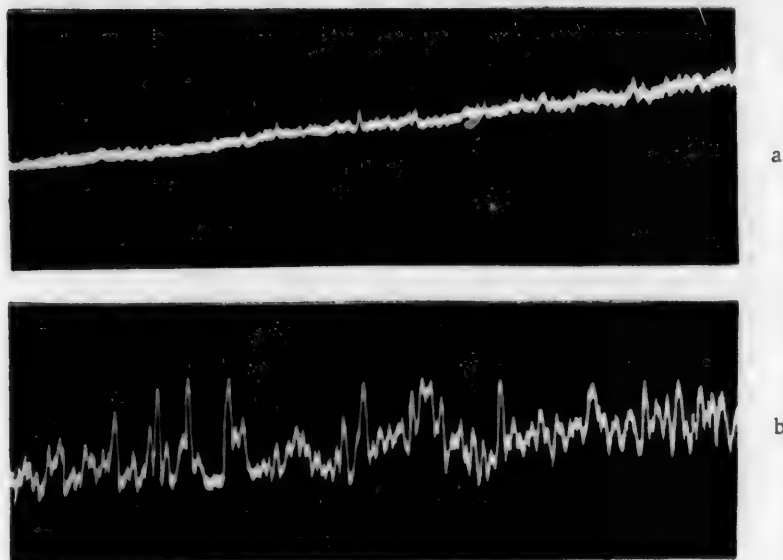


Fig. 5. Profilograms of cobalt deposits (vertical magnification $\times 4000$): a) electrolyte temperature 25° ; b) electrolyte temperature 65° .

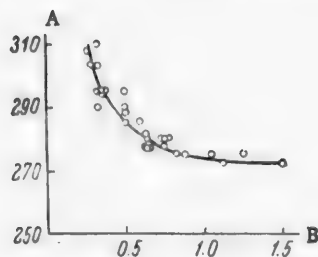


Fig. 6. Relationship between roughness and microhardness of cobalt coatings: A) H (in kg/mm^2); B) h_{av} (in μ).

Effect of electrolyte temperature. This series of experiments was conducted at constant current density ($D_c = 5 \text{ amp}/\text{dm}^2$). The electrolyte temperature was varied between 25 and 90° . The electrolyte pH was maintained in the range of 1.5 to 2.5 . The results are presented graphically in Fig. 4, which shows that temperature variations have a particularly strong influence on roughness of the deposits. The roughness increases with rise of temperature. Profilograms of cobalt deposits formed from electrolytes at 25 and 65° are given in illustration (Fig. 5a and b). The microhardness of cobalt deposits decreases with rise of temperature. This effect is due to decrease of chemical polarization with rise of temperature, which leads to coarsening of the structure of the deposit. The effects of cobalt sulfate concentration (from 100 to $500 \text{ g CoSO}_4 \cdot 7\text{H}_2\text{O}$ per liter) and additions of sodium sulfate (up to $160 \text{ g Na}_2\text{SO}_4$ per liter), boric acid (up to $60 \text{ g H}_3\text{BO}_3$ per liter), the sodium chloride (up to 50 g NaCl per liter) were also tested. It was found that within the stated limits these additives have almost no influence on the roughness and microhardness of cobalt deposits.

Relationship between roughness and microhardness of cobalt deposits. The relationship between the experimental values of roughness and microhardness was plotted graphically (Fig. 6); it was found to be a hyperbolic relationship represented by the expression $H = Kh^{-n}$, where H is the microhardness in kg/mm^2 , h is the roughness in microns, and K and n are coefficients which depend on the nature of the deposited metal. For cobalt $K = 275$ and $n = 0.08$.

Effect of the anode material. The experiments described above were carried out with insoluble platinum electrodes. The possibility of replacing platinum by nickel or lead was investigated. It was considered that in an electrolyte free from Cl^- ions a nickel anode should be in a passive state and should therefore act as an insoluble anode. However, chemical analyses of the electrolyte and cathodic deposits showed that nickel accumulates fairly rapidly in the electrolyte and is deposited jointly with cobalt in the cathode, forming alloys. The relative proportions of nickel and cobalt in the deposit depends on their proportions in the electrolyte, in accordance with the relationship discovered by Fedot'ev and Mikhailov [8]. Nickel therefore cannot be used as an insoluble anode.

After prolonged electrolytic treatment of the electrolyte (10 amp-hr/liter) with a lead anode, lead was determined chemically in the electrolyte and the cathodic deposit. Only traces of lead were detected in the

electrolyte and coating. Therefore lead anodes may be regarded for practical purposes as insoluble. It should be noted that during electrolysis at pH = 3-4 a dense layer of cobalt hydroxide Co(OH)_2 is formed on the anode, and this prevents dissolution of lead. Therefore the pH should be maintained between 3 and 4 at the initial stages of electrolysis.

SUMMARY

1. In a study of the effects of electrolysis conditions on roughness and microhardness of cobalt deposits it was found that the electrocrystallization process is strongly influenced by electrolyte temperature and pH, and the cathodic current density.

2. The following electrolyte composition and process conditions are recommended for production of cobalt deposits of a high degree of surface roughness: cobalt sulfate $\text{CoSO}_4 \cdot 7\text{H}_2\text{O}$, 200 g/liter, pH = 2-3.5, electrolyte temperature 60-70°, cathodic current density from 10 to 25 amp/dm², lead anodes.

LITERATURE CITED

- [1] V. I. Lainer and N. T. Kudryavtsev, *Fundamentals of Electroplating, I* [In Russian] (Metallurgy Press, 1954).
- [2] N. P. Fedot'ev, P. M. Vyacheslavov and N. M. Ostroumova, *J. Appl. Chem.*, 27, No. 1 (1954); 28, No. 4 (1956).*
- [3] N. P. Fedot'ev, P. M. Vyacheslavov and V. V. Bardin, *J. Appl. Chem.*, 28, No. 3 (1956). *
- [4] N. P. Fedot'ev, P. M. Vyacheslavov, N. M. Ostroumov and S. Ya. Grilikhes, *J. Light Ind.*, No. 1 (1957).
- [5] N. P. Fedot'ev, P. M. Vyacheslavov and N. P. Gnusin, *J. Appl. Chem.*, 28, No. 6 (1955). *
- [6] N. P. Fedot'ev and P. M. Vyacheslavov, *Industrial Lab.*, 7 (1952).
- [7] A. L. Rotinyan, É. Sh. Ioffe, E. S. Kozich and Yu. I. Yusova, *Proc. Acad. Sci. USSR* 104, No. 5 (1955).
- [8] N. P. Fedot'ev and S. V. Mikhailov, *Trans. Leningrad Technol. Inst.*, No. 11 (1941).

Received February 11, 1958

*Original Russian pagination. See C.B. Translation.

RATE OF CONTACT REDUCTION OF A METAL FROM SOLUTION

B. V. Drozdov

Contact reduction of a metal from solution is a heterogeneous reaction which takes place on the surface of contact between a metal and a solution. The process therefore consists of the following principal stages: 1) transport of the reacting substances from the volume of the solution to the reacting surface; 2) reaction at the reacting surface and 3) transport of soluble reaction products from the reacting surface into the volume of the solution.

The observed over all rate of the process is determined by its slowest stage, which reflects its principal characteristics.

Studies of the rate of contact reduction have been discussed in many publications [1-12]; some authors, in accepting the electrochemical nature of the reaction, consider that the over all rate is determined to a certain extent by the conditions of supply and removal of the reacting substances [1-5, 7, 10-12]. The opinion has also been advanced that the conditions of transport of the reactants influence only the end of the process, because "at a low concentration of ions in solution the so-called limiting current effect is observed" [8].

The great significance of transport of the reactants is confirmed by the fact that in many cases the reduction is more rapid with elements giving as low emf than with metals giving a high emf. For example, Gliksman, Mouquin, and King [10], who studied the deposition of silver on copper and zinc (from AgNO_3 solutions containing from 0.54 to 5.4 g/liter), showed that in a number of cases the rate of deposition of silver was higher on copper than on zinc under the same conditions, i.e., the influence of the principal electrochemical factors on the over all rate of the process was slight.

Of course, for some reactions conditions may be possible under which the rate of the process is determined by electrochemical factors, such as the precipitation of copper by some types of nickel at room temperature, but such conditions are unusual in practice.

We noted earlier that the influence of transport of the reactants is complicated further by the fact that the second stage of the process involves formation of a solid layer of cathodic deposit through which the reactants must pass. Conditions for diffusion through this film are more difficult than within the solution [1, 2].

Nearly all investigations of contact-reduction rates have been carried out by means of systematic analyses of the reaction products in course of the process. An approach worthy of attention was an attempt to study the process kinetics with a model galvanic cell by determination of the principal electrochemical quantities [11, 12]. The chief difficulty of this method lies in the creation of a model which would have just as low internal and external resistances as the elements involved in electrodeposition.

In this paper we present an account of experiments on the influence of transport of the reactants on the over-all reaction rate; this influence is exerted not only at the end of the process. The investigations were mainly concerned with deposition of copper from solution by means of nickel powder under the conditions used in purification of nickel electrolytes, as this process is characterized by a considerable resistance of the reaction itself.

The view has been put forward that the rate of the process depends on the electrode potentials of the working cell [8]; this is absolutely correct and incontrovertible, but the potentials are determined by a number of factors which include transport of the reactants. Moreover, measurement of the electrode potentials in a working

TABLE 1

Effect of Stirrer Speed on the Rate of Contact Reduction of Copper from Solution. Solution composition: 200 g $\text{NiSO}_4 \cdot 7\text{H}_2\text{O}$, 40 g Na_2SO_4 , 20 g H_3BO_3 , and 5 g NaCl per liter; initial copper content 480 mg/liter temperature 75°

Time (min)	Copper content (mg/liter)			
	without stirring	at stirrer speed, r.p.m.		
		300	600	900
0	480	480	480	480
5	464	443	398	355
10	454	407	340	257
20	450	316	258	240
30	—	241	183	207
60	—	108	58	191
90	—	28	33	199
120	452	15	8	216

TABLE 2

Effect of Stirrer Speed on the Rate of Contact Reduction of Copper from Solution by Nickel Powder. Solution composition: 200 g $\text{NiSO}_4 \cdot 7\text{H}_2\text{O}$, 40 g Na_2SO_4 , 20 g H_3BO_3 and 5 g NaCl per liter; initial copper content 50 mg/liter; temperature 75°

Time (min)	Copper content (mg/liter)			
	without stirring	at stirrer speed, r.p.m.		
		300	600	900
0	51	50	50	52
5	—	48	45	45
10	—	45	37	42
20	—	41	25	37
30	—	33	20	29
60	—	25	16	25
90	—	25	13	21
120	45	20	6	12

The effect of the duration of precipitation of the metal on the temperature coefficient was also studied; it was found that the temperature coefficient decreases as the film of deposited metal becomes thicker, i.e., the influence of transport of the reactants on the over-all rate of the process increases. The results of these experiments (presented below) contradict the views of some authors who consider that a film of precipitated metal offers no resistance to diffusion [9].

Effect of the duration of precipitation of copper by nickel powder (of moderate activity) on the temperature coefficient. Solution composition: 200 g $\text{NiSO}_4 \cdot 7\text{H}_2\text{O}$, 40 g Na_2SO_4 , 20 g H_3BO_3 and 5 g NaCl per liter; initial copper content 0.235 g/liter:

Time from start of reaction (min)	15	30	45	60	120
Temperature coefficient in the 40-70° range (%)	10.0	7.1	4.5	3.7	1.7

contact-reduction cell is difficult and its accuracy is low. Therefore in the present instance the potentials do not constitute a convenient and objective characteristic of the process, such as in electrolysis or in ordinary galvanic cells.

The contacting metals may be characterized by the cell emf, which is easy to measure and determine. However, the emf can in no way be a measure of the true process rate.

The copper-nickel powder cell also contained in solution (200 g $\text{NiSO}_4 \cdot 7\text{H}_2\text{O}$, 40 g Na_2SO_4 and 20 g H_3BO_3 per liter; pH = 5.45) copper (0.26 g/liter) as the sulfate in the cathode compartment. The catholyte and anolyte were separated by a porous diaphragm. The emf of this cell was 523 mv at 17°, and 489 mv at 70°.

On addition of 5 g/liter of NaCl to the solution and decrease of pH to 4.1 the cell emf was 476 mv at 17° and 447 mv at 70°.

Thus, the cell emf decreased by about 6% on increase of temperature from 17 to 70°, whereas the rate of contact reduction increased 3.5-fold. The same is found for the copper-zinc cell.

In order to determine which stage of contact reduction determines the rate of the process, the temperature coefficients of the reaction rate were determined. The temperature coefficient of processes governed by diffusion conditions is, on the average, 1-3% per degree of temperature change, while its value is higher for the kinetic region.

Under conditions of practical significance the temperature coefficient of displacement of copper by zinc powder from sulfate solution is 2.3% at temperatures from 40 to 50°. The temperature coefficient for displacement of silver by zinc is about 2%.

The temperature coefficient of the rate of contact reduction of copper by nickel powder from a nickel electrolyte solution of the composition given above is about 10% at room temperature, while for inactive powders it is greater. For one powder the temperature coefficient was 6% between 17 and 30°, 2.9% between 30 and 75°, and 0.7% between 75 and 101° (for a process one hour in duration).

For these powders the reaction rate is determined by kinetics at room temperature, while above 60° diffusion factors become significant.

TABLE 3

Contact Reduction of Copper by Nickel Powder with Retardation of the Initial Rate of the Process. Solution composition: 2) g $\text{NiSO}_4 \cdot 7\text{H}_2\text{O}$, 40 g Na_2SO_4 and 20 g H_3BO_3 per liter; temperature 75°

Time (min)	Copper content (mg/liter) in solution in experiments		
	I	II	III
0	525	260	60
5	440	231	55
10	263	107	42
15	193	77	38
30	69	24	20
60	23	15	11
120	8	2	2

In these experiments the solution was moved at a constant velocity (about 100 cm per minute) by stirring.

A characteristic sign of diffusion-controlled kinetics is the dependence of reaction rate on stirring rate. It was found that when solutions are purified by the action of powdered metal, the process does not take place to any appreciable extent without stirring or circulation of the liquid; a certain minimum rate of displacement of the powder relative to the solution is necessary for the process to occur. Table 1 contains data on the influence of the stirring rate on the kinetics of removal of copper from nickel solutions by the action of copper powder.

It is clear from Table 1 that the reaction does not proceed without stirring; the decrease of copper concentration during the first twenty minutes was probably the result of agitation of the solution when the powder was put in and the samples taken, as the process subsequently stopped. The optimum stirring in the apparatus used was obtained at 600 revolutions/minute. At 900 rpm the process is more rapid at first, then slows down after 20 minutes, and this is followed by a redissolution process caused by intensified

supply of atmospheric oxygen into the solution as the result of more rapid stirring.

Table 2 contains experimental results for a solution of a lower copper content, which confirm the above conclusions.

Stirring is the main factor which influences transport of the reactants. Transport may be effected in the following ways: 1) transport by current; 2) by natural diffusion; 3) by agitation or circulation of the solution. In all types of contact reduction of metals the electric field usually extends over a very small portion of solution and transport by current is essentially confined to a very small region close to the surface of the contacting metals. The role of natural diffusion is also very small because the diffusional area for a powder is small. Diffusion conditions are especially unfavorable for a powder lying at the bottom of a vessel, and are considerably better for a compact vertical electrode when convection currents are present.

Stirring or circulation of the solution is of primary significance for supply of the reactants from the volume of the solution to the surface.

We also investigated the activation energy of the displacement of copper by nickel powder from sulfate solution; it was found that on increase of temperature a break appears on the $\text{Ln}K-1/T$ linear plot (K is the reaction rate constant and T is the absolute temperature), which approaches to a horizontal line. An explanation of this fact is that transition into the diffusion-controlled region is associated with a decrease of the apparent energy of activation.

It follows that under conditions of practical interest a number of characteristics established experimentally (influence of stirring, temperature coefficient, influence of temperature on the activation energy) show that the rate of the process is determined by the rate of transport of the reactants. Experiments on precipitation of copper from solution onto a lead plate provide good confirmation of the significance of natural circulation. When the plate was in a vertical position the precipitation rate was 1.5 times the rate with the plate horizontal. In the vertical position, the reaction products (heavy salts of lead) fell freely to the bottom of the vessel and a continuous supply of fresh solution could enter the precipitated metal film. With the plate horizontal (the working surface facing upward) the heavy products of reaction were retained by the precipitate and hindered the process. This experiment showed that even the position of the precipitating metal influences the rate of the process.

The rate of contact reduction depends on a large number of factors, which include the properties and amounts of the metals concerned, solution composition, ratio of the weights of the metals to the amount of solution, agitation conditions, temperature, etc. It is difficult to believe that the influence of all conditions for different metals and stages of the process could be embodied in a single equation. The equation put forward earlier by the author [1] for a self-retarding reaction covers the principal relationships under conditions met most often in practice, but it does not account for rarer cases and certain details. For example, it is sometimes found that the rate of the process at the earliest stage is somewhat lower than it is subsequently.

This effect may be attributed either to dissolution of surface films or to overcoming of the retardations accompanying the formation of the first crystal nuclei, as the formation of a new phase is associated with an increase of activation energy (Table 3).

As for any other heterogeneous reaction, the constants in the kinetic equation for contact reduction are somewhat conventional in character (because concentrations are used instead of activities, volume instead of surface concentrations are taken, the dimensions of the reacting surfaces are approximate, etc). For the same reasons the order of reaction is formal. On the one hand, all this leads to difficulties in correlation of constants given by different authors, as is pointed out by Kozlovskii [8]. On the other hand, in view of the good reproducibility of experimental results under definite conditions, certain conclusions may be drawn with the aid of these constants; this is particularly valuable in studies of contact reduction processes, as few reliable methods are available for investigations of such processes.

SUMMARY

1. In practice the contact reduction of metals is usually performed under conditions such that the rate of the process is largely determined by transport of the reactants (i.e., diffusion controls the kinetics), as confirmed by the following experimental results: a) the rate of reaction depends strongly on the agitation conditions; b) the temperature coefficient of the reaction rate is low, and is close to the corresponding coefficient for diffusion; c) the relationship between the activation energy and $1/T$ approaches a horizontal straight line with increase of temperature.

2. The forming film of precipitated metal offers resistance to diffusion; this is confirmed by the fact that the temperature coefficient of the reaction rate decreases with increasing film thickness.

3. The initial formation of cathodic regions involves an increase of the apparent activation energy, so that the reaction slows down during the initial precipitation period.

LITERATURE CITED

- [1] B. V. Drozdov, Proc. 2nd All-Union Conf. on Theoretical and Applied Electrochemistry [In Russian] (Kiev, 1949) p. 106.
- [2] B. V. Drozdov, J. Appl. Chem. 31, No. 2, 211 (1958).*
- [3] M. Centnerszer and W. Heller, Z. Phys. Ch. 161, 113 (1932).
- [4] V. Mayer, Z. Electroch. 39, 439 (1933).
- [5] N. N. Sevryukov, Coll. Sci. trans. Ministry of Nonferrous Metals and Gold [In Russian] 22, 44 (1952).
- [6] I. N. Plaksin, N. A. Suvorovskaya and O. K. Budnikova, Bull. Acad. Sci. USSR OTN, 1 (1948).
- [7] I. N. Plaksin and N. A. Suvorovskaya, Bull. Acad. Sci. USSR, OTN, 3 (1949).
- [8] M. T. Kozlovskii, Mercury and Amalgams in Electrochemical Methods of Analysis [In Russian] (Acad. Sci. Kazakh SSR Press, Alma-Ata, 1956).
- [9] A. A. Bulakh and R. Drachevskaya, J. Appl. Chem. 26, 1225 (1953).*
- [10] G. Glicksman, H. Mouquin and C. King, J. Electroch. Soc. 100, 580 (1953).
- [11] I. Sendzimir and M. Pavelikova, Bull. Polish Acad. Sci. Div. III, 4, 709 (1956).
- [12] I. Sendzimir, Bull. Polish Acad. Sci. Div. III, 4, 715 (1956).

Received February 13, 1958

*Original Russian pagination. See C.B. Translation.

CATHODIC REDUCTION OF FERRIC OXIDE

V. P. Galushko, E. F. Zagorodnyaya

and L. I. Tishchenko

(Dnepropetrovsk State University)

At the present time iron powders are produced industrially by reduction of iron oxides with hydrogen, carbon, carbon monoxide, and natural gases at high temperatures [1], by thermal decomposition of carbonates and various organic salts, by electrolysis of salt solutions, and by mechanical subdivision of the compact or melted metal [2].

Other methods for production of iron powder have not been adopted industrially as yet. Several publications [3-4], and investigations conducted in the electrochemical laboratory of the Dnepropetrovsk University, indicate that subdivided sparingly-soluble compounds of certain metals, including iron, are cathodically reduced to the metals which are liberated in powder form.

The purpose of the present investigation was the study of the effects of electrolyte composition, current density, temperature, and quantity of electricity passed on the cathodic reduction of ferric oxide, Fe_2O_3 , and to determine whether iron powder can be made by this process.

EXPERIMENTAL

The cathode was a rectangular iron or nickel plate, coated on both sides with a paste made from a weighed sample of Fe_2O_3 (chemically pure), with particles < 0.25 mm, and distilled water. The electrode was wrapped in cloth and tied tightly with cord. The anode was cylindrical in shape, made from nickel foil. The mixture of iron powder and Fe_2O_3 formed as the result of cathodic reduction was transferred to a filter, washed with water until the wash waters were neutral to litmus, and dried in air. The content of metallic iron in the mixture was determined by displacement of copper from neutral CuSO_4 solution by the iron, with subsequent titration of the acidified filtrate, containing Fe^{++} ions, by dichromate in presence of phenylanthranilic acid.

The cathode reduction of Fe_2O_3 was effected at constant current strength. In all experiments, unless stated otherwise, the quantity of electricity passed through the cell was the quantity theoretically required for complete reduction of the amount of Fe_2O_3 taken (Q_{theor}). A copper coulometer was connected in the circuit for determination of current efficiency for metallic iron.

The results of cathodic reduction of Fe_2O_3 in certain electrolytes are given in Table 1.

It is evident from Table 1 that cathodic reduction of Fe_2O_3 in neutral K_2SO_4 solution proceeds with a low current efficiency, but addition of NaOH to the solution raises the current efficiency for iron considerably. Even higher current efficiencies are obtained in cathodic reduction of Fe_2O_3 in NaOH solutions, especially at high concentrations (40 and 60%).

The electrolyte chosen for determining the influence of other factors on the process was 40% NaOH solution, as the current efficiency for metallic iron is lower in more dilute NaOH solutions than in 40% NaOH, while if 60% NaOH is used as electrolyte the bath performance deteriorates (a crust is formed on the electrolyte surface and crystals are deposited).

The reduction of Fe_2O_3 is accompanied by liberation of hydrogen at the cathode. In electrolysis of alkali

TABLE 1

Cathodic Reduction of Fe_2O_3 in Various Electrolytes, $t = 80^\circ$, $S_c = 0.7 \text{ cm}^2$, $I = 0.5 \text{ amp}$

Electrolyte composition	Weight taken (g)	Current efficiency for metallic iron (%)
1 N K_2SO_4	0.5	4
1 N $\text{K}_2\text{SO}_4 + 5\% \text{ NaOH}$	0.5	15
1 N $\text{K}_2\text{SO}_4 + 10\% \text{ NaOH}$	0.5	20
1 N $\text{K}_2\text{SO}_4 + 15\% \text{ NaOH}$	0.5	28
5% NaOH	0.5	16
20% NaOH	1.0	37
40% NaOH	1.0	54
60% NaOH	1.0	58

TABLE 3

Effect of Current Density on Current Efficiency for Metallic Iron

Current density (amp/cm ²)	Current efficiency for metallic iron (%)
0.07*	68
0.14	64
0.43	59
0.71	54
1.43	49

*The quantity of electricity in this experiment was $0.5 Q_{\text{theor}}$.

TABLE 5

Effect of the Quantity of Electricity on Current Efficiency for Metallic Iron Electrolyte, 40% NaOH, weight of Fe_2O_3 1 g, $S_c = 0.7 \text{ cm}^2$, $I = 1 \text{ amp}$

Expt. No.	$\frac{Q_{\text{act}}}{Q_{\text{theor}}}$	Current efficiency for metallic iron (%)	Degree of reduction (%)
1	1	49	52
2	1.5	47	74
3	2	45	90
4	3	31	95
5	4	24	98
6	6	16	98

Table 3. The current densities were calculated for the apparent area of the metal cathode. Table 3 shows that the current efficiency falls with increase of current density.

TABLE 2

Effect of Temperature on Current Efficiency for Metallic Iron Electrolyte 40% NaOH, weight of Fe_2O_3 taken 1.0 g, $S_c = 0.7 \text{ cm}^2$, $I = 0.3 \text{ amp}$

Temperature (in $^\circ\text{C}$)	Current efficiency for metallic iron (%)
20	24
50	34
80	59

TABLE 4

Effects of Added Graphite and Iron on the Degree of Cathodic Reduction of Fe_2O_3

Addition	Weight of addition (g)	Degree of reduction of Fe_2O_3 (%)
	No addition	50
Graphite	0.2	70
	0.5	79
Iron	0.5	75*
	1.0	68*

*With correction for added iron.

solutions, hydrogen is liberated at the cathode as the result of decomposition of water molecules [5]:



With increase of alkali concentration the activity of water molecules decreases, the potential of hydrogen evolution increases, and this accounts for the increase of current efficiency when more highly concentrated NaOH solutions are used.

Temperature has a strong influence on cathodic reduction of ferric oxide. It follows from the data in Table 2 that in the cathodic reduction of Fe_2O_3 the current efficiency for metallic iron increase with rise of temperature. At temperatures above 80° evaporation of water from the electrolyte is very considerable, and therefore most of the experiments were performed at 80° .

The current efficiency for metallic iron in cathodic reduction of Fe_2O_3 depends on the cathodic current density. Results obtained in cathodic reduction of Fe_2O_3 at different current densities are given in

TABLE 6

Effects of Ore Particle Size on the Degree of Reduction and the Particle-Size Distribution of the Powder Obtained

Quantity of electricity	Particle size before reduction (mm)	Degree of reduction (%)	Particle-size distribution of powder after reduction (%)			
			to 0.25	0.25-0.5	0.5-1.0	1.0-3.0
$Q_{\text{theor.}}$	to 0.25	68	94	6	—	—
	0.25-0.5	58	12	81	7	—
	0.5-1.0	50	1	4	95	—
	1.0-3.0	41	—	—	4	96
$2 Q_{\text{theor.}}$	to 0.25	—	91	9	—	—
	0.25-0.5	69	17	83	—	—
	0.5-1.0	59	4	5	91	—
	1.0-3.0	58	1	1	2	96

The effects of temperature and current density on current efficiency for metallic iron indicate that these factors influence both cathode processes: evolution of hydrogen and reduction of ferric oxide.

Contact between the Fe_2O_3 grains and the cathode plays a very important part in cathodic reduction of ferric oxide. It was observed that the layers of Fe_2O_3 in good electrical contact with the cathode are the first to undergo cathodic reduction; this is consistent with data on the low conductivity of ferric oxide. The hydrogen which is liberated during reduction of Fe_2O_3 loosens the compact and interrupts contact between the ferric oxide grains and the cathode.

Contact between the Fe_2O_3 particles and the cathode is improved considerably if conducting additives are present in the paste. The data in Table 4 indicate that additions of powdered graphite or metallic iron to Fe_2O_3 increase considerably the percentage reduction of ferric oxide.

The results of the above experiments show that when the theoretical quantity of electricity (Q_{theor}) has been passed through the cell the ferric oxide is incompletely reduced, as hydrogen is simultaneously liberated. For more complete reduction of the Fe_2O_3 taken the quantity of electricity passed must be increased; it follows from the data in Table 5 that for almost complete reduction the quantity of electricity passed must be about four times Q_{theor} .

The powders obtained (Experiments No. 5 and 6, Table 5) contained a small amount of unreduced ferric oxide, mainly on the cloth wrapper; if this is carefully removed it is possible to avoid mixing of the oxide with the iron powder and to obtain a powder containing about 99% of Fe_{met} . The dry iron powder so obtained is gray in color and is finely divided. Despite its high dispersity, the resultant iron powder is resistant to atmospheric oxidation. For example, samples of iron powder remained unchanged in weight when kept in air in the laboratory for 20 days.

The bulk density of the dry powder is 0.8-0.9 g/cc.

The behavior of Krivoi Rog iron ores in cathodic reduction was the same as that of chemically pure ferric oxide.

Experiments were carried out in the cathodic reduction of these ores in order to determine the influence of particle-size distribution on the percentage reduction of ferric oxide. Table 6 contains results obtained in cathodic reduction of ores differing in particle-size distribution, with the use of the theoretical and double the theoretical quantity of electricity. It follows from Table 2 that the percentage reduction falls with increasing size of the ore particles.

In addition, Table 6 contains sieve analysis data on the powders after cathodic reduction. It is seen from these results that ore powders of known particle size are changed somewhat in their particle-size distribution after cathodic reduction, but most of the grains in the powders (80% and over) retain their original size. The observations and results of these experiments indicate that under the conditions used (electrolyte 40% NaOH, temperature 80°) Fe_2O_3 is reduced directly in the solid phase at the cathode.

SUMMARY

1. The effects of electrolyte composition, temperature, current density, quantity of electricity, and certain additives on the degree of cathodic reduction of Fe_2O_3 were studied, and it was found that metallic iron powder can be obtained by cathodic reduction of Fe_2O_3 in an alkaline electrolyte (40% NaOH) at 80°.

2. It was shown in a study of certain characteristics of the resultant iron powder (bulk density, chemical composition, particle size, and atmospheric oxidation) that most of the grains of ferric oxide and Krivoi Rog iron ore retain their original size during cathodic reduction.

3. It is suggested that under the specified electrolysis conditions the cathodic reduction of Fe_2O_3 takes place mainly in the solid phase.

LITERATURE CITED

- [1] V. S. Rakovskii, Proc. 2nd Kiev Conference on Powder Metallurgy [In Russian] (Kiev, 1955).
- [2] O. K. Kudra and E. Gitman, Electrolytic Production of Metallic Powders [In Russian] (Kiev, 1952).
- [3] A. S. Afanas'ev, Sci. Trans. Dnepropetrovsk Metallurgical Inst. "Chemistry and Chemical Technology" 20 (1949).
- [4] A. Sancelme, Ann. de Chim. 12 série 8 (1953).
- [5] A. N. Frumkin, V. S. Bagotskii, Z. A. Iofa and B. N. Kabanov, Kinetics of Electrode Processes [In Russian] (Izd. MGU, 1952).

Received January 20, 1958

THE SYSTEMS WATER-HEXAMETHYLENEIMINE-SODIUM CHLORIDE AND WATER-HEXAMETHYLENEIMINE-SODIUM HYDROXIDE

E. N. Zil'berman and M. M. Bershtein

Hexamethyleneimine (hexahydroazepine) is formed as a by-product in the hydrogenation of adiponitrile to hexamethylenediamine [1]. Hexamethyleneimine is usually extracted from the reaction products in the form of an azeotropic mixture with water. Hexamethyleneimine, which is a secondary aliphatic amine, can be used for various purposes analogously to piperidine. The present investigation was therefore concerned with the problem of a rational method for isolation of hexamethyleneimine from water.

Hexamethyleneimine and water are miscible in all proportions at room temperature. At temperatures above 66.9° two layers are formed [2]. However, the hexamethyleneimine layer still contains a considerable amount of water. The minimum solubility of water in the hexamethyleneimine layer, 29.7%, is found at 140-180°, which is above the boiling points of both components. Therefore separation of hexamethyleneimine and water into layers at high temperatures is not feasible. Hexamethyleneimine may be isolated from water by extraction in benzene [3] followed by distillation of the solvent. However, we consider that displacement of hexamethyleneimine from water by means of an inorganic salt or alkali is a more convenient method under production conditions.

The unlimited mutual solubility of amines and water at low temperatures is usually attributed to formation of chemical compounds which can be decomposed by hydrophilic substances. We therefore studied the possibility of displacing hexamethyleneimine from water by means of sodium chloride or sodium hydroxide. For this purpose mutual solubility in the ternary systems water-hexamethyleneimine-sodium chloride and water-hexamethyleneimine-sodium hydroxide was studied. In view of the fact that when hexamethyleneimine is salted out by these substances it separates out in the form of mixtures containing various amounts of water, and additional distillation is required for its isolation, the composition of the heteroazeotropic mixture water-hexamethyleneimine was also determined.

EXPERIMENTAL

Hexamethyleneimine, the constants of which were given earlier [3], was used in the experiments. Sodium chloride was of the chemically pure grade, and was additionally recrystallized. Commercial solid caustic soda was purified to remove carbonate and used in the form of concentrated aqueous solution.

The construction of binodals was partially based on data on conjugate solutions. The sections of the binodals for which data on the positions of the tie lines were lacking were constructed with the aid of the widely-used "titration" method [3]. A mixture of two components is usually "titrated" by a third component to appearance or disappearance of turbidity. The most convenient procedure in our experiments was titration of homogeneous aqueous solutions of hexamethyleneimine by 25% sodium chloride solution or 10% sodium hydroxide solution in water until the mixture became turbid. The temperature variations were $\pm 0.05^\circ$ (in experiments at 20°) or $\pm 0.2^\circ$ (in experiments at 70 and 65°).

To determine the positions of the tie lines, water, hexamethyleneimine, and the third component were taken in quantities such that two liquid layers approximately equal in volume after mixing (with vigorous stirring)

TABLE 1

Compositions of Conjugate Solutions in the System Water-Hexamethylenimine-Sodium Chloride in Presence of Solid Phase

Temperature (deg)	Composition of layers (%)					
	upper			lower		
	water	hmi •	sodium chloride	water	hmi •	sodium chloride
5	52.4	32.2	15.4	73.5	2.0	24.5
20	42.8	45.9	11.3	72.9	1.3	25.8
35	29.4	63.3	7.3	72.5	1.1	26.4
50	19.1	77.5	3.4	72.4	0.9	26.7
70	10.2	89.4	0.4	72.6	0.6	26.8
90	9.0	90.9	0.1	72.0	0.5	27.5

TABLE 3

Compositions of Conjugate Solutions of a Mixture Containing 49.3% Water, 45.2% Hexamethylenimine, and 5.5% NaOH at Various Temperatures

Temperature (deg)	Composition of layers (%)					
	upper			lower		
	water	hmi •	NaOH	water	hmi •	NaOH
5	25.9	73.9	0.2	85.55	0.65	13.8
20	23.95	75.9	0.15	86.1	0.6	13.3
35	24.5	75.4	0.1	85.9	0.6	13.5
50	20.2	79.7	0.1	86.95	0.55	12.5
65	18.2	81.7	0.1	87.4	0.5	12.1
80	16.4	83.5	0.1	87.7	0.5	11.8

TABLE 2

Mutual Solubility in the System Water-Hexamethylenimine-Sodium Chloride at 70°

Composition of layers (%)					
upper			lower		
water	hmi •	sodium chloride	water	hmi •	sodium chloride
13.5	85.8	0.7	75.3	0.9	23.8
20.3	78.7	1.0	80.8	1.3	17.9
26.9	72.3	0.8	85.7	2.2	12.1
34.8	64.2	1.0	90.1	3.3	6.6
63.2	36.8	—	90.0	10.0	—

TABLE 4

Mutual Solubility in the System Water-Hexamethylenimine-Sodium Hydroxide at 20°

Composition of layers (%)					
upper			lower		
water	hmi •	NaOH	water	hmi •	NaOH
1.2	98.7	0.1	50.6	0.1	49.3
2.9	97.0	0.1	61.9	0.1	38.0
11.6	88.3	0.1	73.8	0.2	26.0
21.2	78.7	0.1	82.9	0.3	16.8
33.3	66.1	0.6	87.9	1.2	9.9
47.6	51.5	0.9	91.1	2.8	6.1

and subsequent settling. When the layers became quite clear samples were taken. In water-hexamethylenimine-

sodium chloride systems hexamethylenimine was determined by direct titration of samples by hydrochloric acid solution in presence of methyl orange, sodium chloride was determined from the chloride content, and water was found by difference. The compositions of conjugate solutions in the system water-hexamethylenimine-NaOH were determined as follows. A weighed sample of solution was put into a Kjeldahl flask, a large excess of water was added, and the azeotropic mixture of water and imine was distilled off. The distillate was collected in standard hydrochloric acid solution. The content of hexamethylenimine in the sample was found from the excess of hydrochloric acid. The NaOH content of the sample was found by acidimetric titration of the residue in the flask after distillation of hexamethylenimine. The points corresponding to the compositions of the original mixture and the conjugate solutions lay on one straight line in the triangular diagrams (unless a solid phase was present). This confirmed the validity of the data obtained by the method described.

For determination of the composition of the heteroazeotropic mixture approximately equal amounts of hexamethylenimine and water were distilled from a Wurtz flask. The mixture in the flask was heterogeneous at the distillation temperature. The distillate, which became homogeneous at room temperature, was titrated by hydrochloric acid and its imine content was found.

RESULTS AND DISCUSSION

Compositions of conjugate solutions in the system water-hexamethylenimine-NaCl in presence of excess

*hexamethylenimine

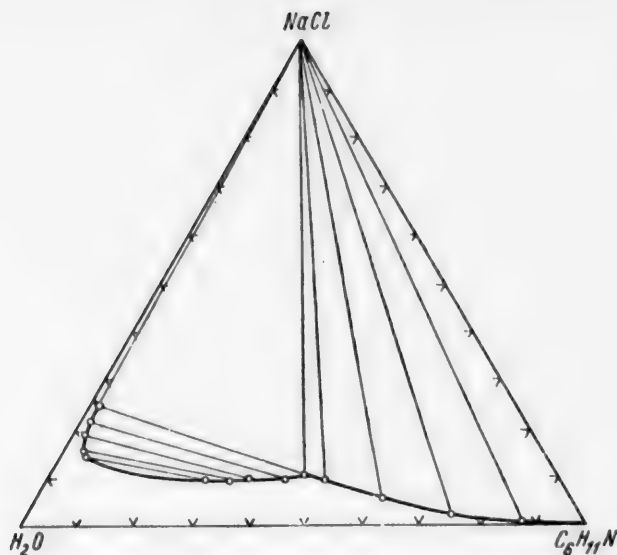


Fig. 1. The system water-hexamethylenimine-sodium chloride at 20°.

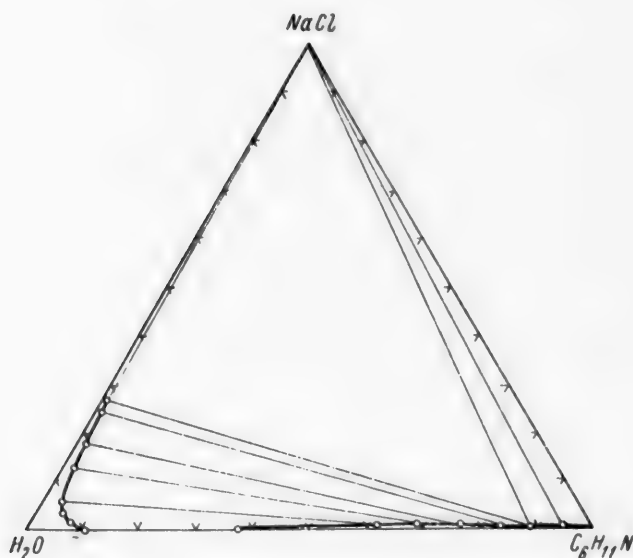


Fig. 2. The system water-hexamethylenimine-sodium chloride at 70°.

solid phase were determined at various temperatures (in the 5-80° range). Mutual-solubility curves for this system at 20° (Fig. 1) and 70° (Fig. 2) were then plotted. Data on the composition of conjugate solutions not saturated with sodium chloride at 70° are presented in Table 2.

The system water-hexamethylenimine-NaOH was also studied in the 5-80° temperature range. To determine the influence of temperature on the heterogenizing effect of the alkali, the compositions of conjugate solutions were determined at different temperatures (Table 3) for the same mixture (water 49.3%, hexamethylenimine 45.2%, and NaOH 5.5%). In addition, mutual solubility diagrams were plotted for this system at 20° (Fig. 3) and 65° (Fig. 4). Table 4 contains data on the compositions of the equilibrium phases of this system at 20°.

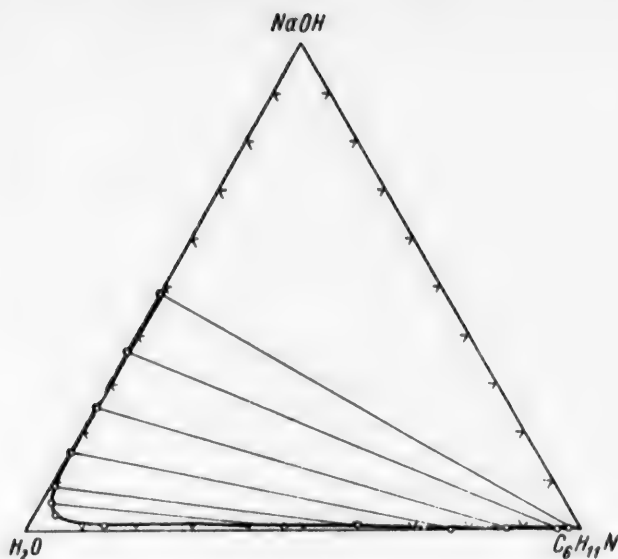


Fig. 3. The system water-hexamethyleneimine-sodium hydroxide at 20°.

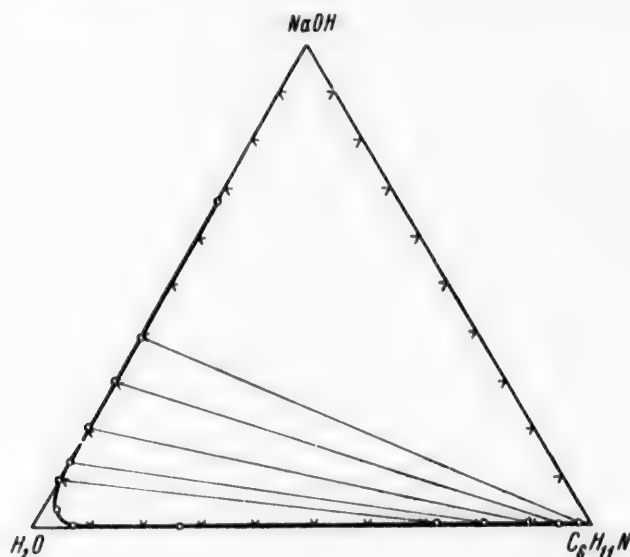


Fig. 4. The system water-hexamethyleneimine-sodium hydroxide at 65°.

The critical points of the investigated mixtures were found by extrapolation of the curve passing through the centers of the tie lines to its intersection with the binodal, or by graphical interpolation [3]. The composition at the critical point for the system with sodium chloride at 20° was found to be: water 70.8%, hexamethyleneimine 17.2%, sodium chloride 12.0%. The mixture corresponding to the critical point for the system with sodium hydroxide at 20° consists of 82.8% water, 15.0% hexamethyleneimine, and 2.2% NaOH. At 65° the composition at the critical point for the same system is 80 parts of water, 20 parts of hexamethyleneimine, and 0.05 part NaOH. The critical points found graphically were in regions where critical opalescence was observed visually.

The heteroazeotropic mixture of hexamethyleneimine and water contained 50.6% of the first component and 49.4% of the second at 751 mm Hg and 95.2°.

The experimental results show that, as expected, the heterogenizing power of NaCl and NaOH increases with temperature. Increase of NaCl or NaOH concentration in the aqueous layer results in an increase of hexamethyleneimine concentration in the conjugate oil layer.

Experimental data on the system with sodium chloride show that at room temperature the upper layer contains approximately equal amounts of water and hexamethyleneimine. It follows that distillation of this mixture yields mainly a homogeneous solution the composition of which corresponds to the azeotropic mixture, and a relatively small amount of anhydrous hexamethyleneimine. A more or less considerable fraction of hexamethyleneimine can be obtained by distillation of the upper layer in the system saturated with sodium chloride and brought to equilibrium at temperatures of 50° and over.

It is much easier to displace hexamethyleneimine from water by means of NaOH. Evidently the alkali, being a more hydrophilic substance, decomposes the amine-water compounds more easily. Even at room temperature in presence of NaOH the hexamethyleneimine content can be raised to about 99% in the oil layer, with 0.1% in the aqueous layer. For separation of the same amount of hexamethyleneimine less alkali is required at high than at low temperatures.

SUMMARY

Mutual solubility has been investigated in the systems water-hexamethyleneimine-sodium chloride and water-hexamethyleneimine-sodium hydroxide, in the 5-80° range, and it was shown that hexamethyleneimine can be salted out of water by sodium chloride at 50° or over, or by addition of sodium hydroxide at room temperature or higher temperatures.

LITERATURE CITED

- [1] E. N. Zil'berman and Z. D. Skorikova, Proceedings of Conference on Heterogeneous Catalysis [In Russian] (Goskhimizdat, Moscow, 1955) p. 471.
- [2] E. N. Zil'berman and Z. D. Skorikova, J. Gen. Chem. 23, 1629 (1953). •
- [3] E. N. Zil'berman, J. Phys. Chem. 26, 1458 (1952).

Received October 21, 1957.

•Original Russian pagination. See C.B. Translation.

THE INFLUENCE OF DYE CONCENTRATION ON LIGHT FASTNESS

Ya. A. Legkun

The rate of fading of organic dyes on textile fibers under the action of light depends on many factors [1], the most important of which are: a) chemical nature of the dye; b) the method of its fixation, i.e., the dyeing method and the nature of the dyed material, and c) composition of the surrounding medium.

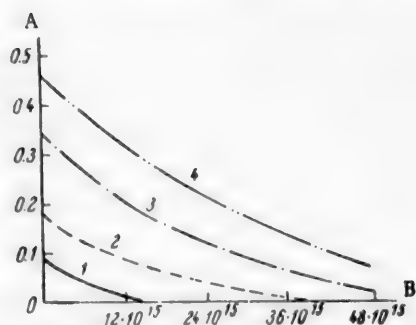


Fig. 1. Effect of degree of irradiation on the content of Direct Light-Fast Sky Blue on the fiber: A) optical density of solutions; B) insolation time (NRD); dye contents of bath (%): 1) 0.5; 2) 1.0; 3) 2.0; 4) 4.

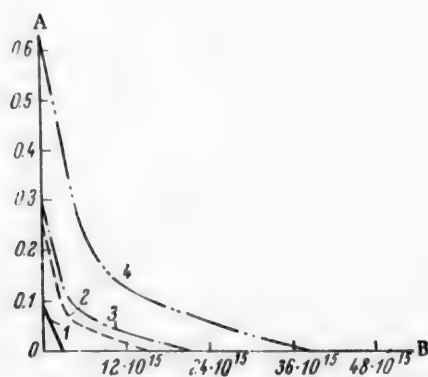


Fig. 2. Effect of degree of irradiation on the content of Direct Pure Sky Blue on the fiber: A) optical density of solutions; B) insolation time (NRD); dye contents of bath (%): 1) 0.5; 2) 1.0; 3) 1.5; 4) 4.

The concentration of the dye on the substrate is also significant in relation to the light fastness of dyeings. It has been shown that the light fastness of dyed textiles depends not only on the presence of oxygen and atmospheric moisture, but also on the amount of dye adsorbed by the fiber [2-5]. However, despite the great practical and theoretical importance of this problem, there is no agreed opinion in the literature on the influence of dye concentration on light fastness. Some authors claim that weaker dyeings are faster to light than saturated dyeings; others are of the opinion that the light fastness of dyes is at a minimum over definite concentration ranges, and yet others state that saturated and light dyeings do not differ in light fastness.

On general theoretical grounds Terenin [1] put forward the view that increase of dye concentration should retard the photochemical reaction of fading because of the strong deactivating influence of identical dye molecules.

The object of the present investigation was to study Terenin's hypothesis experimentally.

EXPERIMENTAL

The material used for the investigation was bright viscose staple fabric No. 4212 [6]. The fabric was dyed by direct dyes often used for dyeing staple fabrics: Direct Light-Fast Sky Blue and Direct Pure Sky Blue [7]. The usual works procedure for viscose staple fabrics [8-10] was followed in preparation and dyeing of the fabrics. The dye concentrations in the bath (in % on the fabric weight) were 0.5, 1.0, 2.0 and 4.0 for Direct Light-Fast Sky Blue and 0.5, 1.0, 1.5 and 4.0 for Direct Pure Sky Blue. The dyed specimens 4 meters long and 0.75 meters wide were exposed to light, the action of atmospheric precipitation (rain) and dew being excluded. The dyeings were insolated in the open air, not under glass, on sunny, cloudy, and dull days, between 8 and 18 hours on a specially equipped platform. The platform was illuminated by direct sunlight on cloudless days from sunrise to sunset. The exposed specimens were fixed

TABLE 1

Variation of the Amount of Dye on the Fiber with the Dye Content of the Bath

Dye content of bath (%) of fabric weight)	Dye on fiber (% of fabric weight)	
	Direct Light-fast Sky Blue	Direct Pure Sky Blue
0.5	0.25	0.28
1.0	0.51	0.75
1.5	—	0.87
2.0	0.97	—
4.0	1.31	1.91

TABLE 3

Decrease of the Amount of Direct Pure Sky Blue on the Fiber After Different Insolation Periods

Amount of Direct Pure Sky Blue	Loss of dye (%) after insolation period (in NRD)						
	0	$3 \cdot 10^{15}$	$6 \cdot 10^{15}$	$9 \cdot 10^{15}$	$12 \cdot 10^{15}$	$15 \cdot 10^{15}$	$18 \cdot 10^{15}$
0.5	100	100	—	—	—	—	—
1.0	100	66.2	83.3	87.5	91.6	100	—
1.5	100	60.3	75.0	82.1	89.3	92.8	96.4
4.0	100	41.3	58.0	75.4	80.3	83.6	85.2

This instrument was installed on the platform used for insolation of the specimens; it was switched on daily at 8 A.M. and recorded the quantity of light energy falling on the earth's surface. The light-energy receiver of the instrument, like the exposed specimens, was placed at an angle of 45° to the horizontal. The total time of insolation (130 days) was divided into 16 equal periods. One insolation period was equivalent to $3 \cdot 10^{15}$ NRD. After each insolation period samples were taken for tests. During the total exposure time the air temperature varied between 18 and 27° , and the relative humidity between 58 and 73%. The degree of fading of the dyeings was determined from the amounts of dye remaining on the fibers after a given number of nominal radiation doses. Sokolov's methods [12-14] were used for determination of the amounts of dye on the fibers before and after insolation and for plotting of concentration curves for the investigated dyes. The FEK-M photoelectric colorimeter was used for the colorimetric determinations.

RESULTS AND DISCUSSION

The following conclusions may be drawn from the curves in Fig. 1 and 2.

1. The amount of dye on unexposed fibers, dyed to different depths by the same dye, increases with the dye concentration (Table 1).
2. Direct Pure Sky Blue is taken up by the fiber to a greater degree than Direct Light-fast Sky Blue.
3. Insolation of dyed fibers results in a decrease of the amount of dye on the fiber (Table 2).

TABLE 2

Decrease of the Amount of Direct Light-Fast Sky Blue on the Fiber After Different Insolation Periods

Amount of Direct light-fast Sky blue	Loss of dye (%) after insolation period (in NRD)						
	0	$3 \cdot 10^{15}$	$6 \cdot 10^{15}$	$9 \cdot 10^{15}$	$12 \cdot 10^{15}$	$15 \cdot 10^{15}$	$18 \cdot 10^{15}$
0.59	100	33.4	55.5	66.7	88.9	100	—
1.0	100	22.3	33.4	38.8	44.4	61.1	66.6
2.0	100	8.8	17.7	33.4	41.2	47.0	52.9
4.0	100	6.6	15.5	23.9	30.5	36.4	43.5

in frames 1 meter wide and 6 meters long. The frames containing the specimens were exposed daily at 8 A.M. and placed at an angle of 45° to the horizontal. After each daily exposure the specimens in their frames were removed and stored in a specially equipped building with conditioned humidity and temperature. The total insolation time was 130 days (May-September 1954).

The insolation time was also determined by means of an electronic light meter, which was used to measure the light energy incident on the earth's surface. The receiver of light energy in the instrument was a vacuum antimony-caesium photocell with an external photoeffect [11]. The indicator in the radiation meter was an electromagnetic counter. One flash of the instrument counter is termed the nominal radiation dose (NRD).

The fading of dyes under the influence of light is unequal in dyeings with different concentrations of dye on the fiber: dye is lost more rapidly from paler dyeings (Table 3). Similar results are obtained with Direct Pure Sky Blue.

It follows that increase of the dye concentration on the fiber leads to increased light fastness of dyeings produced by the same dye to different depths.

4. It was noted earlier that the fiber contains more Direct Pure Sky Blue than Direct Light-fast Sky Blue for all depths, but fading is much more rapid with Direct Pure Sky Blue than with Direct Light-fast Sky Blue probably because of differences in the chemical structure of the dyes.

5. The curves in Fig. 1 and 2 show that different amounts of dye are lost from the fiber over equal insolation periods: the losses of dye are considerably greater during the earlier insolation periods. In our opinion, this effect can be attributed either to the protective action of the products formed by photochemical decomposition of the dyes, or to the protective action of the photodegradation products of cellulose.

In conclusion, I offer my deep gratitude to Academician A. N. Terenin for advice in the course of the present investigation.

SUMMARY

A. N. Terenin's hypothesis, according to which increase of dye concentration leads to increased light fastness of the dyeings, is confirmed experimentally.

LITERATURE CITED

- [1] A. N. Terenin, Photochemistry of Dyes [In Russian] (Izd. AN SSSR, Moscow-Leningrad, 1947).
- [2] J. Joffré, *Bull. Soc. Chim.* 49, 860 (1888).
- [3] J. Joffré, *Bull. Soc. Chim.* 1, 553 (1889).
- [4] M. Kitchelt, *Monatsh. Textil-Ind.* 19, 21 (1904).
- [5] P. Geerman, Coloristic and Textile-Chemical Investigations [In Russian] (Moscow, 1905).
- [6] GOST 5242-50, Silk Dress Fabrics [In Russian].
- [7] Collected Standards and Technical Specifications for Chemical Products, IV [In Russian] (State Standards Press, 1949).
- [8] Handbook on Dyeing and Finishing of Silk Fabrics, edited by A. A. Kop'ev [In Russian] (Moscow, State Light Industry Press, 1953).
- [9] A. Meyer and E. Seitz, Ultraviolet Radiation (IL, Moscow, 1952) [Russian translation].
- [10] K. Ya. Kondrat'ev, Radiant Energy of the Sun [In Russian] (Hydrometeorology Press, Leningrad, 1954).
- [11] M. M. Gurevich, Light and Its Measurement [In Russian] (Izd. AN SSSR, Moscow-Leningrad, 1950).
- [12] A. I. Sokolov, Proc. 4th Conference on Aniline Dye Chemistry and Technology [In Russian] (Izd. AN SSSR, Moscow-Leningrad, 1940).
- [13] R. S. Osipova and S. S. Rakhlina, *Textile Ind.* 8, 8, 28 (1948).
- [14] F. I. Sadov et al., Laboratory Manual for a Course on Chemical Technology of Fibrous Materials [In Russian] (State Light Industry Press, Moscow, 1955).

Received November 18, 1957

SEARCH FOR A METHOD OF ESTIMATING THE PHOTOACTIVE PROPERTIES OF DYES

N. I. Abramova, V. A. Blinov, N. S.

Dokunikhin and V. A. Titkov

Cotton, like other fibers, loses mechanical strength under prolonged action of light and weather, owing to oxidative degradation of cellulose. The loss of fiber strength is much greater if cotton articles dyed by many yellow and orange, and some red and violet vat dyes are exposed to light, air, and moisture.

Numerous investigations have shown that the considerable weakening of dyed fibers as the result of insolation is caused by the sharp intensification of cellulose oxidation in presence of certain vat dyes. Therefore such dyes are usually regarded as substances which activate the photooxidation of cellulose [1-5].

According to Landolt's data, relating in 1933 [6], up to 75% of yellow and orange and up to 50% of red and violet vat dyes have this effect on the fibers. The relative proportions of photoactive and inactive brands in the range of yellow and red vat dyes have not changed substantially since, and therefore the search for substances which do not degrade the fiber remains one of the urgent tasks of vat-dye chemistry.

The search for such dyes is complicated by the lack of sufficiently objective and accurate methods of testing and evaluating photoactive properties. The photoactive properties of dyes are usually estimated from the degree of fiber damage after insolation. The existing methods for determination of the degree of fiber damage are quite adequate for distinguishing between damaged and undamaged fibers, but they are not suitable for determination of small differences in the degree of fiber damage, which is very important in studies of the relationship between the chemical structure and photochemical activity of dyes.

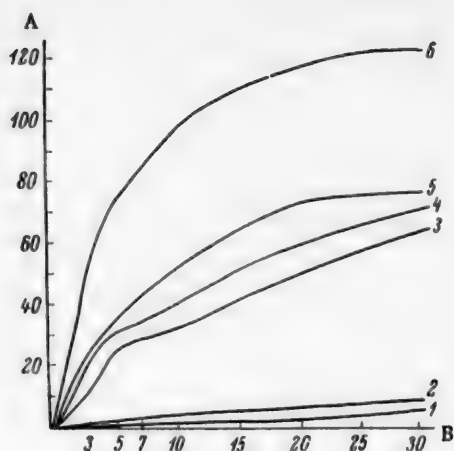
For example, determinations of mechanical properties (tensile strength, abrasion resistance, flex tests) and viscosimetric tests have low sensitivity to small differences in the degree of fiber damage.

Chemical test methods based on determinations of functional groups formed by oxidation or hydrolysis of cellulose are more accurate. Determination of iodine number with the use of weakly alkaline iodine solutions is regarded as one of the most accurate methods for determining aldehyde groups in oxidized fibers [7]. Nevertheless, our experiments showed that owing to the very low absolute contents of aldehyde groups in insolated cellulose estimation of small differences in the degree of fiber damage from iodine numbers is also very difficult.

We developed a method for quantitative determination of the degree of fiber damage and estimation of the photoactive properties of dyes, based on Harrison's qualitative method [8] in which the degree of oxidation of cellulose is characterized by the ability of the fiber to reduce silver from an alkaline solution of a complex silver-thiosulfate compound, which is estimated visually by the degree of blackening of the fabric. In our method the reduced silver was estimated quantitatively, Harrison's method being augmented and modified for the purpose.

The degree of fiber damage was estimated from the amount of reduced silver, and expressed in milliliters of 0.01 N ammonium thiocyanate solution required for titration of the silver reduced by 1 g of fabric. This quantity was termed the silver number.

The stability of the reagent during storage and on heating, its sensitivity to the reducing action of the fiber, reproducibility of the results, and possible side reactions between the reagent and the fiber were all investigated during development of the method.



Effect of treatment time on the silver numbers of fabrics: A) silver number; B) treatment time (minutes); calico: 1) not dyed, not insolated; 2) dyed by Dye No. 3, not insolated; 3) not dyed, insolated for 30 days; 4) dyed by flavanthrone, insolated for 30 days; 5) dyed by Dye No. 2, insolated for 30 days; 6) dyed by Dye No. 3, insolated for 30 days.

The experiments showed that the silver-thiosulfate solution is very sensitive to the reducing action of fibers and that the reproducibility is good.

Rogovin and Shorygina [7] reported that alkaline treatment of partially-oxidized cellulose containing carbonyl groups in positions 2 and 3 of the glucose residue results in breakdown of glucoside linkages and degradation of the cellulose macromolecules. Since the character of cellulose oxidation during insolation has been studied very little, tests were carried out to determine whether the difference between the reducing properties of insolated fibers dyed by active and inactive dyes persists in treatment of the fibers by boiling alkaline silver-thiosulfate solution. The treatment time was varied from 3 to 30 minutes in these tests. The effect of the treatment on undamaged fiber was also investigated.

The results showed that undamaged fabric does not undergo any appreciable changes in the process, as the small values of the silver number increase very little with increase of the treatment time. The silver numbers of insolated specimens, which are oxidized to various extents, increase with increasing treatment time, but the relative difference between the reducing properties of fabric specimens with different degrees of fiber damage persists very distinctly after different boiling times (see diagram).

This method for determination of silver number cannot be used for determining the absolute contents of carbonyl groups in oxidized cellulose because the latter undergoes some additional degradation during treatment in alkaline silver-thiosulfate solution. However, for relative evaluation of the photoactive properties of dyes, including estimations of small differences of photoactive properties, the silver number method is quite suitable by its sensitivity and objectivity.

This was confirmed by additional tests performed with fabric specimens dyed by two active and two inactive dyes; the degree of fiber damage was also determined for these specimens by the iodine number, tensile strength, and viscosimetrically. These last tests were performed on the specimens after brief insolation (10 days).

Comparison of the silver and iodine numbers showed a quite consistent tendency to a progressive increase in the photoactive properties of the dyes. The same result was obtained by determinations of strength loss, and, after brief insolation, by the viscosity characteristics (Table 2).

Of the different complex compounds formed by the interaction of AgNO_3 and $\text{Na}_2\text{S}_2\text{O}_3$, the salts in which the ratio $\text{S}_2\text{O}_3^{2-} : \text{Ag}$ is greater than unity, such as $\text{Na}_3\text{Ag}(\text{S}_2\text{O}_3)_2$ or $\text{Na}_6\text{Ag}_2(\text{S}_2\text{O}_3)_4$, are readily soluble in water and their solutions are fairly stable. The stability of these compounds is even greater in an alkaline medium [9, 10].

The alkaline silver-thiosulfate solution used for the tests had the ratio $\text{S}_2\text{O}_3^{2-} : \text{Ag} \approx 3:1$. When this solution was boiled for 1 hour in a flask under reflux it did not become turbid, Ag_2S was not precipitated, and silver was not reduced. This showed that the reagent is stable when heated and does not undergo side reactions leading to reduction of silver. In the actual tests the boiling time was 5 minutes. When kept in a dark-glass stoppered bottle the solution remained without change for 2-3 days.

The solution was prepared for the tests in sufficient amounts for one day's work, always with freshly-prepared thiosulfate solution.

The sensitivity of the reagent to the reducing action of fibers was verified by tests of the effect of excess reagent on the silver number and by determinations of silver numbers of fabric samples differing very little in the degree of fiber damage. Reproducibility of the results was tested by comparison of the results of duplicate experiments.

TABLE 1

Effect of Treatment Time on Silver Number of Fabric

Treatment time (min)	Silver number of fabrics					
	not insolated		insolated			
	not dyed	dyed by Dye No. 3	not dyed	dyed by Dye No. 1	dyed by Dye No. 2	dyed by Dye No. 3
3	—	1.8	13.8	22.4	26.0	56.4
5	0.4	2.8	25.8	31.8	35.2	75.0
7	—	3.2	29.6	35.0	43.6	86.0
10	1.6	4.2	33.2	42.0	53.6	99.8
20	2.0	7.0	51.8	61.6	75.0	119.0
30	6.0	9.8	66.0	73.2	78.0	126.0

EXPERIMENTAL

Tested materials. Fabric samples differing in the degree of fiber damage were used for development of the method. Fabrics dyed by yellow vat dyes of high and low photoactive characteristics and exposed to the sun for 30 summer days were taken.

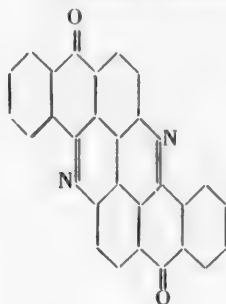
The dyes used were purified, and in some instances specially synthesized, by T. A. Kolobolotskaya. Analyses showed that the dyes were very pure and corresponded to their chemical formulas.

Dye

Chemical structure

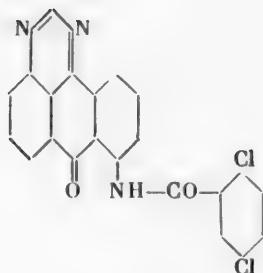
Trade name

No. 1



Indanthrene Yellow G

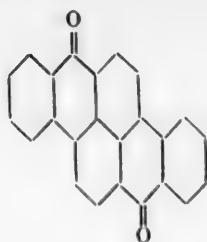
No. 2



Indanthrene Yellow 4GK

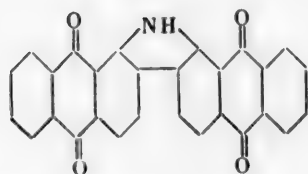
*The dyes are subsequently designated by their numbers.

No. 3



Vat Golden Yellow JK

No. 4



Indanthrene Yellow FFRK

Method for determination of the degree of fiber damage. a) Preparation of alkaline silver-thiosulfate solution: to a freshly-prepared 4% solution of sodium thiosulfate an equal volume of 1% AgNO_3 solution is added gradually with stirring, followed by the same volume of 4% NaOH solution. b) Test procedure: 25 ml of the silver-thiosulfate solution is heated to boiling in a porcelain beaker 50 ml in capacity. The insolated fabric is washed after insolation, dried, cut into fine pieces; a 0.5 g sample is weighed on an analytical balance, added to the solution, and boiled for 5 minutes.

At the end of the treatment the solution is removed from the fabric on a Buchner funnel and the sample is washed with 10% NaNO_3 solution until it is no longer alkaline (phenolphthalein test). It is necessary to use NaNO_3 solution because if distilled water is used for the washing some silver is colloiddally dissolved. The beaker in which the fabric was treated is also rinsed with NaNO_3 solution into the Buchner funnel. The washed fabric is returned to the beaker used for the treatment with silver-thiosulfate solution. The silver deposited on the sides of the funnel is collected by means of pieces of clean filter paper and transferred to the beaker. 25 ml of 20% HNO_3 solution is then added to the beaker and the liquid is heated at $75-80^\circ$ until the silver is completely dissolved.

After the silver has dissolved the solution is filtered through a Buchner funnel, the residue is washed with distilled water to a negative reaction for silver (tested with hydrochloric acid), the filtrate and wash waters are transferred to a flask, and the silver is titrated by 0.01 N ammonium thiocyanate solution, with 10 ml of 10% ferric ammonium alum solution as indicator.

The silver number is represented by the number of milliliters of 0.01 N ammonium thiocyanate solution required for titration of the silver reduced by 1 g of the test fabric.

Determination of the sensitivity of the reagent to the reducing action of the fibers. a) 0.5 g samples of insolated fabric dyed by the inactive Dye No. 1 and the highly active Dye No. 4 were treated with 10, 15, 20, 25, 30 and 35 ml of silver-thiosulfate solution. In the case of Dye No. 1 a low silver number was obtained only after treatment with 10 ml of solution. With Dye No. 4 constant values of the silver number were obtained with 25 ml and over. In either case excess of solution had no effect on the silver number. b) Fabric samples dyed by Dye No. 4 were insolated for 10, 11, 13, 14 and 15 days, after which their silver numbers and tensile strengths were determined. The test results, given below, show that the silver number increases appreciably if the insolation period is increased even by one day, whereas tensile-strength tests do not reveal any difference in the degree of fiber damage in such cases.

Silver - thiosulfate solution taken (ml)	Silver numbers of samples dyed by Dye	
	No. 1	No. 4
10	27.4	—
15	32.4	60.4
20	32.2	77.0
25	30.8	85.6
30	34.8	82.4
35	—	82.4

Insolation time (days)	Silver number	Tensile strength
10	29.8	25.3
11	32.2	24.3
13	35.6	25.1
14	37.4	23.8
15	39.0	24.7

TABLE 2

Results of Viscosimetric Tests

Dye	After 30 days of insolation			Cuprammonium viscosity after 10 days of insolation
	silver number	iodine number	loss of tensile strength (%)	
№ 1	36.6	7.4	38.5	7.8
№ 2	37.6	7.8	43.0	5.6
№ 3	74.2	11.4	49.5	4.3
№ 4	89.2	15.4	60.6	4.0

Reproducibility of the test results. Fabric samples dyed by Dye No. 3 (after 10 days of insolation) and Dye No. 4 (after 30 days of insolation) were used; four determinations (two in each of two duplicate experiments) of silver number were made on these samples. The greatest variation between the results of 4 experiments was 6.8% in the first instance, and 5.9% in the second. In the main experiments deviations between duplicate experiments did not exceed 5-7%.

Silver numbers of samples dyed by Dye

Expt. No.	No. 3	No. 4
1	17.6	44.2
2	16.4	44.1
3	17.5	42.5
4	17.3	45.2

Effect of treatment in alkaline silver-thiosulfate solution on degradation of insolated fibers. Calico samples: 1) not insolated, not dyed and dyed by the photoactive Dye No. 3, and 2) insolated, not dyed and dyed by Dyes No. 1, 2 and 3, were treated at boiling in alkaline silver-thiosulfate solution for 3, 5, 7, 10, 20 and 30 minutes. The test results are given in Table 1 and in the diagram.

Tests by silver and iodine numbers, tensile strength and viscosity. Fabric specimens dyed by the inactive Dyes No. 1 and 2 and the active Dyes No. 3 and 4 were insolated for 30 days for determinations of the silver and iodine numbers and tensile strength, and for 10 days for the viscosity determinations.

The iodine numbers were determined by the method described by Kaverzneva et al. [11]. The tensile strength was determined by means of the Schopper dynamometer by the method described in GOST 3813-47, but with the test length modified, according to the recommendations of the Central Scientific Research Institute of the Cotton Industry, to "zero length," with the dynamometer jaws close up to each other. The viscosity determinations were performed in the Central Scientific Research Institute of the Cotton Industry by A. V. Surovoya's group. The results of the tests are given in Table 2.

SUMMARY

A method has been developed for quantitative determination of the degree of fiber damage, based on the ability of oxidized cellulose to reduce silver from silver-thiosulfate complex compounds.

The method can be used, with adequate sensitivity and accuracy, for comparative evaluation of the photoactive properties of vat dyes, including small differences between compounds similar in chemical structure.

LITERATURE CITED

- [1] C. M. Wittaker, *J. Soc. Dyers Col.* 51, 117 (1935).
- [2] A. Landolt, *Mell. Textilberichte*, 10, 533 (1929).
- [3] F. Scholefield and E. Goodyear, *Mell. Textilberichte*, 10, 867 (1929).
- [4] D. Ashton, S. Clibbens and M. Probert, *J. Soc. Dyers Col.* 65, 650 (1949).
- [5] A. Landolt, *Mell. Textilberichte*, 11, 937 (1930).
- [6] A. Landolt, *Mell. Textilberichte*, 14, 32 (1933).
- [7] Z. A. Rogovin and N. N. Shorygina, *Chemistry of Cellulose and Associated Substances [In Russian]* (Goskhimizdat, 1953) pp. 40-45.
- [8] M. R. Fox, *J. Soc. Dyers Col.* 65, 508 (1949).
- [9] I. L. Khmel'nitskaya and Ya. L. Zil'berman, *J. Gen. Chem.* 11, 1190 (1941).
- [10] H. Baines, *J. Chem. Soc.* 2763 (1929).
- [11] E. D. Kaverzneva, V. L. Ivanov and A. S. Salova, *Bull. Acad. Sci. USSR, Div. Chem. Sci.* 751-761 (1952). *

Received January 20, 1958

*Original Russian pagination. See C.B. Translation.

DYEING OF NITRON FIBERS BY BASIC DYES*

E. S. Roskin, A. A. Kharkharov and A. L. Shapirov

(S. M. Kirov Textile Institute, Leningrad)

It is known that basic dyes give very bright dyeings on protein and cellulose fibers, but their fastness to light, weathering, and wet treatments is low [1]. A distinctive feature of polyacrylonitrile fibers dyed by these dyes is their higher fastness [2-5]. For example, the dye Brilliant Green gave satisfactory fastness to weathering and good fastness to wet treatments on nitron [6].

The high fastness of basic dyes on polyacrylonitrile fibers, in conjunction with their exceptional brightness, makes them especially interesting for dyeing these fibers.

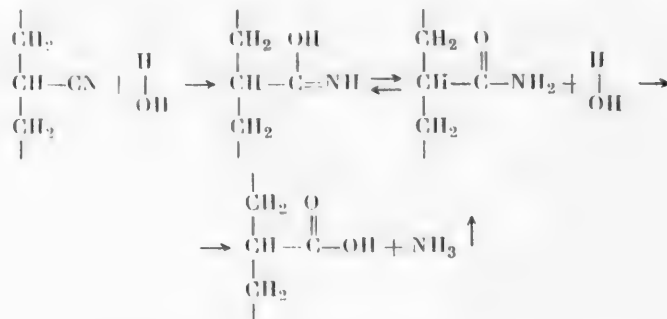
The present investigation was concerned with the influence of time, temperature, concentration, and salt and acid additions on the diffusion of direct dyes into polyacrylonitrile fibers; the aim was to formulate recommendations for practical dyeing. The dyeing was performed in presence of acetic acid, sodium acetate, and OP-10, which is both a surface-active and a dispersing agent.

We found that nitron fiber, which is known to have a high zeta potential [7], adsorbs the colored cations of the investigated dye very intensively. A nitron sample immersed in a boiling bath containing this dye was colored fairly intensively after only 1 minute.

It is possible that the dye combines chemically with the carboxyl groups in the fiber, formed by saponification of nitrile groups in the dyebath or already formed during polymerization of acrylonitrile. Salt formation is accompanied by sorption of the dye by the fiber. The presence of carboxyl groups in fibers may be demonstrated qualitatively by their coloration by weakly alkaline solutions of the colorless carbinol of Brilliant Green. This coloration is produced in nitron fibers (Table 1).

Another qualitative reaction which confirms the presence of carboxyl groups in nitron polyacrylonitrile fiber is the action of a yellow solution of hydrazone-9-acridyl aldehyde base, which colors it the violet color of the salt, as in the case of natural silk.

In the light of the above considerations, the following mechanism may be postulated, in conformity with the theory of A. E. Poral-Koshits, for the interaction of basic dyes with polyacrylonitrile fibers



*Communication IV in the series on the technology of nitron (nitrilon) polyacrylonitrile fibers.

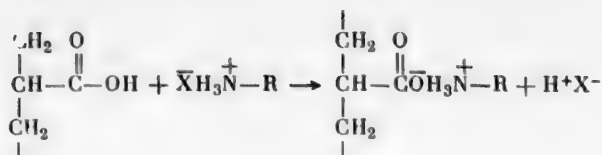


TABLE 1

Fiber	Color produced by alkaline solution of colorless carbinol of Brilliant Green
Silk	Intense green
Wool	Green
Nitron	Pale green
Cuprammonium yarn	Slightly tinted
Cotton	Not colored

TABLE 2*

Dyeing time (min)	Amount of dye adsorbed (% of amount taken)
2	46.6
5	48.5
15	51.4
30	54.7
60	56.0
120	57.4
180	57.4
240	57.4
300	57.4

TABLE 3**

Dyebath ratio	Amount of dye adsorbed by nitron (% of amount taken)
1/30	55.2
1/50	51.8
1/100	49.0
1/150	43.8
1/200	37.8

TABLE 4***

Dyeing temperature (deg)	Amount of dye adsorbed (% of amount taken)
20	31.0
30	35.2
40	37.0
50	39.4
60	46.7
70	49.1
80	49.1
90	49.1
100	49.1

TABLE 5****

Dyeing temperature (deg)	Amount of dye adsorbed (% of amount taken)
20	29.5
30	30.5
40	31.5
50	33.4
60	36.3
70	39.1
80	39.4
90	39.4
100	39.4

TABLE 6*****

Amount of CH ₃ COONa added (% on fiber weight)	Amount of dye adsorbed (% of amount taken)
0	79.3
1	74.7
5	68.3
10	62.0
30	45.1
50	54.9
100	75.9

* 4.5% of dye on the fiber weight taken for the experiment.

** 2.65% of dye on the fiber weight taken for the experiment.

*** 2.16% of dye on the fiber weight taken for the experiment.

**** 6.1% of dye on the fiber weight taken for the experiment.

***** 5.3% of dye on the fiber weight taken for the experiment; pH without acetate; 3.4.

TABLE 7*

Amount of CH_3COONa added (% on fiber weight)	Amount of dye adsorbed (% of amount taken)
0	96.1
1	95.6
5	94.8
10	91.5
20	91.0
50	87.7
100	71.4
200	58.1

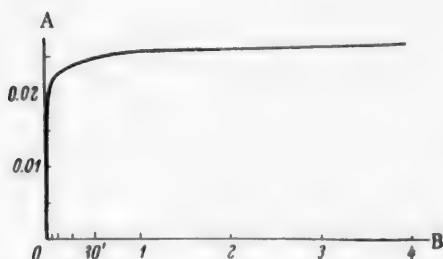


Fig. 1. Effect of dyeing time on the sorption of Brilliant Green: A) amount of dye (in g) taken up by 1 g of nitron; B) time (hours).

TABLE 8**

Bath pH	Amount of dye adsorbed (% of amount taken)
4.9	61.5
4.7	64.2
4.3	71.5
4.2	72.8
3.9	82.5
3.8	86.0
3.6	90.9
3.1	95.0

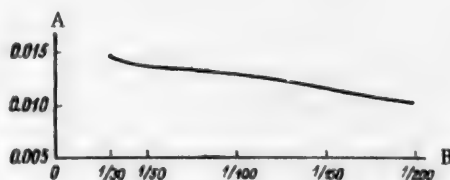


Fig. 2. Effect of dye concentration in the dyebath (liquor ratio) on the sorption of Brilliant Green: A) amount of dye (in g) taken up by 1 g of nitron; B) liquor ratio.

EXPERIMENTAL

The FÉK-M photoelectric colorimeter was used for determinations of the amounts of dye taken up by the fibers. All the determinations were performed with polyacrylonitrile fiber drawn to 300%.

The dyeing conditions were as follows. The nitron samples were immersed in a bath of the following composition (% on fiber weight): 5% dye, 10% glacial acetic acid, 0.5% sodium acetate, 1% OP-10; liquor ratio 1:50.

The dye liquor was brought to the boil during 20 minutes and kept at the boil for 1 hour. The dyed samples were washed in cold water, soap solution (3 g/liter) for 10 minutes at 80°, and cold water again.

The results are presented in Tables 2-8.

DISCUSSION OF RESULTS

Studies of the effect of dyeing time on the adsorption of the dye (Table 2 and Fig. 1) showed that most of the dye is taken up during the first few minutes. Thus, whereas in the first 2 minutes 46.6% of the total amount of dye is taken up, during the subsequent period up to equilibrium an additional 10% of the dye is taken up (the amount of dye taken was 4.5% on the fiber weight). Equilibrium was virtually reached after 1 hour of dyeing at 100°.

Because of the opposite charges present on the dye cations and nitron fibers respectively, it is possible that nearly all of the dye is adsorbed on the fiber surface immediately on immersion. In that case diffusion into the fiber may be very rapid, as the concentration gradient at the surface is high [8]. Subsequently electrostatic forces probably no longer take part in attraction of the dye, and sorption takes place as in the case of substantive dyes. In that case the diffusion rate must gradually diminish as the system approaches equilibrium, because the concentration and the concentration gradient of the dye in the bath both decrease.

* 5.85% of dye on the fiber weight taken for the experiment; pH without acetate, 3.4

** 5.85% of dye on the fiber weight taken for the experiment.

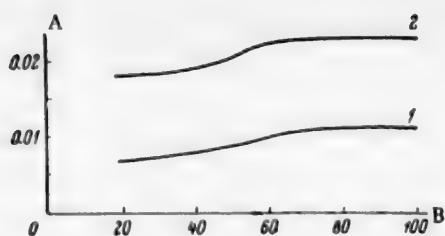


Fig. 3. Effect of temperature on the dyeing of nitron by Brilliant Green: A) amount of dye (in g) taken up by 1 g of nitron; B) temperature (deg); amount of dye (% on fiber weight): 1) 2; 2) 6.

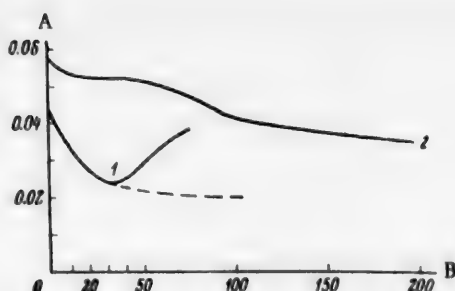


Fig. 4. Effect of added CH_3COONa on the sorption of Brilliant Green: A) amount of dye (in g) taken up by 1 g of nitron; B) amount of CH_3COONa (% on fiber weight); initial pH: 1) 3.4; 2) 2.9.

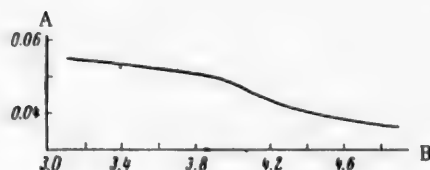


Fig. 5. Effect of dyebath pH on sorption of Brilliant Green: A) amount of dye (in g) taken up by 1 g of nitron; B) pH.

It follows from the foregoing that the rate of dyeing in this instance is determined mainly by forces of electrostatic attraction.

Variations of the dye concentration (Table 3, Fig. 2) have almost no effect on sorption of the dye. Thus, a 7-fold increase in the concentration of Brilliant Green increases the dye adsorption by only 17.4%. It was found in a parallel investigation that in the case of direct dyes a similar increase of concentration increases adsorption by about 700%. This example clearly demonstrates the difference in the nature of interaction of polyacrylonitrile fibers with basic and direct dyes respectively.

As stated earlier, the sorption of a basic dye is determined mainly by electrical attraction forces, and to a smaller extent by the rate of internal diffusion. It is known [8] that the latter slows down with decrease of the concentration and concentration gradient of the dye in the bath. Accordingly, increase of concentration and therefore of the concentration gradient of the dye in the bath must influence the less important factor determining sorption without producing any appreciable increase in the amount of dye taken up. On the other hand, increase of concentration decreases the number of dissociated molecules and thereby has a negative influence on the main cause of dye sorption.

However, as the solution is diluted the influence of concentration and concentration gradient on the rate of external diffusion becomes greater than the influence of dissociation on electrical attraction at the same dilution. Therefore there is a slow decrease of adsorption with decreasing concentration of the solution: 55.2% of the dye is adsorbed at bath ratio 1:30 and 37.8% at bath ratio 1:200.

When polyacrylonitrile fiber of low degree of orientation is dyed by basic dyes, increase of temperature from 20° to the optimum level of 70° increases adsorption by only 10% (Tables 4, 5; Fig. 3), whereas if the same fiber is dyed by direct dyes the same temperature increase raises adsorption by 400%.

Rise of temperature favors disaggregation of the molecules and increases their rate of thermal motion, thereby influencing the rate of external diffusion, which is a factor of secondary significance in this case.

The variation of adsorption of Brilliant Green with the amount of sodium acetate added (Tables 6, 7;

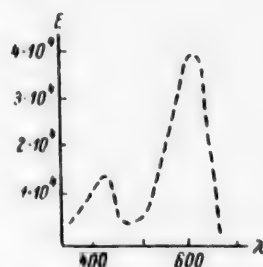


Fig. 6. Absorption spectrum of Brilliant Green in water.

Fig. 4) indicates that the amount of dye taken up decreases with increasing salt concentration.

A possible explanation of this is that the fiber charge is diminished as the result of adsorption of sodium cations. Therefore the dye cations are attracted less strongly to the fiber, and this, of course, affects the dyeing rate.

Thus, introduction of sodium acetate influences the main factor determining the rate of dyeing of polyacrylonitrile fibers by basic dyes, i.e., electrical interaction between the fiber and the dye cations. That is why increase of the amount of salt in the dyebath to 30% on the fiber weight (Table 7, Fig. 4) lowers sorption by nearly 35%. With increase of the salt concentration from 30 to 100% on the fiber weight the amount of dye taken up appears to increase. However, this apparent increase of adsorption is due to formation of the carbinol, which gives a colorless solution.

The effect of the dyebath pH on sorption of the basic dye by nitron is given in Table 8 and Fig. 5. Adsorption of the dye increases with increasing acidity.

An aqueous solution of Brilliant Green has a bluish-green color, which changes to yellowish-green with decrease of pH.

The absorption curve of basic Brilliant Green, which is a monoacid salt, is depicted in Fig. 6. The second maximum on the absorption curve is, as is known, due to the presence of a small amount of the diacid salt in aqueous solutions of Brilliant Green; the absorption maximum of this salt lies in a shorter wave-length region.

Addition of acid to the dye solution evidently increases the amount of diacid salt, and the color of the solution changes from bluish-green to yellowish-green. The cations of the diacid salt of Brilliant Green have a higher charge than the corresponding cations of the monoacid salt. Therefore forces of electrical attraction play a greater part in presence of bivalent cations, and addition of acid (decrease of pH) has a determining influence on the sorption of basic dyes by polyacrylonitrile fibers. It is possible that decrease of pH favors saponification of a larger number of nitrile groups to carboxyls, thereby increasing the amount of dye chemically combined.

SUMMARY

1. The effects of temperature, dyeing time, additions of acid and salt, and concentration and amount of dye in the dyebath on the sorption of Brilliant Green were studied; the hypothesis is put forward that the rate of dyeing of polyacrylonitrile fiber by basic dyes is determined mainly by forces of electrical attraction between the negatively-charged fibers and the dye cations.

2. An attempt is made to explain the mechanism of interaction between polyacrylonitrile fibers and basic dyes.

LITERATURE CITED

- [1] Technical Specifications, Ministry of Chemical Industry USSR, No. 2379-50 [In Russian].
- [2] P. Weyrich, *Das Färben und gleichen der Textilfasern in Apparaten*, B. (1956).
- [3] R. I. Stevens, *Am. Dyestuff Rep.* 13, 409-411 (1954).
- [4] D. I. Crawford, *Canad. Text. Journ.* 61-70 (1954).
- [5] E. Szlosberg, *Am. Dyestuff Rep.* 431-434 (1953).
- [6] E. S. Roskin, *J. Appl. Chem.* 30, No. 1, 124 (1957); 30, No. 7, 1030 (1957).
- [7] T. Vickerstaff, *Physical Chemistry of Dyeing* (IL, 1956) [Russian translation].
- [8] P. V. Moryganov and B. I. Mel'nikov, Note in Vickerstaff's book: *Physical Chemistry of Dyeing* [Russian translation] (1956).

Received January 16, 1958

STABILIZATION OF POLYVINYL CHLORIDE BY SALTS OF STEARIC AND EPOXYSTEARIC ACIDS *

D. M. Yanovskii, A. A. Berlin, E. N. Zil'berman
and N. A. Rybakova

Salts of lead, barium, and other metals are often used for stabilization of polyvinyl chloride [1]. Compounds containing epoxy groups are also effective stabilizers [2, 3]. It has been shown [3, 4] that by the use of mixtures of epoxy compounds with certain salts, such as soaps, thermal stability can be increased to a greater extent than by the use of these stabilizers separately. The patent literature [5] contains references to the use of lead, cadmium, and certain other salts of epoxystearic acid. However, the properties of these compounds have not been described. The literature contains no reports of systematic investigations of the stabilizing effects of stearates, which are widely used in industry, or of epoxystearates. Investigation of the stabilizing action of the latter is of special theoretical and practical interest, as owing to the presence of metal ions and oxirane oxygens in their molecules these compounds may be effective stabilizers for halogenated polymers.

TABLE 1

Effects of Different Stabilizers on Thermal Stability of Polyvinyl Chloride; Amount of Stabilizer Added - 2.5 millimoles per 100 g of polymer

Stabilizers	Stearates		Epoxystearates	
	decomposition temperature (deg)	thermal stability at 175° (min)	decomposition temperature (deg)	thermal stability at 175° (min)
Salts of:				
lead	210	30	216	35
barium	192	25	215	32
calcium	190	13	203	15
cadmium	180	13	195	15
zinc	175	10	180	12
Free acids*	165	8	191	13

* The amounts of stearic and epoxystearic acids added were 5 millimoles per 100 g of polymer.

In continuation of our systematic studies of the relationship between chemical structure and stabilizing effects [3], the present investigation was concerned with the effects of stearates and epoxystearates (the latter synthesized by us) of calcium, barium, cadmium, lead, and zinc on the thermal stability of polyvinyl chloride. This was studied by determinations of the temperature of the start of dehydrochlorination of polyvinyl chloride,

*Communication II in the series on intermediates and auxiliaries in polymer technology.

TABLE 2

Effect of Mixtures of Stearates and Epoxystearates on Thermal Stability of Polyvinyl Chloride

Stabilizer*	Decomposition temperature (deg)				Thermal stability (min)		
	calculated	found	difference between calculated and experimental values	with addition of oxalic acid, 0.75% on weight of polymer	calculated	found	difference between calculated and experimental values
Stearates:							
lead and barium	201	206	+ 5	206.5	27.5	29	+1.5
lead and calcium	200	202	+ 2	202	21.5	24	+2.5
lead and cadmium	195	201	+ 6	201	23.5	26	+2.5
barium and cadmium	186	189	+ 3	188	21.5	23	+1.5
Epoxystearates:							
lead and barium	215.5	205	-10.5	210	33.5	28	-5.5
lead and calcium	209.5	199	-10.5	205	25	20	-5
lead and cadmium	205	195	-10	201	25	24	-1
barium and cadmium	205	197.5	-7.5	201.5	23.5	21	-2.5

*The stabilizer mixtures consisted of equal amounts (1.25 millimole of each per 100 g of polymer) of the corresponding salts.

its stability at 175° (Table 1), and kinetics of dehydrochlorination of polyvinyl chloride (Fig. 1 and 2) in presence of these compounds. The stabilization of polyvinyl chloride by mixtures of equivalent amounts of different stearates or epoxystearates of barium, cadmium, lead, and calcium was also studied (Table 2, Fig. 3 and 4). To demonstrate the synergic effect, Table 2 also contains data calculated for stabilizer mixtures on the assumption that the effects of the individual components of these mixtures are additive. In the case of mixtures containing zinc salts it was of interest to study the stabilizing effects of different compositions.

All the investigated epoxystearates were more effective stabilizers than the corresponding stearates. The cations of the stearates and epoxystearates studied form the following series in order of diminishing effects on the decomposition temperature and thermal stability of polyvinyl chloride and the kinetics of hydrogen chloride evolution on heating: $Pb > Ba > Ca > Cd \gg Zn$.

The stabilizing effects of epoxystearates (Table 1) are almost the same as the effects produced by the action of mixtures of equivalent amounts of epoxystearic acid and stearates of the corresponding metals. Zinc stearate and epoxystearate raise the decomposition temperature and thermal stability of polyvinyl chloride to some extent, but the rate of evolution of free hydrogen chloride is considerably higher in presence of these salts than in presence of the other stearates and epoxystearates investigated (Fig. 1 and 2).

A synergic effect is observed with the use of binary mixtures of lead, barium, calcium, and cadmium stearates. This is confirmed by the fact that the experimental values of decomposition temperature and thermal stability of polyvinyl chloride with addition of stearate mixtures are higher than the values calculated on the assumption that the effects of the stabilizer pairs are additive (Table 2). Moreover the curves representing the kinetics of HCl evolution (Fig. 3) are shifted to the right, when mixed stearates of lead, barium, and cadmium are used, relative to the curves (not shown in Fig. 3) calculated on the same assumption. A similar effect is observed with the use of stearate mixtures containing the calcium salts.

According to patent data [6], the existence of a synergic effect is also assumed when epoxystearate mixtures are used. Our results indicate that an effect the reverse of synergic is observed with the use of binary mixtures of equimolar amounts of lead, barium, calcium, and cadmium epoxystearates. With the mixtures tested the decomposition temperature was lower by 7-15° and thermal stability less by 1-5 minutes than the calculated average values for the respective stabilizer pairs (Table 2). A similar result was obtained in studies of the kinetics of HCl evolution from polyvinyl chloride containing mixtures of epoxystearates. The kinetic curves for

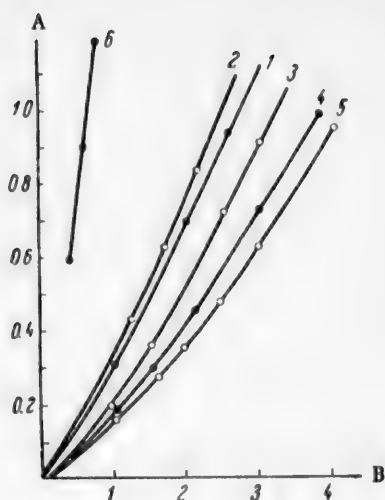


Fig. 1. Kinetics of hydrogen chloride evolution at 175° from polyvinyl chloride containing stearates: A) amount of HCl evolved (% of polymer weight); B) time of heating (hours); stearates used: 1) without stabilizer; 2) Cd; 3) Ca; 4) Ba; 5) Pb; 6) Zn.

the thermal degradation of polyvinyl chloride stabilized by binary mixtures of equimolar amounts of epoxystearates (Fig. 4) lie to the left of the curves (not shown in the figure) calculated on the assumption that the stabilizing effects in the salt pairs are additive.

The probable cause of the reverse synergic effect observed in this case is copolymerization of epoxystearates during heat treatment of polyvinyl chloride. Copolymerization of epoxystearates is catalyzed by hydrogen ions [7], which appear in the system as the result of dehydrochlorination, and the rate of this process is primarily determined by the more reactive epoxy compound. Conversion of monomeric epoxy stabilizers into polymers diminishes the amount of epoxy groups and therefore lowers the thermal stability of the mixture. To confirm this hypothesis, the effect of adding small amounts of oxalic acid to epoxystearate mixtures on the decomposition temperature of polyvinyl chloride was investigated, because it is known that small amounts of oxalic acid inhibit opening of the epoxy ring and thereby partially prevent polymerization of epoxy compounds. It follows from the data in Table 2 that addition of 0.75% of oxalic acid to mixtures of epoxystearates raises the decomposition temperature of polyvinyl chloride by 4-6°, whereas in corresponding experiments with stearates oxalic acid had no influence on the thermal stability of the polymer.

The effects of additions of zinc stearate and epoxystearate to different salts of the same acids are of considerable interest. Table 3 shows that when small amounts of zinc stearate are added to the stearates of different metals there is some increase in the thermal stability of polyvinyl chloride, but if the amount of zinc stearate is increased above 0.1 millimole per 100 g of polymer the thermal stability of the polymer is lowered considerably. Additions of zinc stearate have an analogous effect on the kinetics of HCl evolution when polyvinyl chloride is heated (Fig. 5). Additions of zinc epoxystearate to other epoxystearates, even at a concentration of 0.1 millimole, lower the stabilizing effects of these epoxystearates (Table 3, Fig. 6).

It was thought that the cause of the decrease in thermal stability of polyvinyl chloride on addition of zinc stearate and epoxystearate was the initiating effect on dehydrochlorination of the resin, exerted by the zinc chloride formed by the interaction of hydrogen chloride with stabilizers containing zinc. This hypothesis was

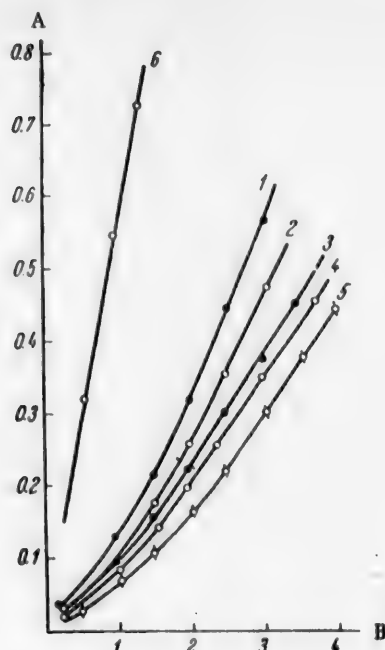


Fig. 2. Kinetics of hydrogen chloride evolution at 175° from polyvinyl chloride containing epoxystearates: A) amount of HCl evolved (% of polymer weight); B) time of heating (hours); epoxystearates used: 1) without stabilizer; 2) Cd; 3) Ca; 4) Ba; 5) Pb; 6) Zn.

TABLE 3

Effects of Additions of Zinc Stearate, Epoxystearate, and Chloride on the Properties of Polyvinyl Chloride Stabilized by Lead, Barium, Calcium, or Cadmium Salts

Stabilizers*	Millimoles added per 100 g of polymer					
	0.1		0.3		0.5	
	decom- position tempera- ture (deg)	thermal stability at 175° (min)	decom- position tempera- ture (deg)	thermal stability at 175° (min)	decom- position tempera- ture (deg)	thermal stability at 175° (min)
Zinc stearate						
Stearates of:						
lead	213	34	205.5	29	202	25
barium	195	28	190	22	185	18
calcium	193	15	191	13.5	189	11.5
cadmium	182	16	176.5	13	173	11
Zinc epoxystearate						
Barium epoxystearate . . .	203	28	191	23	184	17
Zinc chloride						
Without stabilizer	159	—	148	—	—	—
Lead stearate	199	—	192	—	—	—
Lead epoxystearate . . .	202	—	197	—	—	—

*2.5 millimoles per 100 g of polymer.

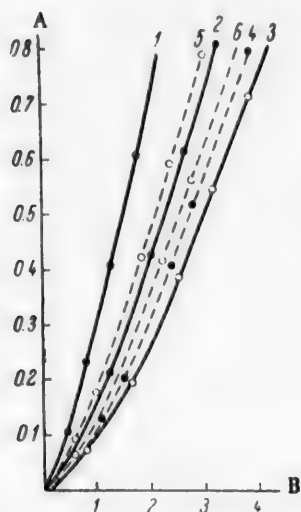


Fig. 3. Kinetics of hydrogen chloride evolution at 175° from polyvinyl chloride containing stearate mixtures: A) amount of HCl evolved (% of polymer weight); B) time of heating (hours); stearate mixtures: 1) Cd; 2) Ba; 3) Pb; 4) Ba and Pb; 5) Ba and Cd; 6) Pb and Cd.

confirmed by experiments on determination of the decomposition temperature of stabilized and nonstabilized polyvinyl chloride in presence of small amounts of zinc chloride (Table 3). Studies of the decomposition kinetics of polyvinyl chloride under such conditions also showed that $ZnCl_2$ catalyzes the process. When polyvinyl chloride is stabilized by zinc salts the adverse effect of $ZnCl_2$ becomes especially pronounced after all the added salt has been expended in combining with the hydrogen chloride, and zinc remains in the system only as the chloride.

EXPERIMENTAL

Polyvinyl chloride resin of PF "special" grade, previously treated as in the earlier investigation [3], was used in the experiments. The original resin without stabilizers had a decomposition temperature of 166° and a thermal stability of 9 minutes. Curves for the dehydrochlorination rate of this resin at 175° are given in Fig. 1 and 2. Methods used for investigation of the stabilized resin were described earlier [3].

In order to obtain comparable data, equivalent amounts of stabilizers per 100 g of polymer were taken in all the experiments; 2.5 millimoles each of lead, barium, or other salts or, 5 meq of oxirane oxygen, while, when mixed stabilizers were used, 1.25 millimole

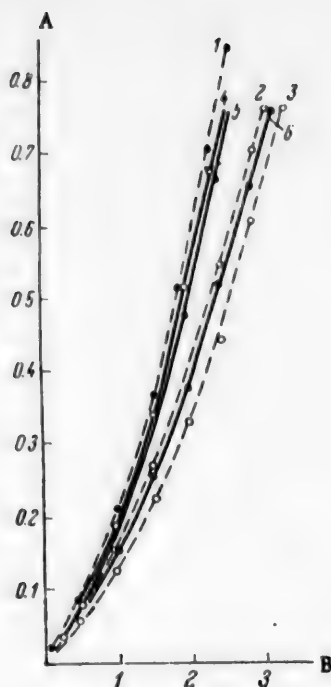


Fig. 4. Kinetics of hydrogen chloride evolution at 175° from polyvinyl chloride containing epoxystearate mixtures: A) amount of HCl evolved (% of polymer weight); B) time of heating (hours); epoxystearate mixtures: 1) Cd; 2) Ba; 3) Pb; 4) Ba and Cd; 5) Pb and Cd; 6) Pb and Ba.

TABLE 4

Analyses and Melting Points of Salts of *Cis*-9,10-epoxystearic Acid

Cis-9,10-epoxystearate	Metal content (%)		Melting point (deg)
	calculated	found	
Lead	25.86	25.00	96-97
Barium	18.78	18.57	188
Calcium	6.32	6.23	112
Cadmium	15.92	15.72	105
Zinc	9.92	10.05	101

Found % Pb 25.0. $C_{36}H_{60}O_8$. Calculated % Pb 25.86.

Cadmium, calcium, barium, and zinc *cis*-9,10-epoxystearates were prepared similarly from the corresponding chlorides. Analytical data and melting points of these salts are given in Table 4.

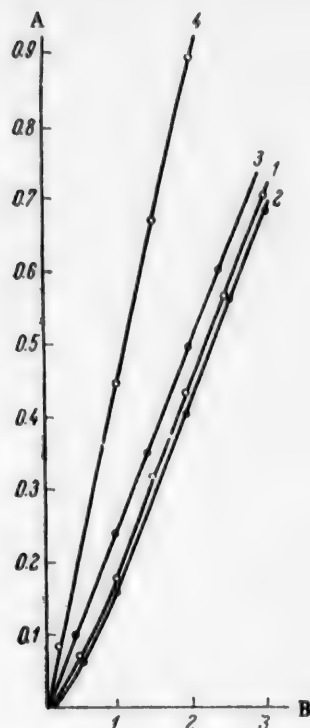


Fig. 5. Kinetics of hydrogen chloride evolution at 175° from polyvinyl chloride stabilized by Ba stearate (2.5 millimoles per 100 g of polymer) with different amounts of Zn stearate: A) amount of HCl evolved (% of polymer weight); B) time of heating (hours); amounts of Zn salt added (millimoles): 1) no addition; 2) 0.1; 3) 0.3; 4) 0.5.

of each salt was usually taken, apart from the experiments with additions of zinc salts (Table 3).

Preparation of salts of *cis*-9,10-epoxystearic acid.

Epoxidation of oleic acid by the action of peracetic acid yielded *cis*-9,10-epoxystearic acid [8], m.p. 58-59° (from acetone), containing 5.36% of oxirane oxygen. 10 g of epoxystearic acid was dissolved in 134 ml of 1% caustic soda, and a solution of 5.6 g of lead nitrate in 30 ml of water was added to this solution at 30-35° with stirring. The precipitate was filtered off, washed with water, and dried. The yield was 13 g of salt, m.p. 96-97°.

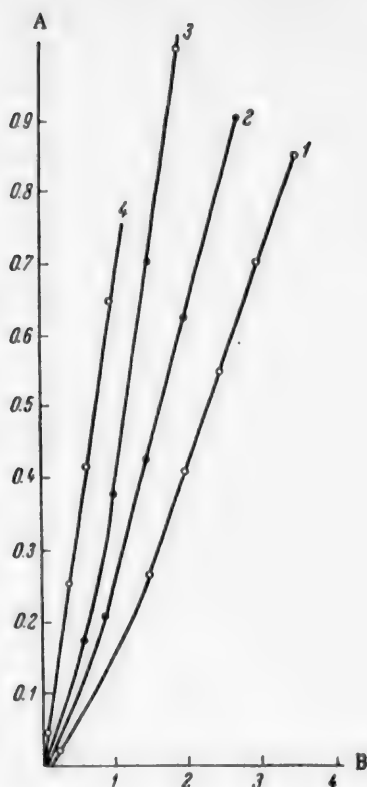


Fig. 6. Kinetics of hydrogen chloride evolution at 175° from polyvinyl chloride stabilized by Ba epoxystearate (2.5 millimoles per 100 g of polymer) with different amounts of Zn epoxystearate: A) amount of HCl liberated (% of polymer weight); B) time of heating (hours); amounts of Zn salt added (millimoles): 1) no addition; 2) 0.1; 3) 0.3; 4) 0.5.

SUMMARY

1. It was shown in a study of the stabilizing effects of Pb, Ba, Ca, Cd and Zn stearates and epoxystearates and their mixtures that epoxystearates are more effective stabilizers than the stearates of the corresponding metals.

2. Mixtures of stearates exhibit a synergic effect, whereas the reverse effect is observed in mixtures of equimolar amounts of epoxystearates.

3. Additions of small amounts of zinc stearate to Pb, Ba, Ca and Cd raise the stabilizing effect slightly; this effect diminishes with increasing contents of the zinc salt.

LITERATURE CITED

- [1] H. V. Smith, *Brit. Plast.* 27, 176 (1954).
- [2] E. S. Narracott, *Brit. Plast.* 24, 341 (1951).
- [3] A. A. Berlin, E. N. Zil'berman, N. A. Rybakova, A. M. Sharetskii and D. M. Yanovskii, *J. Appl. Chem.* 32, No. 4, 863 (1959).
- [4] R. E. Lally, *Paint and Varnish Prod.* 42, 10, 18 (1952).
- [5] F. P. Greenspan and R. J. Gall, U.S. Patent 2,684,353; *Chem. Abs.* 49,11321 (1955).
- [6] H. Murat and F. Higo, *Jap. Patent* 293 (1956); *Chem. Abs.* 51, 6219 (1957).
- [7] A. A. Berlin, in the book: *Advances in Polymer Chemistry and Technology, I* [In Russian] (Goskhimizdat, 1955) p. 67.
- [8] D. Swern, *J. Am. Chem. Soc.* 67, 412 (1945).

Received May 10, 1958

WATER-REPELLENT TREATMENT OF CELLULOSIC MATERIALS BY ORGANOSILICON COMPOUNDS*

M. G. Voronkov and N. V. Kalugin

The available water-repellent treatments for textile fabrics, based on paraffin-stearin emulsions and aluminum salts [1], are inadequate in their adherence to the fabrics. Such finishes have low fastness to laundering, chemical cleaning, and weathering. The combined water-repellent treatment for textiles commonly used in the USSR [1], which involves consecutive treatments with tanning agents, copper and chromium salts, paraffin-stearin emulsion, and aluminum salts, confers only temporary protection against the effects of sunlight, moisture, and microorganisms. As the result of the action of numerous factors (solar radiation, oxidation, abrasion, laundering, weathering, etc) the fabric gradually loses its protective properties.

We tested the durability of the protective effects of the combined treatment on No. 565 tenting under various climatic conditions in the USSR. It was found that the fabrics retain their water repellency for only 3-12 months of continuous use. For example, in the dry hot climatic conditions of Tashkent the fabric loses its water-proofness after 3-4 months; in Batumi, in hot humid conditions, after 4 months; in the Far East, after 6 months; in Western Siberia, after 12 months, etc.

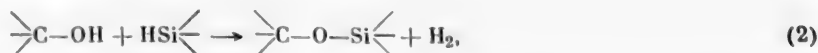
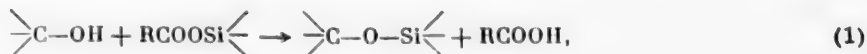
It should be noted that after losing its standard water repellency the fabric still remains hydrophobic for some time, but after 6-8 months restoration of the weatherproofness becomes imperative; this can be achieved by reimpregnation of the fabric in situ.

Our investigations [2-4] have shown that treatment of textile fabrics with organosilicon preparations such as polyalkyl hydrosiloxanes, alkyl acyloxysilanes, and polyalkyl siloxanates (alkyl siliconates) of certain metals in conjunction with impregnation by copper and chromium salts, results in water-repellent finishes which are resistant to weathering, repeated laundering, chemical cleaning, and biological attack.

In our opinion, the high serviceability of organosilicon water-repellent finishes on cellulosic fabrics is primarily due to chemical interaction of reactive functional groups in the monomeric and polymeric organosilicon compounds with hydroxyl groups in cellulose, with formation of C-O-Si linkages.**

Chemical combination between the organosilicon compounds and hydroxyl groups of cellulose takes place during heat treatment of the impregnated fabric. This reaction can also take place at room temperature (especially in presence of catalysts), but much more slowly, requiring weeks and even months for completion.

Our views are confirmed by investigations of model systems, which show that organosilicon compounds containing acyloxy groups [3, 6-9], hydrogen atoms [10-14], or chlorine [15-18] attached to silicon atoms readily react with various mono- and polyhydroxylic organic substances (including cellulose [15] and starch [16]) with formation of condensation products containing C-O-Si linkages, as follows:



*Communication VIII in the series on water-repellent treatment of materials by organosilicon compounds.

**It must be pointed out that some authors [5] hold other views on this subject.

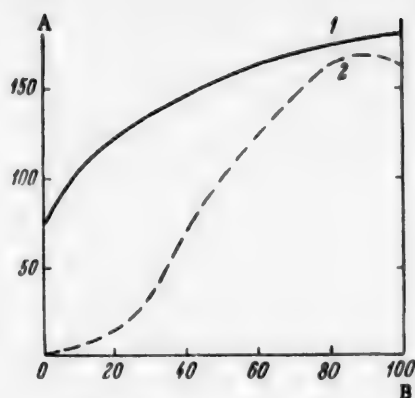


Fig. 1. Water repellency of cotton cloth treated with mixtures of $\text{RSi}(\text{OCOCH}_3)_3$ and $\text{R}_2\text{Si}(\text{OCOCH}_3)_2$ (from Davydova's data [4]): A) water repellency (mm H_2O); B) $\text{RSi}(\text{OCOCH}_3)_3$ content (%); radical R: 1) CH_3 ; 2) C_2H_5 .

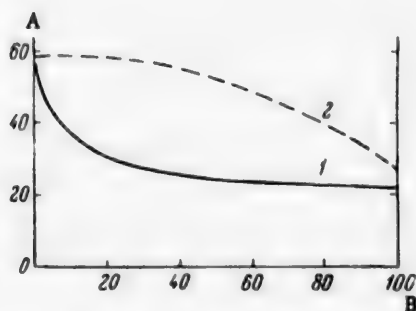
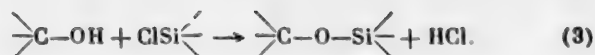
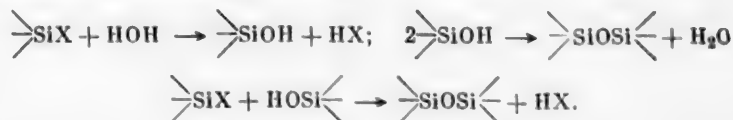


Fig. 2. Water imbibition of cotton cloth treated with mixtures of $\text{RSi}(\text{OCOCH}_3)_3$ and $\text{R}_2\text{Si}(\text{OCOCH}_3)_2$ (from Davydova's data [4]): A) water imbibition (%); B) $\text{RSi}(\text{OCOCH}_3)_3$ content (%); radical R: 1) CH_3 ; 2) C_2H_5 .

materials. Gray cotton and linen fabrics in which the cellulose hydroxyl groups are shielded by accompanying substances (pectins, fats, waxes, resins, etc) are much more difficult to treat, and the coatings formed are less stable.

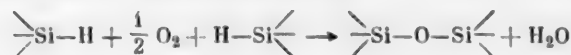
All the foregoing considerations confirm our theoretical views on the chemical nature of the bonding between water-repellent organosilicon coatings and materials containing hydroxyl groups.

An organosilicon compound containing a reactive functional group X attached to the silicon atom ($\text{X} = \text{H}$, OCOR , OR , etc) can also react with water as follows:



As the result of these reactions between the organosilicon compounds and cellulose in the fabric fibers, a chemically-bound water-repellent film is formed on the latter. The hydrophobic properties of this film are determined by orientation of the hydrocarbon radicals of the organosilicon compound in a direction opposite to the fiber surface. In addition, the hydrophobic properties of the fabric, and in particular its decreased moisture absorption, are also due to disappearance of the hydrophilic hydroxyl groups in cellulose as the result of the reaction,* and to shielding of these groups which results from the formation of spatial structures when the cellulose chains are cross linked by the organosilicon molecules. Formation of spatial structures also prevents mutual separation of the cellulose chains and, consequently, penetration of moisture between them.

The existing view [5] that water-repellent polyalkyl hydrosiloxane films are formed by oxidation of Si-H bonds followed by cross linking of the polysiloxane chains



is quite unfounded. On the one hand, we have shown that water-proofing of materials containing OH groups (including cellulose) by the action of polyalkyl hydrosiloxanes proceeds just as successfully in total absence of oxygen or any other oxidizing agents.

On the other hand, we have shown that salts of zinc [11, 13, 14], cadmium, mercury, cobalt, and nickel [11] (for example, their acetates or chlorides), which catalyze reaction (2), are also good catalysts for the water-repellent treatment of cellulosic fabrics and paper [19].

Finally, we have shown that organosilicon polymers which do not contain reactive functional groups and are therefore unable to react chemically with cellulose do not give stable water-repellent coatings on textile fabrics.

The fact that water-repellent organosilicon coatings are stable only on scoured and bleached fabrics also provides evidence in favor of chemical bonding of such coatings by cellulosic

*When acyloxy silanes are used for the treatment, the hydroxyl groups in cellulose are also acetylated.

Results of Chemical Analysis of Fabrics Given Combined Impregnation Treatments,
Before and After Use

Variant No. *	Before use (%)		After 5 months of use in Leningrad (%)		Loss after use (%)	
	Cu	Cr ₂ O ₃	Cu	Cr ₂ O ₃	Cu	Cr ₂ O ₃
Ordinary waterproofed**	0.306	0.128	0.116	0.096	62	25
1	0.498	0.621	0.252	0.487	49	22
2	0.318	0.436	0.228	0.435	28	0.2
4	0.308	0.555	0.229	0.352	26	37
6	0.329	0.538	0.221	0.472	33	12
8	0.266	0.437	0.163	0.400	39	9
10	0.281	0.471	0.229	0.415	18	12
12	0.268	0.572	0.250	0.441	7	23
14	0.252	0.581	0.227	0.471	10	19
16	0.282	0.395	0.189	0.382	33	3
18	0.315	0.397	0.213	0.370	32	7
21	0.437	0.429	0.244	0.377	44	14
22	0.357	0.440	0.214	0.402	20	9
MSN on gray fabric	0.293	0.359	0.239	0.325	18	9
MSN on scoured fabric	0.298	0.407	0.227	0.357	24	12
EN-1 on gray fabric	0.358	0.378	0.344	0.369	39	2
EN-1 on scoured fabric	0.318	0.393	0.268	0.336	15	14

Such reactions are generally undesirable in the waterproofing process, as they prevent chemical reaction of the coating with the hydroxyl groups of the treated material by reactions (1) and (2). In particular, this is confirmed by the fact that when textile fabrics are treated with aqueous emulsions, and especially aqueous solutions of organosilicon preparations, the water-repellent coatings formed are inferior in water repellency, water absorption, and stability to coatings formed by treatment with solutions of the same preparations in inert organic solvents.

At the same time, water present on the treated material in the form of a multimolecular adsorbed film which is not removed on heating to 100-150°, may play a positive role by causing condensation of the organosilicon polymer chains by formation of siloxane cross links. This condensation helps to attach the polymer film around the fiber.

It should be noted that materials treated with trifunctional organosilicon monomers of the type $RSiX_3$, but not with polymers of the type $[R(X)SiO]_n$, become harsher. The explanation is that these monomers form hard, inelastic space polymers. Difunctional monomers of the type R_2SiX_2 [or polymers of the type $(R_2SiO)_n$] do not confer harshness on the treated materials, but do not make them water-repellent either. This is because monomers of the R_2SiX_2 type form on hydrolysis (and in the case of $X = RCOO$ also on pyrolysis) cyclic and linear $(R_2SiO)_n$ molecules which cannot combine with cellulose or with each other. Because of this the cellulose fibers do not become surrounded by continuous films of the organosilicon polymer. However, if mixtures of tri- and difunctional monomers are used, soft water-repellent fabrics with good water-repellency and imbibition characteristics can be obtained (Figs. 1 and 2).

We found that when fabrics are treated with waterproofing organosilicon preparations the latter combine readily with copper and chromium salts to form very stable compounds which persist for a long time in fabrics used in the open air. The results of chemical analyses of No. 565 tenting fabric treated by the combined process and then water proofed by means of organosilicon preparations are given in the table. It is seen that the losses of copper and chromium from a control specimen of water-repellent fabric treated by the usual combined impregnation method were 62 and 25% respectively over a period of five months. In all the variants of the combined impregnation process with the use of organosilicon compounds A-4 (Variants 1-22), MSN, and EN-1,

*The treatment procedures were described previously [2].

**Fabric treated by the usual combined impregnation process (consecutive treatments with tanning agent, copper and chromium salts, paraffin-stearin emulsion, and aluminum acetate).

the copper losses were from 7 to 49%, and chromium losses from 0.2 to 23%; the variations were probably caused by differences in the treatment procedure.

SUMMARY

The nature of the bonding between water-repellent organosilicon coatings and cellulosic fabrics has been studied and it was shown that water-repellent treatment increases the stability of the copper-chromium impregnation treatments which protect the fabrics against the destructive effects of light and microorganisms.

LITERATURE CITED

- [1] P. A. Simigin, M. N. Zusman and F. I. Raikhlin, *Protective Treatments for Textile Materials* [In Russian] (State Light Industry Press, Moscow, 1957); H. Frotcher, *Chemie und physikalische Chemie der Textilhilfsmittel*, Berlin (1955).
- [2] N. V. Kalugin and M. G. Voronkov, *J. Appl. Chem.* 31, 1390 (1958);* in the book: *Chemistry and Practical Applications of Organosilicon Compounds* [In Russian] (Central Office of Technical Information, Leningrad Council of National Economy, 1958) 4, 54.
- [3] M. G. Voronkov and B. N. Dolgov, *Nature* 5, 22 (1954); *J. Leningrad Univ.* 5, 185 (1954).
- [4] V. P. Davydova, *Candidate's Dissertation* [In Russian] (Leningrad, 1958).
- [5] F. Fortress, *Ind. Eng. Ch.* 46, 2325 (1954).
- [6] B. N. Dolgov, V. P. Davydova and M. G. Voronkov, *J. Gen. Chem.* 27, 921, 1593 (1957)*.
- [7] M. G. Voronkov, V. P. Davydova and B. N. Dolgov, *Bull. Acad. Sci. USSR, Div. Chem. Sci.* 698 (1958)*.
- [8] V. P. Davydova and M. G. Voronkov, *J. Gen. Chem.* 28, 1879 (1958)*.
- [9] V. P. Davydova, M. G. Voronkov and B. N. Dolgov, in the book: *Chemistry and Practical Applications of Organosilicon Compounds* [In Russian] (Central Office of Technical Information, Leningrad Council of National Economy, 1958) 1, 204.
- [10] B. N. Dolgov, N. P. Kharitonov and M. G. Voronkov, *J. Gen. Chem.* 24, 1178 (1954)*.
- [11] B. N. Dolgov, N. P. Kharitonov, N. E. Glushkova and Yu. I. Khudobin, *J. Gen. Chem.* 28, 2710 (1958); • *Bull. Acad. Sci. USSR, Div. Chem. Sci.* 113 (1958) •.
- [12] B. N. Dolgov, N. P. Kharitonov and T. V. Tsukshverd, *J. Gen. Chem.* 28, 2714 (1958)*.
- [13] S. Nitsche, *Z. ang. Ch.* 63, 490 (1951).
- [14] M. G. Voronkov and V. N. Zgonnik, *J. Gen. Chem.* 27, 1479 (1957)*.
- [15] H. A. Schugten, I. W. Weaver, and L. D. Reid, *J. Am. Chem. Soc.* 70, 1919 (1948).
- [16] K. W. Kerr and K. C. Hobbs, *Ind. Eng. Ch.* 45, 2542 (1953).
- [17] F. A. Henglein and Makrom, *Chem.* 18-19, 102 (1956); 21, 59 (1956); 24, 1 (1957).
- [18] R. Schwarz, E. Baronetzky and K. Schoelln, *Z. ang. Chem.* 68, 335 (1956).
- [19] N. A. Afonchikov, G. V. Kolobova, P. N. Mikhailov and M. G. Voronkov, *J. Appl. Chem.* 32, 445 (1959)*; in the book: *Chemistry and Practical Applications of Organosilicon Compounds* [In Russian] (Central Office of Technical Information, Leningrad Council of National Economy, 1958) 4, 73.

Received December 27, 1958

*Original Russian pagination. See C.B. Translation.

EFFECTS OF VARIOUS ALDEHYDES ON THE BEHAVIOR OF GLUCOSE IN SULFITE COOKING

S. A. Sapotnitskii and A. G. Moskaleva

Sugars added to cold bisulfite solutions or sulfite liquor combine with bisulfite to form α -hydroxysulfonic acids and lose optical activity in direct proportion to the extent of such combination [1, 2].

When other aldehydes, forming bisulfite compounds of a lower degree of dissociation than those formed with the sugars, were added to such sugar-bisulfite solutions, the sugars were liberated and their optical activity was restored [2]. It was immaterial whether the added aldehydes were aromatic or aliphatic.

When glucose was cooked by the sulfite process in presence of acetaldehyde, the degree of decomposition of the sugar was decreased [3]. This suggested that under the conditions of the sulfite process the presence of acetaldehyde, which forms an almost undissociated bisulfite compound [4], in the cooking liquor prevents combination of sugars with bisulfite and their oxidation to aldonic acids in accordance with H \ddot{a} gglund's hypothetical reaction [5].

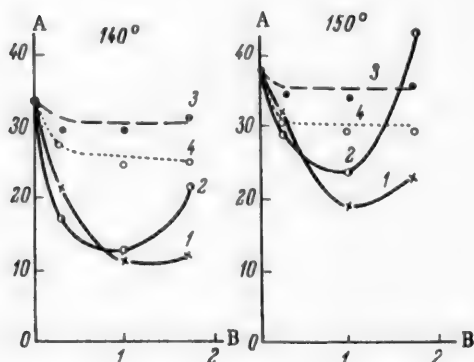


Fig. 1. Effect of aldehyde contents on decomposition of glucose in sulfite cooking: A) amount of glucose decomposed (%); B) amount of aldehyde (moles/mole NaOH); aldehydes: 1) acetaldehyde; 2) formaldehyde; 3) vanillin; 4) benzaldehyde.

In these last experiments the position of the minimum on the curve for glucose decomposition was independent of the cooking temperature or the nature of the base and corresponded to a 1:1 ratio of equivalent concentrations of aldehyde and base, i.e., to the state in which all the bisulfite ions are combined with acetaldehyde.

The question is still being debated whether an oxidation-reduction reaction between sugar and bisulfite can proceed under the conditions of the sulfite cooking process at high temperatures, since the degree of dissociation of sulfurous acid is negligible under these conditions [6]. It has been suggested that the liquor contains no aldehyde-bisulfite compounds at all under the conditions of the sulfite process [7].

Accordingly, our investigations of the influence of aldehydes on the behavior of sugars in sulfite cooking were extended.

Four aldehydes were chosen: two aromatic (vanillin and benzaldehyde) and two aliphatic (acetaldehyde and formaldehyde). Glucose was cooked by the sulfite process in presence of aldehydes in sealed glass tubes placed in an autoclave. The temperature was raised to the required level during 1 hour, and held at that level for 3 hours.

The cooking liquor contained 0.8 mole of total SO_2 and 0.3 mole of NaOH per liter.

In the first series the cooking temperature was 140° , and the glucose concentration was 0.165 mole/liter. In the second series the respective values were 150° and 0.211 mole/liter.

TABLE 1

Effect of Aldehyde Contents on Decomposition of Glucose in Sulfite Cooking; Glucose Concentrations in the Control Cooks Without Aldehyde: 1) before cooking 0.165 mole/liter, after cooking at 140° 0.109 mole/liter; 2) before cooking 0.211 mole/liter, after cooking at 150° 0.132 mole/liter

Aldehydes	Glucose concentrations before cooking (I) and after cooking (II), with aldehyde concentrations (moles per mole of NaOH)					
	0.3		1.0		1.7	
	I	II	I	II	I	II
Temperature 140°						
Acetaldehyde	0.163	0.127	0.163	0.144	0.164	0.144
Formaldehyde	0.164	0.135	0.165	0.144	0.166	0.130
Vanillin	0.160	0.113	0.156	0.110	0.159	0.106
Benzaldehyde	0.161	0.117	0.162	0.122	0.161	0.121
Cooking temperature 150°						
Acetaldehyde	0.213	0.144	0.213	0.172	0.211	0.163
Formaldehyde	0.213	0.151	0.218	0.165	0.230	0.129
Vanillin	0.214	0.141	0.215	0.140	0.207	0.133
Benzaldehyde	0.213	0.144	0.211	0.149	0.211	0.149

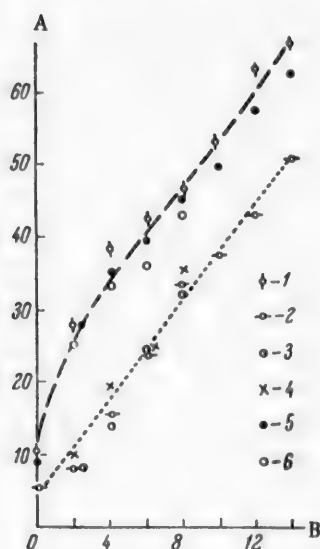


Fig. 2. Effect of aldehyde contents on the course of glucose decomposition during sulfite cooking: A) amount of glucose decomposed (%); B) cooking time at 140° (hours); aldehydes: 1) without aldehyde; 2) acetaldehyde; 3) formaldehyde; 4) butraldehyde; 5) vanillin; 6) benzaldehyde.



Fig. 3. Formation of SO_4^{2-} ions in sulfite cooking of glucose: A) concentration of SO_4^{2-} ions (in g/100 ml); B) cooking time at 140° (hours); NaOH content (mole/liter): I) 0.25; II) 0.375; 1) control cook; 2) glucose with vanillin; 3) glucose with acetaldehyde.

The aldehydes were added in proportions of 0.3 to 1.7 mole per mole of NaOH.

The results are summarized in Table 1. For simplicity, the table gives the glucose concentrations before

TABLE 2

Course of Glucose Decomposition During Sulfite Cooking

Cooking time at 140° (hours)	Glucose concentration (M)		Glucose decomposed (% of initial content)	Cooking time at 140° (hours)	Glucose concentration (M)		Glucose decomposed (% of initial content)
	before cooking	after cooking			before cooking	after cooking	
Glucose without aldehydes				Glucose with acetaldehyde			
0	0.190	0.169	10.6	0	0.184	0.174	5.4
2	0.179	0.129	28.0	2	0.178	0.165	7.8
4	0.184	0.113	38.4	4	0.184	0.155	15.7
6	0.184	0.106	42.6	6	0.184	0.140	23.9
8	0.182	0.098	46.4	8	0.184	0.122	33.6
10	0.190	0.088	53.8	10	0.190	0.119	37.5
12	0.184	0.067	63.5	12	0.179	0.102	43.0
14	0.184	0.060	67.0	14	0.182	0.093	51.0
Glucose with vanillin				Glucose with formaldehyde			
0	0.176	0.161	8.8	2	0.184	0.170	7.9
2	0.170	0.122	28.2	4	0.190	0.154	19.1
4	0.179	0.116	35.0	6	0.182	0.130	28.8
6	0.176	0.107	39.3	8	0.190	0.128	32.5
8	0.176	0.097	45.5	Glucose with butyraldehyde			
10	0.184	0.093	49.5	2	0.179	0.161	10.0
12	0.184	0.078	57.5	4	0.184	0.148	19.7
14	0.182	0.068	62.5	6	0.181	0.137	24.2
Glucose with benzaldehyde				8	0.190	0.122	35.6
2	0.184	0.137	25.4				
4	0.195	0.123	36.5				
6	0.174	0.111	37.1				
8	0.178	0.102	43.3				

and after cooking, while the percentage decomposition of the sugar is represented graphically in Fig. 1.

The curves in Fig. 1 clearly show the influence of the nature of the aldehyde on the decomposition of glucose during sulfite cooking. Aliphatic aldehydes have a strong influence on the degree of decomposition of the sugar. With equivalent concentrations of these aldehydes and the base, the amount of glucose decomposed was about 12% at 140° and about 20% at 150°, whereas, in control cooks without aldehydes, the corresponding values were 34 and 38% respectively.

In presence of aromatic aldehydes the amounts of glucose decomposed were: with vanillin from 30 (at 140°) to 35% (at 150°); with benzaldehyde, from 25 to 35% respectively. The amount of aldehyde added was found to have no effect on the degree of decomposition of glucose — the curves have no minima.

In order to find whether this behavior of aromatic aldehydes is due to the fact that the cooking time was restricted, so that a minimum could occur on either side of the cooking time used, in the next series of experiments the cooking time of glucose (concentration 0.167 mole/liter) was varied from 0 to 14 hours in 2-hour steps.

The composition of the cooking liquor was the same as in the first series of experiments.

The aldehydes were added in the proportion of one mole per mole of NaOH, as the decomposition of glucose was least when aliphatic aldehydes were added in this ratio.

It is clear from Table 2 and Fig. 2 that when glucose is cooked by the sulfite process without added aldehydes under these conditions its decomposition is almost directly proportional to the cooking time, with some acceleration during the first 2 hours.

Aromatic aldehydes have almost no effect on the degree of decomposition of glucose, regardless of the cooking time, whereas aliphatic aldehydes suppress decomposition of glucose to a considerable extent and retain their activity even during very prolonged cooking (14 hours).

The curves for decomposition of glucose in the control cook (without aldehyde) and in cooks with aliphatic aldehydes are almost parallel. It follows, if the course of sulfite cooking of glucose is considered, that aliphatic aldehydes do not prevent decomposition of the sugar, but retard it. For example, 25% of the glucose was decomposed in 2 hours in the control cook, and in 6 hours in cooks with aliphatic aldehydes; 40% was decomposed in 6 hours in the control cook, and in 10.5 hours in the cooks with aliphatic aldehydes.

The influence of the nature of the aldehyde on the degree of decomposition of glucose shows a correlation with the formation of SO_4^{2-} ions the course of sulfite cooking. To confirm this, cooking experiments were performed with 0.2 M glucose solutions at 140°. The total SO_2 content of the cooking liquor was 0.86 mole/liter. To give a fuller idea of the influence of the nature of the aldehydes on oxidation processes, the cooking liquors contained different amounts of NaOH: 0.25 and 0.375 mole/liter.

Figure 3 shows that addition of vanillin to the cooking liquor produced almost no change in the SO_4^{2-} ion concentration, whereas in presence of acetaldehyde the SO_4^{2-} ion concentration of the liquor falls considerably during sulfite cooking. For example, in a liquor containing 0.25 mole NaOH per liter, the SO_4^{2-} ion concentration after 3 hours of cooking was 1.8 g/100 ml in absence of aldehydes, and 0.6 g/100 ml in presence of acetaldehyde. After six hours of cooking the corresponding contents were 2.3 and 1.4 g per 100 ml respectively.

SUMMARY

1. Aliphatic aldehydes added to the cooking liquor decrease the degree of decomposition of glucose during sulfite cooking. The decomposition of glucose is least when the amounts of these aldehydes are sufficient to bind all the bisulfite ions. Addition of aromatic aldehydes to the cooking liquor has little effect on the degree of decomposition of the sugar. The curve for the decomposition of glucose as a function of the aldehyde content does not pass through a minimum in such cases.

2. In a study of the course of decomposition of glucose during sulfite cooking it was shown that the degree of decomposition is almost directly proportional to the cooking time, with some acceleration during the first two hours. Aliphatic aldehydes added to the cooking liquor do not prevent decomposition of the sugar, but merely retard it.

3. In presence of aliphatic aldehydes the formation of SO_4^{2-} ions during sulfite cooking of glucose is diminished. Addition of aromatic aldehydes to the cooking liquor does not decrease the degree of oxidation of SO_2 to SO_4^{2-} .

LITERATURE CITED

- [1] H. H. Browne, J. Org. Chem. 9, 67 (1944).
- [2] S. A. Sapotnitskii and A. G. Moskaleva, Coll. Trans. Sci. Res. Inst. Hydrolysis and Sulfite Alcohol Ind. 5, 5 (1956).
- [3] S. A. Sapotnitskii and A. G. Moskaleva, Coll. Trans. Sci. Res. Inst. Hydrolysis and Sulfite Alcohol Ind. 6 (1958).
- [4] M. A. Gubareva, J. Gen. Chem. 17, No. 12, 2259 (1947).
- [5] E. Hägglund, Ber. 62, 437 (1929).
- [6] S. Rydholm, Svensk Papperstidn. 58, 8, 273 (1955).
- [7] M. G. Eliashberg, Paper Ind. 3, 6 (1950).

Received February 12, 1958

REACTIONS OF ACRICHINE (QUINACRINE HYDROCHLORIDE)
AND RIVANOL (ETHOXYDIAMINOACRIDINE LACTATE)
WITH TANNIN, AND ANALYSIS OF THE LATTER

E. O. Turgel'

It is known that precipitates are formed when solutions of tannins are mixed with solutions of various alkaloids [1, 2] and of other nitrogen-containing basic organic compounds [3, 4]. Some alkaloids give precipitates not only with tannins but also with the related gallic acid [5]. According to Freudenberg [6], these effects are based on chemical reactions leading to formation of sparingly-soluble addition products; this view is confirmed by the work of Haller [4]. On the other hand, in some instances the formation of precipitates can be attributed to mutual coagulation or sensitization [7]. In any event, the significant role of colloidal processes is evident; the action of electrolytes, which in a number of instances cause [2] or accelerate [4] precipitation, is associated with this. In most cases the composition of the precipitates formed was not investigated. Among the few exceptions are quinine tannates which, according to Biginelli [8] and Muraro [8], are formed by reactions of: 1) tannin with quinine base (in alcoholic solutions); 2) tannin with quinine salts (in aqueous solutions). Tannates of the first type (consisting of tannin and quinine base) were termed true tannates, and those of the second type (consisting of tannin and quinine salts) were termed pseudotannates.

It was desired to find whether tannin (and gallic acid) reacts with acrichine. Experiments with another acridine derivative, rivanol, were also carried out.

EXPERIMENTAL

The following compounds were used in the experiments.

a) Gallotannin (five samples) and smoke-tree tannin (one sample). Table 1 contains the results of determinations of moisture and ash contents of these samples by the usual gravimetric methods, and the results of determinations of tannins and nontannins by the All-Union Unified Method (AUM) for tanning extracts [10]. On addition of alcohol [11] to an aqueous solution of Sample No. 4 a slight precipitate was formed; this test gave a negative result with Samples No. 1, 2, 3, 5 and 6. Except when stated otherwise, Sample No. 1 was used.

b) Gallic acid (Schering). Analysis of the crystalline hydrate gave 4.34% H and 44.63% C (calculated: 4.28% H and 44.68% C); the content of water of crystallization was 9.60% (calculated, 9.58%); analysis of the anhydrous substance gave 3.73% H and 49.46% C (calculated: 3.56% H and 49.42% C).

c) Acrichine and rivanol conforming to the specifications of the USSR State Pharmacopoeia [11]. The nitrogen contents found by analysis were 8.27% and 12.15% respectively (by calculation, $C_{23}H_{30}ON_3Cl \cdot 2HCl \cdot 2H_2O$ contains 8.26% nitrogen, and $C_{15}H_{15}ON_3 \cdot CH_3CH(OH)COOH$, 12.24%).

When equal volumes of 1% aqueous solution of tannin and acrichine (or rivanol in parallel experiments) are mixed, no precipitates are formed; however, precipitates appear on addition of electrolytes (Na_2SO_4 is more effective than $NaNO_3$, $NaCl$, or NaH_2PO_4). The precipitates are very bulky because of a high degree of hydration; if the precipitation is carried out at 70-80° the reaction products separate out in the form of a viscous substance of a low degree of hydration, which hardens on cooling. Precipitates are also formed when solutions of acrichine (or rivanol in parallel experiments) and Na_2SO_4 are mixed with aqueous extracts of willow or oak bark, tea, St. John's wort, or sage, bearberry, and red bilberry leaves; it follows that acrichine and rivanol in presence of

TABLE 1

Characteristics of the Original Tannin Samples

Sample No.	Type of tannin	Moisture content (%)	Analytical data (% of bone-dry substance)						
			ash	by AUM		low-molecular impurities			
				tannins	non-tannins	in sample	in mixture of sample with gallic acid (20:1)		in purified product
						calculated	found		
1	Gallotannin	9.67	0.07	95.9	4.1	8.4	12.8	12.5	2.2
2		11.57	0.14	93.7	6.3	14.5	18.7	18.2	—
3		7.85	0.14	94.5	5.5	10.2	14.4	13.9	—
4		11.18	0.25	92.7	7.3	17.5	21.5	21.8	1.2 *
5	Smoke-tree tannin	10.16	0.13	93.8	6.2	14.1	18.2	18.4	—
6		10.82	0.14	97.3	2.7	3.9	8.5	8.1	1.9 1.0 *

*Results corresponding to combined purification by both methods.

electrolytes precipitate not only tannic acid but also other tannins. The behavior of acrichine toward gallic acid differs from that of rivanol. When solutions of acrichine, Na_2SO_4 , and gallic acid are mixed, there is no visible precipitate, whereas rivanol gives a precipitate under these conditions. When alcoholic solutions of the free acrichine and rivanol bases were added to alcoholic solutions of tannin, precipitates were formed in both cases. Precipitates are not formed when alcoholic solutions of the two bases are mixed with alcoholic solutions of gallic acid.

For investigation of the reaction products, the moisture content was determined by drying in a vacuum desiccator to constant weight, and the product was then analyzed for nitrogen and sulfur; the composition was calculated from the analytical data (percentage of acrichine base = 9.518% N, percentage of rivanol base = 6.028% N, percentage of sulfuric acid = 3.058% S). The contents of tannin (or gallic acid) were found by difference. The results are summarized in Table 2.

Analyses of Preparations No. 1 and 2 show that they consisted of tannin and acrichine sulfate (for which $\text{N/S} = 1.31$). It follows that sodium sulfate not only causes coagulation of the reaction products, but also takes part in their formation. The N/S ratio for Preparation No. 4 shows that most of the rivanol in it is present as the sulfate (for which $\text{N/S} = 2.63$), while the rest is apparently in the original lactate form. When rivanol sulfate had been prepared, it was used for formation of Preparation No. 5. Analytical data for the latter indicate that it consists of tannin and rivanol sulfate. Preparations No. 3 and 6 evidently consist of the free bases and tannin. It follows that both acrichine and rivanol, like quinine, form tannates of two types. In evaluation of analytical data on the latter it must be remembered that tannin itself is not an individual substance but a mixture with colloidal properties [1, 7]. Acrichine and rivanol solutions should also have colloidal characteristics owing to the association effects typical of acridine derivatives [12]. Interaction of tannin with acrichine (and also with rivanol) apparently involves both chemical and colloidal processes and leads to the formation of complex mixtures, so that the composition of tannates cannot be expressed in terms of definite stoichiometric formulas. Analysis of Preparation No. 7 showed that only part of the rivanol in it is present as sulfate. From rivanol sulfate we obtained Preparation No. 8, the composition of which corresponds fairly closely to the formula $(\text{C}_{15}\text{H}_{15}\text{ON}_3 \cdot 0.5\text{H}_2\text{SO}_4)_3 \cdot [\text{C}_6\text{H}_2(\text{OH})_3\text{COOH}]_2$ (a substance conforming exactly to this formula should contain 60.93% of rivanol base, 11.80% of sulfuric acid, and 27.27% of gallic acid).

The effects described above may serve as the basis of qualitative tests for tannins and gallic acid; they can be used for removal of tannins and gallic acid, or tannins only, from vegetable extracts. We took advantage of the fact that acrichine precipitates tannins almost quantitatively in developing an analytical method for tannin.

Tannin usually contains variable amounts of organic impurities in addition to its main components—

TABLE 2

Characteristics of Reaction Products

Preparation No.	Reaction product of	Moisture (%)	Contents (% on anhydrous substance)					
			N	S	$\frac{N}{S}$	base	H ₂ SO ₄	tannin (gallic acid)
1	Tannin, Na ₂ SO ₄ , and acrichine	18.29	3.93	2.99	1.31	37.4	9.1	53.5
2	Tannin, Na ₂ SO ₄ , and acrichine (at 70-80°)	10.27	3.66	2.75	1.33	34.8	8.4	56.8
3	Tannin and acrichine base (in alcoholic solutions)	9.57	3.80	—	—	36.2	—	63.8
4	Tannin, Na ₂ SO ₄ , and rivanol	13.15	7.29	2.28	3.20	43.9	7.0	—
5	Tannin, Na ₂ SO ₄ , and rivanol sulfate	16.45	7.21	2.67	2.70	43.5	8.2	48.3
6	Tannin and rivanol base (in alcoholic solutions)	9.67	8.71	—	—	52.5	—	47.5
7	Gallic acid, Na ₂ SO ₄ , and rivanol	12.12	10.17	2.24	4.54	61.3	6.9	—
8	Gallic acid, Na ₂ SO ₄ , and rivanol sulfate	7.02	10.36	3.68	2.82	62.5	11.3	26.2

polygalloylglucoses— and small amounts of mineral substances. The impurities of high molecular weight— starch [13, 14], dextrans [15], and gums [14]— cannot be regarded as characteristic; moreover, qualitative and quantitative determination of these substances does not involve any essential difficulties. Much more typical impurities in tannin are those of low molecular weight, which consist mainly of gallic acid [13, 16], glucose (in smaller amounts) [13, 15], and probably pyrogallol [17]. In contrast to the principal components, these substances are not precipitated by acrichine, but react with iodine in presence of alkali [18, 19], so that they can be determined jointly in the filtrate by means of our iodometric method for gallic acid [19]. The method described below was developed on the basis of a series of experiments.

1 g of tannin is put into a beaker (100-150 ml), about 1 g Na₂SO₄ and 50 ml water is added, the tannin is dissolved (gentle and brief warming is permissible), and the beaker is then placed in a water bath maintained at 70-80°. The solution is allowed to warm through during 2-3 minutes, and acrichine solution (4:100, made with the aid of gentle warming) is added uniformly dropwise with continuous stirring (by means of a glass rod); 20 ml of this solution must be added during 10 minutes. A precipitate of acrichine tannate is formed, and adheres to a considerable extent to the rod and the sides of the beaker. At the end of the precipitation the contents of the beaker are cooled rapidly; with care being taken not to touch the precipitate, the liquid is quantitatively transferred into a 100 ml measuring flask and the level is brought up to the mark by addition of water. The contents of the flask are mixed and then filtered through an ordinary paper filter, the first 35 ml of filtrate being discarded. To remove excess acrichine from the remaining filtrate (A), 50 ml of the filtrate is warmed (in a 100-150 ml beaker) to 70-80°, and 10 ml of 50% KI solution is added (with stirring). When quite cool, the liquid and precipitate is transferred quantitatively into a 100 ml measuring flask and the level is made up to the mark with water. To separate the precipitate, the contents of the measuring flask are mixed and then filtered through an ordinary paper filter, the first 35 ml of the filtrate being discarded. All the remaining filtrate (B) is a solution of the tannin sample free from actual tannins and excess acrichine; it is subsequently used for determination of low-molecular impurities by the method described previously [19] for gallic acid. The average result of 2-3 titrations is used in the calculation. The concentration of impurities in Filtrate B can be calculated, for gallic acid, from the following formula [19]

$$x = \frac{y}{6.275 - 0.023 y} \frac{\text{g gallic acid}}{\text{liter}},$$

where y is the volume of 0.1 N iodine solution taken. Accordingly, the content of low-molecular impurities in the tannin sample is

$$x_1 = \frac{20 y}{6.275 - 0.023 y} \cdot 100$$

or, calculated for the anhydrous substance,

$$x_2 = \frac{2000y}{(6.275 - 0.023y)(100 - b)} \cdot 100$$

where b is the percentage moisture content of the tannin.

The analysis may be interrupted for periods of up to several days after preparation of filtrates A and B, or in the course of the iodometric determination after addition of alkali. A microburet should be used for the titrations.

Deviations from the described procedure may greatly influence the results. However, if the procedure is followed exactly, the results of duplicate analyses are in satisfactory agreement; for example, in analyses of Sample No. 1 the values obtained for the impurity content were 8.3, 8.4 and 8.5%. Average values found in determinations of low-molecular impurities in six tannin samples are given in Table 1. To verify the method, mixtures of these samples with crystalline gallic acid hydrate in 20:1 ratio were prepared and analyzed; the calculated and determined contents of impurities in these mixtures are given in Table 1. Three tannin samples were purified: 1) by extraction in ethyl acetate from a neutralized aqueous solution followed by vacuum distillation of the solvent [6, 16]; 2) precipitation by ether [20] from aqueous solution followed by drying under vacuum at room temperature. Sample No. 1 was purified by the first method; Samples No. 4 and 6 were purified by the first method and then additionally by the second (in addition, Sample No. 6 was subjected to threefold purification by the second method). The purified samples were analyzed (Table 1).

The impurity contents were lowered sharply in all cases (we did not succeed in preparing a sample containing less than 1% impurities). Thus, the recommended method of analysis is suitable for quantitative estimations of the purity of tannin. This conclusion is confirmed by a comparison of the data in Table 1, Columns 6 and 7. Both the test methods, i.e., the All-Union Unified Method based on sorption of tannins by rawhide powder and the recommended method, give the same sequence of the tannin samples in order of purity (No. 6, 1, 3, 5, 2, 4); but the nontannin content determined by the AUM was much lower in each case than the content of low-molecular impurities determined by the recommended method. This may be because rawhide powder can take up considerable amounts of gallic acid in addition to tannins [21]. Because of this, it is doubtful whether analytical methods developed for tanning liquors are suitable for tannin; there are grounds for believing that the recommended method gives a more correct and objective estimation of the degree of purity of tannin. In any event, the recommended method is less time-consuming and gives a much sharper differentiation between different tannin samples.

SUMMARY

Achrichine and rivanol form sparingly-soluble tannates of two types, consisting of tannins and the free bases, and tannins and the salts of these bases respectively. In presence of electrolytes rivanol precipitates tannins and gallic acid from aqueous solutions, while achrichine precipitates tannins but not gallic acid. In addition to the principal components, tannin usually contains organic impurities of low molecular weight which can be determined quantitatively in the filtrate after precipitation of the principal components by achrichine. The results of such determinations give a measure of the degree of purity of the tannin.

LITERATURE CITED

- [1] M. Nierenstein, *The Natural Organic Tannins*, London 12-13, 115-118 (1934).
- [2] A. Ware and V. Smith, *Zbl.* 105, 1, 2169 (1934).
- [3] A. Sanin, *Zbl.* 82, 1, 1899 (1911).
- [4] R. Haller, *Zbl.* 90, 11, 62 (1919).

- [5] A. Grutterink, Z. f. anal. Ch. A. 51, 175 (1912).
- [6] K. Freudenberg, Tannin, Cellulose, Lignin, Berlin, 11, 16 (1933).
- [7] A. Mikhailov, Colloid Chemistry of the Tannins [In Russian] (Moscow-Leningrad, 1935) pp. 16-17, 85-86, 209-211.
- [8] P. Biginelli, Zbl. 78, 11 2063 (1907); 79, 1, 418 (1908).
- [9] F. Muraro, Zbl. 79, 11, 75 (1908).
- [10] Analytical Chemical Control in the Production of Leather and Tanning Extracts (AUM) [In Russian] (Central Sci. Res. Inst. Leather Industry, Moscow, 1955) 1, pp. 178-185.
- [11] USSR State Pharmacopeia, 8th Edition [In Russian] (Moscow, 1952) pp. 38-39, 429-430, 544-545.
- [12] A. Albert, The Acridines, London, 109-113, 182-183, (1951).
- [13] M. Nierenstein, Allen's Commercial Organic Analysis, V, London, 31-32 (1927).
- [14] Chem. Prod. and Chem. News, 16, 14 (1953).
- [15] T. Ullmann, Enzyklopädie der techn. Ch. IX, Berlin-Vienna, 761 (1932).
- [16] E. Fischer, Untersuchungen über Depside und Gerbstoffe Berlin, 23-60, 267, 269 (1919).
- [17] D. Cameron and G. Mc Laughlin, J. Am. Leather Chem. Assoc. 25, 325 (1930).
- [18] H. Meyer, Analysis and Determination of Organic Compounds (Leningrad, 1937) pp. 95, 261 [Russian translation].
- [19] E. O. Turgel', J. Appl. Chem. 30, 819 (1957).*
- [20] P. Sisley, Z. anal. Ch. 34, 102 (1895).
- [21] J. Wilson and E. Kern, Ind. Eng. Chem. 12, 465 (1920).

Received February 11, 1958

*Original Russian pagination. See C.B. Translation.

HYDROCHLORINATION OF DIVINYLCACETYLENE IN A REACTOR WITH AN AIR LIFT

A. E. Akopyan and Zh. A. Kosoyan
(Erevan Polytechnic Institute)

One of the present authors developed a continuous catalytic method for hydrochlorination of divinylacetylene (DVA) [1], based on the reaction



There is no doubt that the proposed method offers a correct solution of all the problems involved in its technical performance, as the process can be continued until the starting materials have been completely consumed, the product is obtained in high yield, the process is safe, and the catalyst can be used for long periods without loss of activity. However, the process involves the use of a reactor equipped with a mechanical stirrer, and this introduces certain complications owing to the corrosive nature of the reaction mixture. It was therefore of definite interest to find whether this process can be effected in a reactor without a mechanical stirrer, but with vigorous agitation of the reaction mixture (the organic and aqueous phases) with simultaneous separation of the reaction product (the oil layer) from the liquid catalyst. The most effective equipment for this purpose proved to be a reactor of the air-lift type, the design of which was chosen after a series of preliminary experiments, in the course of which the equipment was progressively improved by changes in the dimensions and position of the air lift, separator, and the inlet and outlet pipes.

EXPERIMENTAL

The reactor used for the experiments on hydrochlorination of divinylacetylene consisted of a glass tube 35 mm in diameter and 750 mm long. The upper end of the reactor had two connecting branches, one for a thermometer the bulb of which was immersed in the liquid, and one for a water-cooled reflux condenser. The lower end of the reactor was fitted with an outlet tube and stopcock, used for discharging the catalyst from the reactor. The reactor was connected to an air lift, which was a glass tube 14 mm in diameter and 500 mm long, with two inlet tubes 10 mm in diameter for hydrogen chloride and divinylacetylene solution. The level of the first was 30 mm and of the second 90 mm from the lowest point of the air lift. At the level of the upper connecting point of the air lift, but on the other side of the reactor, a separator was attached to the reactor; this had three outlet tubes, one of which was connected to the reactor at a level of 250 mm (from the lower connecting point of the air lift). This reactor was used for a series of experiments for determination of the degree of conversion of the starting substances and yields of reaction products at different volume feed rates of gaseous hydrogen chloride and divinylacetylene solutions.

The apparatus used for continuous hydrochlorination of divinylacetylene is depicted schematically in Fig. 1.

Technical hydrogen chloride was passed through the flask 1, filled with green oil, to remove the small amount of chlorine present. The hydrogen chloride then passed through trap 2, calcium chloride tube 3, and a rotameter 4, into the air lift 5 of the reactor 6 filled with catalyst, the level of which was 50 mm below the upper point of the air lift. The divinylacetylene solution entered the air lift from the header flask 7 through the flow meter 8. The solution flow rate was regulated by means of the flow meter stopcocks, with the solution level constant in the meter. Excess solution passed from the flow meter into the receiver 9. The reactor was

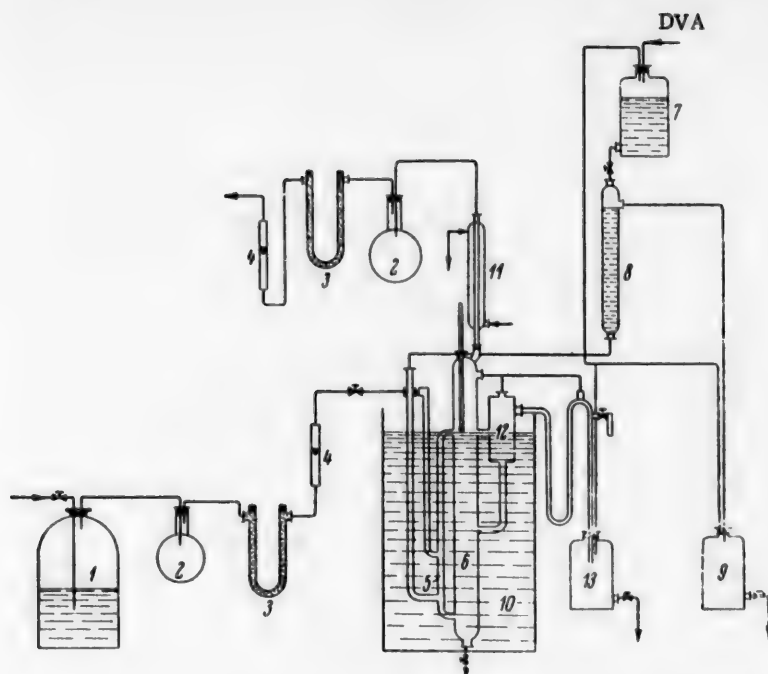


Fig. 1. Apparatus for hydrochlorination of DVA: 1) flask with green oil; 2) spray traps; 3) calcium chloride tubes; 4) rotameters; 5) air lift; 6) reactor; 7) header; 8) flow meter; 9) receiver for solution; 10) thermostatic bath; 11) reflux condenser; 12) separator; 13) receiver for product.

completely immersed in a thermostatically-controlled bath 10. The mixture of inert gases, hydrogen chloride, and vapor of the reaction mixture entered the reflux condenser 11, from which the condensate returned to the reactor and the uncondensed gases escaped into the atmosphere through a spray trap, calcium chloride tube, and rotameter. The incoming and exit gases were dried in calcium chloride tubes in order to improve the accuracy of the rotameter readings and to facilitate calculation of the hydrogen chloride flow rate. The oil layer which accumulated in the reactor during the reaction, together with the catalyst, passed into the separator 12, from which the catalyst flowed back into the reactor along the lower outlet tube, while the upper (oil) layer flowed down the side outlet tube of the separator into the receiver 13 for reaction products.

Solutions of divinylacetylene in xylene, prepared by dissolution of definite amounts of divinylacetylene in xylene, which is inert in the reaction, were used for all the experiments. Divinylacetylene was prepared by vacuum distillation of the works solution, and had the following physical constants: $d_4^{20} = 0.7844-0.7863$, $n_D^{20} = 1.504$, b.p. $46-48^\circ$ at 200 mm.

Effect of the volume feed rate of hydrogen chloride. The experiments of this series were performed at a constant feed rate of the divinylacetylene solution and at constant temperature in the reactor. The hydrogen chloride rate was varied from 55 to 300 liters/hour in the different experiments. The conversion of divinylacetylene in these experiments were estimated by determination of the density of the hydrochlorinated liquid (oil layer), samples of which were taken from a sampling tube (fitted with a stopcock) in the oil-layer line during operation of the apparatus. The samples for analysis were usually taken one hour after the start of an experiment, when the equipment was working quite steadily and the system was in equilibrium. The experiments were performed under the following conditions: amount of catalyst, 500 ml; composition of catalyst (wt. %): CuCl-20, HCl-29, H₂O-51; feed rate of the xylene solution of divinylacetylene (53%), 0.54 liter/hour; density of solution 0.817 g/cc.

The results are plotted in Fig. 2.

It was found that as the hydrogen chloride rate increases the density of the hydrochlorinated liquid and

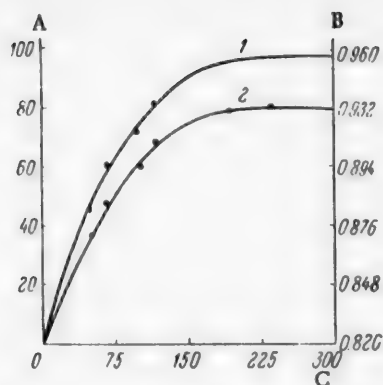


Fig. 2. Effect of the HCl volume feed rate on the process: A) conversion of divinylacetylene (%); B) density of oil layer (g/cc); C) volume feed rate (liters/hour); 1) density of oil layer; 2) conversion of DVA.

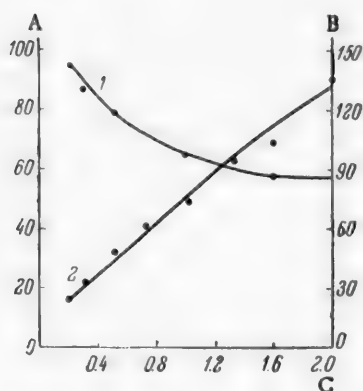


Fig. 3. Effect of the DVA volume feed rate on the process: A) conversion of DVA (%); B) catalyst activity (g/liter·hour); C) volume feed rate (liters/hour); 1) conversion of DVA; 2) catalyst activity.

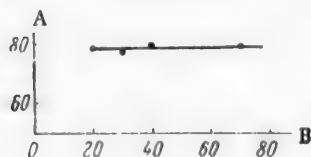


Fig. 4. Effect of concentration on conversion of DVA: A) conversion of DVA (%); B) concentration of DVA (%).

therefore the degree of conversion of divinylacetylene rises to a maximum and then remains almost constant. The probable explanation is that increase of the feed rate of gaseous hydrogen chloride results in intensified agitation and hence to accelerated diffusion of the organic into the aqueous phase; the diffusion in this case determines the rate of the over-all process of divinylacetylene hydrochlorination. Further increase of the hydrogen chloride rate evidently does not accelerate the diffusion any more, and the degree of conversion of divinylacetylene does not increase appreciably. The optimum hydrogen chloride rate is therefore 150–200 liters/hour.

Effect of the volume feed rate of divinylacetylene solution.

The conditions of this series of experiments were exactly the same as before, except that the hydrogen chloride rate was constant (150 liters/hour) and the feed rate of the divinylacetylene solution was varied from 0.3 to 2 liters/hour. The results of these experiments are given in Fig. 3.

It follows from these results that as the feed rate of the divinylacetylene solution increases, the density of the oil layer, and therefore the degree of conversion of divinylacetylene, decreases rapidly at first and then more slowly, while the catalyst output rises steadily. At a feed rate of 0.2 liter/hour it is 23.7 g/hour, whereas at a feed rate of 2 liters/hour it is 140 g/hour. Thus, with a 10-fold increase of the feed rate the conversion of divinylacetylene decreases only by a factor of 1.7, while the catalyst activity increases 6-fold.

The catalyst activity can be calculated from the equation

$$G = 1.1528 \cdot w \cdot a,$$

where G is the dichlorohexadiene yield (in g/hour·liter of catalyst), 1.1528 is the density of dichlorohexadiene, a is the concentration of dichlorohexadiene in the oil layer (in volume fractions), and w is the feed rate of the divinylacetylene solution (liters/hour).

Effect of concentration of divinylacetylene solution. The experiments of these series were performed at constant feed rates of hydrogen chloride (150 liters/hour) and divinylacetylene solution (1.0 liter/hour). The divinylacetylene concentration in solution was varied from 20 to 70%. The results are presented in Fig. 4; it is seen that variations of divinylacetylene concentration have hardly any influence on the degree of conversion, but have a strong influence on the output from the equipment, which is directly proportional to the concentration of divinylacetylene in the original solution.

The use of pure divinylacetylene or of highly concentrated solutions is undesirable owing to the explosive hazards of the peroxides readily formed in pure divinylacetylene by absorption of atmospheric oxygen. A 50–60% solution of divinylacetylene in xylene is more suitable.

Determination of the yields of reaction products. In each experiment about 2 liters of divinylacetylene in xylene solution was hydrochlorinated at a feed rate of 0.6–0.8 liter/hour and a temperature of 56–59°. Seven experiments were performed in a unit with a single reactor, and five in a unit with two reactors in series. The amount of hydrogen chloride consumed was found from the difference

Material Balance for the Process

Amounts (g)							Conversion of starting substances (%)		Yield of dichlorides calculated on converted substances	
starting substances			products							
solution	DVA in solution	HCl	DVA	HCl	di-chloride	residue and losses	HCl	DVA	HCl	DVA
Single reactor										
1387	727	600	152	225	703	248	62.5	79.1	90.5	63.5
1488	715	822	323	552	511	251	32.8	54.7	91.5	73.3
1714	818	641	330	292	669	164	54.2	59.5	98.0	70.3
1724	830	753	385	444	573	188	41.2	53.55	89.5	67.0
1736	816	442	302	92	611	253	79.2	61.0	85.2	61.5
1765	774	1068	408	818	458	158	23.4	48.0	88.5	64.2
1759	874	851	360	531	596	238	37.5	59.0	90.3	60.0
Two reactors										
1633	572	830	100	420	755	127	49.5	82.5	89.0	83.2
1641	609	714	162	269	638	224	62.5	73.4	69.5	74.0
1639	737	571	251	188	697	172	67.0	66.0	87.5	75.0
1647	465	691	82	300	600	181	56.7	82.5	72.7	81.5
1652	465	447	50	000	697	151	100.0	89.3	75.5	87.0

between the weights of solutions taken and obtained and from the rotameter readings, with the concentrations and pressures of the gases before and after the reaction taken into account. The duration of each experiment was 2-3 hours. After each experiment a fraction was isolated from the oil layer at 30-80° and 100-150 mm pressure, and the amount of unconverted divinylacetylene in it was determined. Dichlorohexadiene was then isolated from the residue at 70-78° and 10-12 mm pressure. The purity of the product was estimated by its contents of saponifiable and total chlorine.

Vacuum distillation usually gave 10-20% of a resinous residue. Its chlorine content was 34-38%, whereas that of dichlorohexadiene is 47%. This suggests that the resinous substance is formed by polycondensation of dichlorohexadiene accompanied by liberation of hydrogen chloride. Dichlorohexadiene undergoes polycondensation during distillation of the raw product, under the influence of the certain amount of cuprous chloride dissolved in it and of the high temperature in the still. The results of these experiments are given in the table.

The conversion of hydrogen chloride and divinylacetylene, and the yield of dichlorohexadiene calculated on converted divinylacetylene, are much higher in two reactors in series than in a single reactor, but the catalyst activity is appreciably lower. For fuller utilization of hydrogen chloride, together with intensive agitation of the reaction mixture, hydrogen chloride may be diluted by an inert gas (nitrogen) before entry into the system, or the exit gas may be recycled.

The unchanged divinylacetylene may be returned to the system after isolation from the oil layer. It should be distilled off so that its content in the distillate should be the same as in the original solution (50-60%).

The reaction product, dichlorohexadiene, was also hydrochlorinated in a special experiment. The density and contents of unsaponifiable and total chlorine in the substance before and after the experiment were determined. No changes were found in any of these values ($d_4^{20} = 1.172$, 23.81% of saponifiable chlorine, 46.36% of total chlorine).

Hence it may be concluded that dichlorohexadiene is the final product in the reaction between divinylacetylene and hydrogen chloride, and consequently its yield, calculated on converted divinylacetylene, must be independent of the degree of conversion of divinylacetylene; this conclusion is fully consistent with the experimental results.

SUMMARY

1. Continuous catalytic hydrochlorination of divinylacetylene in an air-lift type of reactor was studied, and the following optimum process conditions were established: feed rates of hydrogen chloride and divinylacetylene solution, 150-200 and 0.6-1.2 liters/hour respectively, concentration of divinylacetylene in the original solution, 50-60%.

2. It is shown that dichlorohexadiene is the final product in the hydrochlorination of divinylacetylene.

3. When dichlorohexadiene is distilled, a resinous product is formed as the result of polycondensation.

LITERATURE CITED

- [1] A. E. Akopyan, J. Appl. Chem. 27, No. 6, 639 (1954). *

Received May 14, 1958

*Original Russian pagination. See C.B. Translation.

CATALYTIC REDUCTION OF ADIPIC ACID DINITRILE TO ϵ -AMINOCAPRONITRILE

L. Kh. Freidlin, A. A. Balandin, T. A. Sladkova,

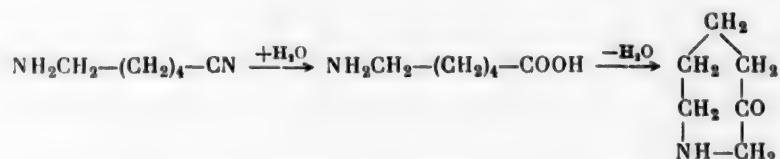
D. I. Lainer and L. G. Emel'yanov

(N. D. Zelinskii Institute of Organic Chemistry, Academy of

Sciences USSR)

State Institute for Planning of Nonferrous Metal Processing Plants

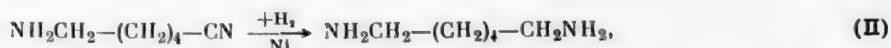
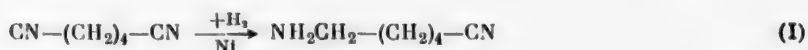
The nitrile of ϵ -aminocaproic acid can be used as an intermediate in the production of capron fiber



The simplest method for its preparation is partial hydrogenation of adiponitrile.

When adiponitrile is hydrogenated in presence of Raney nickel catalyst under pressure, either in static [1] or in dynamic [2] conditions, the principal reaction product is hexamethylenediamine.

The process takes place in stages



and the first stage occurs at a higher rate and under milder conditions than the second.

Arbuzov and Pozhil'tsova [3] were able to effect selective hydrogenation of adiponitrile to ϵ -aminocapronitrile under 0.5-0.7 atmos hydrogen pressure. The reaction is very slow at these pressures. For example, hydrogenation of 10 g of the dinitrile in 150 ml of butanol in presence of 5 g of Raney nickel at 75-80° takes 10 hours.

Zil'berman and Skorikova [1] reported the results of one experiment with a small amount of Raney nickel (2.2% on the weight of dinitrile), in which 51.5% of ϵ -aminocapronitrile was obtained at 142° and 132 atmos, but 35.4% of hexamethylenediamine was also formed.

When the hydrogenation is performed under pressure or in presence of a large volume of active catalyst, the amount of activated hydrogen in the reaction zone is probably considerably greater. Under such conditions the process takes place at a high rate and it is difficult to stop it at the 1st stage: considerable amounts of hexamethylenediamine are formed within a few minutes from the start of hydrogenation. We considered that a catalyst of low activity should be used for selective hydrogenation of adiponitrile to ϵ -aminocapronitrile. It had been shown earlier that a nickel catalyst treated with steam has low activity and selectively accelerates

TABLE 1

Effect of the Catalyst Treatment Temperature. Hydrogenation conditions: temperature 80°, initial pressure 100 atmos, amount of catalyst 20 g, hydrogenation time 2 hours

Expt. No.	Catalyst treat- ment conditions		<u>Dinitrile</u> Ammonia (molar)	Fractional composition of reaction products (wt. %)				
	tempera- ture (deg)	time (hours)		I	II	III	residue	
							tri-amine	dinitrile
1	150	2	1 : 1.52	2.4	24.4	58.5	2.1	12.6
2	180	2	1 : 1.19	3.5	21.7	56.5	3.8	14.5
3	250	2	1 : 2.38	3.8	18.3	52.4	3.2	22.3
4	350	2	1 : 2.51	2.6	14.1	58.0	2.8	22.5

TABLE 2

Effect of Ammonia Content. Hydrogenation conditions: initial pressure 100 atmos

Expt. No.	Temperature (deg)	Dinitrile Ammonia (molar)	Amount of catalyst (g)	Hydrogenation time (hours)	Fractional composition of reaction products (wt. %)				
					I	II	III	residue	
								tri-amine	di-nitrile
5	60	1 : 0.4	10	5	1.3	0.0	6.2	3.6	88.9
6	60	1 : 1.98	10	4	3.7	8.7	55.4	4.1	28.1
7	60	1 : 2.84	20	2	1.3	7.2	55.3	3.8	32.4
8	80	1 : 1.19	19	2	4.2	10.6	56.7	3.8	24.7
9	80	1 : 2.38	20	2	2.6	15.6	59.7	2.2	20.0

hydrogenation of ethylene bonds in presence of aromatic bonds [4]. It is known that nickel, copper, and aluminum form a ternary compound in the proportions of 25:25:50% [5]. Rienacker [6] showed that the activity of reduced nickel-copper catalysts in the hydrogenation of benzene is diminished considerably if their copper content exceeds 20%.

The present investigation was therefore concerned with reduction of the dinitrile in presence of Raney nickel partially deactivated either by additions of copper or titanium, or by treatment with steam under pressure.

EXPERIMENTAL

Preparation of catalysts. Experimental and analytical methods. Nickel catalysts without additives were prepared by exhaustive leaching of powdered 50% Ni-Al alloy by the action of 10% aqueous caustic soda at 95°. The catalyst was washed in water to a neutral reaction and then treated with steam in an autoclave under pressure for 2 hours, taken out, and washed with ethyl alcohol. Nickel catalysts with additions of copper or titanium were made by leaching of the corresponding alloys as described above, but were not treated with steam.

The hydrogenation was performed under static conditions. A steel autoclave 0.5 liter in capacity was charged with 50 ml of the dinitrile and 10-20 g of catalyst. The required quantity of ammonia was then passed into the cooled autoclave from a small weighed cylinder. The hydrogen supply was turned on, and the heater and the mechanism for rotating the autoclave were switched on. After absorption of the amount of hydrogen necessary for reduction of one nitrile group the experiment was stopped. The catalyzate was distilled into fractions corresponding to the boiling points of: hexamethylenimine, 137° (I), hexamethylenediamine, 95-100° at 20 mm (II), and ϵ -aminocapronitrile, 118-120° (20 mm) (III). The high-boiling residue contained bis-hexamethylenetriamine (b.p. 178°, 7 mm) and unchanged adiponitrile. The amine contents of all the fractions were checked acidimetrically, and the content of ϵ -aminocapronitrile in Fraction III was also estimated from the refractive index.

TABLE 3

Effects of Temperature and Pressure. Hydrogenation conditions: molar ratio of dinitrile to ammonia in the original mixture 1:1.55, amount of catalyst 20 g

Expt. No.	Temperature (deg)	Pressure (atmos)	Time (hours)	Fractional composition of reaction products (wt. %)				
				I	II	III	residue	
							tri-amine	di-nitrile
10	25	100	10	2.5	2.9	30.5	6.4	57.7
11	40	100	8	3.9	13.3	55.4	8.5	18.9
12	60	100	2	2.8	7.9	52.3	7.3	29.7
13	60	50	10	1.1	2.1	31.4	4.8	60.0

TABLE 4

Hydrogenation of Adiponitrile over Nickel-Copper Catalyst. Conditions: temperature 80°, pressure 100 atmos

Expt. No.	Composition of original alloy (wt. %)	Dinitrile Ammonia (molar)	Amount of catalyst (g)	Time (hours)	Fractional composition of reaction products (wt. %)				
					I	II	III	residue	
								tri-amine	di-nitrile
14	Ni : Cu : Al 25 : 25 : 50	1 : 0.88	12	—	2.7	0.0	21.5	2.0	73.8
15		1 : 3.04	14	7	2.4	4.2	27.9	5.0	60.5
16		1 : 4.63	12	20	1.0	12.3	52.7	3.2	30.8
17		1 : 1	60	—	9.3	49.2	27.7	9.0	4.8
18	Ni : Cu : Al 10 : 40 : 50	1 : 0.88	37	2	0.0	0.0	3.5	0.0	96.5
19		1 : 3.44	60	10	14.1	1.4	35.0	0.0	49.5
20		1 : 5.29	30	20	2.9	16.2	56.1	0.0	24.8

DISCUSSION OF RESULTS

Table 1 contains the results of experiments on the influence of the temperature of steam treatment of the catalyst on catalyzate composition. The experiments were performed at 80° and 100 atmos in presence of 20 g of catalyst. The table shows that the treatment temperature in the 150-350° range has no appreciable influence on the yield of ϵ -aminocapronitrile, which is 52-58%. The yield of hexamethylenediamine falls from 24 to 14% with increase of the steam treatment temperature from 150 to 350°. The contents of secondary amines in the catalyzates are low (4.5-7.3%).

All the subsequent experiments, summarized in Tables 2 and 3, were carried out with a catalyst treated with steam at 350° for 2 hours.

Table 2 shows the effects of the amounts of catalyst, and of ammonia relative to the weight of dinitrile, on the catalyzate composition. At a 1:0.4 molar ratio of dinitrile to ammonia in the reaction mixture the reaction does not proceed to any appreciable extent (Experiment 5). Change of the dinitrile-ammonia molar ratio from 1:1.2 to 1:2.8 has no effect on the catalyzate composition. The results of Experiments 6 and 7 show that the composition of the reaction products is unchanged if the amount of catalyst is halved. However, the time of reaction is roughly doubled.

Table 3 contains data on the influence of temperature and pressure on the selectivity of the process. These results show that at an initial pressure of 100 atmos the reaction proceeded even at room temperature, but after 0.5 equivalent of hydrogen had been absorbed the reaction ceased (Experiment 10). The yield of ϵ -aminocapronitrile

TABLE 5

Hydrogenation of Dinitrile over Nickel-Titanium Catalyst under Flow Conditions.
Molar ratio of dinitrile to ammonia in the original mixture 1:1.55

Expt. No.	Composition of original alloy (wt. %)	Pressure (atmos)	Temperature (deg)	Dinitrile feed rate (ml/hour)	Fractional composition of reaction products (wt. %)				
					I	II	III	residue	
								tri-amine	di-nitrile
21	Ni:Al 50:50	50	80	70	9.6	78.0	0.0	11.0	1.4
22	Ni:Ti:Al 48:4:48	50	80	70	9.0	45.0	16.0	13.4	17.1
23		20	60	70	0.0	4.0	24.0	2.9	69.1
24		20	60	75	1.1	2.7	24.7	3.4	68.5
25		20	60	45	1.8	9.0	59.7	11.0	18.5

remains almost unchanged over the 40-80° range, and is 52-58%. At 60-80° the reaction time does not exceed 2 hours, and at 40° it is 8 hours. The increase of the hexamethylenediamine yield to 13.3% and the somewhat higher yield of secondary amines in Experiment 11, conducted at 40°, may be attributed to the longer duration of the experiment [1]. Hydrogen was not absorbed at 40° and 25 or 50 atmos pressure. At 60°, and 50 atmos initial pressure, only about 50% of the required volume of hydrogen was absorbed in 10 hours (Experiment 13). The most favorable temperature for production of ϵ -aminocapronitrile under our conditions is 60-80°. Decrease of temperature increases the hydrogenation time and the yields of diamine and secondary amines.

Table 4 contains the results of experiments on hydrogenation of the dinitrile over catalysts containing nickel and copper in 1:1 and 1:4 ratios by weight. It is seen that the activities of these catalysts are low. The principal reaction product is ϵ -aminocapronitrile. The catalyst with the lower copper content is the more active (Experiments 14 and 18). If the amount of this catalyst is increased, the diamine is obtained in substantial yield (Experiments 14 and 17). Therefore the selectivity of the catalyst in Experiments 14-16 may be attributed to an insufficient amount of nickel present in the reaction rather than to changes of catalyst composition. Indeed, Jadot and Braine [7] showed that under harsh temperature and pressure conditions only nitrile groups directly linked to the benzene ring are reduced in presence of Raney-type copper catalysts.

On decrease of the dinitrile-ammonia molar ratio in the original mixture below 1:3.04 the time of hydrogenation in presence of copper-nickel catalysts increases sharply (Experiments 15 and 16, 19 and 20).

Table 5 contains data on hydrogenation of the dinitrile over Raney nickel catalyst containing 4% of titanium by weight. In contrast to all the earlier experiments, these experiments were performed under flow conditions, so that a constant pressure could be maintained in the system. The apparatus and experimental procedure were described earlier [2]. The volume of catalyst was 325 ml, layer height 105 cm, grain size 3-7 mm. The catalyst was prepared by the action of 20% aqueous caustic soda solution on nickel-titanium-aluminum alloy until 40% aluminum had been removed. In Experiment 22, performed at 80°, 50 atmos, 1:1.55 molar ratio of dinitrile to ammonia in the original mixture, and dinitrile feed rate of 70 ml/hour, the yield of hexamethylenediamine was only 45.0%. Under the same conditions 78.0% of the diamine was obtained on the nonpromoted catalyst (Experiment 21).

It follows that the presence of 4% titanium in the original alloy greatly lowers the catalyst activity. This justified tests of the specificity of its action in the process in question.

The results of Experiments 23 and 24 show that at 20 atmos and 60° the yield of ϵ -aminocapronitrile was 24.0%, and of the diamine only 4%. When the dinitrile feed rate was lowered by one third the yield of ϵ -aminocapronitrile reached 59.7%.

SUMMARY

Adiponitrile can be selectively hydrogenated to ϵ -aminocapronitrile in presence of Raney nickel catalyst partially deactivated by steam treatment or by additions of copper or titanium.

LITERATURE CITED

- [1] E. N. Zil'berman and Z. D. Skorikova, Proc. All-Union Conference on Heterogeneous Catalysts in Chemical Industry [In Russian] (1955) p. 471.
- [2] L. Kh. Freidlin, A. A. Balandin, K. G. Rudneva and T. A. Sladkova, Bull. Acad. Sci. USSR, Div. Chem. Sci. 2, 166 (1957).*
- [3] B. A. Arbuzov and E. A. Pozhil'tsova, Bull. Acad. Sci. USSR, Div. Chem. Sci. 1, 65 (1946).
- [4] L. Kh. Freidlin, A. A. Balandin, N. V. Borunova and A. E. Agronomov, Bull. Acad. Sci. USSR, Div. Chem. Sci. 8, 913 (1956).*
- [5] Z. F. Mondolfo, Metallography of Aluminum Alloys (1948).
- [6] G. Rlenacker, Z. anorg. u. allgem. Chem. 274, 47 (1953).
- [7] J. Jadot and R. Braine, Bull. Soc. roy. sci. Liège, 25 (1), 79 (1956).

Received February 27, 1958

*Original Russian pagination. See C.B. Translation.

DECOMPOSITION OF FURAN BY HOT PERHYDROL UNDER PRESSURE

A. P. Salchinkin

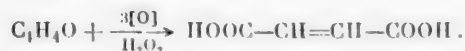
(Chair of Organic, Physical and Colloid Chemistry, the Kuban'
Agricultural Institute)

Certain researches have shown that destructive oxidation of furfural in the liquid phase by concentrated nitric acid, 30% hydrogen peroxide, sodium chlorate and certain other oxidizing agents at elevated temperatures ultimately leads to formation of a number of dicarboxylic acids of technical importance, such as oxalic [1], succinic [2], and fumaric [3]; the formation of maleic acid by oxidation of furfural by atmospheric oxygen in the vapor phase has been reported [4-6]. The formation of these acids must be regarded as the direct consequence of opening of the furan ring, of which furfural is a derivative. Direct oxidation of furan itself is necessary if only because the influence of functional groups which disturb the ring symmetry is thereby eliminated in investigations of the principal stages of the oxidation reaction.

Among the few laboratory investigations of the catalytic oxidation of furan in the vapor phase by hot air in presence of catalysts consisting mainly of vanadium pentoxide we may note the work of Milas and Walsh [4] and of Kalnin', Giller and Tarvid [7, 8]. The results of these studies indicate that the principal solid product formed by oxidation of furan under the conditions described above is maleic acid.

Since the destructive oxidation of furfural proceeds fairly simply and smoothly by the action of 30% hydrogen peroxide, it was decided to use the same oxidizing agent for furan, but under modified conditions because of the volatility and low boiling point of the latter.

If it is assumed that opening of the furan ring terminates in predominant formation of maleic acid, the approximate consumption of oxidizing agent can be estimated from the following scheme:



The results of our experiments on oxidation of furan by hot perhydrol and of studies of the composition of the oxidation products are presented below.*

EXPERIMENTAL

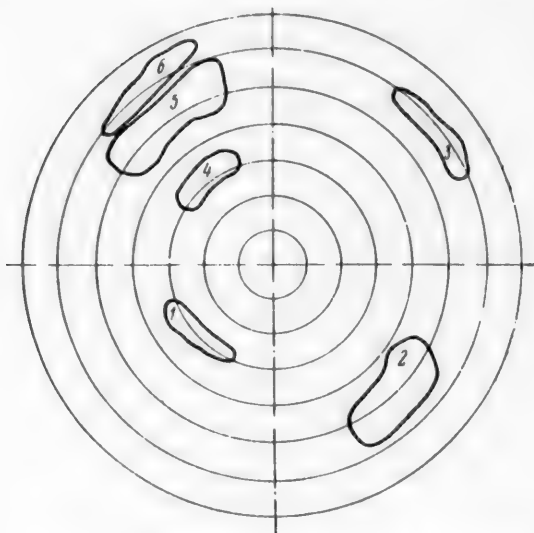
The furan used for the experiments was prepared by decarboxylation of pyromucic acid by Wilson's method [9]. The pyromucic acid used in the preparation was prepared by the method developed in our laboratory [10]. Then pyromucic acid is heated at 205-210°; the furan yield reaches 70% provided that the pyromucic acid content of the samples, as determined by titration, does not fall below 90% and that the receiver is suitably cooled.

Furan fractions boiling in the 31-32° range (at 754 mm) were combined and used for the experiments. The refractive index n_D^{20} was 1.4220, as compared with 1.4216 according to the literature [11].

The strength of the perhydrol, checked by the oxidimetric method, did not exceed 27-28%. Furan was oxidized by perhydrol in sealed glass tubes heated to 160-170°. The tubes, made from No. 23 laboratory glass,

*L. B. Lapkova assisted in some of the experiments on the oxidation of furan.

Organic acids	R _f of acids	
	controls	test mixtures
Tartaric	0.25	0.27
Maleic	0.74	0.71
Succinic	0.77	0.76



Positions of the marker spots and spots for the acids in the tested mixtures: acids: 1,4) tartaric; 2,5) maleic; 3,6) succinic; 1,2,3) markers; 4,5,6) test mixture.

The gas issuing from the tube was passed through a Drechsel flask containing 20 ml of water. The solution in the Drechsel flask had a fruity odor. A portion of the solution gave a distinct iodoform reaction; there was an odor of iodoform followed by a precipitate after a short time. The volume of the reaction mixture diminished by 3-4 ml at the end of the reaction. Of the 10 tubes used 5 exploded during the experiments.

The contents of the five undamaged tubes were combined; the total volume was 88 ml. The liquid was distinctly acid (litmus test). The presence of unchanged hydrogen peroxide was shown by the following test: 2 ml of water and 1 ml of diethyl ether free from alcohol and peroxides were added to 3-5 drops of the mixture. After addition of a small crystal of potassium dichromate the ether layer became blue; this showed the presence of unchanged hydrogen peroxide [13].

The next operation was steam distillation of volatile acids from the acid liquid. The unchanged perhydrol was decomposed by addition of 20 ml of 96% alcohol to the acid liquid before the distillation. The volatile acids were distilled in steam from the reaction mixture until 2-3 drops of condensate gave a faint red color with blue litmus. The volume of condensate was considerable, up to 3 liters. Neutralization of all the volatile-acid fraction in presence of a mixed indicator [14] took 70.85 ml of exactly 1 N caustic soda solution, which is equivalent to 4.25 g of acetic acid.

Part of the neutralized volatile-acid distillate was evaporated in a porcelain basin on a water bath, to leave a dry residue of the salts. The residual dry salts were analyzed for volatile acids [15]. The mercuric oxide test for formic acid was negative. Acetic acid was identified by formation of ethyl acetate. The odor of the ester was quite distinct.

were 125 cm long and 2.2 cm in internal diameter. Furan and perhydrol were taken in 1:5 ratio. The amounts used were 3 ml (2.8 g) of furan and 15 ml of perhydrol.

As furan is volatile and readily inflammable, the closed end of the tube was placed in a vessel with ice before sealing. The sealed tubes were heated in a metal pipe (5 cm in diameter) consisting of two portions 2.5 meters in total length and fitted together with a small gap between. The open region of the sealed tube was heated by means of a burner at this point. The open ends of the outer pipe were firmly plugged (in the event of explosion of the sealed tube). The heating time was 60-70 minutes. The heating temperature was measured by means of a mercury thermometer. For this purpose in three of the experiments a thermometer was placed directly in the tube before it was sealed. The thermometer readings fluctuated in the 160-170° range during the entire reaction period. In the remaining experiments the tubes were heated without thermometers. During the stated time interval the decomposition of the furan taken for the reaction went to completion — the boundary between the furan and perhydrol disappeared and the mixture became homogeneous and colored pale green or slightly yellowish. The tubes were cooled to room temperature and opened. Generally the gas pressure inside the tube was very considerable — the gas stream extinguished the burner flame. The gas was inflammable, it burned with a pale blue flame, and its odor resembled that of acetaldehyde. The presence of aldehyde was confirmed.

When the dry salt residue was heated with soda lime, methane was liberated. The aqueous solution from the distillation flask, free from volatile acids, was transferred to a porcelain basin and evaporated on a water bath until crystallization commenced. The crystalline product was filtered off on a Buchner funnel and recrystallized from hot water in presence of activated charcoal. Large, colorless, distinctly hygroscopic crystals were obtained. When dried in a drying oven the crystals softened at 99° but did not melt completely. The weight of the crystalline product after purification and drying was 9.30 g, or 38.91% of the theoretical yield calculated on the assumption that the oxidation consists predominantly of the conversion of one mole of furan into one mole of maleic acid.

When 2 g of the crystals were recrystallized from dioxane, flaky plates melting at 132-134° were obtained.

It is clear that oxidation of furan by perhydrol gave a mixture of dicarboxylic acids. Tests showed that the dicarboxylic acids do not change the color of bromine water, but alkaline permanganate solution is decolorized instantly. The chemical nature of the components of the acid mixture was investigated by partition paper chromatography [16]. The method recommended for chromatographic analysis of carbohydrates [17], suitably modified for analysis of dicarboxylic acids, proved to be quite suitable for our purpose. Circular chromatograms of the sector type were utilized, with the use of paper disks 7 cm in diameter cut from No. 4 chromatographic paper (made by the Leningrad No. 2 Paper Mill). Concentric circles 1, 2, 3, 4, 5 and 6 cm in diameter were drawn by means of a compass on the disks. Lines at right angles were then drawn to mark out 4 or 8 sectors on each disk. Drops of the unknown solutions and markers, corresponding in number to the number of sectors were applied at the circumference of the 1 cm circle. The markers were 1 N solutions of chemically pure dicarboxylic acids.

The unknown solutions were prepared of the same concentration, calculated as maleic acid, the presence of which was to be expected [4, 7, 8]. The diameter of the spots on the paper was about 3 mm, which corresponds to about 0.5 microliter of solution. A paper wick twisted from a paper strip 0.5 x 0.5 cm was inserted in a hole in the center of the disk.

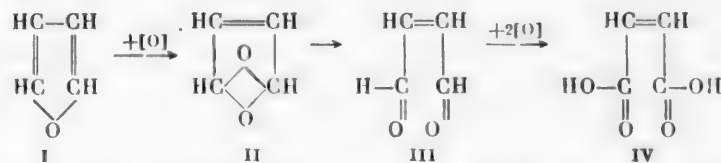
An ordinary desiccator was used as the chromatographic chamber. The prepared paper disk was gripped between two Petri dishes of equal size, 0.5-1 cm smaller than the disk in diameter. The Petri dish contained a glass or porcelain vessel with 2 ml of the motile solvent consisting of butanol, formic acid, and water in 18:2:9 ratio [18].

When the solvent had migrated 6-7 cm along the radius, the chromatogram was taken out and left in air for 4-6 hours. The chromatograms were developed by spraying with a 0.04% solution of bromophenol blue. Curved spots for the acids appeared on a blue background. The decrease of the mobility of acids with increase in the number of polar groups in the molecule is revealed quite distinctly in the circular chromatograms [19]. The acids spots on our chromatograms were in the following sequence of increasing R_f : oxalic - tartaric - malic - succinic - fumaric.

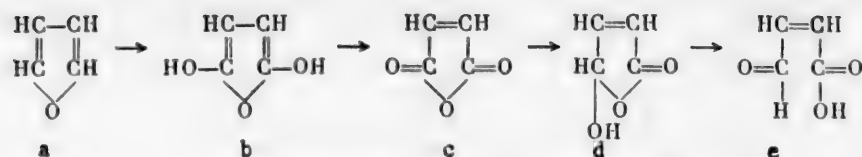
The positions of the spots for the markers and acids of the test mixture are shown in the diagram.

The table contains values of R_f (ratio of the flow rate of the substance to the flow rate of the solvent) for control acids and acids in the tested mixtures.

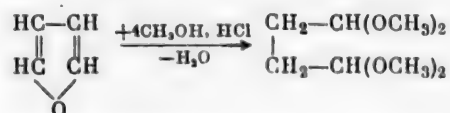
The chemistry of opening of the furan ring by the method of Milas and Walsh [4] is represented by the following scheme:



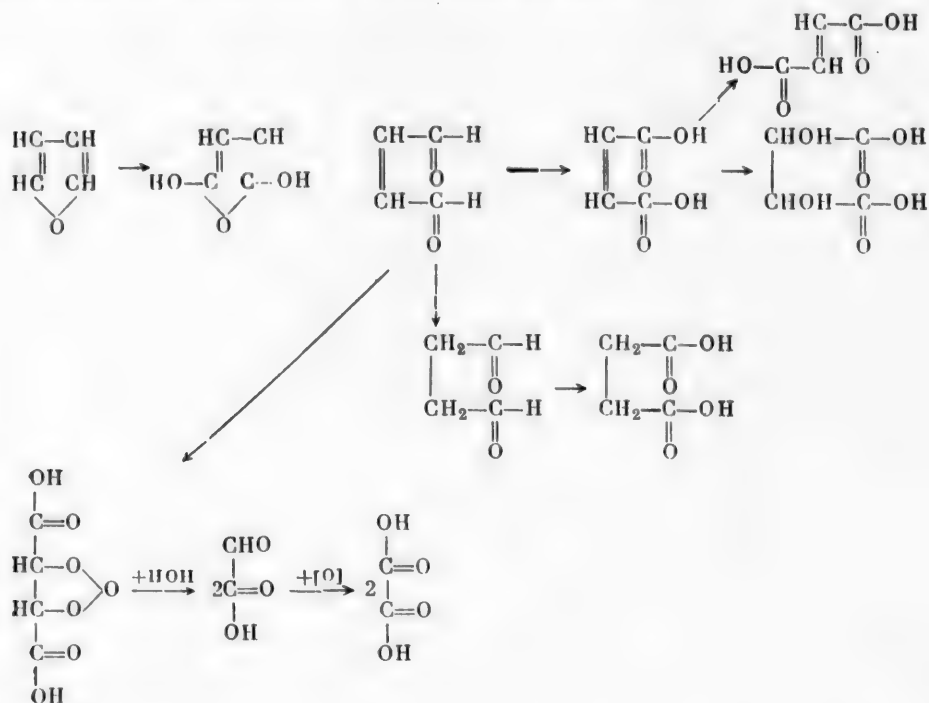
The conversion begins with formation of the hypothetical peroxide (II). However, by analogy with the oxidation of benzene and other aromatic hydrocarbons, the catalytic oxidation of furan may occur by another mechanism, involving hydroxylation of the ring in the α, α positions [7]:



This scheme (presented here in abbreviated form) is confirmed by the following considerations. Liquid-phase catalytic oxidation of furfural in presence of vanadium pentoxide [3] yields maleic monoaldehyde (d) in addition to furmaric acid, whereas breakage of the ring of peroxide (II) should give the dialdehyde and not the monoaldehyde of the same acid; therefore the assumption that the peroxide is formed as an intermediate product is unjustified. Nevertheless, in our opinion the question of the predominant significance of the monoaldehyde of maleic acid in the chain of furan conversions cannot be regarded as finally solved. The formation of 1,4-dicarbonyl compounds by breakage of the furan ring was noted long ago by Harries [20] when furan was heated with methyl alcohol saturated with hydrogen chloride:



Since there is an evident connection between the even number of carbon atoms in the furan ring and the even number of carbon atoms in the carboxylic acids formed from it by decomposition under definite conditions, in our opinion the following reaction scheme for ring opening is possible:



Our proposed mechanism of opening of the furan ring can account for formation of C_2 - C_4 dicarboxylic acids on the basis of common initial conversion stages and of the small number of common intermediate products found up to now among the decomposition products. The central position in the mechanism is occupied by maleic dialdehyde, conversions of which give rise to the formation of dicarboxylic and hydroxydicarboxylic acids.

A method based on direct titration of the hot eluate by a solution of the sodium salt of phenolphthalein [21] was used for quantitative determination of acids in the mixture after chromatographic separation. The titer of the solution was 1270 γ .

5 microliters or 290 γ of substance was transferred consecutively from the solution of the acid mixture onto the chromatogram by means of a graduated pipet.

Taken for titration of acids (ml)	tartaric 0.13	maleic 0.88	succinic 0.10
Found (in γ) (in %)	0.36 12.4	190 65.5	44 15.1

SUMMARY

1. Oxidation of furan by hot perhydrol under pressure is a multistage process which results in the formation of various compounds, among which were detected acetaldehyde, and acetic, tartaric, succinic, and maleic acids. Among the solid dicarboxylic and hydroxydicarboxylic acids the predominant component is maleic acid.

2. A method for analysis of the simplest dicarboxylic acids by paper chromatography is described.

3. A reaction scheme is proposed, representing the consecutive decomposition of furan in the liquid phase at elevated temperatures to yield dicarboxylic acids through maleic dialdehyde.

LITERATURE CITED

- [1] A. P. Salchinkin, Trans. Kuban' Agric. Inst. 2 (30), 220 (1955).
- [2] A. P. Salchinkin, L. B. Lapkova and A. P. Arestenko, J. Appl. Chem. 28, No. 2, 216 (1955).*
- [3] A. M. Bulygina, Oil and Fat Ind. 4, 43 (1934).
- [4] N. A. Milas and W. Walsh, J. Am. Chem. Soc. 57, 8, 1389 (1935).
- [5] E. R. Nielsen, Ind. Eng. Ch. 41, 2, 365 (1949).
- [6] M. V. Tarvid, S. A. Giller and P. I. Kalnin', Bull. Acad. Sci. Latvian SSR 11 (64), 57 (1952).
- [7] P. F. Kalnin', S. A. Giller and M. V. Tarvid, Bull. Acad. Sci. Latvian SSR 3 (44), 443 (1951).
- [8] S. A. Giller and M. V. Tarvid, Bull. Acad. Sci. Latvian SSR 11 (64), 89 (1952).
- [9] Organic Syntheses, 1 (II, Moscow, 1949) p. 449 [Russian translation].
- [10] A. P. Salchinkin and L. B. Lapkova, J. Appl. Chem. 29, No. 1, 141 (1956).*
- [11] Chemical Reagents and Preparations (Handbook) [In Russian] (State Sci. Tech. Press Chem. Lit. Moscow-Leningrad, 1953).
- [12] N. A. Shilov, Volumetric Analysis [In Russian] (Moscow, 1928).
- [13] K. I. Ivanov, V. K. Savinova and E. G. Mikhailova, J. Gen. Chem. 16, No. 1, 65 (1946).
- [14] N. Ya. Dem'yanov and N. D. Pryanishnikov, General Methods of Analysis of Plant Substances [In Russian] (ONTI, Goskhimizdat, Moscow-Leningrad, 1933).
- [15] J. Thorpe and M. Whiteley, Manual of Organic Chemical Analysis (ONTI, Moscow, 1937) [Russian translation].
- [16] A. Frey and D. Wegener, Z. Lebensmittel-untersuch. und Forschung, 104, 2, 127 (1956).
- [17] A. N. Boyarkin, Plant Physiology 2, 3, 298 (1955).
- [18] R. Ya. Shkol'nik, Trans. Commission on Analytical Chem. 6 (9), 502 (1955).
- [19] N. A. Fuks, in the book: Reactions and Methods of Investigation of Organic Compounds [In Russian] (Goskhimizdat, Moscow-Leningrad, 1951) 1, p. 179.
- [20] C. Harries, Ber. 31, 37 (1898).
- [21] N. P. Zueva, Plant Physiology 1, 1, 91 (1954).

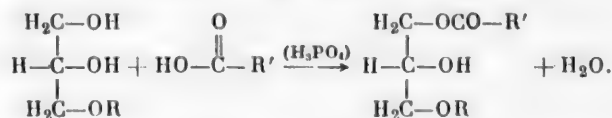
Received April 16, 1958

*Original Russian pagination. See C.B. Translation.

PREPARATION OF ESTERS OF 1-ALKOXYPROPANEDIOL-2,3

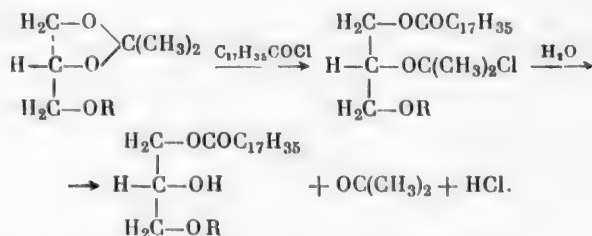
M. S. Malinovskii and V. M. Vvedenskii

It is known that ether-esters of ethylene glycol of the type $\text{ROCH}_2\text{CH}_2\text{OOCCH}_3$ (such as cellosive acetate, etc), are good solvents for nitrocellulose, coumarone, shellac, and certain other resins, and are widely used for such purposes. We considered that esters of glycerol ethers of the general formula $\text{R}'\text{COO}-\text{CH}_2-\text{CH}(\text{OH})-\text{CH}_2\text{OR}$ should be of interest as solvents and plasticizers. Since only a few of these compounds are described in the literature, we undertook the task of their preparation. They were prepared by direct acylation (in presence of 85% phosphoric acid) of glycerol α -monoethers by the corresponding acids:



The following compounds, not described in the literature, were prepared by this method: 1-ethoxy-3-acetatepropanol-2, 1-isopropoxy-3-acetatepropanol-2, 1-n-butoxy-3-acetatepropanol-2; 1-isobutoxy-3-acetatepropanol-2, 1-isoamyloxy-3-acetatepropanol-2, 1-allyloxy-3-acetatepropanol-2, 1-ethoxy-3-propionatepropanol-2, 1-n-butoxy-3-propionatepropanol-2, 1-isoamloxy-3-propionatepropanol-2, 1-ethoxy-3-butyratepropanol-2, 1-n-butoxy-3-butyratepropanol-2, 1-isobutoxy-3-butyratepropanol-2, and 1-isoamyloxy-3-butyratepropanol-2. The yields of the esters reached 70% and sometimes exceeded 90% of the theoretical.

All the esters are colorless and odorless liquids (the only exception is 1-allyloxy-3-acetatepropanol-2, which has a peculiar odor), and are miscible with alcohol, ether, and acetone. In addition to these esters, we prepared 1-ethoxy-3-stearatepropanol-2, 1-butoxy-3-stearatepropanol-2, and 1-isobutoxy-3-stearatepropanol-2 by the method described by Averill [1] from γ -alkoxy- α,β -isopropylideneglycerol and stearoyl chloride (in presence of quinoline) as follows:



The isopropylidene compounds required for the reaction were prepared by the method of Fischer [2] and Irvine et al [3].

To verify the structure of the synthesized esters, some of them were oxidized by chromic anhydride in acetic acid (by the usual method). The oxidation products do not reduce ammoniacal silver oxide solution or Fehling solution, and form semicarbazones with semicarbazide. This shows that the oxidation products contain keto groups formed from secondary alcohol groups in the ethers.

Acylated α -Monoethers of Glycerol

Ester No.	Formulas	Boiling point (deg)	d_4^{20}	n_D^{20}	Yield (%)	Analytical data (%)			
						found		calculated	
						C	H	C	H
1	$\text{CH}_3\text{COOCH}_2\text{CH}(\text{OH})-\text{CH}_2\text{O}-\text{C}_4\text{H}_9$	91 (mm Hg)	1.0683	1.4372		51.26	9.18	51.83	8.70
2	$\text{CH}_3\text{COOCH}_2\text{CH}(\text{OH})-\text{CH}_2\text{O}-\text{CH}(\text{CH}_3)_2$	92 (5)	1.06210	1.4358	69.4	54.19	9.41	54.52	9.15
3	$\text{CH}_3\text{COOCH}_2\text{CH}(\text{OH})-\text{CH}_2\text{O}-\text{C}_4\text{H}_9$	102 (5)	1.0400	1.4404	92.3	56.41	9.41	56.80	9.53
4	$\text{CH}_3\text{COOCH}_2\text{CH}(\text{OH})-\text{CH}_2\text{O}-\text{CH}_2\text{CH}(\text{CH}_3)_2$	102 (5)	1.0267	1.4388	83.7	56.49	9.32	56.80	9.53
5	$\text{CH}_3\text{COOCH}_2\text{CH}(\text{OH})-\text{CH}_2\text{O}-\text{CH}_2\text{CH}_2\text{CH}(\text{CH}_3)_2$	101 (4)	1.0186	1.4374	53.3	58.55	10.06	58.80	9.87
6	$\text{CH}_3\text{COOCH}_2\text{CH}(\text{OH})-\text{CH}_2\text{O}-\text{CH}_2\text{CH}=\text{CH}_2$	97 (5)	1.0709	1.4468	72.1	54.64	8.50	55.15	8.10
7	$\text{C}_4\text{H}_9\text{COOCH}_2\text{CH}(\text{OH})-\text{CH}_2\text{O}-\text{C}_4\text{H}_9$	98-100 (5)	1.0352	1.4408	71.8	54.36	9.41	54.52	9.15
8	$\text{C}_4\text{H}_9\text{COOCH}_2\text{CH}(\text{OH})-\text{CH}_2\text{O}-\text{C}_4\text{H}_9$	104 (5)	1.0287	1.4438	48.6	58.44	10.00	58.80	9.87
9	$\text{C}_4\text{H}_9\text{COOCH}_2\text{CH}(\text{OH})-\text{CH}_2\text{O}-\text{CH}_2\text{CH}_2\text{CH}(\text{CH}_3)_2$	102 (4)	1.0096	1.4445	51.8	60.25	10.40	60.52	10.16
10	$\text{C}_4\text{H}_9\text{COOCH}_2\text{CH}(\text{OH})-\text{CH}_2\text{O}-\text{C}_4\text{H}_9$	105 (7)	1.0364	1.4888	80.5	56.40	9.90	56.80	9.53
11	$\text{C}_4\text{H}_9\text{COOCH}_2\text{CH}(\text{OH})-\text{CH}_2\text{O}-\text{C}_4\text{H}_9$	107 (5)	1.0082	1.4468	71.8	60.20	10.45	60.52	10.16
12	$\text{C}_4\text{H}_9\text{COOCH}_2\text{CH}(\text{OH})-\text{CH}_2\text{O}-\text{CH}_2\text{CH}(\text{CH}_3)_2$	105 (5)	1.0088	1.4466	52.5	60.26	10.36	60.52	10.16
13	$\text{C}_4\text{H}_9\text{COOCH}_2\text{CH}(\text{OH})-\text{CH}_2\text{O}-\text{CH}_2\text{CH}_2\text{CH}(\text{CH}_3)_2$	112 (5)	1.0011	1.4474	32.8	71.63	10.31	62.08	10.41
14	$\text{C}_{17}\text{H}_{33}\text{COOCH}_2\text{CH}(\text{OH})-\text{CH}_2\text{O}-\text{C}_4\text{H}_9$	M.p. 49	—	—	—	71.03	12.26	71.44	12.00
15	$\text{C}_{17}\text{H}_{33}\text{COOCH}_2\text{CH}(\text{OH})-\text{CH}_2\text{O}-\text{C}_4\text{H}_9$	M.p. 50-51	—	—	—	72.02	12.43	72.41	12.15
16	$\text{C}_{17}\text{H}_{33}\text{COOCH}_2\text{CH}(\text{OH})-\text{CH}_2\text{O}-\text{CH}_2\text{CH}(\text{CH}_3)_2$	M.p. 50	—	—	—	72.16	12.56	72.41	12.15

EXPERIMENTAL

Synthesis of 1-butoxy-3-acetatepropanol-2. 37 g of glycerol monobutyl ether and 15 g of glacial acetic acid were mixed with 30 ml of carbon tetrachloride, and 1.5 g of 85% phosphoric acid was added to the mixture. The mixture was heated for 3 hours on a water bath, after which carbon tetrachloride was evaporated off and the residue was distilled under vacuum. The product was a colorless liquid of b.p. 102° (6 mm), d_4^{20} 1.0400, n_D^{20} 1.4404, miscible with alcohol, acetone, and ether. The yield was 92.3% of the theoretical.

Found %: C 56.41, H 9.41. $C_9H_{18}O_4$. Calculated %: C 56.80, H 9.53.

The surface tension α_1 = 43.11 dynes/cm.

The same method was used for preparation of other esters of the type



the properties of which are given in the table (No. 1-13).

Acylated α -Monoethers of Glycerol

Glycerol- γ -ethoxy- α, β -isopropylidene. 60 g of glycerol α -monoethyl ether was mixed with 270 ml of acetone. A small amount of concentrated hydrochloric acid (about 0.1% of the total weight of the reaction mass) was added to the solution. The mixture was left to stand for 24 hours, after which the acid was neutralized by barium carbonate, the acetone was evaporated on a water bath, and the residue was distilled under vacuum. The yield was 50 g (62.5%) of a colorless liquid with a faint odor, which distilled at 41-41° (5 mm); d_4^{20} 0.9580, n_D^{20} 1.4202; found MR_D 42.61, calculated MR 42.97.

Glycerol- γ -butoxy- α, β -isopropylidene of b.p. 64° (5 mm), d_4^{20} 0.9306, n_D^{20} 1.4240, found MR_D 51.88, calculated MR 52.20, was prepared similarly.

Glycerol- γ -isobutoxy- α, β -isopropylidene of b.p. 62° (6 mm), d_4^{20} 0.9300, n_D^{20} 1.4218, found MR_D 51.71, calculated MR 52.20, was prepared by the same method as glycerol- γ -ethoxy- α, β -isopropylidene.

1-Ethoxy-3-stearatepropanol-2. 81.8 g of stearoyl chloride, prepared from stearic acid and phosphorus pentachloride [4], was mixed at room temperature in a round-bottomed flask fitted with a reflux condenser with 48 g of glycerol- γ -ethoxy- α, β -isopropylidene. 38.7 g of quinoline was added to the mixture. Heat was evolved during the reaction. At the end of the reaction the mass was heated on a water bath (at 70°) for 30 minutes and cooled, and then hydrolyzed by addition of 5 N hydrochloric acid. The 1-ethoxy-3-stearatepropanol-2 was filtered off, washed with water, recrystallized twice from 96% ethyl alcohol, and then dried in a desiccator.

The substance consists of white crystals, m.p. 49°, soluble in alcohol and ether.

Found %: C 71.03, H 12.26. $C_{23}H_{46}O_4$. Calculated %: C 71.44, H 12.00.

The other stearate esters detailed in the table (No. 14-16) were prepared similarly.

SUMMARY

Direct acylation (in presence of 85% phosphoric acid) of glycerol α -monoethers by acids gives esters of glycerol monoethers in yields from 70 to 90% of the theoretical. They can be prepared by the action of acid chlorides on isopropylidene derivatives of glycerol monoethers.

LITERATURE CITED

- [1] H. Averill and J. Koche, C. King, J. Am. Chem. Soc. 51, 868 (1929).
- [2] E. Fischer, Ber. 28, 1169 (1895).
- [3] J. Irvine, H. Macdonald and E. Soutar, J. Am. Chem. Soc. 37, 346 (1915).
- [4] F. Kraff and J. Bürger, Ber. 17, 1378 (1884).

Received March 27, 1958

*As in original — Publisher's note.

BRIEF COMMUNICATIONS

REACTIONS OF THE TETRACHLORIDES OF TIN, GERMANIUM AND TITANIUM WITH SILICON-COPPER ALLOY

D. A. Kochkin, M. F. Shostakovskii

and L. V. Musatova

(N. D. Zelinskii Institute of Organic Chemistry, Academy
of Sciences USSR)

In an attempt to use carbon tetrachloride for direct synthesis of organosilicon compounds by the action of carbon tetrachloride vapor on silicon-copper alloy (80:20) at 260-300° we obtained silicon tetrachloride in 85% yield and a small amount of tetrachloroethylene [1, 2].

Patnode and Schiessler [3], who studied the reaction of carbon tetrachloride with silicon-copper alloy (90:10), obtained only tetrachloroethylene and hexadichlorosilane. Silicon tetrachloride was not found in the reaction products. In contrast to the results of Patnode and Schiessler, the formation of silicon tetrachloride was also reported when carbon tetrachloride vapor was passed over ferrosilicon at temperatures above 500° [4].

The present paper deals with a study of reactions of tetrachlorides of other group IV elements—tin, germanium and titanium—with silicon-copper alloy. We found that the tetrachlorides of tin and germanium also react with the alloy at 260-500° with formation of silicon tetrachloride and deposition of metallic tin or germanium on the alloy surface. In distinction from the other group IV elements, titanium tetrachloride does not exchange its chlorine atoms even at 700°.

The ease with which chlorine atoms are exchanged in these tetrachlorides diminishes in the series $C > Sn > Ge > Si > Ti$, which corresponds to the series of increasing bond energies between group IV elements and chlorine (in kcal): $C-Cl-70$, $Sn-Cl-76$, $Ge-Cl-81$, $Si-Cl-87$, $Ti-Cl-102$, given by Cottrell [5].

It follows that under the conditions of our investigation titanium tetrachloride has the greatest thermal stability. The halides of carbon, tin, and germanium have lower bond energies and are converted into silicon tetrachloride by the action of silicon-copper alloy.

An additional explanation of the higher stability of titanium halides is that titanium has more pronounced metallic properties than the other elements in the carbon subgroup of the Mendeleev periodic system.

Because of the inertness of titanium tetrachloride toward silicon-copper alloy it can be used in the direct synthesis of alkyl(aryl) halosilanes as a diluent for the halogen compounds used in the reaction.

EXPERIMENTAL

Reaction of tin tetrachloride with copper-silicon alloy (20:80). A glass tube 18 mm in diameter and 600 mm long, fitted with an electric heater, dropping funnel, receiver, and trap, and cooled in a mixture of acetone and solid carbon dioxide, was packed with 150-200 g of copper-silicon alloy (20:80) in the form of pieces 5-8 mm in diameter. The alloy in the tube was dried in a stream of nitrogen at 200° for 2-3 hours. After the nitrogen had been blown through, the temperature in the reaction tube was raised to 270-300°, and tin tetrachloride, $SnCl_4$ (b.p. 114°, d_4^{20} 2.230; literature data: 114°, d_4^{20} 2.232) was added dropwise from a graduated

TABLE 1

Fractionation of the Products Formed in the Reaction of Tin Tetrachloride with Silicon-Copper Alloy (20:80)

Boiling point (deg)	Yield (%)	d_4^{20}
57-58	66.3	1.5008
57-112	9.2	
112-114	19.0	2.229
High-boiling residue	3.4	

TABLE 2

Fractionation of the Products Formed in the Reaction of Germanium Tetrachloride with Silicon-Copper Alloy at Various Temperatures

Fraction No.	Boiling point (deg)	Yields of fractions (%) of different temperature (deg)		
		300-320	400	500
1	56-58	0.8	26.5	42.0
2	58-80	0.9	1.3	1.2
3	80-83	95.3	60.2	56.0
4	High-boiling residue	1.0	2.1	1.8

products were collected in a receiver cooled in a mixture of ice and salt, and in a trap immersed in a mixture of acetone and solid carbon dioxide. During 34.5 hours 564.0 g of reaction product was obtained; after fractionation, this yielded 550.0 g (92.6% of the theoretical) of germanium tetrachloride (b.p. 82.8° at 756 mm; d_4^{20} 1.873; literature data: b.p. 83.1°, d_4^{20} 1.874).

b) Reaction of germanium tetrachloride with copper-silicon alloy (20:80). The reaction tube was packed with 148.0 g of alloy, and 150 g of germanium tetrachloride was passed during 8.0 hours at 300-320°. The amount of reaction product collected was 107.0 g, containing 0.8 g (0.8%) of silicon tetrachloride and 99.9 g (95.3%) of unchanged germanium tetrachloride. This method was used for the reaction of germanium tetrachloride with the alloy at 400 and 500°. The results of the experiments are given in Table 2.

According to the analytical data, the fraction of b.p. 56-58° consisted mainly of silicon tetrachloride; the fraction of b.p. 80-83° was unchanged germanium tetrachloride.

It follows from the data in Table 2 that germanium tetrachloride is converted into silicon tetrachloride at a higher temperature (about 400-500°) than the tetrachlorides of carbon or tin. Metallic germanium is deposited on the solid mass in the form of a fine powder during the reaction.

SUMMARY

The tetrachlorides of elements of group IV of the periodic system - carbon, germanium, and tin - are converted into silicon tetrachloride when passed over copper-silicon alloy at 260-500°.

dropping funnel at the rate of 20 ml per hour. The total amount of tin tetrachloride added was 120 g. The yield was 95.0 g of liquid products; these were fractionated through a column of 20 theoretical plates into the fractions detailed in Table 1.

According to analytical data, the 1st fraction (b.p. 57-58°; found Cl 83.0%; calculated Cl for SiCl_4 83.4%) was silicon tetrachloride. The 3rd fraction (b.p. 112-114°) was unchanged tin tetrachloride. Metallic tin was deposited in the form of fine granules on the alloy in the reaction tube.

Reaction of titanium tetrachloride with copper-silicon alloy (20:80). The apparatus and method were the same as described above. From 120 to 150 g of titanium tetrachloride (b.p. 132.6° at 743.2 mm, d_4^{20} 1.76, n_D^{20} 1.605; literature data: b.p. 136.5°, d_4^{20} 1.176, $n_D^{16.5}$ 1.61) was passed in each experiment, at temperatures of 300, 400, 500, 600 and 700° respectively. In all cases the titanium tetrachloride was returned unchanged; it was not converted into silicon tetrachloride.

Conversion of Germanium Tetrachloride into Silicon Tetrachloride

a) Preparation of germanium tetrachloride. The glass reaction tube described above was packed with 201.0 g of metallic germanium in the form of 5-10 mm granules. Chlorine gas, previously dried over sulfuric acid and anhydrous calcium chloride, was then passed through at 260-310°. The reaction

LITERATURE CITED

- [1] M. F. Shostakovskii, D. A. Kochkin and L. V. Laine, J. Appl. Chem. 30, 1401 (1957). *
- [2] M. F. Shostakovskii, D. A. Kochkin and L. V. Laine, Authors' Certif. 108316.
- [3] W. J. Patnode and R. W. Schlessler, U.S. Patent 2,381,001 (1945); C.A. 39, 4888 (1945).
- [4] M. G. Voronkov, Work of Russian and Soviet Scientists on the Chemistry of Organosilicon Compounds [In Russian] (Leningrad State Univ. Press, 1952).
- [5] T. L. Cottrell, Strengths of Chemical Bonds (IL, Moscow, 1956) pp. 158-164 [Russian translation].

Received May 8, 1958

*Original Russian pagination. See C.B. Translation.

THERMAL DECOMPOSITION OF CERTAIN SULFATES IN A CURRENT OF STEAM

A. B. Suchkov, B. A. Borok and Z. I. Morozova

Thermal decomposition of sulfates provides solutions to numerous technological problems. These include the production or recovery of sulfuric acid, preparation of pure oxides or hydroxides, phase separation of sulfate mixtures, preparation of double oxides (such as ferrites), and beneficiation of sulfate concentrates.

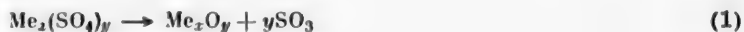
Decomposition of sulfates in a current of steam is of special interest for two reasons. First, this process can be used for direct production of concentrated sulfuric acid [1], and second, in a number of cases the reaction is considerably accelerated by the use of steam. We investigated the thermal decomposition of a number of sulfates in a current of steam. The results are of definite interest.

The apparatus used for the experiments on decomposition in steam was described earlier [1]. The experimental procedure is detailed in the same paper. The decomposition of the sulfates of lithium, sodium, potassium, copper, beryllium, magnesium, calcium, aluminum, titanium, chromium, manganese, iron, cobalt and tin was studied.

The experiments were performed in the 200-1000° temperature range. The results are given in the table. Here, as in the other publications [1, 2] the yield η of sulfuric acid is expressed in molar percentages:

$$\eta = \frac{\text{number of moles of H}_2\text{SO}_4 \text{ obtained} \cdot 100}{\text{number of moles of H}_2\text{SO}_4 \text{ in the original sulfate.}}$$

The table gives the yields (cumulative) of sulfuric acid after definite times in minutes, with water passed at a rate of 0.1 ml per minute. The data in the table, of course, do not present a kinetic picture of the decomposition of sulfates in a current of steam. These results merely show that sulfates are decomposed very rapidly in a current of steam. Our experiments on the decomposition of iron, aluminum, and titanium sulfates in a current of dry argon gave much lower decomposition rates. This is not only because water has a high tendency to decomposing oxide films, but also because the reaction



is accompanied, for a number of sulfates, by the reactions



and



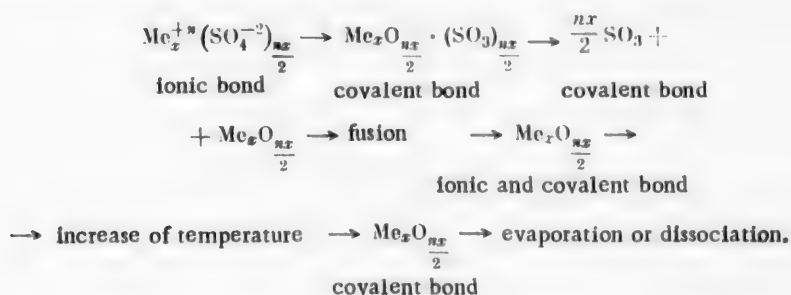
Moreover, it follows from the table that salts containing cations of higher valences decompose at lower temperatures.

When the relative stabilities of salts are considered, it is generally assumed that the stronger the ionic bond in the oxide formed, the greater the weakening of the complex anion in the original sulfate. Comparison of the sulfate decomposition temperature ranges in the table with the lattice energies of the oxides, calculated by Kapustinskii's method, shows that the inverse relationship between them is approximate only.

Results of Experiments on Decomposition of Sulfates

Sulfate	Temperature (deg)	Yield η (molar %) after time (minutes)					
		10	20	30	40	50	60
$\text{Ti}(\text{SO}_4)_2$	400	1.59	2.04	2.24	2.42	2.62	2.80
	500	3.96	6.70	9.31	11.00	12.50	13.92
	600	12.35	24.70	35.80	39.60	42.80	45.50
	700	45.80	63.80	68.00	70.80	72.90	74.80
FeSO_4	400	0.12	0.17	0.19	0.22	0.23	0.24
	500	0.75	1.48	2.23	2.80	3.34	3.83
	600	4.65	9.10	13.80	17.50	21.00	24.10
	700	19.00	33.20	45.00	52.00	57.60	62.30
$\text{Cr}_2(\text{SO}_4)_3$	400	10.02	13.61	15.07	15.97	16.65	17.32
	500	7.00	12.76	17.63	20.75	22.64	23.75
	600	8.80	13.66	16.95	19.70	22.35	24.70
	700	11.09	21.60	32.40	39.40	45.30	48.80
$\text{Al}_2(\text{SO}_4)_3$	400	0.15	0.27	0.35	0.35	0.35	0.35
	500	0.99	1.25	1.36	1.41	1.46	1.50
	600	2.11	2.80	3.32	3.75	4.13	4.40
	700	5.25	8.70	10.65	11.95	12.90	13.50
	800	18.30	32.00	43.60	53.00	58.00	65.50
CuSO_4	600	0.42	0.67	0.74	0.74	0.74	0.74
	700	0.59	1.02	1.32	1.56	1.76	1.92
MnSO_4	600	0.19	0.28	0.28	0.28	0.28	0.28
	700	0.38	0.52	0.56	0.59	0.62	0.65
NiSO_4	600	0.58	0.86	1.02	1.21	1.38	1.55
CaSO_4	1000	0.18	0.34	0.46	0.58	0.71	0.83
BeSO_4	500	0.61	1.14	1.66	2.17	2.60	2.85
	600	1.45	2.72	3.50	3.87	4.10	4.20
Na_2SO_4	900	—	—	—	—	—	0.09
	1000	—	—	—	—	—	0.23
K_2SO_4	1000	—	—	—	—	—	0.73
	200	0.29	0.42	0.53	0.60	0.63	0.65
$\text{Sn}(\text{SO}_4)_2$	250	0.35	0.60	0.84	1.07	1.20	1.25
	300	1.74	3.34	4.82	6.10	7.30	8.00

We consider that differences in the decomposition temperatures of sulfates are associated with the general tendency of inorganic compounds to a transition from ionic to covalent bonding with increase of temperature. This tendency is observed in many classes of inorganic compounds. Transition from the one type of bonding to the other is generally effected through stages of fusion, evaporation, dissociation, or polymorphic transformation. Some classes of compounds show a measure of correlation between bond type and state of aggregation. In the present instance this transition can be represented by the following scheme:



SUMMARY

Decomposition of certain sulfates in a current of steam is an effective means for production of sulfuric acid and the corresponding oxides, and proceeds at lower temperatures than ordinary thermal decomposition.

LITERATURE CITED

- [1] A. B. Suchkov, B. A. Borok and Z. L. Morozova, J. Appl. Chem. 32, No. 6, 1382 (1959).*
- [2] A. B. Suchkov, B. A. Borok and Z. L. Morozova, J. Appl. Chem. 32, No. 7, 1618 (1959).*

Received October 4, 1958

*Original Russian pagination. See C.B. Translation.

THERMAL DECOMPOSITION OF A MIXTURE OF $\text{MnSO}_4 + \text{FeSO}_4$ IN A CURRENT OF STEAM

A. B. Suchkov, B. A. Borok and Z. I. Morozova

The salts used in our experiments on thermal decomposition in a current of steam included the sulfates of iron and manganese. Studies of the thermal decomposition of these salts are of interest from two points of view. First, by lowering the thermal decomposition temperature of FeSO_4 by our method it is possible to recover sulfuric acid from spent pickling liquors. Second, the iron oxide used in the storage-cell industry should be free from manganese. In this connection it is of definite importance to find at what temperatures only ferrous sulfate is decomposed in mixtures of $\text{MnSO}_4 + \text{FeSO}_4$.

There are considerable discrepancies between data of different authors on the thermal decomposition of ferrous sulfate [1-3]. There are relatively few publications on the thermal decomposition of manganese sulfate [4-7].

Analysis of the data in these publications leads to the conclusion that it may be possible to find a temperature at which ferrous sulfate is decomposed while manganese sulfate remains unchanged. This would provide a method for separating the components of the mixture.

EXPERIMENTAL

The apparatus used for thermal decomposition of ferrous and manganese sulfates in a current of steam was described earlier [8]. The characteristic feature of the apparatus is that superheated steam, which entrains sulfur oxides, is passed at a strictly defined rate over the sulfate at a definite temperature. The amounts of liberated oxides can be determined at any required time intervals. The sulfuric acid formed as the result of the decomposition can be concentrated by a special procedure.

Chemically pure salts were used for the experiments. The sulfates were dehydrated in the same apparatus. The dehydration time was 30-40 minutes. During this time $\text{FeSO}_4 \cdot 7\text{H}_2\text{O}$ loses a relatively small amount of sulfur oxides with the water of crystallization; for example, when the temperature is raised uniformly to 400° the loss is 0.125 molar %; up to 500° it is 0.70% and up to 600° , 2.28%. Sulfur oxides are not lost with water of crystallization from MnSO_4 at these temperatures.

Water was fed into the apparatus at the rate of 0.1 ml/minute. The columns of substances used were of approximately the same height. The particle size was kept within the 0.08-0.1 mm range.

DISCUSSION OF RESULTS

The results of some of the experiments are given in Table 1.

In experiments with the circulation unit [8] at 500° the ferric oxide obtained contained spectroscopic traces of impurities and, according to GIPI-4 analyses, it was a pigment of excellent quality. The concentration of the sulfuric acid formed in the process was 96%. The sulfuric acid yield was 50%.

*Here, as before [8], the yield of acid is expressed as a molar percentage (η):

$$\eta = \frac{\text{number of moles of } \text{H}_2\text{SO}_4 \text{ obtained} \cdot 100}{\text{number of moles of } \text{H}_2\text{SO}_4 \text{ in the original sulfate.}}$$

TABLE 1

Results of Experiments on Decomposition of Ferrous and Manganese Sulfates

Salts	Temperature (deg)	H ₂ SO ₄ yield η (in molar %) during reaction time (min)					
		10	20	30	40	50	60
FeSO ₄	400	0.124	0.170	0.194	0.215	0.228	0.243
	500	0.75	1.48	2.23	2.80	3.34	3.83
	600	4.65	9.10	13.80	17.50	21.0	24.1
	700	19.0	33.2	25.0	52.0	57.6	62.3
MnSO ₄	600	0.19	0.28	0.28	0.28	0.28	0.29
	700	0.33	0.52	0.56	0.59	1.62	0.65
	800	1.06	1.56	1.68	1.77	1.86	1.95

TABLE 2

Results of Experiments on Decomposition of Mixtures of FeSO₄ + MnSO₄

Salts	H ₂ SO ₄ yield η (molar %) during reaction time (min)					
	10	20	30	40	50	60
FeSO ₄ + 1% MnSO ₄	6.2	11.6	16.4	20.2	23.0	27.5
FeSO ₄ + 5% MnSO ₄	6.8	13.4	19.4	24.6	29.6	33.0
FeSO ₄ + 10% MnSO ₄	6.0	12.2	17.3	21.5	24.8	28.0

TABLE 3

Results of Experiments on Decomposition of Mixtures in a Circulation Unit

Salts	Mn content in FeSO ₄ after expt.	Iron content in MnSO ₄ after expt. (%)	Degree of decomposition of FeSO ₄ (%)	Amount of MnSO ₄ after expt. (% of original)
FeSO ₄ + 1% MnSO ₄	Traces	7.4	99.8	100
FeSO ₄ + 5% MnSO ₄	"	4.4	99.4	100
FeSO ₄ + 10% MnSO ₄	"	2.34	99.3	100

The data in Table 1 indicate that under these conditions FeSO₄ can be decomposed completely in the 500-600° range, while MnSO₄ remains almost unchanged; moreover, the sulfur oxides liberated by the decomposition of FeSO₄ should retard decomposition of MnSO₄. Experiments on decomposition of sulfate mixtures showed that the optimum temperature, with regard to the rate of the process and the purity of the ferric oxide formed, is 600°. The results of experiments at this temperature are given in Table 2.

These results show that the rate of liberation of sulfur oxides is close to that observed during decomposition of pure FeSO₄. Investigations by electron diffraction and petrographic methods showed total absence of manganese oxides in the solid residues from the experiments.

In order to investigate the efficiency of this process, we decomposed the same mixtures in a circulation unit at 600°. After two hours of reaction the solid residues were washed three times with water, with stirring, at 10:1 liquid-solid ratio. The ferric oxide was filtered off, dried, and analyzed. The filtrate was evaporated to dryness and iron was determined in the residue (the results are summarized in Table 3).

The ferric oxide so obtained also had pigment properties. The yield of sulfuric acid was up to 50%.

SUMMARY

1. By decomposition of ferrous sulfate in a current of steam at 500° it is possible to obtain high-quality ferric oxide and to recover considerable amounts of 96% sulfuric acid.

2. By decomposition of mixtures of ferrous and manganese sulfates in a current of steam at 600°, followed by washing of the solid residue with water, it is possible to obtain ferric oxide free from manganese compounds.

LITERATURE CITED

- [1] S. D. Shargorodskii and K. K. Sigalovskii, *Mem. Inst. Chem. Acad. Sci. Ukrainian SSR* 7, 141 (1940).
- [2] M. E. Pozin and A. M. Ginstling, *J. Appl. Chem.* 23, 1149 (1950).*
- [3] M. E. Pozin and A. M. Ginstling, *J. Appl. Chem.* 24, 134 (1951).*
- [4] K. Friedrich, *Metallurgie*, 7, 323 (1910).
- [5] G. Marchal, *J. Chim. Phys.* 22, 559 (1925).
- [6] Yu. V. Klimenko and A. P. Kvaskov, *Chemical Concentration of Manganese Ores* [In Russian] (Metallurgy Press, 1943).
- [7] V. V. Pechkovskii, *J. Appl. Chem.* 28, 237 (1955).*
- [8] A. B. Suchkov, B. A. Borok and Z. L. Morozova, *J. Appl. Chem.* 32, No. 6, 1382 (1959).*

Received October 4, 1958

*Original Russian pagination. See C.B. Translation.

REACTION OF SILICON WITH HYDROGEN CHLORIDE IN A FLUIDIZED BED

K. A. Andrianov, S. A. Golubtsov and

I. V. Trofimova

In a number of papers [1-4] it is reported that trichlorosilane is formed when hydrogen chloride is passed through a tube filled with crystalline silicon or ferrosilicon. The reaction products contained considerable amounts of silicon tetrachloride in addition to trichlorosilane. The percentage of useful conversion of silicon in this reaction is low, the possibility of regulating the composition of the reaction products is not discussed, and the yield per unit time (productivity) is very low.

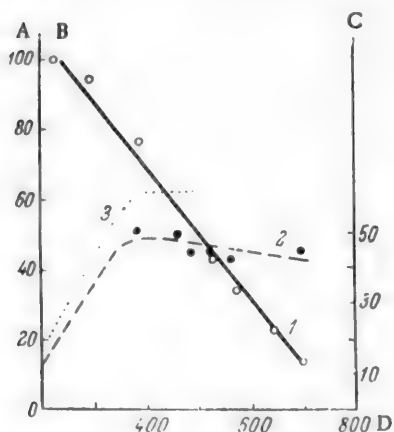


Fig. 1. Effect of reaction temperature on the yield of trichlorosilane: A) HSiCl_3 content of condensate (%), 1; B) degree of conversion (%), 3; C) productivity (g/hour · 100 g), 2; D) temperature (deg).

By analogy with the direct syntheses, described previously, of ethyl- [5, 6], phenyl- [7], and methylchlorosilanes, we effected the reaction between hydrogen chloride and silicon in a fluidized bed, in which silicon powder was agitated by a current of hydrogen chloride. Experiments showed that by this procedure the productivity can be increased sharply (more than 10-fold) and the conversion of silicon improved; it was found that the composition of the reaction products can be regulated by variation of the reaction temperature.

The main product of the reaction between hydrogen chloride and silicon in a fluidized bed is trichlorosilane, formed as follows:



The side reaction of silicon tetrachloride formation



takes place at temperatures above 300°. In addition to trichlorosilane and silicon tetrachloride, the reaction products include dichlorosilane H_2SiCl_2 and high-boiling substances (in all probability chloropolysilanes), but the amounts are very small.

Variations of the composition and yield of reaction products with the temperature are plotted in Fig. 1.

Increase of the reaction temperature to 350-400° results in a considerably increased productivity (yield per unit time) and conversion of hydrogen chloride. Increase of the time of contact between the reactants by increase of the amount of silicon taken from 100 to 180 g raises the conversion of silicon and hydrogen chloride (Table 1).

The results of experiments on the preparation of trichlorosilane by the method described are given in Table 1. Experiments No. 1-9 were carried out in order to determine the effect of temperature on the composition of the reaction products. In experiments No. 10 and 11 the effect of contact time was investigated (by

TABLE 3

Fractionation and Analysis of Reaction Products

Fraction No.	Boiling range (deg)	Condensate from Expt. No. 12 (Table 1)		Condensate from Expt. No. 9 (Table 1)	
		Yield of fraction (wt. %)	trichlorosilane content by analysis (wt. %)	Yield of fraction (wt. %)	trichlorosilane content by analysis (wt. %)
1	30—32	90	100	3	100
2	32—56	Nil	—	7.4	42
3	56—57	Nil	—	84	5
Still residue	3.5	Nil	2.6	Nil
Losses	6.5	—	3	—
Trichlorosilane content of condensate (%):					
from fractionation data (losses as HSiCl_3)		96.5		10.3	
by analysis of condensate		98		14.5	

increase of the amount of silicon taken, with the hydrogen chloride rate maintained at 0.7 liter/minute), and experiments No. 12-14 were carried out by the optimum procedure with the maximum conversion of silicon.

Table 2 contains the principal characteristics of the synthesis of trichlorosilane in a fluidized bed under the optimum conditions, as compared with literature data.

EXPERIMENTAL

The starting materials were hydrogen chloride, made by the action of sulfuric acid (sp. gr. 1.84) on dry common salt, and crystalline silicon of Kr-1 grade.

The apparatus is depicted schematically in Fig. 2. For preparation of the hydrogen chloride, sulfuric acid was added from the dropping funnel 1 into a flask 2 containing common salt. The pressure in the flask was measured by means of the mercury manometer 3. Hydrogen chloride was purified by passage through a vessel 4 with sulfuric acid, and a column 5 packed with small rings, which served as a spray trap. The hydrogen chloride passed through the flow meter 6 into the reactor 7. The reaction products were cooled in the water condenser 8 and partially collected in the receiver 9. Most of the products were condensed in the trap 10, cooled in a mixture of solid carbon dioxide and acetone. The gaseous reaction products were washed with water in the vessel 11 and collected in the gas holder 12.

Experimental procedure. The reactor was charged with silicon crushed to a particle size of 0.075-0.25 mm. The silicon powder was dried at 350-400° for 7-8 hours in a current of nitrogen fed through the meter 6 at a rate of 0.8 liter/minute. The reactor was heated electrically by means of a heater regulated by an LATR-1 autotransformer, and the temperature was checked by means of a thermocouple placed in a socket situated axially in the reactor. The reaction time was 10-12 hours, after which the rate of condensation in the trap 10 fell sharply. At the end of the reaction the reactor was blown through with nitrogen and cooled. The liquid reaction products were fractionated through a packed column with an efficiency of 20 theoretical plates.

By the method developed by S. G. Yagodina and S. V. Syavtsillo, the trichlorosilane content of the mixture can be determined by analytical data on the amount of hydrogen linked to silicon.* The results in Table 3 show satisfactory agreement between the compositions determined by the two methods.

SUMMARY

1. The proposed method for preparation of trichlorosilane mixed with silicon tetrachloride, by the reaction of silicon with hydrogen chloride in a fluidized bed, gives much better yields than those reported in the literature.

*The determinations of hydrogen linked to silicon were performed by S. G. Yagodina.

2. The composition of the reaction products depends on the reaction temperature; the process can be directed toward formation either of trichlorosilane or of silicon tetrachloride.

LITERATURE CITED

- [1] H. Buff and F. Wöhler, *Ann. Chem.* 104, 94 (1857).
- [2] L. Gatterman, *Ber.* 22, 186 (1889); A. N. Warren, *Ch. Eng. News*, 60, 158 (1889).
- [3] F. Combes, *C. r.*, 122, 531 (1896); O. Ruff and K. Albert, *Ber.* 38, 2222 (1905).
- [4] A. G. Taylor and B. V. Walden, *J. Am. Chem. Soc.* 66, 842 (1944).
- [5] K. A. Andrianov, S. A. Golubtsov, L. V. Trofimova, A. S. Denisova and R. A. Turetskaya, *Proc. Acad. Sci. USSR* 108, 3, 465 (1956).*
- [6] K. A. Andrianov, S. A. Golubtsov, L. V. Trofimova and A. S. Denisova, *J. Appl. Chem.* 30, 1277 (1957). *
- [7] K. A. Andrianov, S. A. Golubtsov, N. N. Tishina and L. V. Trofimova, *J. Appl. Chem.* 32, No. 1, 201 (1959). *

Received May 8, 1958

*Original Russian pagination. See C.B. Translation.

TREATMENT OF WASTE WATERS BY DELAYED PRECIPITATION

D. V. Bezuglyi

(V. I. Lenin Polytechnic Institute, Khar'kov)

The structure of a precipitate should correspond to its practical utilization. For example, if a precipitation is used after appropriate treatment as a mineral pigment (lithopone, Prussian blue), the aim in production is to obtain a high degree of dispersity, and difficulties in separating the precipitate from the mother liquor must be overcome. It is much more usual in practice to try to obtain precipitates in the form of well-defined crystals, as such precipitates are much easier to filter off, wash, and transport. In particular, the precipitates formed during treatment of wash liquors from pickling units in metal working factories should conform to these requirements.

Such waters cannot be discharged into public sewage systems without preliminary neutralization of the sulfuric acid and precipitation of iron. Milk of lime is generally used for this purpose; the treatment yields a crystalline precipitate of calcium sulfate and an amorphous precipitate of ferrous hydroxide. Such precipitates are very difficult to separate by filtration; the rate of clarification, considerable at first, slows down progressively. The suspension remains fluid even after prolonged storage, and its content of solids remains low, which makes treatment of the accumulated sludge difficult; it becomes necessary to build costly sludge tanks of high capacity, with appropriate ducts.

On the basis of the general laws governing the formation and growth of solid phases, we have developed a method for precipitation of iron as a coarse precipitate.

TABLE 1

Kinetics of Iron Precipitation by
Ground Shell Rock

Particle-size analysis of shell rock (mm)	Precipitation of iron (%) during boiling time (min)		
	30	60	90
To 0.06	88	96.5	100
0.06—0.088	76	92.5	99
0.088—0.102	62	87	88
0.102—0.2	62	81	87
Chalk-0.102	50	69	85

It is known that the dispersity of a precipitate is determined by the rates of aggregation and orientation; the rate of orientation is a property of a given chemical compound, whereas the rate of aggregation depends on the precipitation conditions (degree of supersaturation, temperature, acidity of the medium, etc). If the degree of supersaturation is low, solid phase formation proceeds with a long induction period and a low rate of crystal growth, so that a coarse precipitate is formed. This is the principle of the delayed-precipitation method.

It is difficult to bring about delayed precipitation if the precipitant is added in the form of solutions of the usual concentrations, as this inevitably leads to local increases of supersaturation and formation of fine precipitates. If extremely dilute solutions are used the precipitation period becomes excessively long.

The delayed-precipitation method has been adopted in industry and analytical practice. For example, in alumina production aluminum hydroxide is precipitated by carbonation of an aluminate solution, i.e., slow neutralization of caustic soda (formed by hydrolysis) by carbonic acid. Much work is being done in analytical chemistry on precipitation from homogeneous solutions [1], for which the term "method of forming reagents" has been suggested by Soviet authors [2]; however, the term "delayed precipitation" is a better description of the nature of the effect.

TABLE 2

Precipitation Data

Precipitation conditions	Volume of sludge (% of initial) after settling time (hours)				Filterability data					
	1	3	18	168	H (cm H ₂ O)	Q	h (cm)	t (sec)	k (cm/sec)	Solids in precipitate (%)
Milk of lime	12.0	—	5.0	1.6	822	2	0.4	60	$4 \cdot 10^{-7}$	—
Shell rock	0.8	0.4	0.4	0.3	830	20	1.3	60	$1.3 \cdot 10^{-5}$	53.1
FeCl ₃ + Ca(OH) ₂	10	—	5.0	5.1	—	—	—	—	—	—
Original shell rock	—	—	—	—	809	30	0.3	60	$0.4 \cdot 16^{-5}$	—

A feature of the use of delayed precipitation in analytical chemistry is that rather costly reagents can be used. Slow increase of the solution pH is necessary for precipitation of hydroxides (basic salts), and compounds soluble in acids; hydrolysis of urea or acid amides is recommended for this purpose [3].

Slow access of oxalate ions into solution is achieved by hydrolysis of dimethyl oxalate or diethyl oxalate [4], and of sulfate ions, by hydrolysis of dimethyl sulfate [5].

It is uneconomic to use such reagents for treatment of pickling liquors; it was necessary to find a cheap precipitant, and finely ground chalk or shell rock proved suitable for the purpose.

In contrast to direct precipitation by the action of calcium hydroxide, the reaction of iron salts with calcium carbonate proceeds through a slow hydrolysis stage with subsequent binding of the sulfuric acid by carbonate; the reaction must therefore be carried out at the boil. The kinetics of iron precipitation by ground shell rock is represented by the data in Table 1. The solution volume was 1 liter, the FeSO₄ concentration was 20 meq/liter, and the weight of shell rock taken was 150% of the theoretical.

We carried out experiments on filtration and sedimentation of precipitates formed by addition of lime in the cold and by retarded precipitation with ground shell rock. The solution contained 0.7 g of FeSO₄ and 0.5 g H₂SO₄ per liter. The period of rapid clarification was observed in a 20-liter bottle, and delayed clarification in a liter cylinder. Delayed precipitation was carried out in 5-liter flasks at the boil, heated for one hour by means of a gas burner. The solutions were made in water containing calcium sulfate; the amount of shell rock was 150% of the theoretical, and its particle-size composition by sieve analysis was: up to 0.06 mm, 14.4%; 0.06 to 0.088 mm, 46.1%; 0.088 to 0.102 mm, 9.8%; 0.102 to 0.2 mm, 30%. The filter area was 41.8 cm². The experimental results are given in Table 2.

The filterability data were calculated by means of the Darcy equation [6]

$$Q = ks \frac{H}{h} t,$$

where Q is the amount of filtrate in time t, for a pressure difference of H cm H₂O and cake thickness h cm, and k is the filterability coefficient in cm/second.

It is seen that when shell rock is used for precipitation the filterability coefficient is about 35 times as great as in precipitation by milk of lime; the filtered precipitate contains about 50% solid matter, loses fluidity, and can be transported in bulk. The structure of the precipitate is such that it can be used for conversion into mineral pigments under suitable conditions. The degree of precipitation depends on the excess of reagent and heating time. With 150% of reagent 80-90% of the iron is precipitated in 45 minutes (subsequently the rate of precipitation diminishes). The residual 10% of iron should be precipitated by milk of lime, as this procedure accelerates the process but does not influence filterability.

Experiments were carried out on neutralization and precipitation of iron from concentrated solutions containing about 200 g of ferrous sulfate and about 50 g of sulfuric acid per liter. Under the same conditions 85% of the iron is precipitated in 2 hours, and 99% in 3 hours. Although the precipitates formed are coarse and form lumps on standing, it is nevertheless probably advantageous to obtain ferrous sulfate from such solutions.

The choice of a method for waste-water treatment must be primarily based on health considerations, pollution of water supplies being inadmissible; the delayed-precipitation method is of interest in this respect, because the sludge can be removed by truck to any suitable dump. However, if waste heat is used as a heat source (spent steam, flue gases), the delayed-precipitation method can also have economic advantages over the usual method of precipitation by milk of lime: capital outlay is reduced considerably because it is unnecessary to construct sedimentation basins, with ducts often of several kilometers leading to them.

In addition, such ducts are unreliable as they may become blocked by coarse deposits.

Waste heat may be utilized in various ways, dependent on the actual conditions. For example, if flue gases are used and their source is at some distance from the pickling plant, treatment of the liquors with calcium carbonate should be performed in two stages: 1) in the cold at the pickling plant, to neutralize acids, and 2) on heating, to precipitate iron, after the clarified neutral liquid has been pumped to the heat source. The heating is effected in a tower sprayed from above with the circulating liquid, and with the flue gas entering from below.

The running costs should be approximately the same in other respects, on the assumption that the cost of grinding the calcium carbonate is equal to the cost of milk of lime.

SUMMARY

1. If coarseness is the main requirement in a precipitate and the presence of excess solid precipitant is not of decisive significance, hydroxides and basic salts of heavy metals can be obtained by the delayed-precipitation method with the use of ground shell rock or chalk.
2. If the delayed-precipitation method is adopted, costly construction becomes unnecessary so that capital outlay is lowered. Separation of the precipitate from the mother liquor, and transport of the precipitate, are easier with this method than with the usual method of direct precipitation by lime.

LITERATURE CITED

- [1] H. H. Willard, *Anal. Chem.*, **22**, 1372 (1950); L. Gordon, *Record of Chem. Progr.*, **17**, 125 (1956).
- [2] A. P. Terent'ev, E. G. Rukhadze and K. N. Litvin, *J. Anal. Chem.*, **11**, 55 (1956).*
- [3] H. H. Willard and N. K. Tang, *J. Am. Chem. Soc.*, **59**, 1190 (1937); H. H. Willard and Sheldon, *Anal. Chem.*, **22**, 1162 (1950).
- [4] H. H. Willard and Coley, *Anal. Chem.*, **20**, 560 (1948).
- [5] P. L. Elving and R. E. Van Atta, *Anal. Chem.*, **22**, 1375 (1950).
- [6] A. V. Nikolaev, *J. Appl. Chem.*, **20**, 187 (1947); L. E. Chernenko and P. A. Rebinder, *Colloid J.*, **12**, 386 (1950).

Received April 26, 1958

*Original Russian pagination. See C.B. Translation.

VOLTAGE BALANCE OF AN ELECTROLYTIC CELL AND POSSIBILITIES OF LOWERING THE SPECIFIC POWER CONSUMPTION IN THE PRODUCTION OF COPPER POWDER

A. V. Pomosov

The high cost of metal powders made electrochemically is due to a considerable extent to the high energy consumption in their production.

When possibilities of lowering the cost of copper powder are considered, attention should be paid to decrease of the specific energy consumption.

The specific energy consumption W depends on the cell voltage U_c and current efficiency η (%):

$$W = \frac{U_c}{a \cdot \eta} \cdot 100,$$

where a is the electrochemical equivalent of copper.

The cell voltage is made up of the following components

$$U_c = \varphi_a - \varphi_c + I_r + \sum \Delta U_{cont}$$

where φ_a is the anode potential, φ_c is the cathode potential, I_r is the ohmic loss of voltage in the electrolyte, and $\sum \Delta U_{cont}$ is the potential drop at the contacts.

The drop at the contacts, in its turn, is made up of the drop of potential between: a) the bus bar and anode bar ΔU_{b-ab} , b) the anode bar and the anode suspension hook ΔU_{ab-h} , c) the hook and the anode ΔU_{h-a} , d) the bar bar and the cathode bar ΔU_{b-cb} , and e) cathode bar and cathode ΔU_{cb-c} .

The potential drop in the bars and electrodes themselves is small and is therefore disregarded.

Calculation of the cell voltage balance by direct measurement of all its components, and subsequent analysis of the balance, makes it possible to detect sources of power loss and to suggest ways of lowering the specific energy consumption.

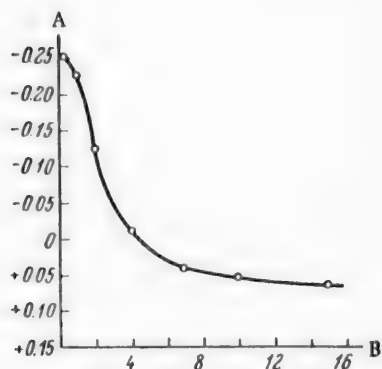
The method for determination of the voltage balance has been described earlier [1, 2].

The formation of a finely divided deposit on the cathode caused considerable difficulties in measurement of the cathode potential. Therefore the cathode potentials were measured immediately after removal of the powderlike deposit. The electrode potentials and voltage drop in the electrolyte were determined by the compensation method. The reference electrode was $Ag|AgCl, KCl\ 0.1\ N$. Since the potential has different values at different points on an electrode, the measurements were performed at 10 points differing in position and depth of immersion, and the average values were taken.

The contact drop was measured by means of a millivoltmeter (accuracy class 0.5). To eliminate the

Voltage Balance at Electrolyte Temperature of 56°

Balance items	Voltage drop	
	in v	in %
Cathode potential	-0.136	6.54
Anode potential	0.353	16.96
Voltage drop in electrolyte	1.420	68.23
Voltage drop at contacts including:	0.1725	8.27
busbar-cathode bar	0.0582	2.79
cathode bar-cathode	0.0032	0.15
busbar-anode bar	0.0444	2.13
anode bar-hook	0.0097	0.46
hook-anode	0.057	2.74
Total	2.0815	100.00
By voltmeter	2.0	
Difference	+0.08	4%



Variations of cathode potential with time at $I = \text{const.}$, $D_c = 1000 \text{ amp/m}^2$; electrolyte containing 32.6 g Cu and 100 g H_2SO_4 per liter; A) potential (v); B) time (minutes).

effects of the magnetic field all the instruments were enclosed in a special iron box. The leads were thick and reliably insulated; they were not allowed to intersect or become coiled, tangled, etc.

The cell used for production of copper powder comprises the following electrochemical system:



The cell cathodes were made from copper starting sheets from the electrolytic copper unit, and anodes from M-1 electrolytic copper.

The electrolyte contained 11.6 g of Cu (as CuSO_4) and 103 g of H_2SO_4 per liter.

The distance between the cathode and anode axes was 60 mm. The current density was 1700 amp/m^2 at the cathode and 1780 amp/m^2 at the anode. The current densities were calculated for the apparent areas of the immersed portions of the electrodes. In view of the formation of a highly disperse deposit, the true current

density at the cathode was considerably lower. During determinations of the voltage balance the electrolysis conditions (electrolyte composition, current load, electrolyte temperature, and interelectrode distances) were kept constant. The voltage balance was determined in production cells of the powdered copper section of the works.* The current efficiency in these cells was 78%. The powders formed had bulk density of 1.45-1.50 g/cc, and had the following particle-size composition: 65-80% of particles of 45μ and smaller, the rest between 45 and 150μ .

The cell voltage balance, presented in the table, was calculated from the determination results.

The cell voltage does not remain constant in time; it is highest at the instant when the powder is removed from the cathode, and then decreases as the metal powder is deposited. This is caused by the rapid growth of the cathodic deposit, with a corresponding change of cathode potential and interelectrode distance. For example, different cells in the section had voltages from 1.5 to 2.25 v; these variations of U_c are caused not only by differences in the age of the deposits, but also by the fact that the electrodes are not in rigidly fixed positions.

*V. M. Sakharova, A. A. Lebedkin, N. A. Golikov, L. L. Soboleva and R. V. Fiks-Shimel' assisted in determinations of the voltage balance.

Variations of the cathode potential with time at constant current, corresponding to an apparent current density of 1000 amp/m², were measured under laboratory conditions.

The results confirm that the cathode potential varies considerably with time. It is seen in the diagram that after removal of the deposit from the cathode the potential shifts by 0.320 v in the positive direction in 15 minutes. Therefore the agreement between the cell voltage found by summation of the results of direct determinations of individual items of the voltage balance and the voltage measured by means of a voltmeter must be regarded as satisfactory.

Analysis of the voltage balance shows that the principal item in it consists of ohmic drop in the electrolyte, and that the losses at the contacts are also considerable.

There are certain possible ways of lowering the cell voltage considerably, and thereby reducing the specific energy consumption.

First, the cell voltage can be lowered by decreasing the ohmic drop in the electrolyte by increases of the electrolyte acidity and temperature. Moreover, increase of temperature should tend to lower the cell voltage as the result of decreased polarization. However, decrease of the cell voltage by increase of electrolyte temperature and acidity does not always reduce the specific energy consumption. Our experiments showed that increase of the electrolyte acidity from 100 to 140 g/liter at current density of 1600 amp/m² and 56° lowers the voltage at the cell terminals by 16-18%. The particle size and bulk density of the powder remain almost unchanged, and the current efficiency drops by only 0.2%. Further acidity increases are inadvisable, as even with 160 g of acid per liter an additional decrease of voltage by 4-5% is accompanied by a 0.8% fall in current efficiency. At higher acidities there is no further decrease of cell voltage, because of increasing cathodic polarization, the current efficiency drops rapidly, and the powder becomes appreciably finer.

The temperature is the second factor with a strong influence both on the cell voltage and the current efficiency. The results of our experiments showed that increase of the electrolyte temperature from 55 to 60° is advisable. In this range a 1° increase of electrolyte temperature reduces the voltage by about 1%. Moreover, if the temperature is raised to 60° the current efficiency increases by 0.3-0.4%. Further increase of temperature is undesirable, as it leads to increase of particle size and less satisfactory operating conditions.

An important item in the balance, the relative proportion of which can be reduced, consists of voltage losses at the contacts. The worst contacts are anode — hook, bus-bar — cathode bar and bus-bar — anode bar. In the first case the voltage losses exceeded 200 mv in some instances, and in the second they reached 100-140 mv. The voltage drop at the contacts increases considerably as the result of contamination with copper powder, and especially owing to crystallization of copper sulfate. The latter is caused by constructive defects in the contacts used at present.

Finally, there is yet another possibility of reducing ohmic losses considerably — by decrease of the inter-electrode distance. However, this can be achieved only by substantial changes of cell design, with automatic removal of the powder from the cathode.

SUMMARY

The specific energy consumption in the production of copper powders can be reduced by increase of the H₂SO₄ content of the electrolyte to 140 g/liter and of the temperature to 60°.

LITERATURE CITED

- [1] M. A. Loshkarev and G. V. Lapp, Trans. Ural Polytech. Inst. No. 24 (Metallurgy Press, 1947).
- [2] A. I. Levin, Trans. Ural Polytech. Inst. No. 27 (Metallurgy Press, 1947).

Received October 28, 1957

USE OF SODIUM THIOSULFATE FOR ANTISEPTIC IMPREGNATION OF WOOD

G. E. Shaltyko, L. I. Pshedetskaya and

K. K. Sergeenkova

(Leningrad Institute of Railroad Transport Engineers)

Sodium thiosulfate is obtained as a by-product in many industries [1].

Thiosulfate decomposes in acid solutions with formation of sulfur dioxide and finely-divided sulfur, which have insecticidal and fungicidal properties [2].

The decomposition of thiosulfate is accelerated in presence of copper salts, when the insoluble and toxic cuprous sulfide Cu_2S [3] is formed in addition to sulfur dioxide and elemental sulfur.

The decomposition of thiosulfate in the reaction with copper sulfate may be represented by the following over all reaction scheme [4]:



Copper sulfate (blue vitriol) has long been used for preservation of wood, but because of the ease with which it is leached out it has little protective effect against the action of wood-rotting fungi [5].

Thiosulfate itself has no fungicidal properties and some fungi can even assimilate sulfur from it [6].

It seems likely that if wood is subjected to a multiple impregnation process, first with aqueous thiosulfate solution and then with copper sulfate solution, a mixture of substances should be formed within the wood and on its surface, and fixed within the wood tissue. This mixture should have good protective properties, with fungicidal effects and only slight leachability.

The present investigation was concerned with combined impregnation of wood by thiosulfate and copper sulfate solutions, and a study of the fungicidal properties of the mixture of substances formed in the process.

Standardized sodium thiosulfate solutions of different concentrations were used for wood impregnation.

After the impregnation the amount of residual thiosulfate in solution was determined, and the percentage of thiosulfate in the treated wood was found by difference. The results are given in Table 1.

Wood samples treated with thiosulfate solutions and samples treated with water under the same conditions were then treated with 3.0% copper sulfate solutions. The samples were then leached out in running water and dried to constant weight at 100-105°. The dry wood samples were then tested for their resistance to a culture of the wood-rotting fungus *Coniophora cerebella*, mainly by the method of the Central Scientific Research Institute of Mechanical Wood Working [7].

This species of fungus was chosen because it is recommended by many workers as the standard organism for tests of this type, and also because copper sulfate is not toxic to it [8, 9].

The extent of fungal attack in the experimental samples was estimated from the amount of growth and weight loss of the samples.

TABLE 1

Absorption of Thiosulfate by Wood

Expt. No.	Thiosulfate concentration (g-equiv/liter)	Thiosulfate contents			
		in original solution (meq)	in solution after treatment of samples (meq)	in samples	
				per g of wood (meq)	%
1	0.11	11	18.4	0.32	5.06
2	0.2	20	16.8	0.39	5.97
3	0.4	40	35.4	0.60	9.49
4	0.5	50	37.6	1.18	18.67
5	0.6	60	48.4	1.25	19.77
6	0.8	80	68.0	1.47	27.25
7	1.0	100	87.8	1.46	27.10
8	1.2	120	107.2	1.47	27.25

TABLE 2

Resistance to Fungal Attack of Wood Samples Impregnated with Thiosulfate and Copper Sulfate Solutions. Average results for 12 samples given in each experiment Culture of *Contophora cerebella* fungus

Expt. No.	Sample weight (g)			Weight loss of samples after mycological tests		Concentration of thio-sulfate solution (g-equiv/liter)	Form of growth on wood samples after four months of contact with fungal culture
	before impregnation	after impregnation	after mycological tests	in g	in % of dry weight		
1*	3.066	2.107	1.754	0.343	16.70	0	Samples covered with abundant mycelium. Surface destruction
2	2.122	2.187	1.920	0.267	12.50	0.11	} Coated with mycelium, partially destroyed on surface
3	2.167	2.252	2.042	0.210	9.23	0.20	
4	2.040	2.136	2.002	0.134	6.27	0.40	
5	1.876	1.976	1.950	0.026	1.40	0.60	} No growth
6	2.186	2.280	2.266	0.024	1.10	0.80	
7	1.895	2.006	1.980	0.019	1.48	1.00	
8	1.922	Control	1.044	0.878	45.68	Control	Samples covered with abundant mycelium, softened, shrunken, crumbled under pressure

*In Experiment No. 1 the samples were impregnated with copper sulfate solution only.

The stability of wood in presence of the fungus was tested for each thiosulfate concentration with 12 wood samples (three sets, each of four samples). The results for a total of 96 samples are given in Table 2.

It follows from the data in Table 2 that combined impregnation of wood by thiosulfate solutions followed by 3% copper sulfate solution, with subsequent leaching of the samples in running water, gives almost complete protection against the wood-rotting fungus at thiosulfate concentration of 0.6 N.

Wood samples impregnated with 3% copper sulfate solution only are attacked and loss up to 16.7% in weight under the same conditions, and control samples lose up to 45.68%.

The average weight loss of the treated samples was 1.2%.

The toxicity of an antiseptic is characterized by its limiting dose, which is the minimum percentage content which protects the wood against fungal attack. The reciprocal of the limiting dose is taken as the measure of the toxicity [10].

The limiting dose of the reaction products formed from thiosulfate and copper sulfate is 5.0‰ and the toxicity is 0.2.

The higher toxicity of the mixture of reaction products formed from thiosulfate and copper sulfate, as compared with copper sulfate alone, may be attributed to the presence of finely-divided sulfur and cuprous sulfide, the toxic properties of which are intensified owing to the synergic effect [11].

EXPERIMENTAL

Starting materials: uniformly chosen samples cut from pine sapwood, 2 x 2 x 1 cm in size (1 cm along the grain); thiosulfate containing 98% $\text{Na}_2\text{S}_2\text{O}_3 \cdot 5\text{H}_2\text{O}$ from the Kohtla-Yarve Combine; copper sulfate containing 96.4% $\text{CuSO}_4 \cdot 5\text{H}_2\text{O}$ and 0.25% of water-insoluble residue.

Sodium carbonate was added to the thiosulfate solutions until alkaline (to phenolphthalein); hydrochloric acid was added to the copper sulfate solution until acid to methyl orange.

Drying and impregnation of wood samples. The wood samples were dried to constant weight in a drying oven at 100-105°.

The samples were impregnated in open vessels at 18-20°. The samples were placed in dry beakers. Each sample was stood on its 2 x 1 cm face and pressed against the bottom of the beaker by means of a springy metal gauze. The samples were kept for 4 hours in thiosulfate solution. After treatment of the samples the residual thiosulfate in each beaker was determined iodometrically, and the amount of thiosulfate absorbed by the wood was found by difference.

After the thiosulfate impregnation the wood samples were treated with 3% copper sulfate solution for 48 hours, then leached in running tap water for 48 hours, and dried to constant weight at 100-105°.

Mycological tests. The fungus *Coniophora cerebella* was grown on wood and was first tested for its wood-rotting capacity. Single rows of glass tubes, about 1.5 cm in diameter, were laid in parallel on the bottom of wide-necked 750 ml conical flasks. Wort agar was then poured in each flask to reach half way up the diameter of the tubes on the bottom of the flask.

The prepared flasks were sterilized, cooled, and sown with the fungus culture. When the mycelium covered the whole row of tubes, wood samples previously sterilized in a burner flame were put into the flasks. The samples were impregnated with thiosulfate and copper sulfate solutions by the combined method, or by copper sulfate solution only.

Four impregnated samples and one control were put into each flask.

The flasks were plugged with cotton wool and kept in a thermostat at 18-21° for the duration of the experiment (four months). The nature of the fungal growth and the state of the samples were observed throughout the experiments.

At the end of the experiments the samples were taken out of the flasks, the fungal growth was scraped off, and the samples were dried to constant weight. The weight loss due to rotting was found from the difference between the dry weights of the samples before and after the experiments.

SUMMARY

1. Wood samples were subjected to combined impregnation with sodium thiosulfate and copper sulfate, and then tested for their resistance against the wood-rotting fungus *Coniophora cerebella*; the mixture was found to have effective fungicidal properties and resistance to leaching.
2. The limiting dose of the sodium thiosulfate-copper sulfate mixture is 5.0‰ and the toxicity is 0.2.

LITERATURE CITED

- [1] M. E. Pozin and B. A. Kopylov, *Chem. Sci. and Ind.* 2, 6, 684 (1957).
- [2] L. K. Tsitovich, *Analysis of Insecticides and Fungicides* [In Russian] (1952).
- [3] V. G. Lilly and H. L. Barnett, *Physiology of the Fungi* (Moscow, 1953) [Russian translation].
- [4] A. I. Ponomarev, *Methods of Chemical Analysis of Minerals and Rocks*, 2 [In Russian] (1955) p. 130.
- [5] V. N. Petri and A. L. Dul'kin, *Wood-Rotting Organisms* [In Russian] (1950) p. 94.
- [6] D. I. Hockenhull, *Biochim. et Biophys. Acta* 3, 326 (1949).
- [7] V. V. Miller and E. I. Meier, *Trans. Central Sci. Res. Inst. Mechanical Wood Working* 2, (8), 40 (1951).
- [8] K. A. Popov and N. I. Tseshinskaya, *Coll. Trans. Central Inst. Sci. Res. and Reconstr. Railroads* 17, 16 (1932).
- [9] D. N. Lektorskiĭ, *Protective Treatments of Wood* 1 [In Russian] (1951) p. 130.
- [10] P. I. Rykachev, *Trans. Central Sci. Res. Inst. Mechanical Wood Working* 2 (8), 228 (1951).
- [11] J. G. Horsfall, *Fungicides and Their Action* (Moscow, 1948) p. 279 [Russian translation].

Received April 12, 1958

METHODS FOR LABORATORY SYNTHESIS OF POLYESTERS

Zh. S. Sogomonyants

Synthetic polyesters are usually made by ester condensation of suitable dicarboxylic acids with glycols.

Until recently the most usual method for carrying out this reaction was by condensation in melts.

In the most fundamental investigations in this field, carried out by Carothers [1], the reaction was conducted under high vacuum in a current of inert gas at high temperatures (200° and over). The method of polycondensate preparation was considerably improved by the use of catalysts and introduction of a preliminary condensation stage [2]; in some cases the reaction temperature could be lowered to 100-120° and esters of much

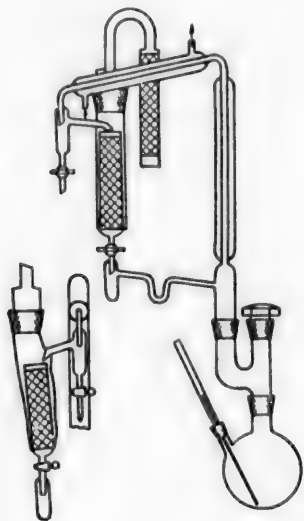


Fig. 1. Batzer's apparatus for preparation of polyesters with azeotropic distillation of the reaction water.

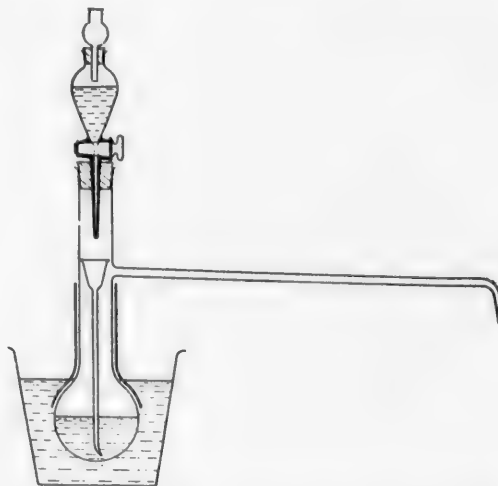


Fig. 2. Apparatus for preparation of small amounts of polyesters with azeotropic distillation of the reaction water.

higher molecular weights could be obtained. However, this method had two essential disadvantages: complicated apparatus was required, and the process took a long time (80-100 hours) because of difficulties in removing the reaction water from the viscous melt.

A detailed paper by Batzer et al. [3] contains the results of experiments on the preparation of polyesters in boiling solvents. The effects of different solvents, concentrations, catalysts, and purity and relative proportions of the components were studied.

The effects of different dehydrating agents and of the polycondensation time on the properties of the polyesters formed were also studied. It was found that with the use of solvents the reaction time does not exceed 20-30 hours, and it is not necessary to use an inert gas or high vacuum. In our experiments, in which we repeated Batzer's procedure for synthesis of polyesters from well-known components (hexamethylene glycol -

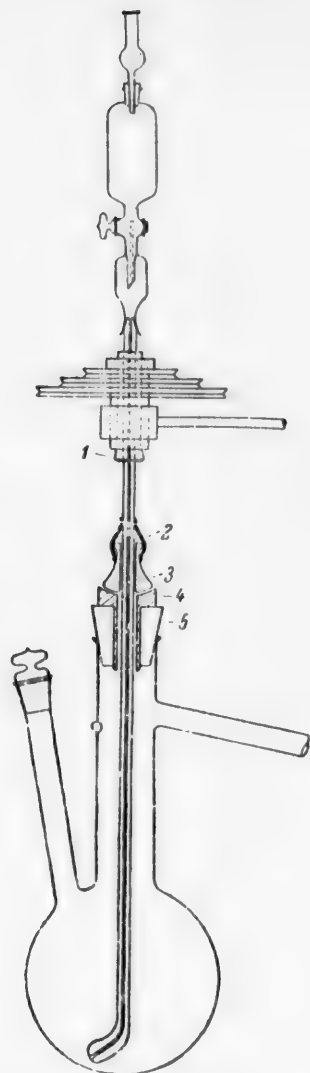


Fig. 3. Apparatus for preparation of polyesters soluble in xylene: 1) grip for stirrer shaft; 2) rubber tube; 3) fluoroplastic ball joint; 4) stainless-steel ball joint; 5) rubber tube.

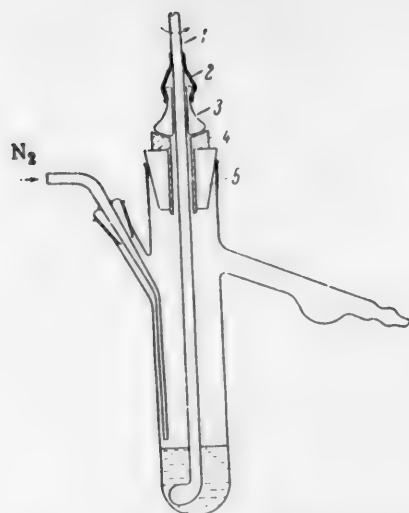


Fig. 4. Apparatus for preparation of polyesters in melts: 1) stirrer; 2) rubber tube; 3) fluoroplastic ball joint; 4) stainless-steel ball joint; 5) rubber tube.

adipic acid, hexamethylene glycol - sebacic acid), we were unable to obtain products of high molecular weight. Brittle products were obtained, which could not be stretched in the cold; the specific viscosity of their 0.5% solutions in benzene did not exceed 0.15. It is possible that we did not reconstruct with sufficient accuracy the apparatus described in Batzer's paper, as the description is not sufficiently detailed. Nevertheless, our experiments justify the conclusion that Batzer's apparatus has a number of disadvantages. First, its design is such that the solvent vapor must traverse a long path before condensation in the straight condenser (Fig. 1). As a result, distillation of the solvent slows down considerably as the solution viscosity increases, so that fresh portions of solvent must be added and heating intensified. This apparatus was particularly inconvenient to use with small amounts of material, as for normal operation the reaction flask must contain not less than 30-40 ml of solvent, apart from the amount in circulation. Therefore small amounts (3-5 g) of polyesters cannot be prepared by Batzer's method because it is

impossible to obtain a high concentration of the reacting substances. Another disadvantage of the apparatus is that solvent and volatile impurities cannot be removed from it at the end of the reaction.

The disadvantages of the Batzer method prompted us to seek more rational conditions for carrying out the polyesterification reaction. As a result three methods were developed, whereby polyesters of fairly high molecular weight could be obtained in the minimum time.

EXPERIMENTAL

Preparation of small amounts of polyesters soluble in xylene. The apparatus suggested for preparation of small amounts (3-6 g) of polyesters, with azeotropic distillation of the water formed in the reaction, consists of

a flask of the Würtz type with an elongated side tube, fitted with a dropping funnel. A long funnel with a slightly curved tip resting on the bottom is inserted in the flask (Fig. 2). The flask volume (25-40 ml) is fairly large, as frothing is possible at the initial reaction stage. The flask was charged with an equimolecular mixture of dicarboxylic acid and glycol, 0.01-0.03 mole of each, p-toluenesulfonic acid (0.3-0.5% on the weight of the mixture), and 3-5 ml of xylene. The flask was heated in a thermostatically-controlled bath containing Wood's alloy at 140-150° for 3 hours so that the reaction mixture boiled gently but xylene did not distill off. The rate of heating was then increased and when the bath temperature reached 160-165° moist xylene was distilled off slowly; at this stage dry xylene, purified by treatment with boiling sulfuric acid (see below) was added continuously at such a rate that its content in the flask was as low as possible. The added xylene entered through the funnel into the depth of the reaction mass heated to above the boiling point of xylene; this ensured good mixing and more effective azeotropic distillation of the reaction water. The long side tube of the flask acted as a condenser for the moist xylene vapor. The heating and distillation of xylene was continued for 15 hours, the amount passed in this time being 250 ml. At the end of this time the funnel was taken out of the flask and the dropping funnel was replaced by a capillary through which purified nitrogen was fed into the flask, while the outlet tube was connected to vacuum.

To remove the solvent and low-molecular substances, the mass was heated under a residual pressure of 1-2 mm for 4 hours; the portion of the flask not heated in the bath was surrounded by a metal case (made from sheet copper or aluminum 0.5-1 mm thick), the lower end of which was immersed in the bath. The polyesters prepared by this method were colorless and had specific viscosity 0.28-0.35 (0.5% solution in benzene). As was noted by Batzer, the purity of the xylene used is very important in the preparation of polyesters. Therefore special care was taken to purify the solvent by the procedure described below.

To 1 liter of xylene 20 ml of concentrated sulfuric acid was added, and the mixture was boiled under reflux for 8-10 hours. The xylene was distilled off, dried by a small amount of calcium chloride, boiled again with 10 ml of sulfuric acid for 6-8 hours, and distilled. During the second boiling the xylene darkened only slightly. The distillate was washed with water, 5 % sodium carbonate solution, water again, dried by calcium chloride, and distilled over phosphorus pentoxide. The xylene purified in this manner remained quite colorless when boiled with p-toluenesulfonic acid for 10 hours.

Preparation of polyesters soluble in xylene from 0.05-0.3 mole lots of starting substances. When the amounts of starting substances exceeded 0.05 mole, it was more convenient to use an apparatus with mechanical stirring (Fig. 3). The reaction vessel was a flask of the Würtz type, 100-250 ml in capacity, with an elongated side tube which acted as a condenser near the top. The flask contained a glass stirrer made from capillary tubing of 1-2 mm internal diameter. The end immersed in the flask was flattened and bent but the capillary remained open. A ball joint made from polychlorotrifluoroethylene (Ftoroplast-3) served as a seal for stirring under vacuum (Fig. 3). The flask contained equimolecular amounts of the starting substances, 0.3-0.5% of paratoluenesulfonic acid monohydrate, and 10-15 ml of xylene. The mixture was heated in a metal bath for three hours so that the solvent boiled gently but did not distill. Xylene was then added through the stirrer tube from a dropping funnel, slowly at first, and then rapidly dropwise. The heating rate was then raised so that the solvent distilled off as rapidly as it was added. The total amount of xylene passed through the reaction mixture was 400-800 ml, in accordance with the amount of mixture, after which side tube was attached to a vacuum source (1-2 mm) and the residual solvent and volatile impurities were distilled off with continuous stirring during 3 hours at 170-180°.

Preparation of polyesters in melts. The apparatus depicted in Fig. 4 was used for preparation of polyesters of high viscosities in the melted state and insoluble in the solvents generally used for azeotropic distillation of reaction water.

This apparatus was used for preparation of polyesters from dimethyl terephthalate and propylene glycol, hexamethylene glycol, and D- and DL-methylhexanediol-1,6. In all the experiments 1.5 mole of dimethyl terephthalate, with 0.25% of lead acetate catalyst. The mixture was melted and heated on a metal bath in a current of purified nitrogen; the working stirrer was connected through a Ftoroplast vacuum seal.

During the first ten hours the temperature of the metal bath was kept at 160-170°, and it was then held at 190° for 2 hours. At the end of this time the nitrogen supply was stopped and the apparatus was connected to vacuum (1-2 mm) through the side tube. The heating was continued under vacuum for 8 hours; during the first two hours the temperature was kept at 190°, after which the rate of heating was increased and the mixture was

held for two hours at 210°, and then for four hours at 240-250°. This method yielded polyesters with specific viscosity from 0.5 to 0.9 (0.5% solution in cresol), almost free from color.

In some cases the polyesters stuck so firmly to the glass that they could only be extracted by cutting off and breaking the lower part of the reaction flask.

LITERATURE CITED

- [1] W. H. Carothers, Collected Papers, New York (1940).
- [2] H. Batzer, Makrom. Chem. 5, 5 (1950).
- [3] H. Batzer, H. Holtschmidt, F. Willoth and B. Mohr, Makrom. Chem. 7, 82 (1951).

Received February 20, 1958

CONTINUOUS METHOD FOR PREPARATION OF 1,4-DICHLOROBUTANE AND DI(4-CHLOROBUTYL) ETHER FROM TETRAHYDROFURAN AND PHOSGENE

V. I. Lutkova and N. I. Kutsenko

Preparation of aliphatic dithalides with halogens in the principal chain of the molecule presents considerable difficulties. In such cases tetrahydrofuran is an intermediate from which compounds such as 1,4-dichlorobutane and di(4-chlorobutyl) ether can be prepared.

A number of bifunctional aliphatic compounds may be synthesized from these dichlorides; synthesis methods have been developed for dinitriles, diamines, dicarboxylic acids, glycols, etc. [1]. It was therefore desirable to develop an efficient method for their preparation, suitable for industrial use.

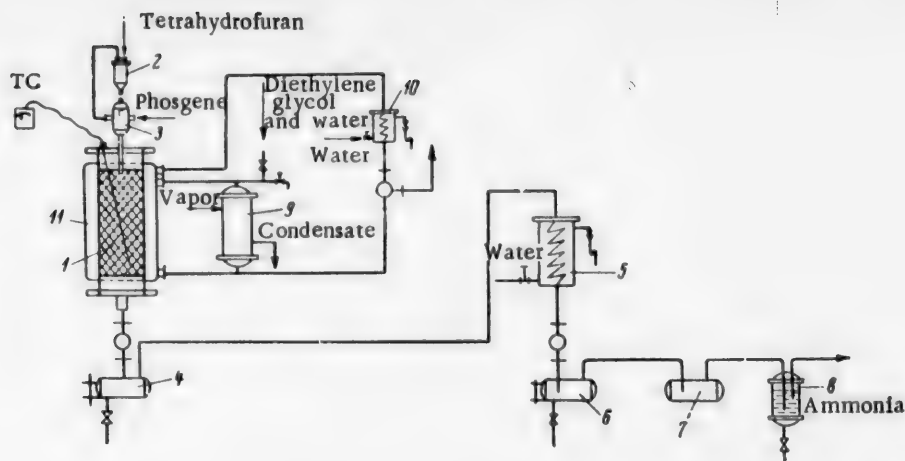
It is known from the literature that 1,4-dichlorobutane and di(4-chlorobutyl) ether can be prepared from tetrahydrofuran by the action of acid chlorides or HCl in presence of various catalysts. The action of thionyl chloride on tetrahydrofuran in presence of stannic chloride [2] or zinc chloride [3, 4] yielded 1,4-dichlorobutane, while in presence of ferric chloride di(4-chlorobutyl) ether was obtained [5]. Di(chlorobutyl) ether was also prepared by the action of phosphorus oxychloride on tetrahydrofuran in presence of sulfuric acid [5]. The preparation of 1,4-dichlorobutane and di(4-chlorobutyl) ether from tetrahydrofuran and phosgene with zinc chloride catalyst has also been described [6-8]. There have been several studies of the preparation of dichlorides from tetrahydrofuran and HCl with different catalysts and under various conditions [9-15].

Most of these preparation methods are of the batch type. Dichlorides have been prepared from tetrahydrofuran with the use of HCl, acid catalysts, and high temperatures and pressures. These conditions involve the use of corrosion-resistant apparatus working under pressure, which makes the process costly.

We have developed a continuous method for preparation of dichlorides from tetrahydrofuran by the action of phosgene in presence of zinc chloride catalyst. The process is effected under atmospheric pressure at 101-102°. Either 1,4-dichlorobutane or di(4-chlorobutyl) ether may be obtained as the end product, according to the amount of catalyst used. The yield of 1,4-dichlorobutane reaches 85-90% of the theoretical, and of di(4-chlorobutyl) ether 50-60%, calculated on tetrahydrofuran. In the first case di(4-chlorobutyl) ether is formed as a by-product; this can be converted into 1,4-dichlorobutane, so that the yield of the latter can be raised to almost the theoretical.

EXPERIMENTAL

The process was carried out in a continuous apparatus (see figure) consisting of a tubular reactor (made of ATM-1 material, which is acid-resistant and has high heat conductivity) 1500 mm long and 36 mm in internal diameter. The reaction tube was packed with Raschig rings. The tube was connected to two consecutive receivers, a condenser, and wash bottles with ammonia solution to absorb unchanged phosgene. The reaction tube was heated by means of a heat carrier consisting of a mixture of diethylene glycol and water, boiling at 107-108°, contained in an external boiler. This method of heating gave a uniform temperature along the entire reactor. The temperature was measured by means of a technical thermometer in the middle of the reactor. The flow meter used for determining the phosgene feed rate was previously calibrated for phosgene. For this calibration phosgene was passed for a definite time into chlorobenzene cooled to -15°, with the meter level constant. Complete absorption of phosgene was checked by the ammonia reaction. The phosgene feed rate was found from



Apparatus for continuous preparation of dichlorides: 1) reactor; 2) header tank; 3) mixer; 4) receiver; 5) condenser; 6) receiver with sorbent; 7) buffer vessel; 8) vessel with ammonia; 9) external boiler; 10) condenser; 11) reactor jacket.

the weight increase of the chlorobenzene after a definite time. In this way a series of points corresponding to different phosgene feed rates was obtained. Tetrahydrofuran containing 10-15% of ZnCl_2 catalyst dissolved in it (the ZnCl_2 dissolved completely only after some phosgene had been passed through the mixture of tetrahydrofuran and catalyst) was fed from a header tank into the reactor at 30 ml/hour. Gaseous phosgene was passed from a cylinder through a manostat and flow meter, connected in parallel, at a rate of 150 ml/minute. The temperature was maintained at 102° . The reaction product was collected in a receiver under the reactor. The next receiver contained petrolatum to trap unconverted tetrahydrofuran carried over with phosgene. At the end of the process nitrogen was blown thoroughly through the system; the product was removed from the receiver and tetrahydrofuran was distilled off at atmospheric pressure on an oil bath. The reaction product was washed with saturated salt solution, neutralized with 10% sodium carbonate solution, washed with water, dried by means of calcined CaCl_2 , and fractionated under vacuum at 13 mm residual pressure. Fractionation yielded:

Fraction I— $48-50^\circ$, 1,4-dichlorobutane, yield 85%

Fraction II— $126-128^\circ$, di(4-chlorobutyl) ether, yield 6.3%

If the amount of catalyst is decreased to 2.5% the yield of 1,4-dichlorobutane falls to 32% and the yield of di(4-chlorobutyl) ether correspondingly rises to 60%

Characteristics of the Dichlorides

1,4-Dichlorobutane is a colorless liquid with a characteristic odor, insoluble in water, soluble in the usual organic solvents; d_4^{20} 1.1288, n_D^{20} 1.4520.

Found %: C 38.24, H 6.28, Cl 55.38; MR 30.38. $\text{C}_4\text{H}_8\text{Cl}_2$. Calculated %: C 38.10, H 6.30, Cl 55.55; MR 30.41.

Di(4-chlorobutyl) ether is a faintly colored, transparent liquid with an unpleasant odor, insoluble in water, soluble in organic solvents; d_4^{20} 1.0747, n_D^{20} 1.4568.

Found %: C 47.68; H 8.47; Cl 35.50; MR 49.95. $\text{C}_8\text{H}_{16}\text{OCl}_2$. Calculated %: C 47.7; H 7.8; Cl 35.69; MR 50.52.

SUMMARY

A continuous method has been developed for preparation of 1,4-dichlorobutane and di(4-chlorobutyl) ether from tetrahydrofuran and phosgene, with zinc chloride catalyst. The process is carried out at atmospheric pressure and $100-102^\circ$. Either dichloride can be obtained as the end product, according to the amount of catalyst used.

The yields reached 90% for 1,4-dichlorobutane, calculated on tetrahydrofuran, and 60% for d(4-chlorobutyl) ether.

LITERATURE CITED

- [1] V. L. Lutkova, *Progr. Chem.* 23, No. 7, 821 (1954).
- [2] Ya. Gol'dfarb and L. Smorgonskii, *J. Gen. Chem.* 8, 1516 (1938).
- [3] H. Krlzikalla, *Referat Lu Hauptlaboratorium Ludwigshafen* (1942).
- [4] V. Lutkova, N. Kutsenko and M. Itkina, *J. Gen. Chem.* 25, 2102 (1955).*
- [5] K. Alexander and L. E. Schniepp, *J. Am. Chem. Soc.* 70, 1839 (1948).
- [6] O. Moldenhauer, Gunther and G. T. Trautmann, *Zbl.* 7400 (1953).
- [7] O. Moldenhauer, *Ann.* 580 169 (1953).
- [8] P. Moshkin, V. Lutkova and N. Kutsenko, *Authors' Certif. No.* 14938 (1955).
- [9] S. Fried and R. D. Kleen, *J. Am. Chem. Soc.* 63, 2691 (1941).
- [10] F. Codignola and M. Piacenza, *Italian patent* 424590 (1947); *C.A.* 43, 4284 (1949).
- [11] *French patent* 864758 (1941); *C.A.* 43, 1433 (1949).
- [12] H. Kroper, *Zbl.* 7403 (1953).
- [13] H. Trieschaumann and F. Mouchen, *Zbl.* 1824 (1954).
- [14] *British patent* 632346 (1947); *C.A.* 44, 6424 (1950).
- [15] N. D. Scott, *U. S. patent* 2491834 (1949); *C.A.* 44, 2542 (1950).

Received April 25, 1958

*Original Russian pagination. See C.B. Translation.

INVESTIGATION OF THE CHEMICAL COMPOSITION OF THE FATTY OIL FROM THE EUROPEAN SPINDLE TREE (EUONYMUS EUROPOEA)

N. I. Simonova

(Leningrad Institute of Motion Picture Engineers)

The European spindle tree contains gutta-percha. According to Shukhobodskii's data [1] the roots of this plant contain up to 7.2% of gutta. Its seeds contain up to 50% of a fatty oil [2, 3], and it can therefore be cultivated as a perennial oil-bearing plant. The oil yield from this plant exceeds the yield from other oil-bearing plants, such as hemp (28-35% fat), flax (35-37% fat), and cotton (20% fat).

It must be noted that the oil of the European spindle tree has not been studied sufficiently.

In 1932 Kraft [4] determined some of its constants, namely the iodine, acid, and saponification numbers.

Subsequently Bogomaz [3] carried out a more detailed study of the physicochemical properties of the European spindle tree. The above-named authors did not investigate the fatty-acid composition of this oil.

The purpose of the present investigation was to study the fatty-acid composition of the oil from the European spindle tree.

Our results showed that the glycerides of this oil contain saturated and unsaturated acids: oleic, linoleic, and linolenic.

EXPERIMENTAL

Two samples of oil were taken for the investigation: 1) oil from the European spindle tree grown in the Northern Caucasus, and 2) oil from the European spindle tree grown in a nursery in the Leningrad region.

The oil yield, by extraction of the ground air-dry seeds with ether in a Soxhlet apparatus, was 45-47%.

The oil was dark green in color and deposited a small amount of precipitate on standing.

General analytical data on the oil are presented in the table.

Isolation of acids from the oil was effected by heating of the oil with alcoholic alkali solution. 300 g of oil was heated for 2 hours with 1125 ml of alcoholic alkali in a flask under reflux. Excess of alcohol was then distilled off, and 1.5 liters of hot water followed by hydrochloric acid was added to the potassium salts of the fatty acids in the flask. The oil which separated out from the cooled solution was extracted in ether. The ether extract was dried by sodium sulfate, and ether was then evaporated off. The acids were yellow-green in color and congealed on standing. The yield was 207 g.

Investigation of solid acids. Solid and liquid acids were separated by the Twitchell method [5]. 50 g of the acids were dissolved in 250 ml of 96% alcohol. The solution was heated to boiling and 250 ml of hot 14.4% alcoholic solution of lead acetate was added. The mixture was heated for 10 minutes on a boiling water bath and then left overnight. On the following day the precipitated lead salts were separated from the liquid and washed with alcohol until the filtrate was free from turbidity on addition of water. For further purification the lead salts insoluble in cold alcohol were recrystallized from hot alcohol containing a little acetic acid.

General Analysis of Oil

Origin of spindle tree	Acid number	Saponification number	Iodine number	Notes
Northern Caucasus, Kislodvsk region	15.1	235.4	101.6	Fresh seeds, with well-preserved arils*
Leningrad province, Siverskaya station	11.7	196.7	100.4	Seeds without arils

*The arils contain about 54.02% of oil, iodine number 105.5, saponification number 210.7, 211.2.

The recrystallized lead salts were decomposed by dilute nitric acid. The liberated acids were extracted in ether. The ether extract was washed several times with water and dried over sodium sulfate. After removal of the ether the acids solidified. The yield of solid acids was 9.5 g. The iodine number was 24.1. From this value it is concluded that the mixture of fatty acids contains 18.4% of saturated acids.

Investigation of liquid unsaturated acids. During the alcohol treatment of the lead salts an unsaturated acid of iodine number 89.6 was isolated; oxidation of this acid by permanganate in alkaline solution yielded dihydroxystearic acid of m.p. 129-130°, indicating the presence of oleic acid in the oil.

The mixture of fatty acids isolated from the lead salts in alcoholic solution had iodine number 126. After the solution had been left for several days the iodine number fell to 120.6, probably owing to oxidation of highly unsaturated acids.

Bromination of unsaturated acids. 10 g of unsaturated acids were dissolved in 100 ml of ethyl ether; the ether solution was cooled in ice and a solution of bromine in ether was added until a permanent color formed (125 ml of 5% solution). The mixture was left overnight in a cold place. A precipitate separated out on standing; this was filtered off, washed with ether, and dried at 80-85°; m.p. 175-176°.

The formation of a hexabromide of m.p. 175-176° indicates the presence of linolenic acid in the oil. According to literature data, its hexabromide melts at 179° [5]. After separation of the precipitated hexabromide the filtrate was treated with sulfite solution to remove excess bromine. The bromine-free filtrate was washed twice with water and dried by sodium sulfate. After removal of the ether the residue was treated several times with hot ligroine. The solution deposited a crystalline substance of m.p. 113-114° on cooling. Further attempts to purify the tetrabromide did not raise its melting point. The formation of a bromide melting at 113-114° indicates the presence of linoleic acid in the oil. Linoleic acid gives a bromide of m.p. 114° [5].

Oxidation of mixed unsaturated fatty acids by the Zaitseva-Gatsury method. 20 g of the acids was mixed with 24 ml of 27% caustic potash solution. 1350 ml of water was added to the potassium salts so formed. To this solution 1350 ml of 1.5% potassium permanganate solution was added cautiously with continuous stirring. The mixture was left to stand at room temperature for 20 hours.

On the following day the precipitated manganese dioxide was filtered off and washed several times with water. Acidification of the filtrate by 10% sulfuric acid gave a white curdy precipitate of a mixture of hydroxy acids and unchanged fatty acids.

The acids were filtered off and washed with water. The yield of acids was 8.8 g, m.p. 113-114°.

When the acid mixture was treated with ligroine 3.1 g of substance of m.p. 53-54° was extracted. The acid number was determined. 0.1920 g of substance took 39.81 mg KOH.

	Found	: acid no. 207.3
$C_{16}H_{32}O_2$	Calculated:	acid no. 197.33
$C_{18}H_{36}O_2$	Calculated:	acid no. 218.92.

On the assumption that the saturated acids are palmitic and stearic, it follows from the acid number of 207.3 that the mixture contains 49.4% of palmitic and 51.6% of stearic acid.

The residue from the ligroine treatment was extracted in ethyl ether in a Soxhlet apparatus; the substance extracted in ether had m.p. 132-133° after recrystallization from hot alcohol. A mixed sample of the substance with dihydroxystearic acid, which corresponds to oleic acid, gave no melting-point depression; the two substances were therefore identical. Determination of the acid number of dihydroxystearic acid of m.p. 132-133° gave the following results. 0.1470 g of substance took 26.54 mg KOH.

Found : acid no. 180.5
 $C_{18}H_{36}O_4$. Calculated: acid no. 178.7

This indicates the presence of oleic acid in the original mixture.

The residue from the ether extraction was treated with hot water. The hot aqueous solution deposited a precipitate of m.p. 165-169° on cooling. The acid number was determined. 0.240 g of substance took 38.98 mg KOH.

Found : acid no. 162.4
 $C_{18}H_{36}O_6$. Calculated: acid no. 161.2.

The formation of tetrahydroxystearic acid indicates the presence of linoleic acid in the mixture of acids. This result confirms the data obtained in bromination of the acids.

A hydroxy acid of m.p. 201-202° was isolated from the aqueous solution; this indicates the presence of linolenic acid in the oil. Hexahydroxystearic acid melts at 203-205°.

Preparation of the methyl esters of the fatty acids. The quantitative composition of the mixture of fatty acids was investigated by the Kaufman method [6], based on the iodine and thiocyanate numbers. The methyl esters of the fatty acids were prepared for this purpose.

A flask fitted with a reflux condenser contained 40 g of fatty acids dissolved in 250 ml of methyl alcohol; 2.5 ml of concentrated sulfuric acid was added to this solution. The mixture was heated for 3 hours on a boiling water bath, excess alcohol was distilled off, and the residual reaction product was poured out into 200 ml of water. The esters were extracted by means of ethyl ether. After removal of the solvent the mixture of esters was distilled at 2 mm in a CO_2 atmosphere. Most of the esters distilled at 171-183°. The ester distillate was a transparent, slightly yellowish liquid. The yield was 34.2 g, iodine number 96.0, thiocyanate number 74.5.

Calculation of the contents of methyl esters of saturated and unsaturated acids in the mixture by Kaufmann's method [6] gave the following results (in %): saturated acids 19.3, oleic acid 55.8, linoleic acid 19.3, linolenic acid 5.6.

SUMMARY

1. The seeds of the European spindle tree contain 45-47% of oil.
2. The oil contains saturated acids, and oleic, linoleic, and linolenic acids.

LITERATURE CITED

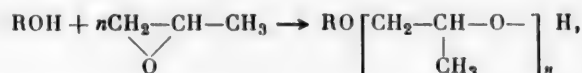
- [1] V. A. Shukhobodskii, Dissertation [In Russian] (Botanical Institute, 1953).
- [2] V. Lykov, Oil and Fat Ind. 6, 401 (1936).
- [3] V. A. Bogomaz, Trans. Forestry Inst. 11, 285 (1953).
- [4] D. Kraft, Oil and Fat Ind. 6, 55-56 (1932).
- [5] A. Gryuk, Analysis of Fats and Waxes, 43, 318, 294 (1932).
- [6] H. P. Kaufmann, Investigations in the Field of Fat Chemistry (1937) [Russian translation].

Received April 25, 1958

PREPARATION OF MONOMETHYL ETHERS OF POLYPROPYLENE GLYCOLS

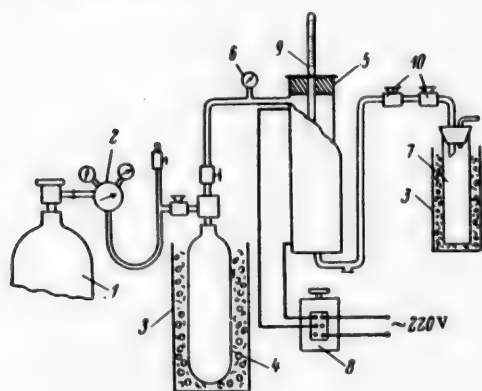
S. M. Gurvich, V. R. Likhterov and
V. S. Etlis

Condensation of propylene oxide with methanol, giving a mixture of monomethyl ethers of propylene glycols (1), occurs in accordance with the scheme:



where n may have various values.

It should be noted that primary ethers are formed when alkaline catalysts (sodium methylate, caustic soda, tributylamine) are used [1-5]. Whereas in presence of acid catalysts (sulfuric acid, boron trifluoride) [1, 2, 4] a mixture of primary and secondary isomeric ethers is formed. Until now the reaction of propylene oxide with methanol has been studied mainly in relation to isolation and study of low-molecular reaction products with $n = 1$ or 2 [1, 2, 4, 6, 7].



Preparation of mixed methyl ethers of polypropylene glycols: 1) nitrogen cylinder; 2) reducing valve; 3) cooling vessel; 4) cylinder; 5) electrically-heated reactor; 6) manometer; 7) receiver; 8) LATR transformer; 9) thermometer in sheath; 10) needle valve.

The aim of the present investigation was to find the optimum conditions for a continuous process of preparation of mixture (1) with $n = 3-5$ predominant. It was also desired to isolate the individual ethers in the mixture (1).

The results showed that the yield of the required fraction, consisting mainly of mixture (1) with $n = 3-5$, increases with increase of the molar ratio of propylene oxide to alcohol, and of the amount of caustic soda. In the light of these results and also of data reported by one of us earlier [5], we used a continuous laboratory unit, shown schematically in the figure, for preparation of (1). With this apparatus up to 5 different factors can be varied: the molar ratio of propylene oxide to methanol, the amount of catalyst (caustic soda), reaction time, temperature, and pressure. It was shown that the optimum molar ratio of propylene oxide to methanol is 1:0.2, as at lower ratios the conversion of propylene oxide and methanol is incomplete (24-56% of the former and 6-17% of the latter remains unchanged). Conversion of propylene oxide is likewise incomplete if the amount of catalyst

is reduced to 0.15% from 2.0% at the optimum component ratio. The best results were obtained at low pressures (2-5 atmos) and high temperatures (120-140°). At 1:0.2 ratio of the original components and a caustic soda concentration of 2.0-2.3%, conversion of propylene oxide and alcohol was complete, with a high percentage

Constants and Analytical Data for Monomethyl Ethers of Di-, Tri-, Tetra- and Pentapropylene Glycols

Monomethyl ether (1) of	Boiling point/ pressure (deg/mm)	d_4^{20}	n_D^{20}	Molar refraction		Molecular weight		Carbon (%)		Hydrogen (%)	
				found	cal- culated	found	cal- culated	found	cal- culated	found	cal- culated
Dipropylene glycol	90—91/12*	0.9375**	1.4229***	39.40	39.34	152	148	56.70	56.80	10.49	10.80
Tripropylene glycol	100/2	0.9684	1.4302****	55.04	54.83	204	206	58.37	58.20	10.50	10.66
Tetrapropylene glycol	124—5/2	0.9773	1.4350	70.58	70.33	259	264	59.36	59.15	10.65	10.60
Pentapropylene glycol	151—5/2	0.9832	1.4382	86.12	85.83	315	322	59.84	59.63	10.75	10.56

* Literature data: b.p. 76.1/10 ***** [6].

** Literature data: d_4^{20} 0.950 [6]; 0.9488 [7].

*** Literature data: n_D^{20} 1.419 [6]; 1.4200 [7].

**** Literature data: n_D^{25} 1.4277 [7].

***** As in original — Publisher's note.

content of (1) with $n = 3-5$ (45-50%), even when the mixture was in the reaction zone for only a short time (50 minutes). Moreover, the fact that low pressures can be used is itself an important advantage from the design and technological aspects, as compared with synthesis at 13-14 atmos.

For investigation of the reaction product it was fractionated through a laboratory column of 30 theoretical plates, with isolation of individual compounds (1) of $n = 3, 4$ and 5. The monomethyl ethers of di-, tri-, tetra-, and pentapropylene glycols were obtained pure by repeated fractionation of the first fractions (see table).

EXPERIMENTAL

The starting substances — propylene oxide, methanol, and caustic soda — were placed in the required proportions into a small cylinder cooled in ice to prevent premature reaction. The mixture was forced into the reactor by means of compressed nitrogen, with simultaneous collection of the product from the reactor in a graduated receiver cooled in ice. The reactor was made from special steel, with electrical surface heating, in the form of a cylindrical vessel 200 cc in capacity with a screw lid; it was previously filled with the prepared product (1) and heated to the required temperature. The pressure in the reactor and the residence time of the mixture in the reaction zone were easily regulated by a system of valves; any desired temperature could also be easily established. The collected product was fractionated.

SUMMARY

A continuous laboratory unit was used for investigating the effects of the molar ratio of propylene oxide to methanol, amount of caustic soda, reaction time, temperature, and pressure on the composition of the mixture of monomethyl ethers of polypropylene glycols formed in the reaction. It was found that the optimum conditions for obtaining the maximum contents of a mixture of the monomethyl ethers of tri-, tetra-, and pentapropylene glycols are: pressure 2-5 atmos, temperature 120-140°, reaction time 50-120 minutes, propylene oxide — methanol ratio 1:0.2, and caustic soda concentration 2.0-2.3%.

LITERATURE CITED

- [1] A. A. Petrov, J. Gen. Chem. 14, 1038 (1944).
- [2] A. A. Petrov, J. Gen. Chem. 16, 1206 (1946).

- [3] H. C. Chitwood and B. T. Freure, *J. Am. Chem. Soc.* 68, 680 (1946).
- [4] W. Reeve and A. Sadle, *J. Am. Chem. Soc.* 72, 1251 (1950).
- [5] S. M. Gurvich, *J. Gen. Chem.* 25, 1713 (1955).*
- [6] J. Biglon, *Ind. Chim.* 40, 249 (1953).
- [7] H. A. Pecorini and J. T. Banchero, *Ind. Eng. Ch.* 48, 1287 (1956).

Received March 25, 1958

*Original Russian pagination. See C.B. Translation.

OXIDATIVE AMMONOLYSIS OF γ -PICOLINE IN THE VAPOR PHASE*

B. V. Suvorov, S. R. Rafikov, V. S. Kudinova
and B. A. Zhubanov

In recent years derivatives of isonicotinic acid have been used in medicine. Its hydrazides, which have proved to be effective drugs in the treatment of tuberculosis, are especially widely used [1]. This has led to increased interest in new methods for preparation of isonicotinic acid. Several methods for its synthesis have been described [2], the most promising of which are based on catalytic vapor-phase oxidation of γ -picoline by atmospheric oxygen, as processes of this type are continuous and do not involve the use of scarce oxidizing agents or acid-resistant equipment.

According to literature data [3] the yield of isonicotinic acid by direct catalytic oxidation of γ -picoline is low, probably because of its great tendency to undergo decarboxylation [4].

The reaction proceeds more smoothly if the oxidation is performed in presence of ammonia. The nitrile of isonicotinic acid formed in the process can be subsequently saponified by any of the known methods to give free isonicotinic acid. Several patents deal with production of the nitrile of isonicotinic acid by oxidation of γ -picoline in presence of ammonia [5] with catalysts consisting of oxides of variable-valence metals: vanadium pentoxide or mixtures of vanadium, molybdenum, and phosphorus oxides. It is reported [6] that isonicotinonitrile can be obtained in yields of up to 23% by oxidation of γ -picoline in presence of vanadium oxide catalyst on alumina.

In the present investigation isonicotinonitrile was synthesized by our method of oxidative ammonolysis of organic compounds, which can be used for preparation of many nitriles in good yields [7].

γ -Picoline was isolated as the oxalate from a technical β -picoline fraction [8]. After recrystallization from anhydrous ethyl alcohol the oxalate melted at 139-140°. It was decomposed by 60% aqueous caustic soda. The liberated γ -picoline was extracted in ether. The ether extract was dried over calcined magnesium sulfate, the solvent was evaporated off, and the residue was fractionated at atmospheric pressure. The fraction of b.p. 140-140.5° (at 690 mm) and n_D^{20} 1.5050 was taken for the experiments. Its yield was about 11% on the γ -picoline fraction taken.

Ammonolysis of γ -picoline was effected in a unit of the flow type [7]. The catalyst was granulated tin vanadate. At the end of the experiment the system used for collecting the reaction products was washed through with water. The aqueous solution was extracted with ether. The extract was dried over calcined magnesium sulfate and fractionated. Isonicotinonitrile distilled at 186-187°. The melting point of the substance so prepared was not below 79°.

The nitrile was boiled with 60% sulfuric acid to give isonicotinic acid, which melted at 313-314° in a sealed capillary tube. A mixed sample with pure isonicotinic acid gave no depression. It should be noted that if isonicotinonitrile is saponified by dilute aqueous ammonia under pressure, the acid is also formed in almost quantitative yield.

To determine the optimum conditions for preparation of isonicotinonitrile, several series of experiments

*Communication XXII in the series on oxidation of organic compounds.

Effects of Reaction Temperature and Space Velocities on the Yield of Isonicotinonitrile
(Contact time 0.55-0.65 second)

Reaction temperature (deg)	Space velocity (liters/liter catalyst • hour)				Nitrile yield (%)
	γ -picoline	air	ammonia	water	
360	0.057	2320	10.37	27.23	63.0
375	0.049	2320	8.69	22.80	55.0
390	0.049	2320	9.21	24.22	55.0
360	0.019	1740	11.80	73.10	47.7
375	0.026	1740	10.60	65.20	54.6
390	0.024	1740	10.10	62.00	59.1
360	0.031	2952	4.69	29.0	62.5
375	0.029	2952	4.04	25.6	71.6
390	0.028	2952	5.96	21.4	62.8
405	0.030	2952	2.98	18.8	53.6

were carried out with different contact times, space velocities, and proportions of the starting materials.

The maximum yield of isonicotinonitrile was obtained at 375°, space velocity of γ -picoline 0.3, ammonia 4.0, water 25, and air 2950 liters per liter of catalyst per hour; it was over 70% on the γ -picoline taken. Results obtained in some other experiments are also given in the table for comparison.

SUMMARY

Isonicotinonitrile can be obtained in yields of over 70% by catalytic ammonolysis of γ -picoline in presence of a vanadium catalyst.

Saponification of the nitrile in an acid medium, or under pressure in presence of dilute aqueous ammonia, gives isonicotinic acid in high yield.

LITERATURE CITED

- [1] M. N. Shchukina, G. N. Pershin, O. O. Makeeva, et al., Proc. Acad. Sci. USSR 84, 981 (1952).
- [2] M. Yu. Lidak, S. A. Giller and N. N. Naumenko, Bull. Acad. Sci. Latvian SSR 12 (77), 83 (1953); British Patent 709176; Chem. Abs. 49,9044 (1955); M. V. Rubtsov, E. S. Nikitskaya and Ya. D. Yanina, J. Gen. Chem. 24, 1648 (1954)*.
- [3] R. W. Lewis and O. W. Brown, Ind. Eng. Ch. 36, 890 (1944); T. Ishiguro and I. Utsami, J. Pharm. Soc. Japan 72, 709 (1952); Ch. A. 47, 2174 (1953); F. E. Cislak and W. R. Wheeler, British Patent 563273; Chem. Abs. 40, 2472 (1946); U.S. Patent 2437938; Chem. Abs. 43, 4204 (1949).
- [4] Heterocyclic Compounds, I (IL, Moscow, 1955) p. 442 [Russian translation].
- [5] W. I. Denton and R. B. Bishop, U.S. Patent 2592123; Ch. A. 47, 616 (1953); F. Porter, M. Erchak Jr., N. Cosby and John N. Cosby; U.S. Patent 2510605; Ch. A. 45, 187 (1951).
- [6] G. Maynrmik, F. Moschetto, H. S. Bloch and L. V. Scudl, Ind. Eng. Ch. 44, 1630 (1952).
- [7] B. V. Suvorov, M. I. Khmura, A. D. Kagarlitskii, B. A. Zhubanov and M. V. Prokof'eva, Authors' Certif. No. 110059 (1957); S. R. Rafikov, B. V. Suvorov, M. I. Khmura and V. S. Kudanova, Proc. Acad. Sci. USSR 113, 355 (1957);* S. R. Rafikov and B. V. Suvorov, Authors' Certif. No. 113518 (1958).
- [8] K. Oyaniodo, U. Hamatsu and T. Dannoura, Ann. Rept. Takamine Lab. 5, 11 (1953).

Received October 11, 1958

*Original Russian pagination. See C.B. Translation.

SECOND INTERNATIONAL CONFERENCE ON THE PEACEFUL USES OF ATOMIC ENERGY, GENEVA, 1958

The science of nuclear energy is developing more and more intensively year by year. This is confirmed by the exhibition at the First International Conference on Peaceful Uses of Atomic Energy in Geneva in August 1955, where only 8 countries were represented, and the exhibits were accommodated quite easily in a few rooms and corridors of the Palace of Nations. The exhibits of the 20 countries participating in the exhibition of the Second International Conference needed much more space, and the exhibition was transferred to the park of the Palace of Nations, where the pavilion specially built for it occupied nearly one half of a hectare.

The Second International Conference on the Peaceful Uses of Atomic Energy, held in Geneva from September 1 to 13, 1958, attracted an enormous amount of attention. About 5000 scientists and experts from 66 countries and a number of international organizations took part in its work.

Soviet scientists have also made a large contribution to the development of nuclear power. At the exhibition the Soviet Union demonstrated 5 types of thermonuclear installations, which aroused special interest in the conference delegates. Our exhibits included the installation "Al'fa" and the well known "Ogra," models of power atomic power stations being built in the Soviet Union, a model of the "Lenin," the first atomic ice-breaker in the world, unique physical apparatus, etc.

The exhibits shown demonstrated once again the great number and diversity of uses of atomic energy for peaceful purposes.

The results of scientific investigations in various branches of nuclear physics, reactor physics, experience in the operation of atomic power plants, and results obtained by the uses of atomic energy in medicine, geology, biology, chemical technology, and industry were reported in nearly 2500 papers presented at the Conference.*

The Soviet delegation presented about 200 papers (twice as many as at the First Geneva Conference). In addition, after the address by the leader of the Soviet delegation, V. S. Emel'yanov, who discussed the future of atomic power in the USSR, the conference delegates were presented with a four-volume collection containing the results of 100 previously unpublished theoretical and experimental investigations carried out by Soviet scientists on controlled thermonuclear reactions.

The problem of controlled thermonuclear reactions was the center of attention of the participants at the Second International Conference. The well-known French chemist F. Perrin, present of the Conference, pointed out the problems associated with the synthesis of light nuclei were the most important of the topics discussed at the conference. It is therefore easy to understand the interest aroused by the paper, prepared by L. A. Artsimovich and read by E. I. Dobrokhotov, on investigations of controlled thermonuclear reactions in the USSR.

The problem of controlled nuclear reactions has received much attention in the USSR since the inception of atomic power technology. Work in this field has also been carried out in other countries.

The Soviet Government initiated the publication of research results in this field. In 1956 the Soviet Academician L. V. Kurchatov presented a paper at the British research center in Harwell on the possibilities of

*A systematic list of the papers presented at the Second International Conference on the Peaceful Uses of Atomic Energy is given in the journal *Atomnaya Energiya* (Vol. 5, No. 3, September 1958). A list of papers is also given in "express information" leaflets of the Main Administration for Utilization of Atomic Energy, the Council of Ministers USSR: Express Information No. 24 (102), June 23, 1958, Papers 1-966; No. 25 (103), June 30, 1958, Papers 967-1925; No. 26 (104), July 7, 1958, Papers 1926-2489.

effecting thermonuclear reactions in a gaseous discharge. The great significance of Kurchatov's Harwell lecture was noted repeatedly at the conference; this lecture not only destroyed the atmosphere of secrecy which surrounded thermonuclear research, but also activated work in other countries in this field. The French scientist P. Hubert reported that France started work on controlled synthesis only after Kurchatov's lecture. After this lecture publications of researches carried out in England and the United States gradually began to appear.

Discussion at the conference of the research done in this field showed that Soviet and foreign scientists, taking different routes, obtained identical results.

At the present time, despite the wide extent of researches into controlled thermonuclear reactions, they are still at the stage of exploration of various approaches to the problem, and none of these approaches has been explored enough to justify the claim that it ensures success.

A most important condition for success in these researches is the preservation and further development of the international scientific cooperation which originated at the Second International Conference.

A. K. Krasin reported on the performance of the first industrial atomic power plant in the world, which commenced operation two years before the British power plant at Calder Hall and three and one half years before the American plant at Shippingport. The first Soviet atomic power plant supplies current for industrial purposes and is also used for research work.

The conference delegates listened with great attention to a paper, full of factual data, on the use of radioactive isotopes in the USSR, presented by one of its authors, A. V. Topchiev, who stressed the importance of utilizing nuclear radiations in chemical technology.

V. I. Veksler reported on the work of the physicists of the United Nuclear Research Institute in Dubno, who developed an ingenious method for studying the structure of atomic nuclei and their constituents — protons and neutrons. The first results indicate that not only the atomic nuclei but the nucleons themselves are complex systems.

Considerable interest was also aroused by the paper on the atomic ice breaker "Lenin," presented by A. P. Aleksandrov. He stated that the atomic ice breaker Lenin will be the most powerful ice breaker in the world, with a turboelectric power unit of 44,000 horse power.

N. A. Dollezhal' presented new data on uranium-graphite reactors with superheating of high-pressure steam.

The paper presented by S. A. Skvortsov was concerned with water-water power reactors.

The papers presented by the Soviet delegation at the conference also included papers on changes in the mechanical properties of metallic constructional materials under the influence of neutron bombardment (N. F. Pravdyuk, S. T. Konobeevskii, et al.), on the interaction of plutonium with other metals in relation to their positions in the Mendeleev periodic system (A. A. Bochvar et al.), on the refining of beryllium and other metals by condensation on heated surfaces (K. D. Sinelnikov et al.), on phase diagrams of certain uranium and thorium systems (O. S. Ivanov and T. A. Badaeva), on binary phase diagrams of $\text{UO}_2\text{--Al}_2\text{O}_3$, $\text{UO}_2\text{--BeO}$, $\text{UO}_2\text{--MgO}$ (P. P. Budnikov, S. G. Tresvyatskii and V. I. Kushakovskii), on the chlorination of UO_2 and PuO_2 by carbon tetrachloride (I. V. Badaev and A. N. Vol'skii), etc.

The conference attracted much new data which must now be carefully examined. This will be assisted by publication of the conference proceedings. At the present time the Press of the Main Administration on the Utilization of Atomic Energy (Atomizdat) is preparing, for publication in 1959, the papers presented to the Second International Conference on Peaceful Uses of Atomic Energy by Soviet scientists (6 volumes), and selected papers by foreign scientists (10 volumes).

BOOK REVIEWS

GRANULATED BLAST-FURNACE SLAGS AND SLAG CEMENTS

P. P. Budnikov and I. L. Znachko-Yavorskii

The Chinese Press of the Building Materials Industry, Peking, 1956, 224 pp.

The chemical and mineralogical composition, structure, and hydraulic behavior of various blast-furnace slags are described systematically and in great detail. Moreover, the authors have proposed the use of blast-furnace slags as the argillaceous material for cement production by the wet process. The equipment and methods used for granulation of blast-furnace slags are described. A detailed account is given of the production technology of various slag cements, their constructional properties, and fields of application. The book is therefore a most valuable contribution to the literature, for production and utilization of cement and for scientific research in the cement industry.

In the first chapter, in the section entitled "Chemical composition of blast-furnace slags," it is shown that the utilization of granulated blast-furnace slags with high contents of manganese and magnesium oxides for cement production is technologically feasible.

In the section "Mineralogical composition and structure of blast-furnace slags" it is shown in the light of the theory of electrolytic dissociation that silica and alumina are present as nonequilibrium SiO_4^{4-} and AlO_4^{5-} groups in the glassy mass of granulated blast-furnace slags. In water they react with Ca^{2+} and Mg^{2+} cations, thus conferring hydraulic properties on the slag.

In the section "Hydraulic properties of blast-furnace slags" an account of the nature of activity and its determination in various slags is followed by a description of new trends in the production of cements from slags (for example, blast-furnace slag cement by V. V. Serov's process). All this is of great practical importance for research in the field of slag-cement production.

In the second chapter the activities of slags determined by different methods are compared; the dry and semidry granulation processes are shown to have technical and economic advantages over the wet process.

The last two chapters contain a very detailed account of the authors' views on the principles of hardening of various slag cements and of their sulfate resistance.

These features of the book are of great value to us Chinese cement scientists, and for our work.

However, the book does not contain a detailed account of investigations of slags of different chemical compositions and grades, carried out by GOST methods. There is no account of the use of the polarization microscope whereby the refractive indices of the glassy mass of slags can be utilized for control of cement quality during production.

In 1956 the engineers T'ao Ch'en Ku and Mieh Ti Shen of the Scientific Research Institute of Cement (Chinese Peoples' Republic) suggested a method for production of nepheline-sulfate cement (a sort of sulfate-slag cement with regard to the nature of its hardening), and carried it out in practice. This cement is made from 45-50% of nepheline (a by-product of the aluminum industry, containing 21-25% SiO_2 , 6-13% Al_2O_3 , 41-45% CaO and 2-4% Na_2O), 30-35% of granulated blast-furnace slag, 14-16% of anhydrous calcium sulfate (calcined at 600-700°), and 2-3% of slaked lime. Mixing and fine grinding of this mixture gives a hydraulic cement of "500" and sometimes of "600" grade.

The investigations carried out in our Institute on the influence of temperature on the hardening of slag

Portland cements have shown that the strength of concrete made from slag Portland cement containing 30% of basic or acid slag after steaming at $80 \pm 5^\circ$ for 6-16 hours does not exceed $0.3 R_{28}$ with ordinary hardening. This effect is not mentioned in the book.

Moreover, there is a contradiction between the results of practical experience of the use of sulfate-slag cement in a lime-cement-sand mortar (1:4-1:1:9) for brick laying (p. 174) and the specific properties of this cement (Chapter Four). An explanation of this point would be desirable in a new edition.

This book is a very valuable manual on cement technology. It has been translated into Chinese and is one of the most widely-used Soviet technical books for specialists in the cement industry.

Tung T'i-kun (Deputy Director, Scientific Research
Institute of Cement)
Lo Hsiu Shun (Engineer)

INHIBITORS OF METAL CORROSION

I. N. Putilova, S. A. Balezin and
V. P. Barannik

Goskhimizdat, Moscow, 1958, 184 pp., 5000 copies.

The book deals with protection of metals against corrosive attack. The authors of the book, who are university workers, are well-known specialists in this field. They were awarded the Stalin prize for their development of a number of inhibitors of acid corrosion. Their experience and the most important research results are presented in the book. In addition, literature data on the work of other authors, both Soviet and foreign, are extensively represented.

The theory of inhibitor action is discussed, and an account is given of the most important inhibitors of metal corrosion in water, aqueous solutions of acids, alkalies, and salts, under atmospheric conditions, and in nonaqueous liquid media. Although the book is in the nature of a monograph, it is written in a simple style which makes it suitable for university students, teachers, and wide circles of scientific and technical workers in various branches of industry.

The present state of scientific knowledge in the field is reflected in the book, which contains experimental data.

Chapter I deals with classification of inhibitors and a discussion of their action. They aptly classify inhibitors as follows: inhibitors type A, which form the so-called protective films on the metal surfaces, inhibitors type B, which reduce the corrosiveness of the medium with respect to the metal, and, finally, mixed inhibitors type AB, which have the combined effects of types A and B, or the predominant effect of either one of these types. Inhibitors of types A and B are, in their turn, subdivided into groups according to their influence on corrosion kinetics. The authors' proposed classification facilitates the subsequent consideration of the extensive experimental data presented in the book. The same chapter deals with the influence of inhibitor concentration on the rate of corrosion, the effects of temperature on inhibitor action, the action of mixtures of inhibitors, and certain other topics.

Chapter II is concerned with various theories of the mechanism of inhibitor action, including the adsorption theory, the overvoltage theory, and the film theory. It should be noted that this chapter is less successful than Chapter I or the following chapters. There are some superficialities, inaccuracies, and even a few errors in the discussion of certain theoretical publications by a number of authors. In our opinion, the role of electrochemical processes is underestimated in discussions of certain, often contradictory, experimental data. The conclusion that "changes of electrochemical parameters cannot be the cause of retardation of metal corrosion" is unjustified, and the example given in illustration is erroneous (p. 69). In the next edition, which is highly necessary, Chapter II must be thoroughly revised, with a more careful analysis and correlation of different theories of inhibitor action.

The interest of Chapters III, IV and V lies in the fact that they contain a detailed review of the experimental data and important scientific achievements in the original investigations by the authors.

The most corrosive media are aqueous solutions of acids. The authors present data on the action of their inhibitors ChM and PB in such media and discuss the results of over 10 years' experience of the transport of inhibited hydrochloric acid in ordinary tank cars. It must be pointed out that such transportation became possible only after the authors' discovery of inhibitor PB.

Corrosion in aqueous alkalis (Chapter IV) has been studied less thoroughly. This chapter is therefore short; it describes inhibitors of corrosion of aluminum, zinc, and iron in alkalis. Inhibition of corrosion in water and in aqueous salt solutions, and inhibitors of atmospheric corrosion are discussed in greater detail (Chapter V).

The last chapter (VI) is concerned with inhibitors of corrosion in nonaqueous liquid media. This section is also of considerable interest, because a variety of nonaqueous liquids corrosive to metals is used in modern technology. Therefore corrosion processes are often much more rapid in such media than in aqueous solutions. This chapter contains a review of inhibitors for media containing alcohols and phenols, for halogenated hydrocarbons, and for liquid hydrocarbons. As the authors correctly point out, this review "cannot be regarded as exhaustive." This section should be extended in the next edition (with tables and graphs representing experimental data, as in the preceding chapters).

Inhibitors of acid corrosion are widely used for chemical removal of oxides (rust) from metal surfaces. The rate of solution of the rust remains the same or is reduced slightly, whereas dissolution of the metal is very sharply retarded. Inhibitors also retard diffusion of hydrogen into metal and thereby reduce embrittlement. The authors give effective formulations for removal of rust and for subsequent passivation of the metal surface. Another important feature is their proposed method of rust removal by means of etching pastes; suitable fillers are added to the formulation to give it a consistency convenient for application by means of a brush. This is especially necessary when the parts to be cleaned are too large for the pickling bath, or for cleaning of metallic ceilings and, in general, of surfaces sloping at various angles. The recommended pastes have good properties: the rate of dissolution of the rust is considerable, the adhesion to metal is adequate, and the corrosive action on the metal under the paste is slight.

Methods of preparation and use of acid-corrosion inhibitors and of etching and passivating pastes are given in appendices. These are five in number. The data presented there are especially useful for practical purposes, as the titles indicate: 1) use of the ChM pickling additive; 2) chemical removal of rust from steel with the use of inhibitors; 3) use of hydrochloric acid for removal of boiler scale; 4) derusting and passivation of metals by means of pastes; 5) protection of metals against atmospheric corrosion by means of paper impregnated with inhibitors. In contrast to the main text, the appendices are printed in small type.

We think it would be better to combine the appendices in a separate chapter, say VII, and to provide literature references as in all the other chapters. The practical significance of the data in the appendices also justifies this.

The authors made fairly complete use of the available literature and patents, and of their own publications, in the compilation of the book. A list of literature references is given in each chapter and in the introduction (a total of 330 references is cited). This makes it possible to obtain more detailed information on the subject matter of each chapter.

All metals are susceptible to corrosion, although to different extents. Therefore the publication of a book which has the protection of metals against this "disease" as its aim can only be welcomed. The authors have accomplished a large and necessary task. Their book will be widely used by industrial workers, university teachers, and students. It should be noted that the book has been translated and published in England.

G. P. Khomchenko

Physical Chemistry

**PHYSICAL CHEMISTRY Section
of the
PROCEEDINGS OF THE ACADEMY OF SCIENCES
OF THE USSR (DOKLADY)**

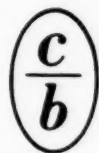
including all reports on:

**Chemical Kinetics
Interface Phenomena
Electrochemistry
Absorption Spectra
and related subjects**

As in all sections of the Proceedings, the papers are by leading Soviet scientists. Represents a comprehensive survey of the most advanced Soviet research in physical chemistry. The 36 issues will be published in 6 issues annually. Translation began with the 1957 volume. Translation by Consultants Bureau bilingual chemists, in the convenient C. B. format.

Annual subscription	\$160.00
Single issues	35.00
Individual articles	5.00

Cover-to-cover translation, scientifically accurate. Includes all diagrammatic and tabular material integral with the text; clearly reproduced by multilith process; staple bound.



CONSULTANTS BUREAU, INC.
227 W. 17th St., NEW YORK 11, N. Y.

PROCEEDINGS OF THE FIRST ALL-UNION CONFERENCE ON RADIATION CHEMISTRY, MOSCOW, 1957

THIS UNPRECEDENTED RUSSIAN CONFERENCE on Radiation Chemistry, held under the auspices of the *Division of Chemical Sciences, Academy of Sciences, USSR* and the *Ministry of Chemical Industry*, aroused the interest of scientists the world over. More than 700 of the Soviet Union's foremost authorities in the field participated and, in all, fifty-six reports were read covering the categories indicated by the titles of the individual volumes listed below. Special attention was also given to radiation sources used in radiation-chemical investigations.

Each report was followed by a general discussion which reflected various points of view in the actual problems of radiation chemistry: in particular, on the *mechanism of the action of radiation on concentrated aqueous solutions*, on the *practical value of radiation galvanic phenomena*, on the *mechanisms of the action of radiation on polymers, etc.*

The entire "Proceedings" may be purchased as a set, or individual volumes may be obtained separately as follows:

- Primary Acts in Radiation Chemical Processes**
(heavy paper covers; 5 reports, approx. 38 pp., illus., \$25.00)
- Radiation Chemistry of Aqueous Solutions**
(heavy paper covers, 15 reports, approx. 83 pp., illus., \$50.00)
- Radiation Electrochemical Processes**
(heavy paper covers, 9 reports, approx. 50 pp., illus., \$15.00)
- Effect of Radiation on Materials Involved in Biochemical Processes**
(heavy paper covers, 6 reports, approx. 34 pp., illus., \$12.00)
- Radiation Chemistry of Simple Organic Systems**
(heavy paper covers, 9 reports, approx. 50 pp., illus., \$30.00)
- Effect of Radiation on Polymers**
(heavy paper covers, 9 reports, approx. 40 pp., illus., \$25.00)
- Radiation Sources**
(heavy paper covers, 3 reports, approx. 20 pp., illus., \$10.00)

PRICE FOR THE 7-VOLUME SET

: \$125.00

NOTE: Individual reports from each volume available at \$12.50 each. Tables of Contents sent upon request.

CB translations by bilingual scientists include all photographic, diagrammatic, and tabular material integral with the text.

CONSULTANTS BUREAU, INC.

227 WEST 17TH STREET, NEW YORK 11, N. Y.

